

[2014]

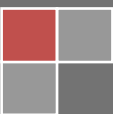
[International Journal of Computational Engineering Research]

[Frequency: 12 issues per year]

[International Journal of Computational Engineering Research(IJCER) is an intentional online Journal in English monthly publishing journal. This Journal publish original research work that contributes significantly to further the scientific knowledge in engineering and Technology.]

Volume 4, Issue 5, May, 2014

IJCER



Editorial Board

Editor-In-Chief

Prof. Chetan Sharma

Specialization: Electronics Engineering, India
Qualification: Ph.d, Nanotechnology, IIT Delhi, India

Editorial Committees

DR.Qais Faryadi

Qualification: PhD Computer Science
Affiliation: USIM(Islamic Science University of Malaysia)

Dr. Lingyan Cao

Qualification: Ph.D. Applied Mathematics in Finance
Affiliation: University of Maryland College Park,MD, US

Dr. A.V.L.N.S.H. HARIHARAN

Qualification: Phd Chemistry
Affiliation: GITAM UNIVERSITY, VISAKHAPATNAM, India

DR. MD. MUSTAFIZUR RAHMAN

Qualification: Phd Mechanical and Materials Engineering
Affiliation: University Kebangsaan Malaysia (UKM)

Dr. S. Morteza Bayareh

Qualificatio: Phd Mechanical Engineering, IUT
Affiliation: Islamic Azad University, Lamerd Branch
Daneshjoo Square, Lamerd, Fars, Iran

Dr. Zahéra Mekkioui

Qualification: Phd Electronics
Affiliation: University of Tlemcen, Algeria

Dr. Yilun Shang

Qualification: Postdoctoral Fellow Computer Science
Affiliation: University of Texas at San Antonio, TX 78249

Lugen M.Zake Sheet

Qualification: Phd, Department of Mathematics
Affiliation: University of Mosul, Iraq

Mohamed Abdellatif

Qualification: PhD Intelligence Technology
Affiliation: Graduate School of Natural Science and Technology

Meisam Mahdavi

Qualification: Phd Electrical and Computer Engineering

Affiliation: University of Tehran, North Kargar st. (across the ninth lane), Tehran, Iran

Dr. Ahmed Nabih Zaki Rashed

Qualification: Ph. D Electronic Engineering

Affiliation: Menoufia University, Egypt

Dr. José M. Merigó Lindahl

Qualification: Phd Business Administration

Affiliation: Department of Business Administration, University of Barcelona, Spain

Dr. Mohamed Shokry Nayle

Qualification: Phd, Engineering

Affiliation: faculty of engineering Tanta University Egypt

CONTENTS:

S.No.	Title Name	Page No.
Version I		
1.	Automated Glaucoma Screening using CDR from 2D Fundus Images Sushma G.Thorat	01-07
2.	Model of Quantum Computing in the Cloud: The Relativistic Vision Applied in Corporate Networks Chau Sen Shia , Mario Mollo Neto , Oduvaldo Vendrametto	08-26
3.	Extended version of Leach and its comparison with Energy aware multi-hop multi-path Hierarchy Protocol Prof. Greeshma Arya , Prof. D.S Chauhan , Ridhi Khanna , Nehal Mittal, Amandeep	27-35
4.	A Review on HADOOP MAPREDUCE-A Job Aware Scheduling Technology Silky Kalra , Anil lamba	36-40
5.	Harmonic Reduction by Using Shunt Hybrid Power Filter Kavita Dewangan, Prof. Pawan C. Tapre	41-49
6.	Determination of Optimal Account and Location of Series Compensation and Svs for an Ac Transmission System B.Suresh Kumar	50-57
Version II		
1.	Strength and Durability of Fly Ash, Cement and Gypsum Bricks Nitin S. Naik, B.M.Bahadure, C.L.Jejurkar	01-04
2.	An Extensive Hypothetical Review on Call Handover Process in Cellular Network Vaibhav V.Kamble , Shubhangi G. Salvi, Bharatratna P. Gaikwad , Rahul B. Gaikwad	05-08
3.	Extensions of Enestrom-Kakeya Theorem M. H. Gulzar	09-18

4.	Analysis of Vulnerability Assessment in the Coastal Dakshina Kannada District, Mulki to Talapady Area, Karnataka S. S. Honnanagoudar , D. Venkat Reddy, Mahesha. A	19-24
5.	Robotics Helicopter Control and its Applications in Engineering Prof.Dr.Eng.PVL Narayana Rao, Mr.Jemal Ahmed Andeta, Mr.Habte Lejebo Leka, Mr.AbrahamAssefa Simmani, Er.Pothireddy Siva Abhilash	25-30
6.	Design and Implementation Of A Microcontroller-Based Keycard Aneke Chikezie,Ezenkwu Chinedu Pascal,Ozuomba Simeon	31-39
7.	A Review on Parallel Scheduling of Machines and AGV'S in an FMS environment Prof.Mallikarjuna ,Vivekananda , Md.Jaffar , Jadesh , Hanumantaraya	40-47
8.	Mapreduce Performance Evaluation through Benchmarking and Stress Testing On Multi-Node Hadoop Cluster Urvashi Chaudhary ,Harshit Singh	48-51

Version III

1.	Characteristics of soils for underground pipeline laying in the southwest Niger Delta Uko, E. D., Benjamin, F. S. and Tamunobereton-ari, I.	01-18
2.	Efficient Ranking and Suggesting Popular Itemsets In Mobile Stores Using Fp Tree Approach B.Sujatha Asst prof ,Shaista Nousheen Asst.prof , Tasneem rahath Asst prof, Nikhath Fatima	19-30
3.	Elaboration of stochastic mathematical models for the prediction of parameters indicative of groundwater quality Case of Souss Massa – Morocco Manssouri T. , Sahbi H. , Manssouri I.	31-40
4.	Experimental Studies of the Statistical Properties of Network Traffic Based on the BDS-Statistics Alexey Smirnov , Dmitriy Danilenko	41-51

5.	Area-Delay Efficient Binary Adders in QCA D.Thirupathi Reddy M.Tech, Soma Prneeth Reddy , Katasani Sandeep Kumar Reddy, Suddamalla Nagadastagiri Reddy, S.K. khasid	52-56
6.	Efficient Multicast Algorithms for Wireless Mesh Networks Dr.Sivaagorasakthivelmurugan , P.Ravi Shankar	57-62
7.	Subaltern Voice in Shakespeare: A Study in the Tempest Tribeni Mandal	63-67
8.	Modeling of Sokoto Cement Production Process Using A Finite Automata Scheme: An Analysis Of The Detailed Model Z. Ibrahim, A.A. Ibrahim ,I. A. Garba	68-74
9.	Clustering Techniques to Analyze Communication Overhead in Wireless Sensor Network Prof. Arivanantham Thangavelu , Prof. Abha Pathak	75-78

Automated Glaucoma Screening using CDR from 2D Fundus Images

Sushma G.Thorat

M.E.(Electronics and Telecommunication)
Siddhant college of engineering,Saudumbare,Pune

Abstract:

Glaucoma is a chronic eye disease that leads to blindness. This disease cannot be cured but we can detect the disease in time. Current tests using intraocular pressure (IOP) measurement are not sensitive enough for population based glaucoma screening. Optic nerve head assessment in retinal fundus images is more promising and superior than current methods. This paper proposes segmentation of optic disc and optic cup using superpixel classification for glaucoma screening. In optic disc segmentation, clustering algorithms are used to classify each superpixel as disc or non-disc. For optic cup segmentation, in addition to the clustering algorithms, the Gabor filter and thresholding is used. . The segmented optic disc and optic cup are then used to compute the cup to disc ratio for glaucoma screening. The Cup to Disc Ratio (CDR) of retinal fundus camera image is the primary identifier to confirm glaucoma for a given patient.

Index terms: Glaucoma Screening, Gabor Filter, Intraocular pressure, Optic cup segmentation, Optic disc segmentation, Thresholding, CDR.

I. INTRODUCTION

Glaucoma is a chronic eye disease of the major nerve of vision, called the optic nerve which is progressively damaged. If glaucoma is not diagnosed and treated in time, it can progress to loss of vision and even blindness. Glaucoma usually causes no symptoms early, it can only be diagnosed by regular eye examinations. It is predicted to affect around 80 million people by 2020[1].

There are different methods to detect glaucoma: assessment of (1) raised intraocular pressure (IOP), (2) abnormal visual field,(3) damaged optic nerve head. The IOP measurement using non-contact tonometry is not sensitive enough for population based glaucoma screening. A functional test through vision loss requires special equipment only present in territory hospitals and therefore unsuitable for screening. Optic nerve head assessment can be done by a trained professional. However manual assessment is subjective, time consuming and expensive. Hence, automatic optic nerve head assessment would be very beneficial.

In the previous work on “Classifying glaucoma with image-based features from fundus photographs”[2], the features are normally computed at the image-level and we use image features for binary classification between glaucomatous and healthy subjects[3]. Many glaucoma risk factors are considered, such as vertical cup to disk ratio(CDR),disc diameter, peripapillary atrophy(PPA),etc.Among of these CDR is commonly used. A larger CDR indicates a higher risk of glaucoma. There has been some research into automatic CDR measurement from 3D images[4]. The 3D images are not easily available and high cost of obtaining 3D images makes it inappropriate for a large scale screening program. This paper proposes an automatic glaucoma screening using CDR from 2D fundus images.

II. Literature Survey

[1] Effects of Preprocessing Eye Fundus Images on Appearance Based Glaucoma Classification:

Early detection of glaucoma is essential for preventing one of the most common causes of blindness. Our research is focused on a novel automated classification system based on image features from fundus photographs[5] which does not depend on structure segmentation or prior expert knowledge. Our new data driven approach that needs no manual assistance achieves an accuracy of detecting glaucomatous retina fundus images comparable to human experts. In this paper, we study image preprocessing methods to provide better input for more reliable automated glaucoma detection. We reduce disease independent variations without removing information that discriminates between images of healthy and glaucomatous eyes. In particular,

nonuniform illumination is corrected, blood vessels are inpainted and the region of interest is normalized before feature extraction and subsequent classification.

[2] Locating the Optic Nerve in a Retinal Image Using the Fuzzy Convergence of the Blood Vessels

We describe an automated method to locate the optic nerve in images of the ocular fundus. Our method uses a novel algorithm we call fuzzy convergence to determine the origination of the blood vessel network[6]. We evaluate our method many images of healthy retinas and diseased retinas, containing such diverse symptoms as tortuous vessels, choroid revascularization, and hemorrhages that completely obscure the actual nerve. We also compare our method against three simpler methods, demonstrating the performance improvement. All our images and data are freely available for other researchers to use in evaluating related methods.

[3] Detection of Optic Disc in Retinal Images by Means of a Geometrical Model of Vessel Structure

We present here a new method to identify the position of the optic disc (OD) in retinal fundus images. The method is based on the preliminary detection of the main retinal vessels[7]. All retinal vessels originate from the OD and their path follows a similar directional pattern (parabolic course) in all images. To describe the general direction of retinal vessels at any given position in the image, a geometrical parametric model was proposed, where two of the model parameters are the coordinates of the OD center. Using as experimental data samples of vessel centerline points and corresponding vessel directions, provided by any vessel identification procedure, model parameters were identified by means of a simulated annealing optimization technique. These estimated values provide the coordinates of the center of OD.

[4] Detecting the Optic Disc Boundary in Digital Fundus Images Using Morphological, Edge Detection, and Feature Extraction Techniques.

Optic disc (OD) detection is an important step in developing systems for automated diagnosis of various serious ophthalmic pathologies. This paper presents a new template-based methodology for segmenting the OD from digital retinal images. This methodology uses morphological and edge detection techniques followed by the Circular Hough Transform to obtain a circular OD boundary approximation. It requires a pixel located within the OD as initial information. For this purpose, a location methodology based on a voting-type algorithm is also proposed. The algorithms were evaluated on many images and the results were fairly good.

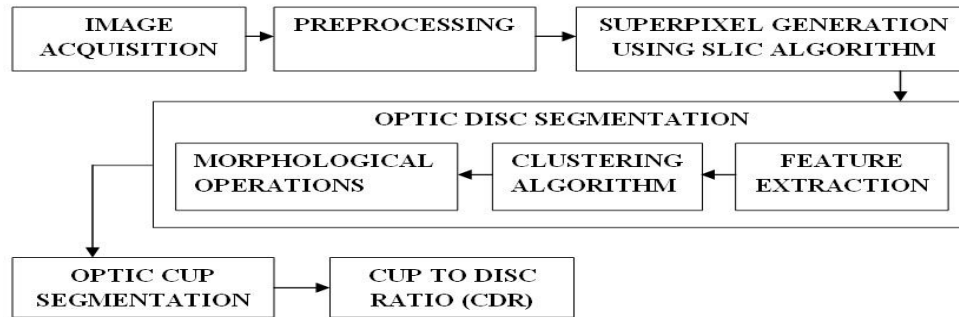
[5] Optic Nerve Head Segmentation

Reliable and efficient optic disk localization and segmentation are important tasks in automated retinal screening. General-purpose edge detection algorithms often fail to segment the optic disk due to fuzzy boundaries, inconsistent image contrast or missing edge features. This paper presents an algorithm for the localization and segmentation of the optic nerve head boundary in low-resolution images (about 20 /pixel). Optic disk localization is achieved using specialized template matching and segmentation by a deformable contour model. The latter uses a global elliptical model and a local deformable model with variable edge-strength dependent stiffness. The algorithm is evaluated against randomly selected images from a diabetic screening program. Ten images were classified as unusable; the others were of variable quality. The localization algorithm succeeded on all but one usable image.

III. PROPOSED SYSTEM

This paper focuses on automatic glaucoma screening using CDR from 2D fundus images. This paper proposes superpixel classification based disc and cup segmentations for glaucoma screening. In this proposed approach, preprocessing such as image filtration, color contrast enhancement are performed which is followed by a combined approach for image segmentation and classification using texture, thresholding and morphological operation. Multimodalities including K-Means clustering, Gabor wavelet transformations are also used to obtain accurate boundary delineation. We incorporate prior knowledge of the cup by including location information for cup segmentation. Based on the segmented disc and cup, CDR is computed for glaucoma screening.

IV. PROPOSED SYSTEM BLOCK DIAGRAM



4.1. Image acquisition:

The retina can be observed and recorded using several methods including Fluorescein Angiograms (FA), Transient Visual Evoked Potential (TVEP) or fundus camera. FA is a medical estimation tool that injects fluorescein into the body before image capture so vessel features (arteries, capillaries and veins) can stand out and be photographed

4.1. Image Preprocessing:

First, we need to enhance the image that we are going to use. We can either apply basic filter techniques or we can use histogram equalization techniques for the process of histogram equalization. We also found some techniques to generate too noisy images for glaucoma detection (histogram equalization adaptive histogram equalization or color normalization). Thus, we have selected methods which are well-known in medical image processing and preserve image characteristics. Naturally, the proposed system can be improved in the future with adding new methods. In detecting abnormalities associated with fundus image, the images have to be preprocessed in order to correct the problems of uneven illumination problem, nonsufficient contrast between exudates and image background pixels and presence of noise in the input fundus image. Aside from aforementioned problems, this section is also responsible for color space conversion and image size standardization for the system.

One of the problems associated with fundus images is uneven illumination. Some areas of the fundus images appear to be brighter than the other. Areas at the centre of the image are always well illuminated, hence appears very bright while the sides at the edges or far away are poorly illuminated and appears to be very dark. In fact the illumination decreases as distance from the centre of the image increase. Many methods were tried in resolving this problem of un-even illumination, among which are the use of Naka Rushton method and Adaptive Histogram Equalization Method (AHM). AHM gives better performance, higher processing speed and work well for all images of different sizes, hence the reason for it being used as method of correcting un-even illumination.

4.2. Superpixel Generation:

They have been proved to be useful in image segmentations in various images of scene, animal, human etc.

Slc Algorithm:

This paper uses the simple linear iterative clustering algorithm (SLIC) to aggregate nearby pixels into superpixels in retinal fundus images[8]. Compared with other superpixel methods, SLIC is fast, memory efficient and has excellent boundary adherence. SLIC is also simple to use with only one parameter, i.e., the number of desired superpixels. We introduce a new superpixel algorithm, simple linear iterative clustering (SLIC), which adapts a k-means clustering approach to efficiently generate superpixels. Despite its simplicity, SLIC adheres to boundaries as well as or better than previous methods. At the same time, it is faster and more memory efficient, improves segmentation performance, and is straightforward to extend to superpixel generation. SLIC is simple to use and understand.

By default, the only parameter of the algorithm is k , the desired number of approximately equally-sized superpixels. For color images in the CIELAB color space, the clustering procedure begins with an initialization step where k initial cluster centers $= l_i, a_i, b_i, x_i, y_i$ are sampled on a regular grid spaced S pixels apart. To produce roughly equally sized superpixels, the grid interval is $S = N/k$. The centers are moved to seed locations corresponding to the lowest gradient position in a 3×3 neighborhood. This is done to avoid centering a superpixel on an edge, and to reduce the chance of seeding a superpixel with a noisy pixel.

Next, in the assignment step, each pixel i is associated with the nearest cluster center whose search region overlaps its location. This is the key to speeding up our algorithm because limiting the size of the search

region significantly reduces the number of distance calculations, and results in a significant speed advantage over conventional k -means clustering where each pixel must be compared with all cluster centers. This is only possible through the introduction of a distance measure D , which determines the nearest cluster center for each pixel.

4.3. Optic Disc Segmentation:

4.3.1. Background:

The segmentation estimates the disc boundary, which is a challenging task due to blood vessel occlusions, pathological changes around disc, variable imaging conditions, etc. Feature Extraction techniques like clustering algorithm and morphological operations are used for optic disc segmentation[9]. Circular Hough transform is also used to model the disc boundary because of its computational efficiency.

K-means clustering algorithm:

K-Means algorithm is an unsupervised clustering algorithm that classifies the input data points into multiple classes based on their inherent distance from each other. The algorithm assumes that the data features form a vector space and tries to find natural clustering in them.

K-Means algorithm is an unsupervised clustering algorithm that classifies the input data points into multiple classes based on their inherent distance from each other. The algorithm assumes that the data features form a vector space and tries to find natural clustering in them. The points are clustered around centroids μ_i , $i = 1 \dots k$ which are obtained by minimizing the objective

$$\sum_{j=1}^K \sum_{i=1}^X \|X_i^{(j)} - c_j\|^2$$

where $\|x_i - c_j\|^2$ is a chosen distance measure between a data point x_i and the cluster centre c_j , is an indicator of the distance of the n data points from their respective cluster centres.

- Compute the intensity distribution (also called the histogram) of the intensities.
- Initialize the centroids with k random intensities
- Repeat the following steps until the cluster labels of the image do not change anymore.
- Cluster the points based on distance of their intensities from centroid intensities replicated with the mean value within each of the array and then the distance matrix is calculated.

$$c^{(i)} := \arg \min_j \|x^{(i)} - \mu_j\|^2$$

- Compute the new centroid for each of the clusters.

$$\mu_i := \frac{\sum_{i=1}^m 1\{c^{(i)} = j\} x^{(i)}}{\sum_{i=1}^m 1\{c^{(i)} = j\}}$$

Where k is a parameter of the algorithm (the number of clusters to be found), i iterates over the all the intensities, j iterates over all the centroids and μ_i are the centroid intensities.

4.3.2. Feature extraction:

Gabor Filter:

In image processing, a Gabor filter, named after Dennis Gabor, is a linear filter used for edge detection. Frequency and orientation representations of Gabor filters are similar to those of the human visual system, and they have been found to be particularly appropriate for texture representation and discrimination. In the spatial domain, a 2D Gabor filter is a Gaussian kernel function modulated by a sinusoidal plane wave. The Gabor filters are self-similar: all filters can be generated from one mother wavelet by dilation and rotation.

Gabor filters are directly related to Gabor wavelets, since they can be designed for a number of dilations and rotations. However, in general, expansion is not applied for Gabor wavelets, since this requires computation of bi-orthogonal wavelets, which may be very time-consuming. Therefore, usually, a filter bank consisting of Gabor filters with various scales and rotations is created. The filters are convolved with the signal, resulting in a so-called Gabor space. This process is closely related to processes in the primary visual cortex. Jones and Palmer showed that the real part of the complex Gabor function is a good fit to the receptive field

weight functions found in simple cells in a cat's striate cortex. The Gabor space is very useful in [image processing](#) applications such as [optical character recognition](#), [iris recognition](#) and [fingerprint recognition](#). Relations between activations for a specific spatial location are very distinctive between objects in an image. Furthermore, important activations can be extracted from the Gabor space in order to create a sparse object representation. Among various wavelet bases, Gabor functions provide the optimal resolution in both the time (spatial) and frequency domains, and the Gabor wavelet transform seems to be the optimal basis to extract local features for several reasons. The problem with cup and disc segmentation is that the visibility of boundary is usually not good especially due to blood vessels. Gabor wavelets can be tuned for specific frequencies and orientations which is useful for blood vessels. They act as low level oriented edge discriminators and also filter out the background noise of the image. Since vessels have directional pattern so 2-D Gabor wavelet is best option due to its directional selectiveness capability of detecting oriented features and fine tuning to specific frequencies

4.4 Optic Cup Segmentation:

We can use thresholding or binarization for Optic Cup segmentation Process. This process will convert the given image into a thresholded or binarized image where we can easily get our Optic Cup. Binary images are produced from color images by segmentation. Segmentation is the process of assigning each pixel in the source image to two or more classes. If there are more than two classes then the usual result is several binary images.

The simplest form of segmentation is probably [Otsu thresholding](#) which assigns pixels to foreground or background based on grayscale intensity. Another method is the [watershed algorithm](#). [Edge detection](#) also often creates a binary image with some pixels assigned to edge pixels, and is also a first step in further segmentation.

4.4.1. Binarization:

Binarization is a process where each pixel in an image is converted into one bit and you assign the value as '1' or '0' depending upon the mean value of all the pixel. If greater than mean value then its '1' otherwise its '0'.

4.4.2 Thresholding:

Thresholding is the simplest method of image [segmentation](#). From a [grayscale](#) image, thresholding can be used to create [binary images](#).

During the thresholding process, individual [pixels](#) in an image are marked as "object" pixels if their value is greater than some threshold value (assuming an object to be brighter than the background) and as "background" pixels otherwise. This convention is known as threshold above. Variants include threshold below, which is opposite of threshold above; threshold inside, where a pixel is labeled "object" if its value is between two thresholds; and threshold outside, which is the opposite of threshold inside. Typically, an object pixel is given a value of "1" while a background pixel is given a value of "0." Finally, a binary image is created by coloring each pixel white or black, depending on a pixel's labels.

Threshold selection:

The key parameter in the thresholding process is the choice of the threshold value (or values, as mentioned earlier). Several different methods for choosing a threshold exist; users can manually choose a threshold value, or a thresholding algorithm can compute a value automatically, which is known as automatic thresholding

A simple method would be to choose the [mean](#) or [median](#) value, the rationale being that if the object pixels are brighter than the background, they should also be brighter than the average. In a noiseless image with uniform background and object values, the mean or median will work well as the threshold, however, this will generally not be the case. A more sophisticated approach might be to create a [histogram](#) of the image pixel intensities and use the valley point as the threshold.

The histogram approach assumes that there is some average values for both the background and object pixels, but that the actual pixel values have some variation around these average values. However, this may be computationally expensive, and image histograms may not have clearly defined valley points, often making the selection of an accurate threshold difficult. In such cases a [unimodal threshold selection algorithm](#) may be more appropriate.

Morphological operation:

The disc and cup boundary detected from the segmentation methods may not represent the actual shape of the disc and cup since the boundaries can be affected by a large number of blood vessels entering the disc. Therefore the morphological operations are employed to reshape the obtained disc and cup boundary. Then CDR is calculated by taking the ratio of the area of cup to OD.

4.5. CDR Calculation and Diagnosis:

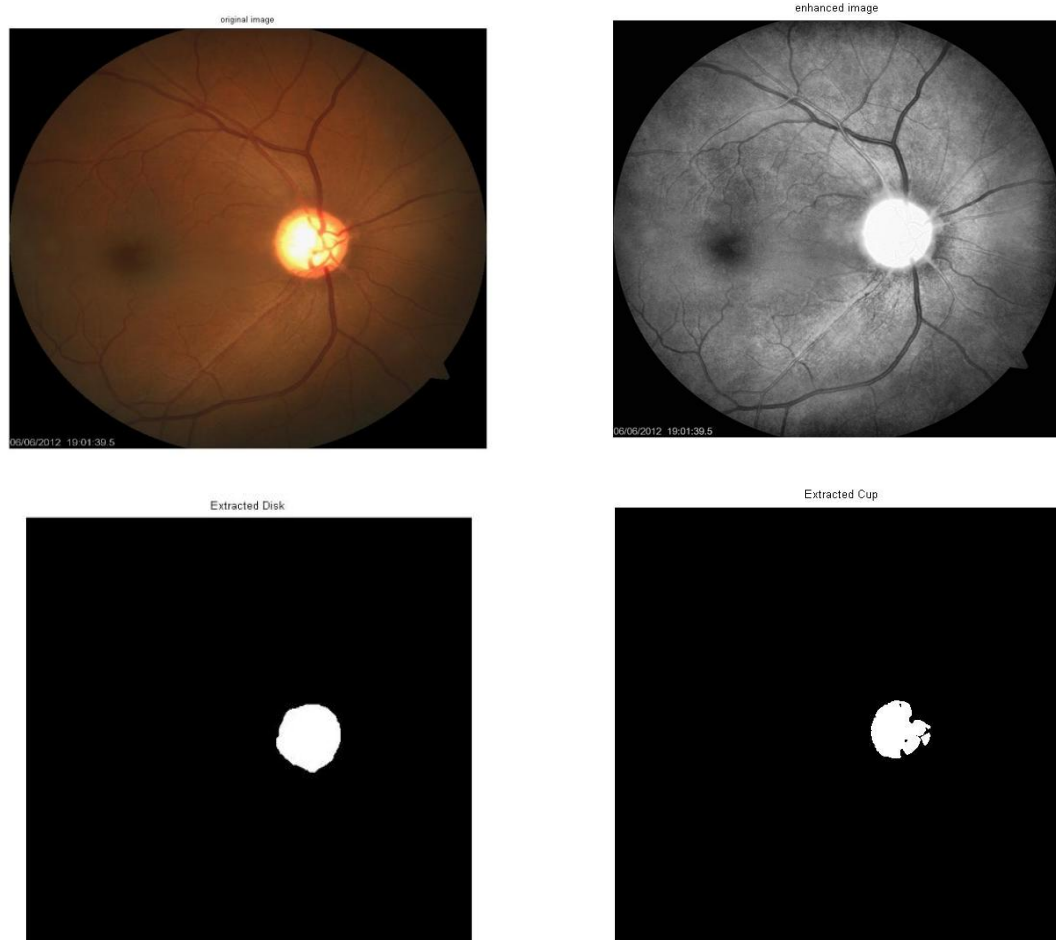
After obtaining the disc and cup, various features can be computed. We follow the clinical convention to compute the CDR. As mentioned in the introduction, CDR is an important indicator for glaucoma screening computed as

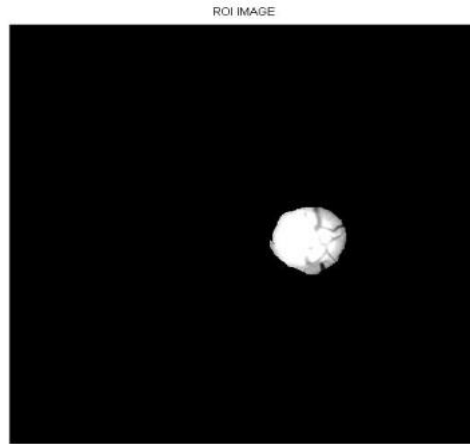
$$\text{CDR} = \text{Area of Cup} / \text{Area of Disc}$$

The computed CDR is used for glaucoma screening. When CDR is greater than a threshold, it is glaucomatous, otherwise it will be considered as a healthy one.

V. EXPERIMENTAL RESULT

Our experiments uses 2326 images from 2326 different subject eyes including 650 from the Singapore Malay Eye study (SiMES) and 1676 from Singapore Chinese Eye Study (SCES). We evaluate the proposed disc segmentation and cup segmentation method using the manual boundary as “ground truth” Among the 2326 eyes, 168 SiMES and 46 SCES eyes are diagnosed as glaucomatous by ophthalmologists.





VI. CONCLUSIONS

In this paper, I present superpixel classification based methods for disc and cup segmentation for glaucoma screening. It has been demonstrated that CSS is beneficial for both disc and cup segmentation. In disc segmentation, HIST and CSS complement each other as CSS responds to blobs and provides better differentiation between PPA and discs compared with histograms. Reliability score is an important indicator of the automated results. I have demonstrated that, by replacing circular Hough transform based initialization with the proposed one for active shape model, I am able to improve the disc segmentation. In future work, multiple kernel learning [65] will be used for enhancement. The accuracy of the proposed method is much better than the airpuff IOP measurement and previous CDR based methods.

REFERENCES

- [1] H. A. Quigley and A. T. Broman, "The number of people with glaucoma worldwide in 2010 and 2020," *Br. J. Ophthalmol.*, vol.90(3), pp. 262–267, 2006.
- [2] R. Bock, J. Meier, G. Michelson, L. G. Nyl, and J. Honegger, "Classifying glaucoma with image-based features from fundus photographs," *Proc. of DAGM*, pp. 355–364, 2007.
- [3] A. Aquino, M. Gegundez-Arias, and D. Marin, "Detecting the optic disc boundary in digital fundus images using morphological, edge detection, and feature extraction techniques," *IEEE Trans. Med. Imag.*, vol. 29, pp. 1860–1869, 2010.
- [4] Z. Hu, M. D. Abramoff, Y. H. Kwon, K. Lee, and M. K. Garvin, "Automated segmentation of neural canal opening and optic cup in 3-d spectral optical coherence tomography volumes of the optic nerve head," *Inv Ophthalmol Vis Sci.*, vol. 51, pp. 5708–5717, 2010.
- [5] J. Meier, R. Bock, G. Michelson, L. G. Nyl, and J. Honegger, "Effects of preprocessing eye fundus images on appearance based glaucoma classification," *Proc. CAIP*, pp. 165–172, 2007.
- [6] A. Hoover and M. Goldbaum, "Locating the optic nerve in a retinal image using the fuzzy convergence of the blood vessels," *IEEE Med. Imag.*, vol. 22, pp. 951–958, 2003.
- [7] M. Foracchia, E. Grisan, and A. Ruggeri, "Detection of optic disc in retinal images by means of a geometrical model of vessel structure," *IEEE Trans. Med. Imag.*, vol. 23, no. 10, pp. 1189–1195, 2004.
- [8] R. Achanta, A. Shaji, K. Smith, A. Lucchi, P. Fua, and S. Susstrunk, "Slic superpixels compared to state-of-the-art superpixel methods," *IEEE Trans. Pattern Anal. and Mach. Intell.*, vol. 34, pp. 2274–2281, 2012.
- [9] J. Cheng, J. Liu, D. W. K. Wong, F. Yin, C. Cheung, M. Baskaran, T. Aung, and T. Y. Wong, "Automatic optic disc segmentation with peripapillary atrophy elimination," *Int. Conf. of IEEE Eng. in Med. And Bio. Soc.*, pp. 6624–6627, 2011.

Model of Quantum Computing in the Cloud: The Relativistic Vision Applied in Corporate Networks

Chau Sen Shia¹ Mario Mollo Neto² Oduvaldo Vendrametto³

¹Doctor, Production Engineering, Postgraduate Department of Production Engineering, University Paulista UNIP. São Paulo, SP – Brazil

²Doctor, Production Engineering, Postgraduate Department of Production Engineering, University Paulista UNIP. São Paulo, SP – Brazil,

³Doctor, Production Engineering, Postgraduate Department of Production Engineering, University Paulista UNIP. São Paulo, SP – Brazil,

ABSTRACT

Cloud computing has is one of the subjects of interest to information technology professionals and to organizations when the subject covers financial economics and return on investment for companies. This work aims to present as a contribution proposing a model of quantum computing in the cloud using the relativistic physics concepts and foundations of quantum mechanics to propose a new vision in the use of virtualization environment in corporate networks. The model was based on simulation and testing of connection with providers in virtualization environments with Datacenters and implementing the basics of relativity and quantum mechanics in communication with networks of companies, to establish alliances and resource sharing between the organizations. The data were collected and then were performed calculations that demonstrate and identify connections and integrations that establish relations of cloud computing with the relativistic vision, in such a way that complement the approaches of physics and computing with the theories of the magnetic field and the propagation of light. The research is characterized as exploratory, because searches check physical connections with cloud computing, the network of companies and the adhesion of the proposed model. Were presented the relationship between the proposal and the practical application that makes it possible to describe the results of the main features, demonstrating the relativistic model integration with new technologies of virtualization of Datacenters, and optimize the resource with the propagation of light, electromagnetic waves, simultaneity, length contraction and time dilation.

Key-words: Virtualization, Datacenters, Relativity, Quantum Mechanics, Corporate Networks.

I. INTRODUCTION

To offer companies the opportunity to dissociate their information technology needs and of your cloud computing infrastructure is able to offer, in the long run, savings companies, included the reduction of infrastructure costs and payment models based on the use of services (2009 ISACA). The low cost of cloud computing and its ability to dynamically resource expansion make it boost innovation for small business in development (VAJPAYEE, 2011). According to Fusco and Sacomano (2009), the network of companies and the importance of communications in environments of computer networks have been important in the world of modern business and social networks, because the reality is increasingly volatile and dynamic has brought the need to speed up processes, business and organizations, therefore internationalize should be the presence of competitive thinking and strategic alignment of that reality. According to Tonini, oak and Spinola (2009), for competitive advantage, companies must continually update themselves on technology; get maturity in processes and eliminating operational inefficiencies. This requires an involvement of people, processes and the Organization as a whole.

Currently the companies are organizing network format, and business processes among the organizations increasingly use the applications that process and provide information for the operation of this new arrangement. The new organization is a combination of various organizations, composed of interconnected cells with several access points provided by the infrastructure of information technology (IT), while the central element of processing and storage of information and data in the cloud is the *Datacenter* (VERAS, 2009).

The present work aims to establish a model of integration in networks of alliances with companies applying the theories of physics and cloud computing virtualization to understand the basics of relativity and its application in the communication between companies as strategic business processes and relationships between organizations. The proposal introduces a relativistic and quantum model using the fundamentals of physics. In this context there is the possibility of alliances and resource sharing, to enter into multilateral agreements, involving organizational relationships, interpersonal and inter-organizational.

II. THEORETICAL FRAMEWORK

This section describes the main aspects and justifications for the construction of the system proposed in this paper and are related to: cloud computing, theory of relativity, alliances and corporate networks, propagation of light, optics, time dilation, length contraction, electromagnetic waves, field and magnetic forces, quantum mechanics and virtualization.

2.1. Service design principles

A design paradigm, in the context of business automation is considered the approach that governs the design of logic, which consists of set of rules (or principles) complementary that define collectively the broad approach represented by paradigm. The fundamental unit of service-oriented logic is the "service" and in itself represents a distinct design paradigm. Each service gets its own distinct functional context and has a set of capabilities related to this context via public service contract (ERL, 2009).

In this context, the practice and the fundamentals of service contracts allow for greater interoperability, alignment of business and technology domain, greater organizational agility, greater diversification of suppliers, lower workload, low service coupling, service abstraction, and reuse of service and reduced amount of application-specific logic.

2.2. Alliances and networks of enterprises

The role of the Alliance will make the difference in getting the results of the companies involved in the business. Thus it is important to create solid alliances, but well developed, sufficiently flexible to include changes, as the market environment and corporate objectives change and the relationship evolve. The rings can be threatened only if the expected benefits of the relationship growing ever smaller, or if the behavior of any of the parties is deemed to be opportunistic, (FUSCO and SACOMANO, 2009). In this context, the relationship and the types of relationships should establish the density, the centralization and fragmentation of the network, establishing measures of position of the actors in the network. A network can be coordinated by applying the concepts of network centralization.

A central actor joining several other actors who are not connected with other groups, this central actor then plays the role of coordinating and controlling other actors. This actor can add to the actors don't low density plants offering guidance to perform certain task. In this way the density and centralization indicate how the network (as a whole) is structured. Already fragmentations are disconnected subnets where the actors don't relate to other groups of actors. A high fragmentation means that there exists a strong cohesion, but locally the actors may be strongly cohesive (LAZZARINI, 2008).

2.3. Integration of relativistic model in enterprise networks

Computer networking computing is a set of virtual resources and accessibility of user-friendly *hardware* (physical), *software* (logical), and services development platform. Its resources can be configured easily to fit a workload (*Workload*) variable, allowing the optimization of the use of resources and replace it assets. These features and services are developed using new virtualization technologies, which are: application architectures and service-oriented infrastructure and technologies based on the internet as a means to reduce the resource usage costs of hardware and software you used for processing, storage and networking (ERL, 2009).

2.4. Fundamentals of physics

Physical descriptions of the chapters are based on the fundamentals of light, optics, relativity, electromagnetic waves, quantum mechanics, quantum physics and quantum computing, according to the authors Young and Freedman (2009), Knight, Randall (2009), Ernesto F. Galvão (2007), Herbert a. Pohl (1971) and Michael a. Nielsen and Isaac I. Chuang (2005).

2.4.1. Propagation of light and optics

The first evidence of the wave properties of light occurred around 1665. Only in 1873, James Clerk Maxwell predicted the existence of electromagnetic wave and calculated the speed of its spread, however the

work carried out by Heinrich Hertz (1887) showed that the light is actually an electromagnetic wave. However the wave nature of light to be understood should be linked to the emission and absorption of light so that it is revealed the corpuscular nature of that light. In addition, the energy carried by the light wave is concentrated in discrete packets known as photons or quanta. For the description of the propagation of light using the wave model, but your explanation is accomplished through the issuance and absorption of light (YOUNG and FREEDMAN, 2009).

Electromagnetic sources are accelerated electric charges, thus all bodies emit electromagnetic radiation known as thermal radiation, so any form of matter hot is a light source. The light can also be produced by electrical discharges in ionized gases, therefore light source uses the phosphor material to convert ultraviolet radiation of a mercury arc into visible light. In any light source these electromagnetic waves propagate in a vacuum to the speed of light ($c = 2,99792458 \times 10^8$ m/s) (YOUNG and FREEDMAN, 2009).

The wave properties of light can be dealt with through the wave optics. In this way are used models of rays of light to study the propagation of light in reflection and refraction. A wave of light when it reaches a smooth surface (split between two transparent media) frequently this wave is partially reflected and refracted. The refractive index of a material ($n = c/v$) plays a key role in geometrical optics and its propagation is slower through a material than in a vacuum. The letter "c" corresponds to the speed of light in vacuum, while "v" is the speed of light in the material. Therefore the propagation of light through any material has the value of "n" always greater than 1 and in vacuum your value is equal to 1 (YOUNG and FREEDMAN, 2009).

The direction of (A) ray of light varies when it passes from one material to another with different refractive index. Already in relation to frequency "f" (wave characteristics of light) the wave does not vary when this is just a material for another. Figure 1 shows the effects of rays of light.

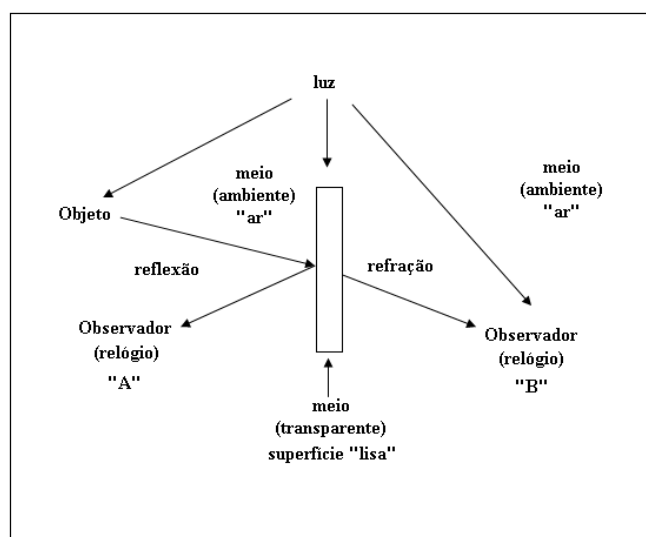


Figure 1-Propagation of light and optics, author.

Figure 1 represents a model that describes the wave properties of light. The main components are the objects, the air, the observers, the light spreads (reflection and refraction) and the light. According to Oliveira (2005), to focus on a surface separating two media with different refractive index, a beam of light is partially reflected and partially refracted. Faced with a smooth surface and a half transparent both the observer and observer B can view the object at the same time when this object receives the light, because according to Einstein's theory of relativity there is not a universal reference system. Considers that the physical phenomena (in same conditions), are identical in all inertial reference systems.

2.4.2. Relativity and light

At the beginning of this century, two theoretical systems that profoundly altered the foundations of classical physics were the theory of quanta, developed by Max Planck (1857-1947) and the history of relativity of Albert Einstein (1879-1955), because these theories together, interpret the universe from the microcosm to the macrocosm of the atom intergalactic spaces (RAMALHO, IVAN, NICHOLAS and TOLEDO, 1976).

Second Ramalho, Ivan, Nicholas and Toledo (1976), aspects and the notion of relativity were proposed by Galileo and Newton in their times ("the physical phenomena are relative to reference systems"). Space and time appear to be simple concepts as it is possible to measure distances by means of a ruler or a train. With a timer it is possible to record the time of occurrence of events. Einstein's theory already altered our understanding of some fundamental concepts of physics. Has real consequences for modern technology and understanding of the universe we live in (KNIGHT, 2009).

Einstein's theory of relativity the consequence there is a universal reference system. In their postulate of the theory of special relativity relates that "the laws of physics are identical in reference systems, in rectilinear motion and uniform, some in relation to others". This postulate is of the opinion that the physical phenomena (in same conditions), are identical in all inertial reference systems, because there is no universal reference system. Therefore we do not know of the existence of any experience able to determine if a system is at rest or uniform rectilinear and moves against an arbitrary reference inertial system (RAMALHO, IVAN, NICHOLAS and TOLEDO, 1976). To Einstein: a) the speed of light is a universal constant, b) is the same in all inertial reference systems, c) in a vacuum does not depend on the motion of the light source and has equal value in all directions.

As Young and Freedman (2009), the theory of relativity has introduced significant changes, since it states that the laws of physics should be the same in any inertial reference system. Since the speed of light in vacuum should always be the same in any system of reference. The main consequences of these statements are:

- [1] An event that occurs simultaneously to another relative to an observer may not occur simultaneously in relation to another observer.
- [2] When there is relative motion between two observers and they effect measures of time and distance intervals, the results obtained may agree.
- [3] So that the law of conservation of energy and the law of conservation of linear momentum are valid in any inertial reference system, Newton's second law and the equations for the kinetic energy and momentum must be reworded.

It is known that the Faraday induction law is compatible with the principle of relativity, because all the laws of electromagnetism are the same in all inertial reference systems. Another important fact that must be cited is also the prediction of propagation velocity of electromagnetic waves in a vacuum, which were deduced from the Maxwell equations stating that light and all electromagnetic waves travel in a vacuum with a constant speed of 299,792,458 m/s ($c = 3.0 \times 10^8$ m/s) which is the speed of light. According to Einstein's postulate, the speed of light in vacuum is always the same in any inertial reference system and does not depend on the speed of the source (YOUNG and FREEDMAN, 2009). According to Einstein's postulate, the movement of the light after that abandons the font cannot depend on the motion of the source, because an inertial observer cannot move with the speed of light.

On the relativity of simultaneity, it is known that the measure of the time and a time interval involves the concept of simultaneity. Concurrency is not an absolute concept, because if two events occur simultaneously or not, that depends on the reference system. Concurrency plays an important role in the measurement of time intervals. Thus we conclude that intervals of time between two events may be different in different reference systems, can also time dilation occurs. The distance between two points also depends on the reference system (not just the time interval between two events) and where is the observer. Can occur what we call length contraction, the relative velocity does not suffer contraction. There is no length contraction when two rules are arranged in directions perpendicular to the direction of relative velocity (YOUNG and FREEDMAN, 2009). The fundamental principal of relativity is named event. An event is an occurrence in a physical space set point and in a second set of time. Events can be observed and measured by observers who use different benchmarks, because an event is what actually happens. Concurrency is determined already inquiring when the event actually occurred, and not when it was seen or observed (KNIGHT, 2009).

According to the principle of relativity, all laws of physics are the same in any inertial frame of reference. All observers not matter how each move in relation to the other, realize that all the light waves (regardless of its sources) spread in relation to their respective benchmarks with the same speed of light ($c = 3 \times 10^8$ m/s). Any experiment conducted to compare the value of the speed of light in relation to different benchmarks reveals that propagates with the same speed of light in any inertial frame, is independent of how the frames move towards others (KNIGHT, 2009).

The special theory of relativity of Einstein (1905) is based on two assumptions: there is a reference to determine whether a body is in absolutely rest and the speed of light is independent of the speed of its source. This theory of special relativity Einstein invented the theory of general relativity, which describes gravity as geometrical property of space and time (GAZINELLI, 2013).

According to Knight (2009), Einstein's theory of relativity forced a review of the concepts of space and time, because the experiments revealed that the classical distinction between particles and waves there at atomic level. Already, it is known that light behaves as a particle, while the electrons (or entire atoms) behave as waves. While in theory of quantum physics (early 1920) Atomic particles are described as wave function.

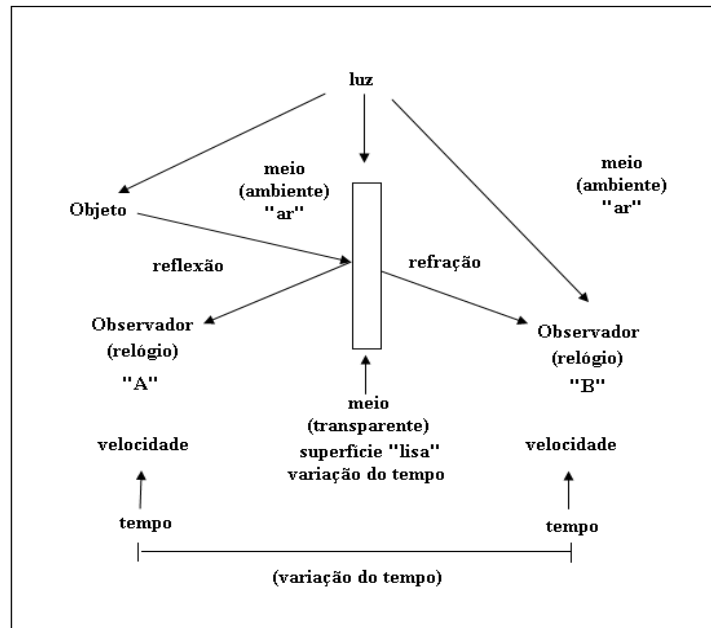


Figure 2-Relativity of simultaneity and time, author.

Figure 2 shows the light on the object according to the vision of observers A and B (standing) at the same time the incidence of light on a transparent medium. Time variation is established in relation to the observers, the reflection and refraction of light on the object and the trajectory of the light in relation to the smooth surface. It is observed that the light cannot depend on the motion of the source, because an inertial observer cannot move with the speed of light, the principle of relativity of simultaneity.

2.4.2.1. Time dilation and length contraction

The length $L = x_2 - x_1$ bar, measured in the frame R, is less than the length $L' = x'_2 - x'_1$ the same bar, measured in the frame R', excited about μ speed R, is called length contraction (RAMALHO, IVAN, NICHOLAS and TOLEDO, 1976).

The principle of relativity leads to the conclusion that the time is not the same for the two reference frames that move one to the other. A temporal dilation can be defined as $\Delta t = \Delta \tau / \sqrt{1 - \beta^2} \geq \tau$. the main aspect of relativity is that all are equally valid and inertial everything we know about the referential is as they move towards others (KNIGHT, 2009). The concept of time dilation is used whenever they are compared the intervals between events compared to observers in different inertial reference systems. For a non-inertial reference system with high speed time is longer compared to inertial reference time is shorter (YOUNG and FREEDMAN, 2009).

In addition to the time interval, the distance between two events depends also on the reference system, where the observer is (also involves the concept of simultaneity). The length measured in the reference system in which the body is at rest is the length itself, already the length measured in any other reference system that moves is the length contraction (YOUNG and FREEDMAN, 2009). Shortening the distance between two objects, as measured by an observer moving relative to the objects is called the spatial contraction. The length of the object is maxim with respect to the reference in that the object is at rest. The length of the object is smaller when measured relative to any frame in which the object is in motion (KNIGHT, 2009)..

2.4.3. Electromagnetic waves

Maxwell and Hertz and other established that light is an electromagnetic wave, interference, diffraction and polarization provide evidence of the wave nature of light. When observed closely the emission, absorption and scattering of electromagnetic radiation have completely different aspects of light, because the energy of a quantized electromagnetic wave. The light is emitted and absorbed in packets with defined energies, known as photons or quanta, and the energy of a single photon is proportional to the frequency of the radiation. The energy of an atom is also quantized, because its internal power cannot assume any value, only some values of energy known as energy levels (YOUNG and FREEDMAN, 2009). According to Pohl (1971), the unit of energy quanta was the first to introduce the concept of a quantum of energy, because it found that the energy was transferred into units or packages (called quanta) that became more evident by the photoelectric effect, played by Einstein.

Electromagnetic waves arise as a result of two effects: a variable magnetic field produces an electric field and a variable electric field produces a magnetic field. In this way these two fields constantly add in its spread through space. As Maxwell, if at a point P is produced a variable electric field \vec{E} so will induce a magnetic field variable \vec{B} with time and with distance from point P. Furthermore, the vector \vec{B} will induce a variable vector \vec{E} , which also varies with time and with distance from the variable magnetic field. This reciprocal induction magnetic and electrical fields, variables with the time and distance, it becomes possible to spread this induction sequence through space. Therefore, an electrical disturbance in the point P, due to oscillation of electrical charges, these travel to distant points through the mutual formation of electrical and magnetic fields variables (RAMALHO, IVAN, NICHOLAS and TOLEDO, 1976). The demonstration of the speed of propagation of an electromagnetic wave in vacuum, according to Maxwell is equal to the speed of light in vacuum (where $v = 3 \times 10^8$ m/s), where v is the speed of propagation of an electromagnetic wave in vacuum.

On the airwaves, it is known that in frequency between 10^4 to 10^7 Hz, are very well reflected by the ionized layers of the upper atmosphere (known as the ionosphere). This reflection allows radio waves to be detected at large distances from the network, because it has a wavelength of tens to thousands of meters and useful for transmission of information. These waves can be transmitted from one continent to another by means of artificial satellites (RAMALHO, IVAN, NICHOLAS and TOLEDO, 1976).

2.4.4. Field and magnetic forces

The classical physics was formed for mechanics, electromagnetism and thermodynamics. The phenomena of electricity and magnetism were studied experimentally and its fundamental laws were discovered. Later, James Clark Maxwell, Hans Christian Oersted and Michael Faraday, were able to gather in a single theory the phenomena of electricity, introducing the concept of electromagnetic field. The magnetic field continuously occupies a region of space that is characterized by two vector quantities (electric and magnetic fields). The speed of propagation of electromagnetic waves in vacuum is identical to the speed of light and it is concluded that the light is a kind of electromagnetic wave. They thus unify into a single optical phenomena and theory of electromagnetism. Then the thermodynamics completes the picture of classical physics, because it deals with the concepts of energy, temperature and heat. The theory of unification continued with Maxwell's electromagnetic theory, which united electrical, magnetic and optical phenomena (GAZZINELLI, 2013).

As Young and Freedman (2004), a magnetic interaction can be described as: a) a live load or an electric current creates a magnetic field in their neighborhoods (in addition to the electric field), b) the magnetic field exerts a force about any other current or load that moves within the field. The magnetic field is a vector field associated with each point in space.

Magnetic forces only act on moving charges and it turns out that the electrical and magnetic interactions are related. However the magnetic force depends on the speed of the particle, unlike electric force which is always the same is independent of charge be at rest or in motion. An electric charge in motion does not suffer from magnetic forces action, but creates a magnetic field when you're on the move, already the symmetry properties of the magnetic field can be related to ampere's law. That same electric field can also vary with time (known as displacement current) to produce a magnetic field (YOUNG and FREEDMAN, 2004).

Regarding the photo-electric effect it is known that an electromagnetic radiation, focuses on a surface of a metal, electrons can be expelled this surface and this phenomenon (discovered by Hertz in 1887), is called Photo-electric effect, which was explained later by Einstein in 1905. Einstein proposed that the photo-electric effect, one photon of radiation incident, when a metal is completely absorbed by a single electron, yielding your energy instantly, so the electron of metal with an additional power. Einstein suggests, so that the light is composed of photons and that this can be absorbed by the metal just one at a time, and there is no fractions of a photon. For Einstein "the energy of the electron must increase with the frequency and has nothing to do with the intensity of the radiation. However the energy received by an electron, by absorbing a photon is always the same (RAMALHO, IVAN, NICHOLAS and TOLEDO 1976).

2.4.5. Quantum mechanics

The quantum nature of light is used to explain properly the photo-electric effect is in contradiction with the wave nature of light, however allows you to justify the interference and diffraction phenomena of light. Despite that the two theories are completely different are also needed to explain a single physical phenomenon. To reconcile these facts was presented the "dual" nature of light, where in certain phenomena the light behaves as a wave nature and in other, particle nature. The same beams of light can deflator around an obstacle and focus on the surface of the metal, causing the photo-electron emission. To Louis De Broglie (1924), if the light has dual nature, also a particle could behave similarly, and then relates the wave characteristic with particle size. With it your chance other physicists have developed quantum mechanics who favored the exact description of

Atomic phenomena, because it changed the way of looking at nature in terms of probability terms and not in terms of certainty (RAMALHO, IVAN, NICHOLAS and TOLEDO, 1976).

As Max Planck (1900), an electron oscillating with frequency "f", emit (or absorb) an electromagnetic wave of the same frequency, but energy is not emitted (or absorbed) continuously, and in discontinuous servings (particles that carry each a number of well-defined energy) called photons. The energy of each photon is called a quantum or quanta (in the plural). An oscillating electron cannot absorb (or issue) energy continuously (or an electron absorbs (or send) a quantum or anything).

In 1982 Richard Feynman published a work in which he argued the simulation of particles that behave according to quantum mechanics. He had observed that even simple problems of quantum physics seem to require an immense number of computational steps in its resolution seemed to be in the category of intractable problems. For him the quantum properties of the simpler system would help in more complex systems simulation, thus a quantum computer could be more efficient than a usual computer, the question is: "what kind of problem could be solved more quickly in a quantum computer than a classical computer?" (GALVÃO, 2007).

Today we know that the main problems that can be solved by quantum computers are the simulation of quantum systems proposed by Feynman (simulation of new devices and materials), factoring and search in a database. In 1984, Charles Bennett and Gilles Brassard developed the first absolute security protocol, which involves the exchange of quantum particles of light (photons), assuming only the quantum mechanics is an accurate description of nature. One of the main advantages has its origins in the phenomena of superposition and entanglement (GALVÃO, 2007).

2.5. Integration of relativistic computing and virtualization

The choice of measurement of properties chosen for the actors are "subject" that have two possible values (business or social) and "duration" which also have only two values (long and short). So, measuring these properties can determine the existing correlations of these results. The application of quantum mechanics, establish the superposition States of the objects (actors) and their behaviors (some aspects) as if they were in multiple positions at the same time, because in this state it is possible to be manipulated and measured. When measuring the properties "subject" and "duration" of the companies involved after the connection, it is possible to obtain by analogy the importance and the possible values that will determine the correlations of these properties.

With the application of relativity of simultaneity seeks to establish a measurement and time interval in the interaction between the actors of a company network in relation to systems of references and events. Through the theory of relativity applies the concept of space and time of cloud computing (virtualization), in addition to the exchange of services between the actors of a communication network with the use of the internet. The fundamentals applied in the construction of the proposed model will serve as the basis for the construction of the graphical interface of the classic model (space, time, speed) Newtonian and relativistic model (space, time, speed) of Einstein. Already the foundations of physics, structure the foundations for the construction of quantum computation.

III. METHODOLOGY AND MATERIALS

This research work is classified as applied, are proposing a model based on data collection and aims to generate possible knowledge of practical application to resolve specific problems of connection between corporate networks and cloud computing virtualization.

As for the approach, this research is quantitative, as it seeks to explain through quantifiable data, show relationships of phenomena observed with proof (or not) of the hypothesis established, delineated on the collection of data to prove systematically confirmation (or not) of this hypothesis. This work is an exploratory research, because of the importance of this study, aims to enhance the application of network model in companies with cloud computing virtualization, using the fundamentals of Physics in a relativistic view.

The surveys conducted have provided a better understanding of the matter proposed in this work and offered a clearer vision of the problem and of ideas. The research also involved bibliographic survey, interviews with other teachers in the areas of physics and computer science who had practical experience problems searched for a greater understanding and dimension of this study. In this context it was possible to better clarify about the subject, to then propose the model proposed. Technical procedures were already structured in: characterization of the study, data collection, data analysis, application of physics, simulation of the values and presentation (charts and graphs). We used the concepts of physics laws of reflection and refraction, reflection and the Huygens principle, interference of light, diffraction, wave-particle duality, electromagnetic phenomena, Galileo and Einstein relativity, simultaneity, time dilation, spatial contraction, mechanics and quantum physics. In addition, were supplemented with the fundamentals of corporate networks and cloud computing.

To obtain the data collected was used in a sample table with the following structure: date, time, machine, OS, connection time, processing speed, RAM, period, wavelength, connection speed, distance and frequency. Through this infrastructure was able to access and perform measurements of the environment offered by internet and cloud computing virtualization for verification of connections in distributed environment and cloud computing virtualization. Then were formulated mathematical and physical expressions, generated from the data entries which resulted in the data presented in tables and charts. It was elaborated the relativistic model architecture of network of companies and of application of virtualization of computers based on the frequency of wave. As a constraint to the model presented adopted the magnetic wave velocity (speed of light), as a means of propagation for the connection between the actors of a network of companies in virtualization of *Datacenters*.

3.1. Scope of the experimental work

Models will be developed on the basis of the results generated by connections of computers in internet networks and cloud computing virtualization to deepen the knowledge and behavior of the virtual machines. Will be monitored and compared with the basics presented by Relativistic Physics. Then mathematical arguments will be constructed to validate the applications of Physics in computer network environment, using the registered virtual stopwatch. For the study and analysis of the results presented will use as a basis the mechanics and quantum physics for the deepening of quality of information. Through simulations and tests will be established the limits of Royal connections and relativist and show the results achieved and also the differences established by connections registered by machines available (beginning of tunneling between the network nodes).

3.2. Project Architecture

The relativity is space and time. The difficulty is that some aspects of relativity seem to be incompatible with the laws of electromagnetism, especially the laws that govern the propagation of light waves. Special relativity Einstein involves spatial contraction and time dilation (KNIGHT, 2009). Based on these strong foundations established the structure of architecture and the proposal of this work.

As Knight (2009) it is known that no object has a "true" speed, because its speed towards someone is moving or stopped. The most that is possible is the specification of the speed of an object relative to a coordinate system. However the definition of reference can be based on: the referential) extends infinitely in all directions, b) are observers at rest relative to its benchmark, c) the number of observers and the amount of equipment used is enough to measure the positions and the velocities with any level of accuracy established.

In the proposed architecture in this work, it is considered that all components (objects) belong to a single inertial frame, where all observers are at rest, in relation to the other and belong to the same benchmark.

The principle of Galilean relativity "the laws of mechanics are the same in all inertial reference frames". To the principles of relativity, all laws of physics are the same in any inertial frame (all results of the theory of relativity based on this postulate). And whereas Maxwell's equations of electromagnetism which are laws of physics, they are also true in any inertial frame and predict that electromagnetic waves (including light) propagate with the speed $c = 3.00 \times 10^8$ m/s, so the light propagates with the speed "c" in all inertial reference frames (KNIGHT, 2009).

According to the experiments performed in the laboratory to compare the value of the speed of light in relation to different benchmarks, reveal that light propagates with 3.00×10^8 m/s for any inertial, regardless of how the frames move towards others (KNIGHT, 2009). In this way the architecture (proposed), considers how inertial frame the principle of relativity to the components: actors, *Datacenters* and quantum computations.

For the fundamental entity of relativity physics is the event (occurrence physics in a point set space and in a second set of time), which can be observed and measured by observers who use different benchmarks. It is also possible to quantify where and when an event occurs using coordinates (x, y, z) and the instant of time "t" which are known as space-time coordinates of the event, because an event is what actually happens. However when two events occur in different positions, but at the same time measured in some benchmark are known as simultaneous. Concurrency is determined inquiring when the event actually occurred, and not when it was seen or observed (KNIGHT, 2009). The observation of events of architecture proposal on simultaneity between the components (objects) located in layers (A), (B) and (C) because "t" is the second time in the event (communication) actually occurs between the components (objects) of architecture (considering the fact that light propagates the 300×10^8 m/s events occur simultaneously).

Physical studies reveal that the light travels equal distances in equal time intervals, because the light propagates at a speed "c" in relation to all the references independent of the motion of objects. According to the theory of relativity "two events that occur simultaneously in a referential S are not simultaneous in another frame S' in relative motion to S" (known as relativity of simultaneity). Therefore the proposed architecture is based on the propagation of light in all reference frames and all components (objects) represented by the layers

(A), (B) and (C), in addition, it is considered just a benchmark as qualitative measurement. As Knight (2009), the principle of relativity concludes that the time is not the same for the two reference frames that move a in relation to the other, since the space is different from moving a referential in relation to another.

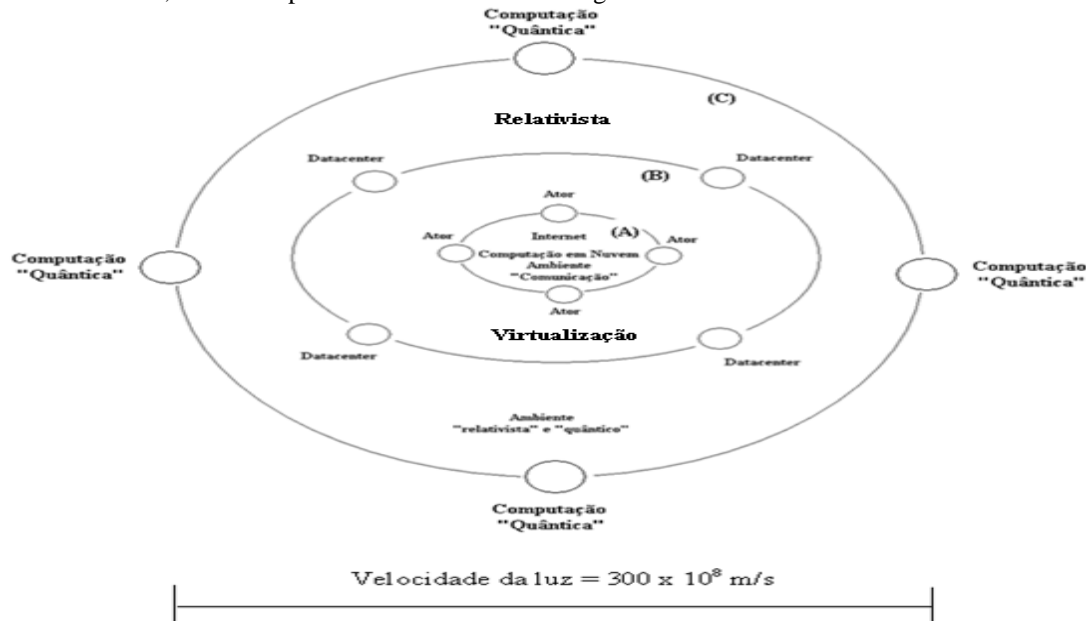


Figure3-relativistic model architecture business networks, author.

Figure 3 above shows how inertial reference the light for the connection between the components (objects) arranged in layers A, B and c. in the layer are the major features of the internet, cloud computing and communication protocols. B layer the components and features of virtualization provided by *Datacenters*, already in the C layer quantum computing resources (a new technology necessary for the application of the relativistic model).

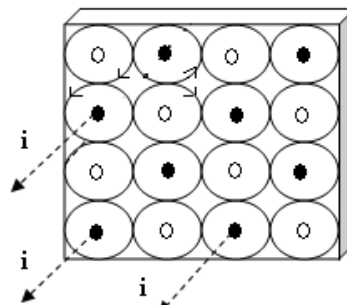


Figure 4 – array of circular motion of magnetic field and electric current, author.

Figure 4 above represents an array where the coils are located where they are traversed chains or not, in each one of these coils to generate electromagnetic fields. In addition, it also shows the meanings of the fields (clockwise or anti-clockwise) when currents are applied in their coils. When circulating current in a coil electromagnetic fields of their neighborhoods may be clockwise or counter-clockwise, because it depends on the intensity of the current that runs through each of their specific coils. The result of these movements are the records that identify the frequencies waves, which quantifies its corresponding value (can be considered the principle of quantum memory) of stored information and also possible to be recovered (through the specific frequencies).

The superposition is a technical term that describes one of the main features of microscopic objects that follow the rules of quantum mechanics. The quantum superposition is the possibility of a quantum object takes a peculiar combination of properties that would be mutually exclusive in accordance with our intuition. Quantum mechanics allows making predictions in terms of probabilities which can be described through the probability amplitudes. Can be manipulated and measured which usually alter the probability amplitudes associated with each position, because it depends on the probability amplitudes immediately before the measurement (GALVÃO, 2007).

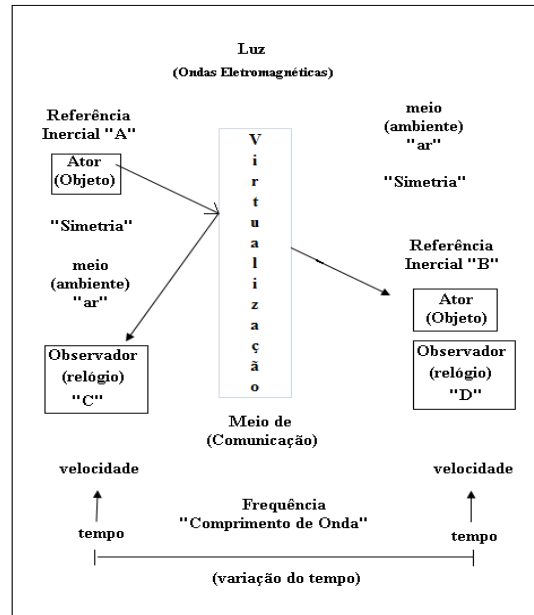


Figure 5 – relativistic Model and application of virtualization to cloud computing, author.

Based on the foundations of quantum mechanics in Figure 5 above, shows the superposition of the propagation speed of the media in relation to speed and time and the application of the frequency and wavelength. The transmission of the communication established between companies can be measured through its properties. Such properties can be the "subject" (social or business) or the "duration" (short or long) in the exchange of information between them, thus characterized the superposition that occurs on virtualization offered by quantum computation. Under these conditions the relativistic space and time are applied to connection speed or tunneling in relation to the speed of light.

One of the key concepts in relativity is the concurrency, and is associated with the relativity of time (OLIVEIRA, 2005). An exchange of information between the actor (or company) "A" frame with the frame "C" Observer are simultaneous events when they occur at the same time. For a connection speed with very high speeds (according to Einstein's theory of relativity) time under these conditions can dilate (known as time dilation), your route will be larger and thus the observer "C" will take longer to receive the connection and the information sent. The actor already inertial reference "D" will receive the connection before both of which (A and D Company) are running within the virtualization environment.

Light is an electromagnetic wave and its energy transported by the light wave is concentrated in discrete packets known as photons or quanta. Aspects of health and corpuscular of light apparently contradictory are explained were reconciled with the development of quantum electrodynamics (YOUNG and FREEDMAN, 2009). As Galvão (2009), distant quantum particles seem to be communicating, so that the measures of its properties are correlated. Figure 6 shows the correlation between the actors (or businesses) on a communication, exchange of information or services. These correlations are the measurements of the properties of the actors (or companies) that are: "subject" who own the business or social values and "duration" that have the values, long or short. These measures allow to quantify the correlations that exist between companies, which are monitored by the layer of cloud computing and virtualization are also represented by tables 1 and 6 figures below. The light has an undulating phenomenon (according to Maxwell electrodynamics) for this reason will always be an electromagnetic wave in any inertial frame (travel with the same speed of light, $c = 3 \times 10^8$ m/s), thus it can be concluded that the speed of propagation of the communication and exchange of messages between the companies has the same value in all inertial systems (maintains the integrity the sending and receiving such information) provided that use light waves on the connection between companies (principle of implementation of quantum computation).

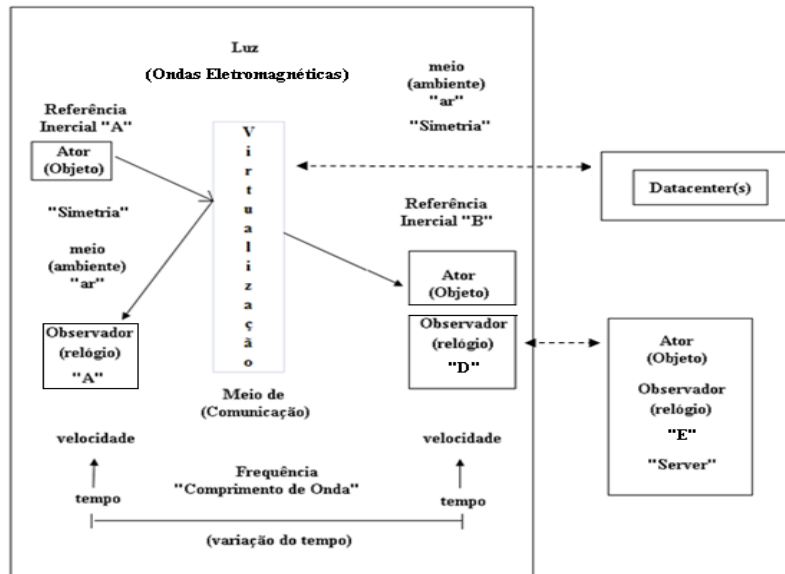


Figure 6 – Relativistic Model and the application of the wave frequency and virtualization in cloud computing, author.

Figure 6 shows the behavior of light and its undulating phenomenon (according to electrodynamics of Maxwell), for this reason will always be an electromagnetic wave in any inertial frame (travel with the same speed of light, $c = 3 \times 10^8$ m/s), thus it can be concluded that the speed of propagation of the communication and exchange of messages between the companies has the same value in all inertial systems (maintains the integrity and shipping receipt of this information), since that uses light waves on the connection between companies (principle of implementation of quantum computation). Established (first) the connection (using electromagnetic connections), to carry out the exchange of information, so the data can be packaged and transmitted by electromagnetic field (using the C layer of architecture proposal).

3.3. Details of the components

Will be developed an infrastructure model to test, simulating the connections with the virtualization tunneling with the *Datacenters* and using different computer speeds and models. In this way these components will extend the communication resources of educational institutions that are connected on the network to facilitate transactions and exchanges of services between these institutions.

In this project the main components are: the *Datacenters*, the doors of communication between the structures of clouds Computing Virtualization, networking organizations, service models, electromagnetism and the foundations of relativity.

3.4. Tools used

The main tools used are: the hosting cloud computing, *web* technologies, the models of enterprise network services, and the application of electromagnetism in communications transmissions.

3.5. Application environments

The environment for realization will be built using internet networks, cloud computing, virtualization, *Datacenters* and networks of educational institution as intra-organizational type. The infrastructure for the implementation of the case study should be built using computers of different sizes and characteristics, where they will be interconnected in a network of computers using virtualization of these machines. Aiming at the application and realization of this work is its implementation with the cloud computing and basics of relativity to be able to demonstrate its advantages.

IV. ANALYSIS OF RESULTS

The tables below show the results of the data collected for the analysis of the implementation of the modifications of the Galilean relativity, time contraction, time dilation and the relativistic momentum.

1	Data	Hora	Máqui	Sistema Operacional	Tempo UOL	Velocidade	Memória RAM
70	21/1/2014	09h14	A	XP	8,56	2,67	3,00
71	21/1/2014	09h14	A	XP	2,31	2,67	3,00
72	21/1/2014	09h14	A	XP	2,72	2,67	3,00
73	21/1/2014	09h14	A	XP	3,00	2,67	3,00
78	21/1/2014	15h02	A	XP	9,21	2,67	3,00
79	21/1/2014	15h02	A	XP	2,84	2,67	3,00
80	21/1/2014	15h02	A	XP	2,91	2,67	3,00
81	21/1/2014	15h02	A	XP	3,13	2,67	3,00
86	22/1/2014	09h10	A	XP	24,32	2,67	3,00
87	22/1/2014	09h10	A	XP	3,88	2,67	3,00
88	22/1/2014	09h10	A	XP	2,84	2,67	3,00
89	22/1/2014	09h10	A	XP	2,84	2,67	3,00
94	22/1/2014	13h26	A	XP	31,91	2,67	3,00
95	22/1/2014	13h26	A	XP	3,13	2,67	3,00
96	22/1/2014	13h26	A	XP	2,82	2,67	3,00
97	22/1/2014	13h26	A	XP	2,97	2,67	3,00
106	23/1/2014	08h00	A	XP	9,06	2,67	3,00
107	23/1/2014	08h00	A	XP	2,79	2,67	3,00
108	23/1/2014	08h00	A	XP	3,09	2,67	3,00
109	23/1/2014	08h00	A	XP	2,84	2,67	3,00
114	23/1/2014	14h48	A	XP	30,25	2,67	3,00
115	23/1/2014	14h48	A	XP	3,25	2,67	3,00
116	23/1/2014	14h48	A	XP	2,93	2,67	3,00
117	23/1/2014	14h48	A	XP	2,75	2,67	3,00
123			A	XP	6,29	2,67	3,00

Table 1-Data collection of server and client environment computing, author.

Table 1 shows the results applied in a computer PC (*Personal Computer*) Intel processor speed of 2.67 GHZ, XP operating system (from *Microsoft*) with the amount of 3.00 GB RAM, where they were recorded: the dates, times and the time required to connect to a site (UOL). At the end of the table is recorded the average time for the connections and the main features of the machine used in the environment (client/server) on the internet and how tunneling was carried out of the connection with the *Datacenter*.

1	Data	Hora	Máqui	Sistema Operacional	Tempo UOL	Velocidade	Memória RAM
6	18/1/2014	11h45	B	XP	13,09	1,73	2,00
7	18/1/2014	11h45	B	XP	9,90	1,73	2,00
8	18/1/2014	11h45	B	XP	12,72	1,73	2,00
9	18/1/2014	11h45	B	XP	9,78	1,73	2,00
14	18/1/2014	11h59	B	XP	14,90	1,73	2,00
15	18/1/2014	11h59	B	XP	9,87	1,73	2,00
16	18/1/2014	11h59	B	XP	9,85	1,73	2,00
17	18/1/2014	11h59	B	XP	12,88	1,73	2,00
22	18/1/2014	22h20	B	XP	12,91	1,73	2,00
23	18/1/2014	22h20	B	XP	9,72	1,73	2,00
24	18/1/2014	22h20	B	XP	14,79	1,73	2,00
25	18/1/2014	22h20	B	XP	12,81	1,73	2,00
30	19/1/2014	16h13	B	XP	28,19	1,73	2,00
31	19/1/2014	16h13	B	XP	9,81	1,73	2,00
32	19/1/2014	16h13	B	XP	12,69	1,73	2,00
33	19/1/2014	16h13	B	XP	10,75	1,73	2,00
38	19/1/2014	18h15	B	XP	18,28	1,73	2,00
39	19/1/2014	18h15	B	XP	9,81	1,73	2,00
40	19/1/2014	18h15	B	XP	12,97	1,73	2,00
41	19/1/2014	18h15	B	XP	9,94	1,73	2,00
124			B	XP	12,78	1,73	2,00

Table 2-Data collection of server client environment computing, author.

Table 2 shows the results applied in a computer *Notebook* Intel processor 1.73 GHZ speed, operating system XP (from *Microsoft*) with the amount of 3.00 GB RAM, where they were recorded: the dates, times and the time required connecting to a site (UOL). At the end of the table is recorded the average time for the connections and the main features of the machine used in the environment (client/server) on the internet and how tunneling was carried out of the connection with the *Datacenter*.

1	Data	Hora	Máquina	Sistema Operacional	Tempo UOL	Velocidade	Memória RAM
61	20/1/2014	14h42	C	Windows 7	0,90	2,50	6,00
66	20/1/2014	20h42	C	Windows 7	35,56	2,50	6,00
67	20/1/2014	20h42	C	Windows 7	0,78	2,50	6,00
68	20/1/2014	20h42	C	Windows 7	1,25	2,50	6,00
69	20/1/2014	20h42	C	Windows 7	1,88	2,50	6,00
74	21/1/2014	09h16	C	Windows 7	5,69	2,50	6,00
75	21/1/2014	09h16	C	Windows 7	0,97	2,50	6,00
76	21/1/2014	09h16	C	Windows 7	0,68	2,50	6,00
77	21/1/2014	09h16	C	Windows 7	0,81	2,50	6,00
82	21/1/2014	15h03	C	Windows 7	5,44	2,50	6,00
83	21/1/2014	15h03	C	Windows 7	1,00	2,50	6,00
84	21/1/2014	15h03	C	Windows 7	0,97	2,50	6,00
85	21/1/2014	15h03	C	Windows 7	0,56	2,50	6,00
90	22/1/2014	09h12	C	Windows 7	5,84	2,50	6,00
91	22/1/2014	09h12	C	Windows 7	0,88	2,50	6,00
92	22/1/2014	09h12	C	Windows 7	0,85	2,50	6,00
93	22/1/2014	09h12	C	Windows 7	0,75	2,50	6,00
98	22/1/2014	13h28	C	Windows 7	6,32	2,50	6,00
99	22/1/2014	13h28	C	Windows 7	1,00	2,50	6,00
100	22/1/2014	13h28	C	Windows 7	1,06	2,50	6,00
101	22/1/2014	13h28	C	Windows 7	0,78	2,50	6,00
125			C	Windows 7	3,05	2,50	6,00

Table 3 — Data collection of server client environment computing, author.

Table 3 shows the results applied in a computer *Notebook* Intel processor 2.50 GHZ speed, operating system Windows 7 (from *Microsoft*) with the amount of 6.00 GB RAM, where they were recorded: the dates, times and the time required to connect to a site (UOL). At the end of the table is recorded the average time for the connections and the main features of the machine used in the environment (client/server) on the internet and how tunneling was carried out of the connection with the *Datacenter*.

1	Data	Hora	Máquina	Sistema Operacional	Tempo UOL	Velocidade	Memória RAM
102	22/1/2014	13h39	D	Windows 7	6,69	1,20	2,00
103	22/1/2014	13h39	D	Windows 7	7,81	1,20	2,00
104	22/1/2014	13h39	D	Windows 7	8,72	1,20	2,00
105	22/1/2014	13h39	D	Windows 7	5,00	1,20	2,00
110	23/1/2014	08h02	D	Windows 7	8,00	1,20	2,00
111	23/1/2014	08h02	D	Windows 7	10,73	1,20	2,00
112	23/1/2014	08h02	D	Windows 7	11,63	1,20	2,00
113	23/1/2014	08h02	D	Windows 7	8,41	1,20	2,00
118	23/1/2014	14h53	D	Windows 7	8,84	1,20	2,00
119	23/1/2014	14h53	D	Windows 7	3,38	1,20	2,00
120	23/1/2014	14h53	D	Windows 7	6,97	1,20	2,00
121	23/1/2014	14h53	D	Windows 7	12,50	1,20	2,00
126			D	Windows 7	8,22	1,20	2,00

Table 4 — Data collection of server client environment computing, author.

Table 4 shows the results applied in a computer *Notebook* Intel processor 1.20 GHZ speed, operating system Windows 7 (from *Microsoft*) with the amount of 2.00 GB RAM, where they were recorded: the dates, times and the time required to connect to a site (UOL). At the end of the table is recorded the average time for the connections and the main features of the machine used in the environment (client/server) on the internet and how tunneling was carried out of the connection with the *Datacenter*.

	E	F	G	H	I	J	K	L	M	N
1	Tempo UOL	Velocidade(GHZ)	Memória RAM(GB)	T(Período) seg	Comprimento de onda(cm)	Velocidade Conexão(cm/s)	Comprimento de onda(cm)	Distância(cm)	Tempo(seg)	Frequência (GHZ)
110	8,00	1,20	2,00	0,00000000833	25,00	0,0313	0,00000000026	0,25	8,00	1,2
111	10,73	1,20	2,00	0,00000000833	25,00	0,0233	0,00000000019	0,25	10,73	1,2
112	11,63	1,20	2,00	0,00000000833	25,00	0,0215	0,00000000018	0,25	11,63	1,2
113	8,41	1,20	2,00	0,00000000833	25,00	0,0297	0,00000000025	0,25	8,41	1,2
114	30,25	2,67	3,00	0,00000000375	11,24	0,0037	0,00000000001	0,11	30,25	2,67
115	3,25	2,67	3,00	0,00000000375	11,24	0,0346	0,00000000013	0,11	3,25	2,67
116	2,93	2,67	3,00	0,00000000375	11,24	0,0383	0,00000000014	0,11	2,93	2,67
117	2,75	2,67	3,00	0,00000000375	11,24	0,0409	0,00000000015	0,11	2,75	2,67
118	8,84	1,20	2,00	0,00000000833	25,00	0,0283	0,00000000024	0,25	8,84	1,2
119	3,38	1,20	2,00	0,00000000833	25,00	0,0740	0,00000000062	0,25	3,38	1,2
120	6,97	1,20	2,00	0,00000000833	25,00	0,0359	0,00000000030	0,25	6,97	1,2
121	12,50	1,20	2,00	0,00000000833	25,00	0,0200	0,00000000017	0,25	12,50	1,2
122	Tempo UOL	Velocidade	Memória RAM	T(Período) seg	Comprimento de onda(cm)	Velocidade Conexão(cm/s)	Comprimento de onda(cm)	Distância(cm)	Tempo(seg)	Frequência (GHZ)
123	13,93	2,67	3,00	0,00000000988	29,64	0,1081	0,00000000047	0,30	13,93	
124	38,50	1,73	2,00	0,00000002692	80,75	0,2938	0,00000000127	0,81	38,50	
125	14,39	2,50	6,00	0,00000001134	34,02	0,1563	0,00000000067	0,34	14,39	
126	12,97	1,20	2,00	0,00000001083	32,49	0,0548	0,00000000036	0,32	12,97	
127										
128						Veloc. Relat.		Dist. Relat.	Tempo Relat.	
129						0,108129243		0,296434695	13,931607143	
130						0,293844001		0,807545236	38,504000000	
131						0,156295539		0,340154494	14,392500000	
132						0,054835504		0,324906367	12,970000000	
133										
134						Varição Veloc. Relat.		Varição	Varição	
135						0,000029243		0,003565305	0,001607143	
136						0,000044001		0,002454764	0,004000000	
137						0,000004461		0,000154494	0,002500000	
138						0,000035504		0,004906367	0,000000000	

Table 5 – Time dilation and contraction of space, author.

Table 5 shows the results presented in the analysis of the connections established by physical machines of different characteristics, applying the concepts of virtualization, calculations of tunneling: period, wavelength, frequency, time and distance and time variations relativists. Table 6 shows the more detailed results and explains the time dilation and contraction of space in virtualization environment.

	0,0740	0,00000000062		
	0,0359	0,00000000030	0,25	6,97
	0,0200	0,00000000017	0,25	12,50
(cm)	Velocidade Conexão(cm/s)	Comprimento de onda(cm)	Distância(cm)	Tempo(seg)
	0,1081	0,00000000047	0,30	13,93
	0,2938	0,00000000127	0,81	38,50
	0,1563	0,00000000067	0,34	14,39
	0,0548	0,00000000036	0,32	12,97
	Veloc. Relat.		Dist. Relat.	Tempo Relat.
	0,108129243		0,296434695	13,931607143
	0,293844001		0,807545236	38,504000000
	0,156295539		0,340154494	14,392500000
	0,054835504		0,324906367	12,970000000
	Varição Veloc. Relat.		Varição	Varição
	0,000029243		0,003565305	0,001607143
	0,000044001		0,002454764	0,004000000
	0,000004461		0,000154494	0,002500000
	0,000035504		0,004906367	0,000000000

Table 6 – Part of time dilation and contraction of space, author.

Table 6 shows the results of the calculations in relation to the values of the variations set out in simulations of virtualization connections compared to the speed of light. Are described the values of speeds, distances covered, time and variations in virtualization environment reached relativists. The wavelength for the computer operating system, XP, the tunneling period is $9,88 \times 10^{-10}$ s, the wavelength of $4,7 \times 10^{-13}$ m and

frequency equal to 1.5 Ghz, which according to the classification of the electromagnetic spectrum is in the range of electromagnetic radiation. On computer B, XP operating system, the period of the tunneling is $26,92 \times 10^{-10}$ sec, and the wavelength of $12,7 \times 10^{-13}$ m and frequency equal to 11.3 Ghz, which according to the classification of the electromagnetic spectrum is in the range of electromagnetic radiation. To computer C, the operating system Windows 7, the tunneling period is $11,34 \times 10^{-10}$ sec, and the wavelength of $6,7 \times 10^{-13}$ m and frequency equal to 2.25 Ghz, which according to the classification of the electromagnetic spectrum is in the range of electromagnetic radiation. To computer D, operating system Windows 7, the tunneling period is $10,83 \times 10^{-10}$ sec, and the wavelength of $3,6 \times 10^{-13}$ m and frequency equal to 0.71 Ghz, which according to the classification of the electromagnetic spectrum is in the range of electromagnetic radiation. Occurs, so a variation of the tunneling of computers A, B, C and D in the virtual environment in relation to the speed of light which are: for the computer to 0.00000000036% in relation to the speed of light; to computer B of 0.00000000098% in relation to the speed of light; to computer C of 0.00000000052% in relation to the speed of light; to computer D of 0.00000000018% in relation to the speed of light.

1	Data	Hora	Máqui	Sistema Operacional	Tempo Conexão	Tempo UOL	Velocidade	Memória RAM	Velocidade	Memória RAM
18	18/1/2014	11h27	A-->B	XP-->XP	5,50	2,60	2,67	3,00	1,73	2,00
19	18/1/2014	11h27	A-->B	XP-->XP	5,50	2,88	2,67	3,00	1,73	2,00
20	18/1/2014	11h27	A-->B	XP-->XP	5,50	2,85	2,67	3,00	1,73	2,00
21	18/1/2014	11h27	A-->B	XP-->XP	5,50	3,22	2,67	3,00	1,73	2,00
30	18/1/2014	11h50	A-->B	XP-->XP	1,50	1,12	2,67	3,00	1,73	2,00
31	18/1/2014	11h50	A-->B	XP-->XP	1,50	1,06	2,67	3,00	1,73	2,00
32	18/1/2014	11h50	A-->B	XP-->XP	1,50	1,21	2,67	3,00	1,73	2,00
33	18/1/2014	11h50	A-->B	XP-->XP	1,50	1,16	2,67	3,00	1,73	2,00
38	18/1/2014	22h15	A-->B	XP-->XP	1,50	32,81	2,67	3,00	1,73	2,00
39	18/1/2014	22h15	A-->B	XP-->XP	1,50	19,25	2,67	3,00	1,73	2,00
40	18/1/2014	22h15	A-->B	XP-->XP	1,50	18,84	2,67	3,00	1,73	2,00
41	18/1/2014	22h15	A-->B	XP-->XP	1,50	12,50	2,67	3,00	1,73	2,00
46	19/1/2014	16h18	A-->B	XP-->XP	1,69	18,82	2,67	3,00	1,73	2,00
47	19/1/2014	16h18	A-->B	XP-->XP	1,69	12,22	2,67	3,00	1,73	2,00
48	19/1/2014	16h18	A-->B	XP-->XP	1,69	17,62	2,67	3,00	1,73	2,00
49	19/1/2014	16h18	A-->B	XP-->XP	1,69	18,81	2,67	3,00	1,73	2,00
54	19/1/2014	18h17	A-->B	XP-->XP	1,68	16,88	2,67	3,00	1,73	2,00
55	19/1/2014	18h17	A-->B	XP-->XP	1,68	17,59	2,67	3,00	1,73	2,00
56	19/1/2014	18h17	A-->B	XP-->XP	1,68	17,35	2,67	3,00	1,73	2,00
57	19/1/2014	18h17	A-->B	XP-->XP	1,68	12,04	2,67	3,00	1,73	2,00
152			A-->B	XP-->XP	2,57	12,44	2,67	3,00	1,73	2,00

Table 7 – Computer data collection in virtualization environment, author.

Table 7 shows the results applied in a computer PC (*Personal Computer*) Intel processor speed of 2.67 GHZ, XP operating system (from Microsoft) with the amount of 3.00 GB RAM and another computer of processor speed of 1.73 GHZ, XP operating system (from Microsoft) with the amount of 2.0 GB RAM, where they were registered: dates, schedules and the time required to connect to a site (UOL). At the end of the table is recorded the average time for the connections and the main characteristics of the machines used in the virtualization environment of cloud computing.

1	Data	Hora	Máqui	Sistema Operacional	Tempo Conexão	Tempo UOL	Velocidade	Memória RAM	Velocidade	Memória RAM
22	18/1/2014	11h37	B-->A	XP-->XP	1,22	3,75	1,73	2,00	2,67	3,00
23	18/1/2014	11h37	B-->A	XP-->XP	1,22	3,38	1,73	2,00	2,67	3,00
24	18/1/2014	11h37	B-->A	XP-->XP	1,22	3,34	1,73	2,00	2,67	3,00
25	18/1/2014	11h37	B-->A	XP-->XP	1,22	3,35	1,73	2,00	2,67	3,00
26	18/1/2014	11h45	B-->A	XP-->XP	1,33	2,97	1,73	2,00	2,67	3,00
27	18/1/2014	11h45	B-->A	XP-->XP	1,33	0,97	1,73	2,00	2,67	3,00
28	18/1/2014	11h45	B-->A	XP-->XP	1,33	1,37	1,73	2,00	2,67	3,00
29	18/1/2014	11h45	B-->A	XP-->XP	1,33	1,10	1,73	2,00	2,67	3,00
34	18/1/2014	11h57	B-->A	XP-->XP	1,03	3,37	1,73	2,00	2,67	3,00
35	18/1/2014	11h57	B-->A	XP-->XP	1,03	4,22	1,73	2,00	2,67	3,00
36	18/1/2014	11h57	B-->A	XP-->XP	1,03	3,90	1,73	2,00	2,67	3,00
37	18/1/2014	11h57	B-->A	XP-->XP	1,03	4,15	1,73	2,00	2,67	3,00
42	18/1/2014	22h23	B-->A	XP-->XP	1,47	4,31	1,73	2,00	2,67	3,00
43	18/1/2014	22h23	B-->A	XP-->XP	1,47	3,38	1,73	2,00	2,67	3,00
44	18/1/2014	22h23	B-->A	XP-->XP	1,47	3,56	1,73	2,00	2,67	3,00
45	18/1/2014	22h23	B-->A	XP-->XP	1,47	3,37	1,73	2,00	2,67	3,00
50	19/1/2014	16h21	B-->A	XP-->XP	1,47	3,53	1,73	2,00	2,67	3,00
51	19/1/2014	16h21	B-->A	XP-->XP	1,47	3,19	1,73	2,00	2,67	3,00
52	19/1/2014	16h21	B-->A	XP-->XP	1,47	3,32	1,73	2,00	2,67	3,00
53	19/1/2014	16h21	B-->A	XP-->XP	1,47	3,28	1,73	2,00	2,67	3,00
58	19/1/2014	18h23	B-->A	XP-->XP	1,63	3,56	1,73	2,00	2,67	3,00
59	19/1/2014	18h23	B-->A	XP-->XP	1,63	3,25	1,73	2,00	2,67	3,00
60	19/1/2014	18h23	B-->A	XP-->XP	1,63	7,91	1,73	2,00	2,67	3,00
61	19/1/2014	18h23	B-->A	XP-->XP	1,63	3,32	1,73	2,00	2,67	3,00
153			B-->A	XP-->XP	2,09	3,46	1,73	2,00	2,67	3,00

Table 8 – data collection the virtualization environment computing, author.

Table 8 shows the results applied in a computer *Notebook* Intel processor 1.73 GHZ speed, operating system XP (from Microsoft) with the amount of 2.00 GB RAM and another computer PC (*Personal Computer*) speed of 2.67 GHZ processor, XP operating system (from Microsoft) with the amount of 3.0 GB RAM, where they were registered: dates, schedules and the time required to connect to a site (UOL). At the end of the table is recorded the average time for the connections and the main characteristics of the machines used in the virtualization environment of cloud computing.

1	Data	Hora	Máquina	Sistema Operacional	Tempo Conexão	Tempo UOL	Velocidade	Memória RAM	Velocidade	Memória RAM
89	20/1/2014	20h47	A-->C	XP-->Windows 7	0,94	1,31	2,67	3,00	2,50	6,00
94	21/1/2014	09h18	A-->C	XP-->Windows 7	1,25	1,19	2,67	3,00	2,50	6,00
95	21/1/2014	09h18	A-->C	XP-->Windows 7	1,25	1,07	2,67	3,00	2,50	6,00
96	21/1/2014	09h18	A-->C	XP-->Windows 7	1,25	0,81	2,67	3,00	2,50	6,00
97	21/1/2014	09h18	A-->C	XP-->Windows 7	1,25	1,56	2,67	3,00	2,50	6,00
102	21/1/2014	15h06	A-->C	XP-->Windows 7	1,25	0,46	2,67	3,00	2,50	6,00
103	21/1/2014	15h06	A-->C	XP-->Windows 7	1,25	1,21	2,67	3,00	2,50	6,00
104	21/1/2014	15h06	A-->C	XP-->Windows 7	1,25	1,72	2,67	3,00	2,50	6,00
105	21/1/2014	15h06	A-->C	XP-->Windows 7	1,25	1,63	2,67	3,00	2,50	6,00
110	22/1/2014	09h15	A-->C	XP-->Windows 7	0,62	0,75	2,67	3,00	2,50	6,00
111	22/1/2014	09h15	A-->C	XP-->Windows 7	0,62	1,00	2,67	3,00	2,50	6,00
112	22/1/2014	09h15	A-->C	XP-->Windows 7	0,62	0,94	2,67	3,00	2,50	6,00
113	22/1/2014	09h15	A-->C	XP-->Windows 7	0,62	1,09	2,67	3,00	2,50	6,00
118	22/1/2014	13h29	A-->C	XP-->Windows 7	1,34	0,72	2,67	3,00	2,50	6,00
119	22/1/2014	13h29	A-->C	XP-->Windows 7	1,34	0,59	2,67	3,00	2,50	6,00
120	22/1/2014	13h29	A-->C	XP-->Windows 7	1,34	0,47	2,67	3,00	2,50	6,00
121	22/1/2014	13h29	A-->C	XP-->Windows 7	1,34	1,06	2,67	3,00	2,50	6,00
154			A-->C	XP-->Windows 7	1,07	1,19	2,67	3,00	2,50	6,00

Table 9 – Data collection the virtualization environment computing, author.

Table 9 shows the results applied in a computer PC (*Personal Computer*) Intel processor speed of 2.67 GHZ, XP operating system (from Microsoft) with the amount of 3.00 GB RAM memory and other computer *Notebook* processor 2.5 GHZ speed, operating system Windows 7 (from Microsoft) with the amount of 6.0 GB RAM where were recorded: the dates, times and the time required to connect to a site (UOL). At the end of the table is recorded the average time for the connections and the main characteristics of the machines used in the virtualization environment of cloud computing.

1	Data	Hora	Máquina	Sistema Operacional	Tempo Conexão	Tempo UOL	Velocidade	Memória RAM	Velocidade	Memória RAM
90	20/1/2014	20h49	C-->A	Windows 7-->XP	0,91	3,54	2,50	6,00	2,67	3,00
91	20/1/2014	20h49	C-->A	Windows 7-->XP	0,91	3,44	2,50	6,00	2,67	3,00
92	20/1/2014	20h49	C-->A	Windows 7-->XP	0,91	2,25	2,50	6,00	2,67	3,00
93	20/1/2014	20h49	C-->A	Windows 7-->XP	0,91	3,41	2,50	6,00	2,67	3,00
98	21/1/2014	09h21	C-->A	Windows 7-->XP	1,13	3,38	2,50	6,00	2,67	3,00
99	21/1/2014	09h21	C-->A	Windows 7-->XP	1,13	3,31	2,50	6,00	2,67	3,00
100	21/1/2014	09h21	C-->A	Windows 7-->XP	1,13	3,28	2,50	6,00	2,67	3,00
101	21/1/2014	09h21	C-->A	Windows 7-->XP	1,13	3,12	2,50	6,00	2,67	3,00
106	21/1/2014	15h08	C-->A	Windows 7-->XP	1,25	3,19	2,50	6,00	2,67	3,00
107	21/1/2014	15h08	C-->A	Windows 7-->XP	1,25	4,21	2,50	6,00	2,67	3,00
108	21/1/2014	15h08	C-->A	Windows 7-->XP	1,25	3,44	2,50	6,00	2,67	3,00
109	21/1/2014	15h08	C-->A	Windows 7-->XP	1,25	3,57	2,50	6,00	2,67	3,00
114	22/1/2014	09h18	C-->A	Windows 7-->XP	0,94	3,47	2,50	6,00	2,67	3,00
115	22/1/2014	09h18	C-->A	Windows 7-->XP	0,94	3,50	2,50	6,00	2,67	3,00
116	22/1/2014	09h18	C-->A	Windows 7-->XP	0,94	3,19	2,50	6,00	2,67	3,00
117	22/1/2014	09h18	C-->A	Windows 7-->XP	0,94	3,28	2,50	6,00	2,67	3,00
122	22/1/2014	13h32	C-->A	Windows 7-->XP	1,06	3,60	2,50	6,00	2,67	3,00
123	22/1/2014	13h32	C-->A	Windows 7-->XP	1,06	3,25	2,50	6,00	2,67	3,00
124	22/1/2014	13h32	C-->A	Windows 7-->XP	1,06	3,37	2,50	6,00	2,67	3,00
125	22/1/2014	13h32	C-->A	Windows 7-->XP	1,06	3,41	2,50	6,00	2,67	3,00
155			C-->A	Windows 7-->XP	1,09	3,56	2,50	6,00	2,67	3,00

Table 10 – Data collection the virtualization environment computing, author.

Table 10 shows the results applied in a computer *Notebook* processor 2.5 GHZ speed, operating system Windows 7 (from Microsoft) with the amount of 6.0 GB RAM and another computer of type PC (*Personal Computer*) Intel processor speed of 2.67 GHZ, XP operating system (from Microsoft) with the amount of 3.00 GB RAM where were recorded: the dates, times and the time required to connect to a site (UOL). At the end of the table is recorded the average time for the connections and the main characteristics of the machines used in the virtualization environment of cloud computing.

1	Data	Hora	Máquina	Sistema Operacional	Tempo Conexão	Tempo UOL	Velocidade	Memória RAM	Velocidade	Memória RAM
126	22/1/2014	13h46	A-->D	XP-->Windows 7	3,10	8,84	2,67	3,00	1,20	2,00
127	22/1/2014	13h46	A-->D	XP-->Windows 7	3,10	17,16	2,67	3,00	1,20	2,00
128	22/1/2014	13h46	A-->D	XP-->Windows 7	3,10	13,85	2,67	3,00	1,20	2,00
129	22/1/2014	13h46	A-->D	XP-->Windows 7	3,10	20,12	2,67	3,00	1,20	2,00
134	23/1/2014	08h04	A-->D	XP-->Windows 7	2,06	6,28	2,67	3,00	1,20	2,00
135	23/1/2014	08h04	A-->D	XP-->Windows 7	2,06	4,81	2,67	3,00	1,20	2,00
136	23/1/2014	08h04	A-->D	XP-->Windows 7	2,06	12,03	2,67	3,00	1,20	2,00
137	23/1/2014	08h04	A-->D	XP-->Windows 7	2,06	4,47	2,67	3,00	1,20	2,00
142	23/1/2014	14h54	A-->D	XP-->Windows 7	1,91	8,28	2,67	3,00	1,20	2,00
143	23/1/2014	14h54	A-->D	XP-->Windows 7	1,91	3,47	2,67	3,00	1,20	2,00
144	23/1/2014	14h54	A-->D	XP-->Windows 7	1,91	4,50	2,67	3,00	1,20	2,00
145	23/1/2014	14h54	A-->D	XP-->Windows 7	1,91	4,09	2,67	3,00	1,20	2,00
156			A-->D	XP-->Windows 7	2,36	8,99	2,67	3,00	1,20	2,00

Table 11 – Data collection the virtualization environment computing, author.

Table 11 shows the results applied in a computer PC (*Personal Computer*) Intel processor speed of 2.67 GHZ, XP operating system (from Microsoft) with the amount of 3.00 GB RAM memory and other computer *Notebook* processor 1.2 GHZ speed, operating system Windows 7 (from Microsoft) with the amount of 2.0 GB RAM where were recorded: the dates, times and the time required to connect to a site (UOL). At the end of the table is recorded the average time for the connections and the main characteristics of the machines used in the virtualization environment of cloud computing.

1	Data	Hora	Máquina	Sistema Operacional	Tempo Conexão	Tempo UOL	Velocidade	Memória RAM	Velocidade	Memória RAM
130	22/1/2014	13h49	D-->A	Windows 7-->XP	1,71	4,06	1,20	2,00	2,67	3,00
131	22/1/2014	13h49	D-->A	Windows 7-->XP	1,71	3,63	1,20	2,00	2,67	3,00
132	22/1/2014	13h49	D-->A	Windows 7-->XP	1,71	3,38	1,20	2,00	2,67	3,00
133	22/1/2014	13h49	D-->A	Windows 7-->XP	1,71	3,41	1,20	2,00	2,67	3,00
138	23/1/2014	08h07	D-->A	Windows 7-->XP	1,84	3,37	1,20	2,00	2,67	3,00
139	23/1/2014	08h07	D-->A	Windows 7-->XP	1,84	3,18	1,20	2,00	2,67	3,00
140	23/1/2014	08h07	D-->A	Windows 7-->XP	1,84	3,37	1,20	2,00	2,67	3,00
141	23/1/2014	08h07	D-->A	Windows 7-->XP	1,84	3,22	1,20	2,00	2,67	3,00
146	23/1/2014	14h59	D-->A	Windows 7-->XP	2,12	3,54	1,20	2,00	2,67	3,00
147	23/1/2014	14h59	D-->A	Windows 7-->XP	2,12	3,21	1,20	2,00	2,67	3,00
148	23/1/2014	14h59	D-->A	Windows 7-->XP	2,12	3,50	1,20	2,00	2,67	3,00
149	23/1/2014	14h59	D-->A	Windows 7-->XP	2,12	4,03	1,20	2,00	2,67	3,00
157			D-->A	Windows 7-->XP	1,89	3,49	1,20	2,00	2,67	3,00

Table 12 – Data collection the virtualization environment computing, author.

Table 12 shows the results applied in a computer *Notebook* Intel processor 1.2 GHZ speed, operating system Windows 7 (from Microsoft) with the amount of 2.00 GB RAM and another computer PC (*Personal Computer*) speed of 2.67 GHZ processor, XP operating system (from Microsoft) with the amount of 3.0 GB RAM where were recorded: the dates, times and the time required to connect to a site (UOL). At the end of the table is recorded the average time for the connections and the main characteristics of the machines used in the virtualization environment of cloud computing.

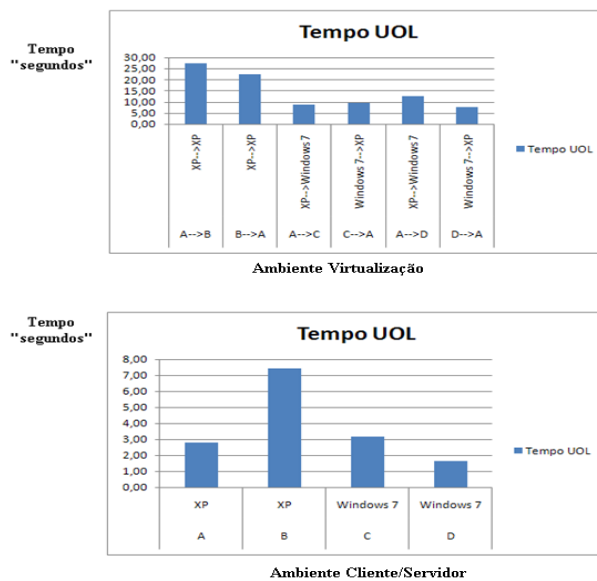


Figure 7-Graphical analysis of client/server environments and virtualization, author.

Considering the observations and graphical analysis of results presented in Figure 7, the machines and operating systems used have a speed rating and access to the site "UOL" in ascending order the computers: D, A, C and B. However, when running in the virtual environment the slower computers can be faster when run on faster computers or vice-versa.

Máquina	Sistema Operacional	Tempo Conexão	Tempo UOL	Velocidade	Memória RAM	Velocidade	Memória RAM
A->B	XP->XP	9,24	27,16	2,67	3,00	1,73	2,00
B->A	XP->XP	7,51	22,25	1,73	2,00	2,67	3,00
A->C	XP->Windows 7	3,62	8,87	2,67	3,00	2,50	6,00
C->A	Windows 7->XP	3,75	9,42	2,50	6,00	2,67	3,00
A->D	XP->Windows 7	4,25	12,48	2,67	3,00	1,20	2,00
D->A	Windows 7->XP	3,21	7,49	1,20	2,00	2,67	3,00

Máquina	Sistema Operacional	Tempo UOL	Velocidade	Memória RAM
A	XP	2,76	2,67	3,00
B	XP	7,44	1,73	2,00
C	Windows 7	3,15	2,50	6,00
D	Windows 7	1,65	1,20	2,00

$\lambda=v*T$ (cm)	Velocidade de Conexão (cm/s)
16,69	13,68
13,23	12,36
12,81	11,97
0,13	11,97
0,00	0,00
0,00	0,00

Figure 8 – Analysis of the results of the client/server environments and virtualization, author.

Figure 8 shows the connection speeds of the machines tested and the average data transmission in the virtual environment. The results of their frequencies and wavelengths are within the ranges of UHF frequencies above, according to the table of frequency spectra in Figure 9 the standardization ITU (*International Telecommunications Union-Telecommunication*).

Alto frequência High frequency	HF	7	3-30 MHz	100 m – 10 m
Muito alta frequência Very high frequency	VHF	8	30-300 MHz	10 m – 1 m
Ultra alta frequência Ultra high frequency	UHF	9	300-3000 MHz	1 m – 100 mm
Super alta frequência Super high frequency	SHF	10	3-30 GHz	100 mm – 10 mm
Extra alta frequência Extremely high frequency	EHF	11	30-300 GHz	10 mm – 1 mm
			Acima dos 300 GHz	< 1 mm

Figure 9 – Table of frequency Spectra ITU-T (*International Telecommunications Union-Telecommunication*).

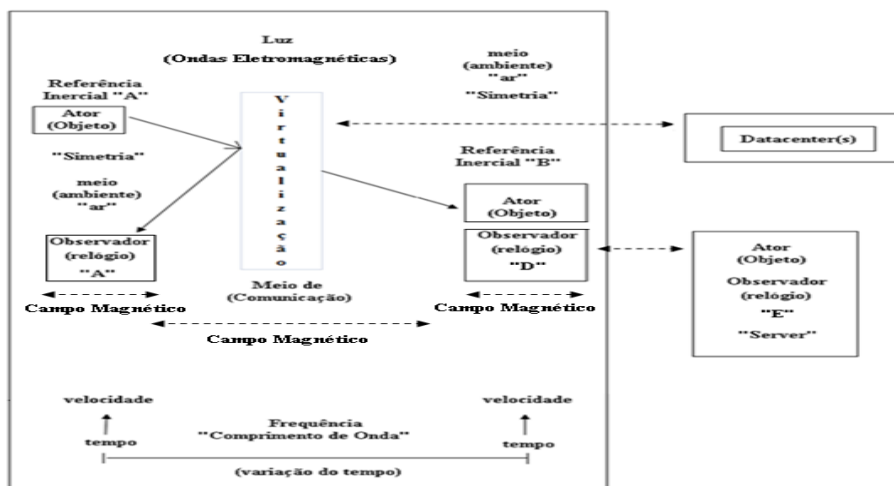


Figure 10 – Analysis of the magnetic field on the virtualization environments, objects and time, author.

Figure 10 shows the relationship and the results obtained in this work on the relativistic vision applied to virtualization in corporate networks using the principles of tunneling to connect and Exchange data on cloud computing. It is observed that the light and the magnetic field have a direct influence in relation to objects: actor, the observers, the time registered by watches, the frequency waves, the speed and the means of communication established by virtualization. Virtualization allows the resources of *Datacenters* are shifted to the virtualization environment, with this we can observe the concepts of relativity about the time relativity related concurrency.

Considering the evolution of semiconductor technology and its limits of *chips* CMOS (Metal Oxide Semiconductor), an issuer of waves from the 340 Mhz frequency, the UHF wave spectrum (*Ultra High Frequency*), thus going on to work in the field of the effects of quantum physics (JUNIOR, SAUVÉ and MC, 1996). At this frequency the behavior of the electrons becomes unpredictable (known as tunneling of electrons). In virtualization these limitations will not exist, because the tunneling and behavior in data exchange and communications are under the responsibility only of the magnetic fields or speed of light. Because it notes that the displacement of objects horizontally about virtualization does not suffer from magnetic field deviation, however when moving horizontally virtualization the magnetic field points to the original position of the displacement, thus it is considered that the speed of light is a universal constant, is the same in all inertial reference systems in the vacuum, does not depend on the motion of the light source and has equal value in all directions, according to the postulate of Einstein's special theory of relativity. Under these conditions the length contraction may occur, but the relative speed does not suffer contraction. There is also the physical occurrence in a point set space and moment of time. In accordance with the principles of relativity, all the physical laws are the same in relation to any reference, because the speed of light is independent of how the references to move towards others.

V. CONCLUSION

This work had as objective to analyze and propose a model and quantum relativistic vision with the possibility of being implemented with the principles of Physics in virtualization of *Datacenters* in corporate networks. On the basis of the comments of the applications and infrastructure and internet technologies the IT environment has reduced their costs with the use of virtualization of *Datacenters*. In physics light wave property in addition to being an electromagnetic wave is associated with the emission and absorption of light, also carries energy and light source, which are present in the electronic components in computers. So it is known that the direction of a ray of light varies as it passes from one material to another with different refractive index, but in relation to the wave frequency does not vary according to the laws of physics and theory of Einstein should be the same in any inertial reference systems. The theory of relativity and concurrency involves the main concepts of measure of time and time intervals and describes that concurrency is not an absolute concept, because two events occur simultaneously or not. Concurrency is important for the measurement of time intervals and length contraction may occur, while the relative velocity does not suffer contraction. An event is a fundamental principal of relativity and can be observed and measured by observers in different frames, whereas in concurrency, event is what actually happens. All the laws of physics are the same in relation to any reference and the value of the speed of light in different references propagate with the same speed of light in any inertial frame of reference. These concepts and fundamentals are parts of application virtualization of *Datacenters*.

The choice of measurements of the properties for the actors in the virtualization environment determines the correlations that exist for these results, because the application of quantum mechanics establishes the super positions of the actors (companies) and behaviors as if they were in multiple places simultaneously. However, the study and the results presented can serve as a basis for further work involving quantum computing vision applied in corporate networks and the presentation of the structure to the development of a quantum computer.

BIBLIOGRAPHICAL REFERENCES

- [1] CHAVES, Sidney. **A questão dos riscos em ambientes de computação em nuvem**, Universidade de São Paulo, São Paulo, 2011.
- [2] ERL, Thomas. **SOA Princípios de Design de Serviços**, Pearson Education do Brasil, São Paulo- SP, 2009.
- [3] FUSCO, José Paulo Alves e SACOMANO, José Benedito. **Alianças em redes de empresas: modelo de redes simultâneas para avaliação competitiva**, Editora Arte & Ciência, São Paulo – SP, 2009.
- [4] GALVÃO, Ernesto F.; **O que é computação quântica**, Vierira & Lent Editorial Ltda, Rio de Janeiro – RJ, 2007.
- [5] GAZZINELLI Ramayana; **Quem tem medo da física quântica**, Editora UFMG – MG, 2013.
- [6] JUNIOR TEIXEIRA, José Helvécio; SAUVÉ, Jacques Phillippe e MOURA, José Antão Beltrão. **Do Mainframe para Computação Distribuída**, Livraria e Editora Infobook S.A. Rio de Janeiro – RJ, 1996.
- [7] KNIGHT, Randall; **Física uma Abordagem Estratégica**, Bookman, Porto Alegre – RS, 2009.
- [8] LEHMAN, T. J.; VAJPAYEE, S.; **We've Looked at Clouds from Both Sides Now**. In: Annual SRII Globa Conference, San Jose, CA (US): Institute Electrical and Electronics Engineers (IEEE), p.342-348, 2011.
- [9] MOREIRA, Rui e CROCA, José; **Diálogos sobre Física Quântica dos paradoxos à não-linearidade**, Capax Dei, Rio de Janeiro – RJ, 2010.
- [10] OLIVEIRA, Ivan S.; **Física Moderna a Física Clássica, a Relatividade, a Mecânica Quântica e a Estrutura do Átomo**, Editora Livraria da Física, São Paulo – SP, 2005.
- [11] POHL, Herbert A.; **Introdução à mecânica quântica**, Editora da Universidade de São Paulo – SP, 1971.
- [12] RAMALHO, Junior Francisco; IVAN; Cardoso dos Santos José; NICOLAU Gilberto Ferraro e TOLEDO, Soares Paulo Antonio de; **Os fundamentos da física Eletricidade e Física Moderna**, Editora Moderna Ltda, São Paulo – SP, 1976.
- [13] YOUNG, Hugh D. and FREEDMAN, Roger A. **Física IV Ótica e Física Moderna**, Pearson Education do Brasil, São Paulo-SP, 2009.
- [14] YOUNG, Hugh D.; e FREEDMAN, Roger A. ; **Física III Eletromagnetismo**, Editora Pearson Education do Brasil, São Paulo – SP, 2004.

Extended version of Leach and its comparison with Energy aware multi-hop multi-path Hierarchy Protocol

¹, Prof. Greeshma Arya, ², Prof. D.S Chauhan, ³, Ridhi Khanna,
⁴, Nehal Mittal, ⁵ Amandeep
^{1, 3, 4}, Dept of ECE, IGDTUW, Delhi, India
², Dept of Electrical Science, Utrakhand Technical University

ABSTRACT:

Wireless sensor networks are generally battery limited deployed in remote and crucial areas where continuous monitoring is essential. One of the main design issues for such a network is conservation of the energy available in each sensor node. Increasing network lifetime is important in wireless sensor networks. The proposed scheme describes a new way to select the Cluster head. Analysis shows that the extended version or enhanced LEACH protocol balances the energy expense, saves the node energy and hence prolongs the lifetime of the sensor network. Also a comparison between LEACH, proposed scheme (extended version) and Energy aware multi-hop multi-path hierarchy protocol (EAMMH) is presented.

KEYWORDS: Cluster head(CH), Energy conservation, Energy level, Optimum distance, Comparison, LEACH, EAMMH, Energy Efficient, Multi Path, Multi Hop, Lifetime.

I. INTRODUCTION

LEACH is a clustering-based protocol. LEACH is one of the first hierarchical routing approaches for sensors networks. It randomly selects a few sensor nodes as cluster heads (CHs) and rotate this role to evenly distribute the energy load among the sensors in the network. In LEACH, the cluster head (CH) nodes compress data arriving from nodes that belong to the respective cluster, and send an aggregated packet to the base station in order to reduce the amount of information that must be transmitted to the base station (negotiation). WSN is considered to be a dynamic clustering method.

Section 1-Study of LEACH protocol

Operation of Leach

It has 2 phases :

1. Set up State Phase

2. Steady State Phase

In the setup phase, the clusters are organized and CHs are selected.

In the steady state phase, the actual data transfer to the base station takes place.

The duration of the steady state phase is longer than the duration of the setup phase.

During the setup phase, a predetermined fraction of nodes, p , elect themselves as CHs.

A sensor node chooses a random number, r , between 0 and 1. Let a threshold value be $T(n)$. If this random number is less than a threshold value, $T(n)$, the node becomes a cluster-head for the current round. The threshold value is calculated based on an equation that incorporates the desired percentage to become a cluster-head, the current round, and the set of nodes that have not been selected as a cluster-head in the last $(1/P)$ rounds, denoted by G .

$$T(n) = \frac{p}{1 - p \cdot (r \cdot \text{mod} \frac{1}{p})} \quad \forall n \in G$$

$$T(n) = 0 \quad \forall n \text{ not } \in G$$

where G is the set of nodes that are involved in the CH election.

Each elected CH broadcasts an advertisement message to the rest of the nodes in the network that they are the new cluster-heads. All the non-cluster head nodes, after receiving this advertisement, decide on the cluster to which they want to belong. This decision is based on the signal strength of the advertisement. The non cluster-head nodes inform the appropriate cluster-heads that they will be a member of the cluster. After receiving all the messages from the nodes that would like to be included in the cluster and based on the number of nodes in the cluster, the cluster-head node creates a TDMA schedule and assigns each node a time slot when it can transmit. This schedule is broadcast to all the nodes in the cluster.

During the steady state phase, the sensor nodes can begin sensing and transmitting data to the cluster-heads. The cluster-head node, after receiving all the data, aggregates it before sending it to the base-station. The energy spend by any transmitter to send a L-bit message over a distance d is,

$$S(i).E = E_{Tx}(l, d) = \begin{cases} \{L.E_{elec} + \epsilon_{fs} \cdot d^2 & \text{if } d \leq d_o\} \\ \{L.E_{elec} + \epsilon_{mp} \cdot d^4 & \text{if } d > d_o\} \end{cases}$$

Where $d_o = \sqrt{\frac{\epsilon_{fs}}{\epsilon_{mp}}}$

This is the energy dissipated in sending the data packets to the base station. This gives also gives the estimate of the remaining energy with the node. After a certain time, the network goes back into the setup phase again and enters another round of selecting new CH.

II. RELATED WORK

The idea proposed in LEACH has been an inspiration for many hierarchical routing protocols, although some protocols have been independently developed[1] . Taxonomy of the different architectural attributes of sensor networks is developed [2] . Further improvements on LEACH protocol for wireless sensor networks has been developed where both security & efficiency features have been dealt with [3]. Here the sensing area has been divided into a number of equilateral areas, called as clusters. Each cluster consists of six equilateral triangles called cells. The protocol consists of a number of rounds but after forming the clusters they do not change in each round. Both each equilateral triangle & each equilateral hexagon has same number of nodes. In each cell one cell head is selected & one CH is selected is chosen from six cell heads. The data are sent to the base station by using the multi-hop manner through a secure path consisting of cluster heads. The analysis shows that the improved protocol saves nodes energy, prolongs WSN lifetime, balances energy expenses and enhances security for WSNs.

To allow a single-tier network to cope with additional load & to be able to cover a large area of interest without degrading the service, networking clustering has been pursued in some routing approaches[4] . The hierarchical routing protocols involve nodes in multi-hop communication within a particular cluster to efficiently maintain the energy consumption of sensor nodes as well as perform data aggregation fusion to decrease the number of transmitted messages in the sink. Cluster formation is typically based on the energy reserve of sensors and sensor's proximity to the cluster head[5][6] . LEACH is one of the first hierarchical routing approaches for sensors networks.

Section 2-Proposed Scheme

The aim of LEACH protocol is to minimize energy consumption or in other words, to maximize the network lifetime. To make this happen several ideas are proposed for CH selection but they were based on mainly the node's (to be selected as CH) energy level. The node having greater energy level will be selected as CH most of the times. But here in the new proposed scheme not only the node's energy level is considered but also it's location or position both within the CH & from outside the cluster(neighbour clusters) are considered.

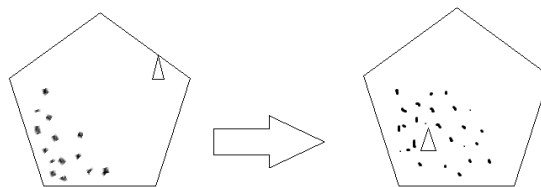
We know that there may a number of nodes in a cluster & there is always a CH. Suppose for example, if the CH lies at a distant position from the majority of nodes. So to communicate between CH & sensor nodes, since the distance between them is high, energy consumption for the communication is also high. That means, the higher the distance between CH & sensor nodes the greater the energy consumption.

Here a new idea to select the CH is given below :

1. Select the CH in the dense node zone.

To illustrate this say for example, you are announcing something. If the persons, for whom your announcement is, are very far from you, you have to shout more to make them listen to it but if those persons are near to you, you won't have to shout that much.

That means, if nodes are near to the CH, energy consumption is less.



2. Suppose a cluster is surrounded by 6 clusters. So 6 CH can communicate with the central CH. This central CH should be at an optimum distance from those CH. That means the distance between them should be balanced or on average.

Say, C0,C1,C2,C3,C4,C5,C6 are the CH of cluster 0(central cluster),cluster 1, cluster 2, cluster 3, cluster 4, cluster 5, cluster 6 respectively. There should not be a huge difference among distances between C0-C1,C0-C2,C0-C3,C0-C4,C0-C5,C0-C6.

Hence, energy consumption will be in control.

$$T(n) = \frac{p}{1-p \cdot (r \bmod \frac{1}{p})} \left(\frac{S(i).E}{E_{max}} \right) \left(\frac{D_{avg}}{\sum D_{inter_nodes}} \right) \quad \forall n \in G$$

$$T(n) = 0 \quad \forall n \text{ not } \in G$$

Where S(i).E is the current energy of each node and E_{max} is the initial energy of each node.

D_{avg} is the average distance from all other nodes in the cluster.

D_{inter_node} is the distance between any two nodes in the cluster.

Here with the original formula two factors are multiplied.

- Average distance from other nodes in same cluster/∑ inter-node distance

This factor checks whether the node, to be selected as CH, belongs to a density popular area as well as the distance from the node to the other nodes within the cluster is on average.

- Current energy of the node/Initial energy of each node

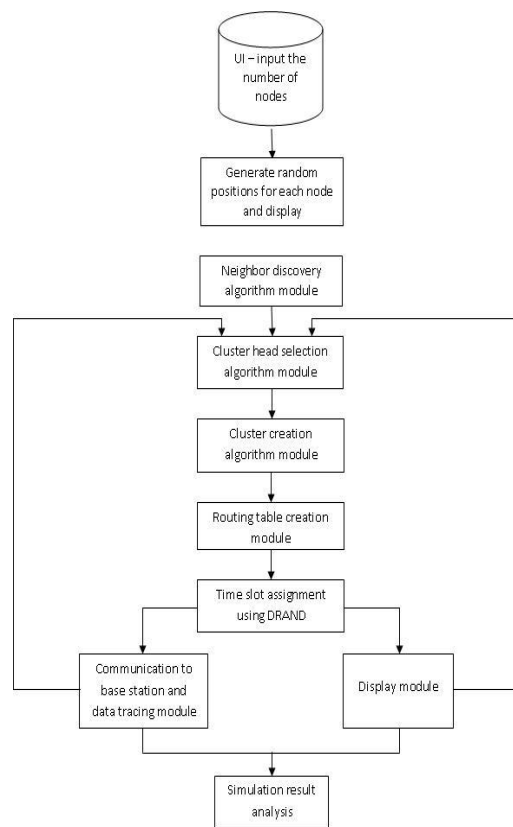
This factor suggests that each node computes the quotient of its own energy level and the aggregate energy remaining in the network. With this value each node decides if it becomes cluster-head for this round or not. High-energy nodes will more likely to become cluster-heads than low-energy nodes.

Section 3-Energy-aware multi-hop, multi-path hierarchy (EAMMH)

Clustering provides an effective way for prolonging the lifetime of a wireless sensor network. This paper elaborately compares two renowned routing protocols namely, LEACH and EAMMH for several general scenarios, and brief analysis of the simulation results against known metrics with energy and network lifetime being major among them. In this paper will the results and observations made from the analyses of results about these protocols are presented.

EAMMH routing protocol was developed by inducing the features of energy aware routing and multi-hop intra cluster routing [7]. The operation of the EAMMH protocol is broken up into rounds where each round begins with a set-up phase, when the clusters are organized, followed by a steady- state phase, when data transfers to the base station occur. The below flow chart describes the overview of the protocol initially the user has to give the input which is in the form of number of nodes.

Once the nodes are deployed, every node uses the neighbor discovery algorithm to discover its neighbor nodes. Using the cluster head selection algorithm cluster heads are selected among the nodes. These cluster heads broadcasts the advertisement message to all its neighboring nodes and thus clusters are formed with a fixed bound size. Each node in the cluster maintains routing table in which routing information of the nodes are updated. DRAND (distributed randomized time slot assignment algorithm) [8] method is used, it allows several nodes to share the same frequency channel by dividing the signal into different time slots. The cluster head aggregates the data from all the nodes in the cluster and this aggregated data is transmitted to the base station.



Setup Phase

Initially, after the node deployment the neighbor discovery takes place. This can be done using many methods like: k-of-n approach, ping, beacon messaging.

After the neighbor discovery, when cluster are being created, each node decides whether or not to become a cluster-head for the current round. This decision method is similar to the one used in LEACH. The setup phase operates in the following sequence:

1. CH (Cluster Head) Selection
2. Cluster Formation

Data Transmission Phase

Once the clusters are created, the sensor nodes are allotted timeslots to send the data. Assuming nodes always have data to send, they transmit it at their allotted time interval.

When a node receives data from one its neighbors, it aggregates it with its own data. While forwarding the aggregated data, it has to choose an optimal path from its routing table entries. It uses a heuristic function to make this decision and the heuristic function is given by,

$$h = K (E_{avg} / h_{min} * t)$$
 where K is a constant, E_{avg} is average energy of the current path, h_{min} is minimum hop count in current path, t = traffic in the current path.

The path with highest heuristic value is chosen. If this path's $E_{min} >$ threshold, it is chosen. Else the path with the next highest heuristic value is chosen, where

$E_{min} = E_{avg} / \text{const}$

The constant may be any integer value like 10.

If no node in the routing table has E_{min} greater than threshold energy, it picks the node with highest minimum energy.

The information about the paths and routing table entries at each node becomes stale after a little while. The heuristic values calculated based on the stale information often leads to wrong decisions. Hence the nodes are to be supplied with fresh information periodically. This will increase the accuracy and timeliness of the heuristic function. During the operation of each round, the necessary information is exchanged at regular intervals. The interval of periodic updates is chosen wisely such that the node does not base its decisions on the stale information and at the same time, the periodic update does not overload the network operation.

III. SIMULATION

- (A).LEACH and proposed scheme are compared using MATLAB.
- (B).Both LEACH and EAMMH are simulated using MATLAB.
- (C).Finally the three protocols are compared for energy consumption and lifetime.

The parameters taken into consideration while evaluating EAMMH and LEACH are as follows.

- 1.Round Number vs Number of Dead Nodes
- 2.Round Number vs Average Energy of Each node.

To simplify the simulation of these protocols few assumptions are made. They are as follows:

- 1. Initial energy of nodes is same.
- 2. Nodes are static
- 3. Nodes are assumed to have a limited transmission range after which a another equation for energy dissipation is used.
- 4. Homogeneous distribution of nodes.
- 5. Nodes always have to send the data.

Details of the simulation environment are mentioned in Table 1, given below:

Table 1: Simulation Details

Simulation Area	200*200
Base Station Location	(150,100)
Channel Type	Wireless Channel
Energy Model	Battery
<u>Transmission Amplifier</u>	
Efs	10pJ/bit/m2
Emp	0.0013pJ/bit/m4
Data Aggregation Energy	5nJ/bit
<u>Transmission</u>	
Energy, E_{Tx}	50nJ/bit
Receiving Energy, E_{Rx}	50nJ/bit
Packet size	4000bits
CH proportion	P=0.2
Number of nodes	200
Initial energy	1 J

Results:

(A). LEACH and proposed scheme are compared using MATLAB.

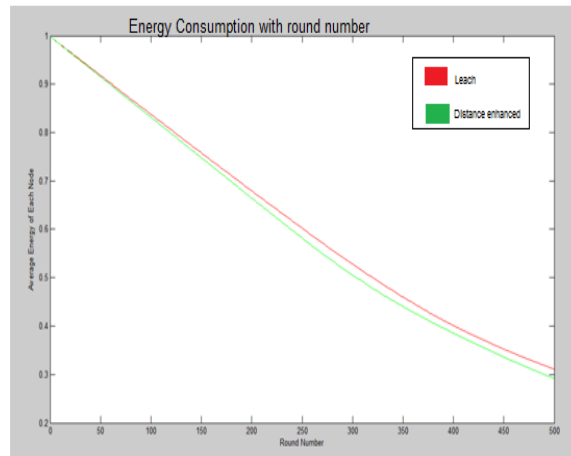


Fig. 2. Dissipation of energy in each node.

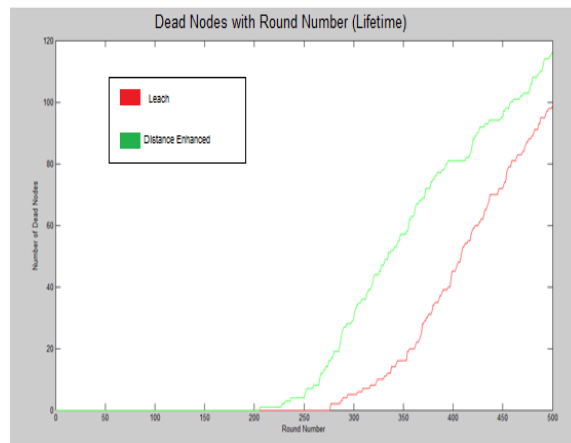


Fig. 3. Number of nodes dying with time

Since the goal is to maximize the lifetime of the network or to minimize the energy consumption, according to the new proposed formula the lifetime of the network will be greater than the Leach, as seen by the above graphs.(Fig.2,3)

The new proposed scheme obviously has future scope for betterment of increasing network lifetime. There will be more advancement in placing CH over the cluster to minimize energy conservation. The two new factors need further studies and practical implementation to understand their exact importance and efficiency.

(B). Both LEACH and EAMMH are simulated using MATLAB

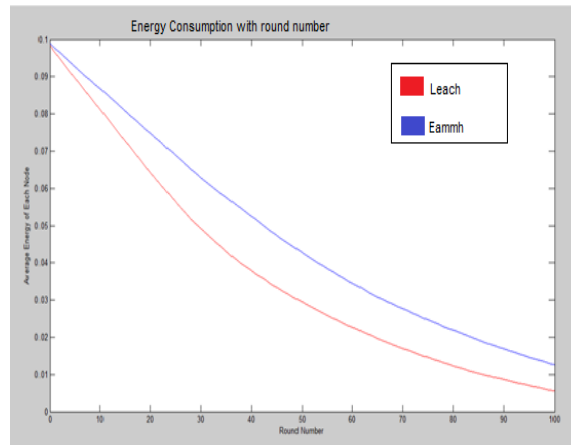


Fig. 4. Dissipation of energy in each node.

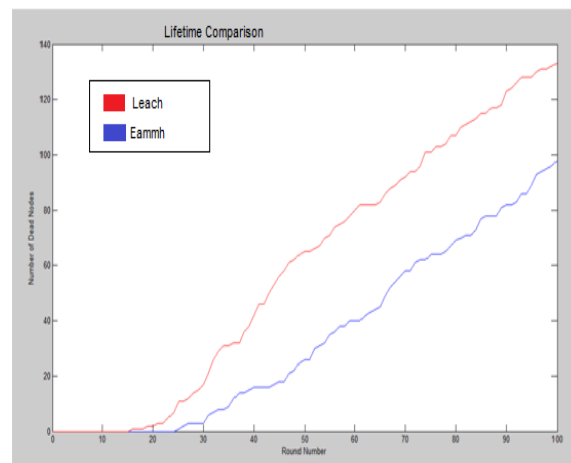


Fig. 5. Number of nodes dying with time

It is evident that for each probability level as the number of nodes increase EAMMH is seen to perform better in terms of average energy of each node (Fig.4) and the total number of dead nodes (Fig.5). However for a lesser number of total number of nodes, LEACH is found to perform better. We observe from most cases that even though EAMMH performs better, the first dead node in most of the operations is by EAMMH. LEACH on the other hand has a delayed time in getting the first dead node but a larger number of nodes run out of energy in a short period of time subsequently. We observe that LEACH at 0.05 probability is better than EAMMH, while at a probability of 0.1, EAMMH outperforms LEACH by a factor of 23% and at 0.2 probability by a factor of around 46%.

Even though LEACH employs Multi-hop mechanisms, EAMMH with the usage of Multi-path and hierarchical routing parameters and techniques with the inclusion of Multi-hop can perform with much better energy efficiency than LEACH in cases where more number of nodes are involved. In cases when there are a few nodes as an intra-cluster routing mechanism can add to the overhead of the node, LEACH in its simple mode of operation proves to be more energy efficient.

(C). Comparison of all three protocols using MATLAB

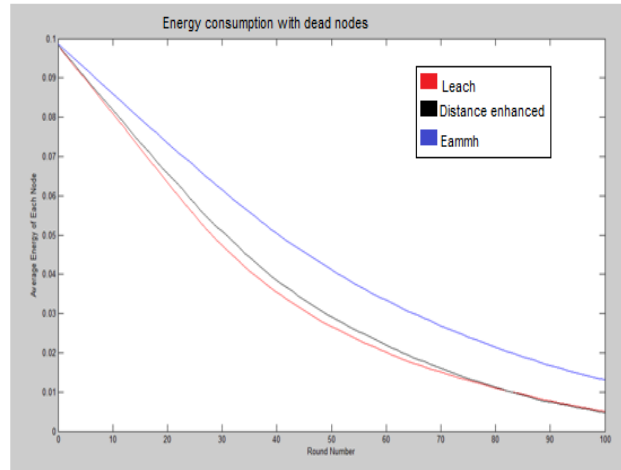


Fig. 6. Dissipation of energy in each node.

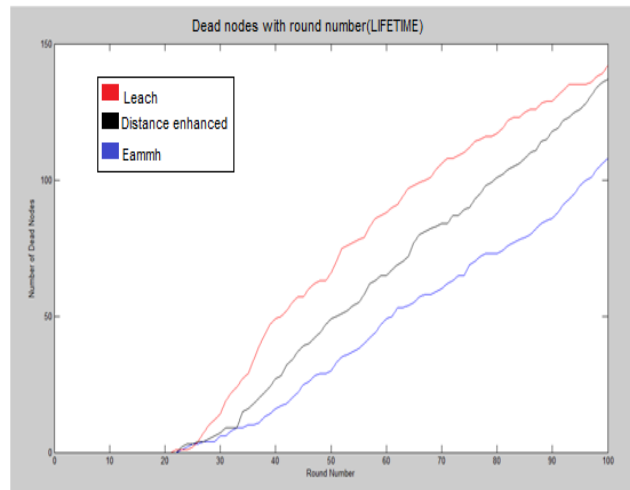


Fig. 7. Number of nodes dying with time

As seen from the above figures Eammh outperforms leach and the proposed scheme in terms of lifetime and using energy judiciously. Throughput, however, is almost the same when we talk of leach and scheme proposed. From the brief analyses of the simulation we have come to a conclusion that LEACH can be preferred in cases of smaller networks where the total number of nodes is less than fifty where it performs slightly better than EAMMH and EAMMH can be chosen in larger networks and also when the heuristic probability of Cluster Head selection is more. Although proposed scheme is always better than leach as it takes into account the energy levels of each node and the distance of cluster head from the sensor nodes and the sink.

The following table briefly describes various properties of differences and similarities in these three protocol.

S.no	Property of comparison	Leach	Propos-ed scheme	Eammh
1.	GPS requirement	No	No	Yes
2.	Multi-path routing	No	No	Yes
3.	Multi-hop routing	Yes	Yes	Yes
4.	Failure recovery	Yes	Yes	Yes
5.	Lifetime	Low	Medium	High
6.	Energy Consumption	High	Medium	Low
7.	Energy Distribution	Uniform	Uniform	Uniform
8.	Cluster head selection	Random	Determini-stic	Random
9.	Throughput	Low	Medium	Medium

Fig. 8. Table of comparison

IV. CONCLUSION AND FUTURE WORK

Wireless Sensor Networks are usually spread over large areas are recently finding applications in many fields. In this regard, there is a requirement of methods which can manage the WSN's in a better way. Wireless Sensor Networks are powered by the limited capacity of batteries. The main challenge in the design of protocols for Wireless Sensor Network is energy efficiency due to the limited amount of energy in the sensor nodes. The ultimate motive behind any routing protocol is to be as energy efficient as possible to keep the network running for a longer period of time. In this paper we have presented a detailed description of Leach, distance enhanced leach(proposed) and Eammh protocols. The factors included in leach are there in the new proposed scheme. Hence the proposed one is improved compared to the previous LEACH algorithm in terms of energy conservation.

If we analyze the new mathematical formula for increasing network lifetime, we will find enhanced results with the new. The new proposed scheme obviously has future scope for betterment of increasing network lifetime. There will be more advancement in placing CH over the cluster to minimize energy conservation.

REFERENCES

- [1]. W. Heinzelman, A. Chandrakasan and H. Balakrishnan, "Energy-Efficient Communication Protocol for Wireless Microsensor Networks," Proceedings of the 33rd Hawaii International Conference on System Sciences (HICSS '00), January 2000.
- [2]. Jamal N. Al-Karaki Ahmed E. Kamal – "Routing Techniques in Wireless Sensor Networks: A Survey" Dept. of Electrical and Computer Engineering Iowa State University, Ames, Iowa 50011.
- [3]. S. Tilak et al., "A Taxonomy of Wireless Microsensor Network Models",in ACM Mobile Computing and Communications Review(MC2R) June 2002.
- [4]. ZHANG Yu-quan, WEI Lei – "IMPROVING THE LEACH PROTOCOL FOR WIRELESS SENSOR NETWORKS"; School of Information and Electronics, Beijing Institute of Technology, Beijing 100081.
- [5]. A. Buczak and V. Jamalabad, "Self-organization of a Heterogeneous Sensor Network by Genetic Algorithms," *Intelligent Engineering Systems Through Artificial Neural Networks*, C.H. Dagli, et.(eds.), Vol. 8, pp. 259-264, ASME Press, New York, 1998
- [6]. C.R. Lin and M. Gerla, "Adaptive Clustering Mobile Wireless Networks," *IEEE Journal on Selected areas in Communications*, Vol. 15, No. 7, September 1997.
- [7]. Monica R Mundada, V CyrilRaj and T Bhuvanewari "Energy Aware Multi-Hop Multi-Path Hierarchical (EAMMH) Routing Protocol for Wireless Sensor Networks" European Journal Of Scientific Research ISSN 1450-216X Vol. 88 No 4 October, 2012
- [8]. Valerie Galluzzi and Ted Herman "Survey: Discovery in Wireless Sensor Networks"International Journal of Distributed Sensor Networks Volume 2012

A Review on HADOOP MAPREDUCE-A Job Aware Scheduling Technology

Silky Kalra¹, Anil lamba²

1 M.Tech Scholar, Computer Science & Engineering, Haryana Engineering College Jagadhari, Haryana,

2 Associate Professor, Department of Computer Science & Engineering, Haryana Engineering College Jagadhari, Haryana

ABSTRACT:

Big data technology remodels many business organization perspective on the data. conventionally, a data framework was like a gatekeeper for data access. such frameworks were built as monolithic “scale up”, self contained appliances. Any added scale required added resources, which often exponentially multiplies cost. One of the key approaches that have been at the center of the big data technology landscape is Hadoop. This research paper includes detailed view of various important components of Hadoop, job aware scheduling algorithms for mapreduce framework, various DDOS attack and defense methods.

KEYWORDS: *Distributed Denial-of-Service (DDoS), Hadoop, Job aware scheduling, Mapreduce,*

I. INTRODUCTION

MapReduce is currently the most famous framework for data intensive computing. MapReduce is motivated by the demands of processing huge amounts of data from a web environment. MapReduce provides an easy parallel programming interface in a distributed computing environment. Also MapReduce deals with fault tolerance issues for managing multiple processing nodes. The most powerful feature of MapReduce is its high scalability that allows user to process a vast amount of data in a short time. There are many fields that benefit from MapReduce, such as Bioinformatics, machine learning, scientific analysis, web data analysis, astrophysics, and security. There are some implemented systems for data intensive computing, such as Hadoop. An open source framework, Hadoop resembles the original MapReduce.

With increasing use of the Internet, Internet attacks are on the rise. Distributed Denial-of-Service (DDoS) in particular is increasing more. There are four main ways to protect against DDoS attacks: attack prevention, attack detection, attack source identification, and attack reaction. DDoS attack is one such threat which is distributed form of Denial of Service attack in which service is consumed by an attacker and legitimate user can not use the service. DDoS attack is one such threat which is distributed form of Denial of Service attack in which service is consumed by attacker and legitimate user can not use the service. We can find a solution against DDoS attack, but they are based on a single host and lacks performance so here Hadoop system for distributed processing is used.

II. HADOOP

The GMR(Google map reduce) was invented by Google back in their earlier days so they could usefully index all the rich textural and structural information they were collecting, and then present meaningful and actionable results to users. MapReduce(you map the operation out to all of those servers and then you reduce the results back into a single result set), is a software paradigm for processing a large data set in a distributed parallel way. Since Google’s MapReduce and Google file system (GFS) are proprietary, an open-source MapReduce software project, Hadoop, was launched to provide similar capabilities of the Google’s MapReduce platform by using thousands of cluster nodes[1]. Hadoop distributed file system (HDFS) is also an important component of Hadoop, that corresponds to GFS. Hadoop consists of two core components: the job management framework that handles the map and reduces tasks and the Hadoop Distributed File System (HDFS). Hadoop’s job management framework is highly reliable and available, using techniques such as replication and automated restart of failed tasks.

2.1 Hadoop cluster architecture

A small Hadoop cluster includes a single master and multiple worker nodes. The master node consists of a JobTracker, TaskTracker, NameNode and DataNode. A slave or *worker node* acts as both a DataNode and TaskTracker, though it is possible to have data-only worker nodes and compute-only worker nodes. These are normally used only in nonstandard applications. Hadoop requires [Java Runtime Environment \(JRE\)](#) 1.6 or higher. The standard start-up and shutdown scripts require [Secure Shell](#) to be set up between nodes in the cluster.

In a larger cluster, the HDFS is managed through a dedicated NameNode server to host the file system index, and a secondary NameNode that can generate snapshots of the namenode's memory structures, thus preventing file-system corruption and reducing loss of data.

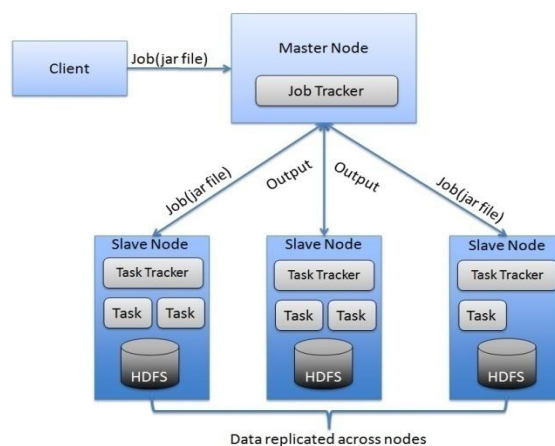


Figure 1. shows Hadoop multinode cluster architecture which works in distributed manner for MapReduce problem.

Similarly, a standalone JobTracker server can manage job scheduling. In clusters where the Hadoop MapReduce engine is deployed against an alternate file system, the NameNode, secondary NameNode and DataNode architecture of HDFS is replaced by the file-system-specific equivalent.

2.2 Hadoop distributed file system

HDFS stores large files (typically in the range of gigabytes to terabytes^[13]) across multiple machines. It achieves the reliability by replicating the data across multiple hosts, and hence does theoretically not require RAID storage on hosts (but to increase I/O performance some RAID configurations are still useful). With the default replication value, 3, data is stored on three nodes: two on the same rack, and one on a different rack.

The HDFS file system includes a so-called *secondary namenode*, which misleads some people into thinking ^[citation needed] that when the primary namenode goes offline, the secondary namenode takes over. In fact, the secondary namenode regularly connects with the primary namenode and builds snapshots of the primary namenode's directory information, which the system then saves to local or remote directories. These checkpoint images can be used to restart a failed primary namenode without having to replay the entire journal of file-system actions, then to edit the log to create an up-to-date directory structure. Because the namenode is the single point for storage and management of metadata, it can become a bottleneck for supporting a huge number of files, especially a large number of small files. HDFS Federation, a new addition, aims to tackle this problem to a certain extent by allowing multiple name-spaces served by separate namenodes.

An advantage of using HDFS is data awareness between the job tracker and task tracker. The job tracker schedules map or reduce jobs to task trackers with an awareness of the data location. For example: if node A contains data (x,y,z) and node B contains data (a,b,c), the job tracker schedules node B to perform map or reduce tasks on (a,b,c) and node A would be scheduled to perform map or reduce tasks on (x,y,z). This reduces the amount of traffic that goes over the network and prevents unnecessary data transfer.

2.3 Hadoop V/S Dbms

However, no compelling reason to choose MR over a database for traditional database workloads

MapReduce is designed for one-off processing tasks

- Where fast load times are important
- No repeated access. It decomposes queries into sub-jobs, schedules them with different policies.

DBMS	HADOOP
In a centralized database system, you've got one big disk connected to four or eight or 16 big processors. But that is as much horsepower as you can bring to bear	In a Hadoop cluster, every one of those servers has two or four or eight CPUs. You can run your indexing job by sending your code to each of the dozens of servers in your cluster, and each server operates on its own little piece of the data. Results are then delivered back to you in a unified whole.
To DBMS researchers, programming model doesn't feel new	Hadoop MapReduce is a new way of thinking about programming large distributed systems
Schemas: DBMS require them	Schemas: - MapReduce doesn't require them - Easy to write simple MR problems - No logical data independence

Table1. Comparison of Approaches

III. DISTRIBUTED DENIAL OF SERVICE ATTACK

A denial-of-service attack (DoS attack) is an attempt to make a computer resource unavailable to its intended users[1]. Distributed denial-of-service attack (DDoS attack) is a kind of DoS attack where attackers are distributed and targeting a victim. It generally consists of the concerted efforts of a person, or multiple people to prevent an Internet site or service from functioning efficiently or at all, temporarily or indefinitely.

3.1 How DDoS Attack works

DDoS attack is performed by infected machines called bots and a group of bots is called a botnet. This bots (Zombie) are controlled by an attacker by installing malicious code or software which acts as per command passed by an attacker. Bots are ready to attack any time upon receiving commands from the attacker. Many types of agents have scanning capability that permit to identify open port of a range of machines. When the scanning is finished, the agent takes the list of machines with open port and launches vulnerability-specific scanning to detect machines with un-patched vulnerability. If the agent found a machine with vulnerability, it could launch an attack to install another agent on the machine.

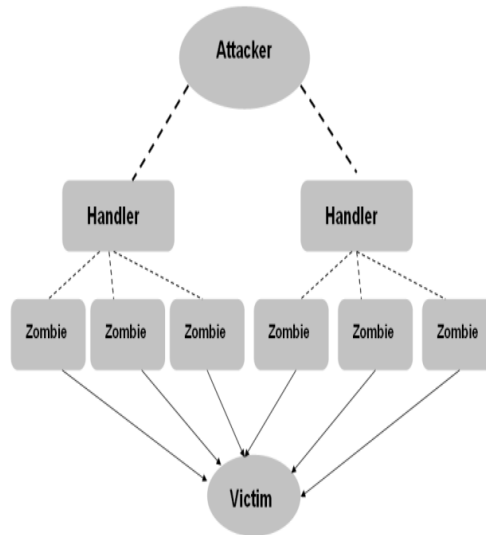


Fig 2. shows DDoS attack architecture, explaining its working mechanism.

IV. FAIR SCHEDULER

The core idea behind the fair scheduler is to assign resources to jobs such that on average over time, each job gets an equal share of the available resources. This behavior allows for some interactivity among Hadoop jobs and permits greater responsiveness of the Hadoop cluster to the variety of job types submitted.

The number of jobs active at one time can also be constrained, if desired, to minimize congestion and allow work to finish in a timely manner. To ensure fairness, each user is assigned to a pool. In this way, if one user submits many jobs, he or she can receive the same share of cluster resources as all other users (independent of the work they have submitted).

V. 5. RELATED STUDY

In [1], Prashant Chauhan, Abdul Jhummarwala, Manoj Pandya in December, 2012 provided an overview of Hadoop. This type of computing can have a homogeneous or a heterogeneous platform and hardware. The concept of cloud computing and virtualization has derived much momentum and has turned a more popular phrase in information technology. Many organizations have started implementing these new technologies to further cut down costs through improved machine utilization, reduced administration time and infrastructure costs. Cloud computing also confronts challenges. One of such problem is DDoS attack so in this paper author will focus on DDoS attack and how to overcome from it using honeypot. For this here open source tools and software are used. Typical DDoS solution mechanism is a single host oriented and in this paper focused on a distributed host oriented solution that meets scalability.

In [2], Jin-Hyun Yoon, Ho-Seok Kang and Sung-Ryul Kim, in 2012, proposed a technique called "triangle expectation" is used, which works to find the sources of the attack so that they can be identified and blocked. To analyze a large amount of collecting network connection data, a sampling technique has been used and the proposed technique is verified by experiments.

In [3], B. B. Gupta, R. C. Joshia, Manoj Misra, in 2009, the main aim of this paper is First is to demonstrate a comprehensive study of a broad range of DDoS attacks and defense methods proposed to fight with them. This provides a better understanding of the problem, current solution space, and future research scope to fight down against DDoS attacks. Second is to offer an integrated solution for entirely defending against flooding DDoS attacks at the Internet Service Provider (ISP) level.

In [4], Yeonhee Lee, Youngseok Lee, in 2011 proposed a novel DDoS detection method based on Hadoop that implements an HTTP GET flooding detection algorithm in MapReduce on the distributed computing platform.

In [5], Matei Zaharia, Dhruba Borthakur, Joydeep Sen Sarma, Khaled Elmeleegy, Scott Shenker, Ion Stoica, in April 2009, provided an overview of Sharing a MapReduce cluster between users. It is attractive because it enables statistical multiplexing (lowering costs) and allows users to share a common large data set. They evolved two simple techniques, delay scheduling and copy-compute splitting, which improve throughput and response times by factors of 2 to 10. Although we concentrate on multi-user workloads, our techniques can also increase throughput in a single-user, FIFO workload by a factor of 2.

In [6], Radheshyam Nanduri, Nitesh Maheshwari, Reddy Raja, Vasudeva Varma, in 2011, proposed an approach which attempts to hold harmony among the jobs running on the cluster, and in turn minimize their runtime. In their model, the scheduler is made mindful of different types of jobs running on the cluster. The scheduler tries to assign a task on a node if the incoming task does not affect the tasks already running on that node. From the list of addressable pending tasks, our algorithm picks out the one that is most compatible with the tasks already running on that node. They bring up heuristic and machine learning based solutions to their approach and attempt to maintain a resource balance on the cluster by not overloading any of the nodes, thereby cutting down the overall runtime of the jobs. The results exhibit a saving of runtime of around 21% in the case of heuristic based approach and approximately 27% in the case of machine learning based approach when compared to Yahoo's Capacity scheduler.

In [7], Dongjin Yoo, Kwang Mong Sim, in 2011, compare contrasting scheduling methods, evaluating their features, strengths and weaknesses. For settlement of synchronization overhead, two categories of studies; asynchronous processing and speculative execution are addressed. For delay scheduling in Hadoop, Quincy scheduler in Dryad and fairness constraints with locality improvement are addressed.

VI. CONCLUSION AND FUTURE WORK

Traditional scheduling methods perform very poorly in mapreduce due to two aspects

- running computation where the data is
- Dependence between map and reduce task .

The Hadoop accomplishment creates a set of pools into which jobs are placed for selection by the scheduler. Each pool can be assigned shares to balance the resources across jobs in pools. By default, all pools have same shares, but we can configure accordingly to provide more or fewer shares depending upon the job type.

REFERENCES

- [1] Prashant Chauhan, Abdul Jhummarwala, Manoj Pandya, "Detection of DDoS Attack in Semantic Web" International Journal of Applied Information Systems (IJ AIS) – ISSN : 2249-0868 Foundation of Computer Science FCS, New York, USA Volume 4– No.6, December 2012 – www.ijais.org, pp. 7-10
- [2] Jin-Hyun Yoon, Ho-Seok Kang and Sung-Ryul Kim, Division of Internet and Media, Konkuk University, Seoul, Republic of Korea h2jhyoon@gmail.com, hsriver@gmail.com, kimsr@konkuk.ac.kr pp. 200-203
- [3] B. B. Gupta, Joshi, R. C. and Misra, Manoj (2009), 'Defending against Distributed Denial of Service Attacks: Issues and Challenges', Information Security Journal: A Global Perspective, 18: 5, 224 – 247
- [4] Yeonhee Lee, Chungnam National University, Daejeon, 305-764, Republic of Korea, yhlee06@cnu.ac.kr.
- [5] Matei Zaharia, Dhruba Borthakur, Joydeep Sen Sarma, Khaled Elmelegy, Scott Shenker, Ion Stoica, "Job Scheduling for Multi-User MapReduce Clusters", University of California, Berkeley, Facebook Inc, Yahoo! Research Electrical Engineering and Computer Sciences University of California at Berkeley Technical Report No. UCB/EECS-2009-55 <http://www.eecs.berkeley.edu/Pubs/TechRpts/2009/EECS-2009-55.html> April 30, 2009
- [6] Radheshyam Nanduri, Nitesh Maheshwari, Reddy Raja, Vasudeva Varma, "Job Aware Scheduling Algorithm for MapReduce Framework" by In 3rd IEEE International Conference on Cloud Computing Technology and Science Athens, Greece. Report No: IIT/TR/2011/-1, Centre for Search and Information Extraction Lab, International Institute of Information Technology, Hyderabad - 500 032, INDIA, November 2011, pp. 724-729
- [7] Dongjin Yoo, Kwang Mong Sim, A comparative review of job scheduling for mapreduce Multi-Agent and Cloud Computing Systems Laboratory, School of Information and Communication, Gwangju Institute of Science and Technology (GIST), Gwangju, IEEE CCIS2011, 978-1-61284-204-2/11/\$26.00 ©2011 IEEE, pp.353-358
- [8] Mirkovic and P. Reiher, A Taxonomy of DDoS Attack and DDoS Defense Mechanisms, ACM SIGCOMM CCR, 2004
- [9] H. Sun, Y. Zhang, and H. Chao, A Principal Components Analysis-based Robust DDoS Defense System, IEEE ICC, 2008
- [10] Y. Lee, W. Kang, and Y. Lee, A Hadoop-based Packet Trace Processing Tool, TMA, April 2011
- [11] Jeffrey Dean and Sanjay Ghemawat. Mapreduce: simplified data processing on large clusters Commun. ACM, 51(1):107– 113, 2008.
- [12] Jaideep Dhok, Nitesh Maheshwari, and Vasudeva Varma. Learning based opportunistic admission control algorithm for mapreduce as a service. In ISEC '10: Proceedings of the 3rd India software engineering conference, pages 153–160. ACM, 2010.
- [13] Richard O. Duda, Peter E. Hart, and David G. Stork. Pattern Classification (2nd Edition). Wiley-Interscience, edition, November 2000.
- [14] Geoffrey Holmes Bernhard Pfahringer Peter Reutemann Ian H. Witten Mark Hall, Eibe Frank. The weka data mining software. SIGKDD Explorations, 11(1), 2009.
- [15] Hadoop Distributed File System. http://hadoop.apache.org/common/docs/current/hdfs_design.html.
- [16] Fair Scheduler. http://hadoop.apache.org/common/docs/r0.20.2/fair_scheduler.html.
- [17] Capacity Scheduler. http://hadoop.apache.org/common/docs/r0.20.2/capacity_scheduler.html.
- [18] Quan Chen, Daqiang Zhang, Minyi Guo, Qianni Deng, and Song Guo. Samr: A self-adaptive mapreduce scheduling algorithm in heterogeneous environment. In Computer and Information Technology (CIT), 2010 IEEE 10th International Conference on, 29 2010.
- [19] J. Polo, D. Carrera, Y. Becerra, V. Beltran, J. Torres, and E. Ayguade and. Performance management of accelerated mapreduce workloads in heterogeneous clusters. In Parallel Processing (ICPP), 2010 39th International Conference on, pages 653 –662, 2010.
- [20] Aameek Singh, Madhukar Korupolu, and Dushmanta Mohapatra. Server-storage virtualization: integration and load balancing in data centers. In Proceedings of the 2008 ACM/IEEE conference on Supercomputing, SC '08, pages 53:1–53:12, Piscataway, NJ, USA, 2008. IEEE Press.

Harmonic Reduction by Using Shunt Hybrid Power Filter

Kavita Dewangan¹, Prof. Pawan C. Tapre²

¹ SSTC (SSGI), Junwani, Bhilai and 490001, India

² Prof. of SSTC (SSGI), Junwani, Bhilai and 490001, India

ABSTRACT:

This project report presents design, simulation and development of passive shunt filter and shunt hybrid power filter (SHPF) for mitigation of the power quality problem at ac mains in ac-dc power supply feeding to a nonlinear load. The power filter is consisting of a shunt passive filter connected in series with an active power filter. At first passive filter has been designed to compensate harmonics. The drawback associated with the passive filter like fixed compensation characteristics and resonance problem is tried to solve by SHPF. Simulations for a typical distribution system with a shunt hybrid power filter have been carried out to validate the presented analysis. Harmonic contents of the source current has been calculated and compared for the different cases to demonstrate the influence of harmonic extraction circuit on the harmonic compensation characteristic of the shunt hybrid power filter.

Keywords: active power filter, alternating current, direct current, harmonic compensation, modeling, Shunt passive filter, shunt hybrid power filter,

I. INTRODUCTION

Now a day's power electronic based equipment are used in industrial and domestic purpose. These equipments have significant impacts on the quality of supplied voltage and have increased the harmonic current pollution of distribution systems. They have many negative effects on power system equipment and customer, such as additional losses in overhead and underground cables, transformers and rotating electric machines, problem in the operation of the protection systems, over voltage and shunt capacitor, error of measuring instruments, and malfunction of low efficiency of customer sensitive loads. Passive filter have been used traditionally for mitigating the distortion due to harmonic current in industrial power systems. But they have many drawbacks such as resonance problem, dependency of their performance on the system impedance, absorption of harmonic current of nonlinear load, which could lead to further harmonic propagation through the power system.

To overcome of such problem active power filters is introduced. It has no such drawbacks like passive filter. They inject harmonic voltage or current with appropriate magnitudes and phase angle into the system and cancel harmonics of nonlinear loads. But it has also some drawbacks like high initial cost and high power losses due to which it limits there wide application, especially with high power rating system.

To minimize these limitations, hybrid power filter have been introduced and implemented in practical system applications. Shunt hybrid filter is consists of an active filter which is connected in series with the passive filter and with a three phase PWM inverter. This filter effectively mitigates the problem of a passive and active filter. It provides cost effective harmonic compensation, particularly for high power nonlinear load.

II. SHUNT HYBRID POWER FILTER

2.1 Introduction

Hybrid filters provide cost-effective harmonic compensation particularly for high-power nonlinear load. A parallel hybrid power filter system consists of a small rating active filter in series with a passive filter. The active filter is controlled to act as a harmonic compensator for the load by confining all the harmonic currents into the passive filter. This eliminates the possibility of series and parallel resonance.

The schematic diagram of the shunt hybrid power filter (SHPF) is presented in Fig.1. The scheme contains the three phase supply voltage, three phase diode rectifier and the filtering system consists of a small-rating active power filter connected in series with the LC passive filter. This configuration of hybrid filter ensures the compensation of the source current harmonics by enhancing the compensation characteristics of the passive filter besides eliminating the risk of resonance. It provides effective compensation of current harmonics and limited supply voltage distortion. The hybrid filter is controlled such that the harmonic currents of the nonlinear loads flow through the passive filter and that only the fundamental frequency component of the load current is to be supplied by the ac mains.

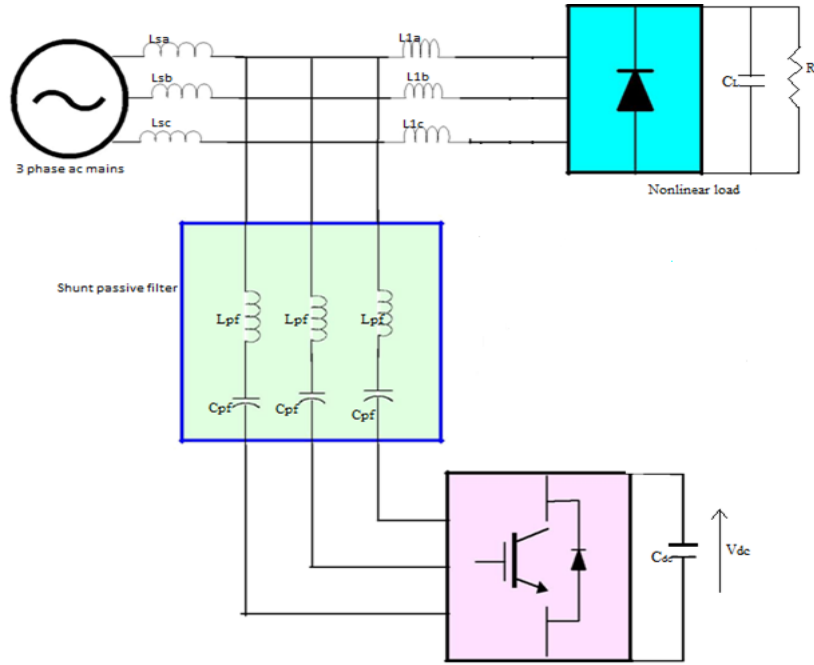


Fig.1 Schematic diagram of 3-phase SHPF Supplying power to Nonlinear Load

2.2 Modeling of the SHPF

2.2.1 Model in a-b-c reference frame:

Kirchhoff's law of voltage and currents applied to this system provide three differential equations in the stationary "a-b-c" frame (for k = 1, 2, 3)

$$V_{sk} = L_{PF} \frac{di_{ck}}{dt} + R_{PF} i_{ck} + \frac{1}{C_{PF}} \int i_{ck} dt + V_{KM} + V_{MN} \quad (1)$$

Differentiating (1) we get

$$\frac{dV_{sK}}{dt} = L_{PF} \frac{d^2 i_{cK}}{dt^2} + R_{PF} \frac{di_{cK}}{dt} + \frac{1}{C_{PF}} i_{cK} + \frac{dV_{KM}}{dt} + \frac{dV_{MN}}{dt} \quad (2)$$

Assume that the zero sequence current is absent in a three phase system and the source voltages are balanced, so we obtain:

$$V_{MN} = -\frac{1}{3} \sum_{k=1}^3 V_{kM} \quad (3)$$

We can define the switching function C_k of the converter k^{th} leg as being the binary state of the two switches S_k and S'_k . Hence, the switching C_k (for k = 1, 2, 3) is defined as

$C_k = 1$, if S_k is On and S'_k is Off,

$C_k = 0$, if S_k is Off and S'_k is On.

Thus, with $V_{kM} = C_k V_{dc}$, and from (4), the following relation is obtained:

$$\frac{d^2 i_{cK}}{dt^2} = -\frac{R_{PF}}{L_{PF}} \frac{di_{cK}}{dt} - \frac{1}{C_{PF} L_{PF}} i_{cK} - \frac{1}{L_{PF}} \left(C_K - \frac{1}{3} \sum_{m=1}^3 C_m \right) \frac{dV_{dc}}{dt} + \frac{1}{L_{PF}} \frac{dV_{sK}}{dt} \quad (5)$$

Let the Switching state function be defined as

$$q_{nk} = \left(C_K - \frac{1}{3} \sum_{m=1}^3 C_m \right)_n \quad (6)$$

The value of q_{nk} depends on the switching state n and on the phase k. This shows the interaction between the three phases. Conversion from $[C_k]$ to $[q_{nk}]$ is as follows

$$q_{n1} = \frac{2}{3} C_1 - \frac{1}{3} C_2 - \frac{1}{3} C_3 \quad (7)$$

$$q_{n2} = -\frac{1}{3}C_1 + \frac{2}{3}C_2 - \frac{1}{3}C_3 \tag{8}$$

$$q_{n3} = -\frac{1}{3}C_1 - \frac{1}{3}C_2 + \frac{2}{3}C_3 \tag{9}$$

Hence we got the relation as

$$\begin{bmatrix} q_{n1} \\ q_{n2} \\ q_{n3} \end{bmatrix} = \frac{1}{3} \begin{bmatrix} 2 & -1 & -1 \\ -1 & 2 & -1 \\ -1 & -1 & 2 \end{bmatrix} \begin{bmatrix} C_1 \\ C_2 \\ C_3 \end{bmatrix} \tag{10}$$

The matrix in (10) is of rank 2 q_{nk} has no zero sequence components. By the analysis of the dc component of the system it gives

$$dV_{dc} = \frac{1}{C_{dc}} i_{dc} = \frac{1}{C_{dc}} \sum_{k=1}^3 q_{nk} i_{ck} \tag{11}$$

With the absence of zero sequence components in i_k and q_{nk} one can get

$$\frac{dV_{dc}}{dt} = \frac{1}{C_{dc}} (2q_{n1} + q_{n2})i_{c1} + \frac{1}{C_{dc}} (q_{n1} + q_{n2})i_{c2} \tag{12}$$

Hence the complete model of the active filter in “a-b-c” reference frame is obtained as follows

The application of (5) for phase 1 and 2 with (13)

$$\begin{aligned} L_{PF} \frac{d^2 i_{c1}}{dt^2} &= -R_{PF} \frac{di_{c1}}{dt} - \frac{1}{C_{CF}} i_{c1} - q_{n1} \frac{dV_{dc}}{dt} + \frac{dV_{s1}}{dt} \\ L_{PF} \frac{d^2 i_{c2}}{dt^2} &= -R_{PF} \frac{di_{c2}}{dt} - \frac{1}{C_{CF}} i_{c2} - q_{n2} \frac{dV_{dc}}{dt} + \frac{dV_{s2}}{dt} \\ C_{dc} \frac{dV_{dc}}{dt} &= (2q_{n1} + q_{n2})i_{c1} + (q_{n1} + q_{n2})i_{c2} \end{aligned} \tag{13}$$

The above model is time varying and nonlinear in nature.

2.2.2 Model Transformation in to “d-q” reference frame:

Since the steady state fundamental components are sinusoidal, the system is transformed into the synchronous orthogonal frame rotating at constant supply frequency. The conversion matrix is

$$C_{dq}^{123} = \sqrt{\frac{2}{3}} \begin{bmatrix} \cos\theta & \cos(\theta - 2\pi/3) & \cos(\theta - 4\pi/3) \\ -\sin\theta & -\sin(\theta - 2\pi/3) & -\sin(\theta - 4\pi/3) \end{bmatrix} \tag{14}$$

where $\theta = \omega t$, and the following equalities hold:

$$C_{123}^{dq} = (C_{dq}^{123})^{-1} = (C_{dq}^{123})^T$$

Now (13) is

$$\frac{dV_{dc}}{dt} = \frac{1}{C_{dc}} (q_{n1})^T (i_{c123}) \tag{15}$$

Applying coordination transformation

$$\frac{dV_{dc}}{dt} = \frac{1}{C_{dc}} [C_{123}^{dq} (q_{ndq})^T] [C_{123}^{dq} (i_{dq})] = \frac{1}{C_{dc}} [(q_{ndq})^T] [(i_{dq})] \tag{16}$$

On the other hand, the two first equations in (13) are written as

$$\frac{d^2 [i_{c12}]}{dt^2} = -\frac{R_{PF}}{L_{PF}} \frac{d}{dt} [i_{c12}] - \frac{1}{C_{PF} L_{PF}} [i_{c12}] - \frac{1}{L_{PF}} [q_{n12}] \frac{dV_{dc}}{dt} + \frac{1}{L_{PF}} \frac{d}{dt} [V_{c12}] \tag{17}$$

The reduced matrix can be used

$$C_{dq}^{12} = \sqrt{2} \begin{bmatrix} \cos(\theta - \frac{\pi}{6}) & \sin\theta \\ -\sin(\theta - \frac{\pi}{6}) & \cos\theta \end{bmatrix} \tag{18}$$

It has the following inverse

$$C_{12}^{dq} = \sqrt{\frac{2}{3}} \begin{bmatrix} \cos\theta & -\sin\theta \\ \sin(\theta - \frac{\pi}{6}) & \cos(\theta - \frac{\pi}{6}) \end{bmatrix} \tag{19}$$

Apply this transformation into (17)

$$\frac{d^2 [C_{12}^{dq} [i_{dq}]]}{dt^2} = -\frac{R_{PF}}{L_{PF}} \frac{d}{dt} [C_{12}^{dq} [i_{dq}]] - \frac{1}{C_{PF} L_{PF}} [i_{dq}] - \frac{1}{L_{PF}} [C_{12}^{dq} [q_{ndq}]] \frac{dV_{dc}}{dt} + \frac{1}{L_{PF}} \frac{d}{dt} [C_{12}^{dq} [V_{dq}]] \quad (20)$$

With the following matrix differential property

$$\frac{d [C_{12}^{dq} [i_{dq}]]}{dt} = C_{12}^{dq} \frac{d}{dt} [i_{dq}] + \left(\frac{d}{dt} C_{12}^{dq} \right) [i_{dq}] \quad (21)$$

$$\frac{d^2 [C_{12}^{dq} [i_{dq}]]}{dt^2} = C_{12}^{dq} \frac{d^2}{dt^2} [[i_{dq}]] + \left(\frac{d}{dt} C_{12}^{dq} \right) \left[\frac{d}{dt} [i_{dq}] \right] + \left(\frac{d}{dt} C_{12}^{dq} \right) \frac{d}{dt} + \left(\frac{d^2}{dt^2} C_{12}^{dq} \right) [[i_{dq}]] \quad (22)$$

Now the following relation is derived:

$$\frac{d^2 [i_{dq}]}{dt^2} = - \begin{bmatrix} \frac{R_{PF}}{L_{PF}} & -2\omega \\ 2\omega & \frac{R_{PF}}{L_{PF}} \end{bmatrix} \frac{d [i_{dq}]}{dt} + \begin{bmatrix} -\omega^2 + \frac{1}{L_{PF} C_{PF}} & -\omega \frac{R_{PF}}{L_{PF}} \\ \omega \frac{R_{PF}}{L_{PF}} & -\omega^2 + \frac{1}{L_{PF} C_{PF}} \end{bmatrix} [i_{dq}] - \frac{1}{L_{PF}} [q_{ndq}] \frac{d [V_{dc}]}{dt} + \frac{1}{L_{PF}} \frac{d}{dt} [V_{dc}] + \frac{1}{L_{PF}} \begin{bmatrix} 0 & -\omega \\ \omega & 0 \end{bmatrix} [V_{dq}] \quad (23)$$

Now the complete model in the d-q frame is obtained from (16) and (23)

$$\begin{aligned} L_{PF} \frac{d^2 i_d}{dt^2} &= -R_{PF} \frac{di_d}{dt} + 2\omega L_{PF} \frac{di_d}{dt} - \left(-\omega^2 L_{PF} + \frac{1}{C_{PF}} \right) i_d + \omega R_{PF} i_q - q_{nd} \frac{dV_{dc}}{dt} + \frac{dV_d}{dt} - \omega V_q \\ L_{PF} \frac{d^2 i_q}{dt^2} &= -R_{PF} \frac{di_q}{dt} - 2\omega L_{PF} \frac{di_q}{dt} - \left(-\omega^2 L_{PF} + \frac{1}{C_{PF}} \right) i_q - \omega R_{PF} i_d - q_{nq} \frac{dV_{dc}}{dt} + \frac{dV_q}{dt} + \omega V_d \\ C_{dc} \frac{dV_{dc}}{dt} &= q_{nd} i_d + q_{nq} i_q \end{aligned} \quad (24)$$

The model is time invariant during a given switching state.

2.3 Harmonic current control

$$\begin{aligned} L_{PF} \frac{d^2 i_d}{dt^2} + R_{PF} \frac{di_d}{dt} + \left(-\omega^2 L_{PF} + \frac{1}{C_{PF}} \right) i_d &= 2\omega L_{PF} \frac{di_q}{dt} + \omega R_{PF} i_q - q_{nd} \frac{dV_{dc}}{dt} + \frac{dV_d}{dt} - \omega V_q \\ L_{PF} \frac{d^2 i_q}{dt^2} - R_{PF} \frac{di_q}{dt} + \left(-\omega^2 L_{PF} + \frac{1}{C_{PF}} \right) i_q &= -2\omega L_{PF} \frac{di_d}{dt} - \omega R_{PF} i_d - q_{nq} \frac{dV_{dc}}{dt} + \frac{dV_q}{dt} + \omega V_d \end{aligned} \quad (25)$$

$$\begin{aligned} V_d &= 2\omega L_{PF} \frac{di_q}{dt} + \omega R_{PF} i_q - q_{nd} \frac{dV_{dc}}{dt} + \frac{dV_d}{dt} - \omega V_q \\ V_q &= 2\omega L_{PF} \frac{di_d}{dt} - \omega R_{PF} i_d - q_{nq} \frac{dV_{dc}}{dt} + \frac{dV_q}{dt} + \omega V_d \end{aligned} \quad (26)$$

Now the transfer function of the model is:

$$\frac{I_d(S)}{V_d(S)} = \frac{1}{L_{PF} S^2 + R_{PF}(S) + 1/C_{PF} - L_{PF} \omega^2} \quad (27)$$

Transfer function of the P-I controller is given as

$$G_i(S) = \frac{U_d(S)}{I_d(S)} = \frac{U_q(S)}{I_q(S)} = K_p + \frac{K_i}{S} \quad (28)$$

The closed loop transfer function of the current loop is

$$\frac{I_q(S)}{I_q^*(S)} = \frac{I_d(S)}{I_d^*(S)} = \frac{K_p}{L_{PF} S + \frac{R_{PF}}{L_{PF}} S^2 + \left(\frac{1}{C_{PF} L_{PF}} - \omega^2 + \frac{K_p}{L_{PF}} \right) S + \frac{K_i}{L_{PF}}} \quad (29)$$

The control loop of the current i_q is shown in the fig.2 below and the control law is

$$q_{nd} = \frac{2\omega L_{PF} \frac{di_q}{dt} + \omega R_{PF} i_q + \frac{dV_d}{dt} - \omega V_q - u_d}{\frac{dV_{dc}}{dt}}$$

$$q_{nq} = \frac{2\omega L_{PF} \frac{di_d}{dt} + \omega R_{PF} i_d + \frac{dV_q}{dt} - \omega V_d - u_q}{\frac{dV_{dc}}{dt}} \quad (30)$$

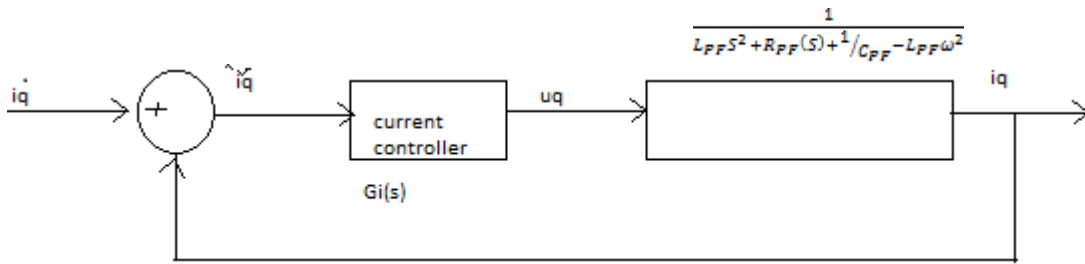


Fig.2 Control loop of the current.

Note that the inputs q_{nd} and q_{nq} consist of a nonlinearity cancellation part and a linear decoupling compensation part.

2.4 Regulation of DC voltage

The active filter produces a fundamental voltage which is in-phase with fundamental leading current of the passive filter. A small amount of active power is formed due to the leading current and fundamental voltage of the passive filter and it delivers to the dc capacitor. Therefore, the electrical quantity adjusted by the dc-voltage controller is consequently i_q^* . To maintain V_{dc} equal to its reference value, the losses through the active filter's resistive-inductive branches will be compensated by acting on the supply current.

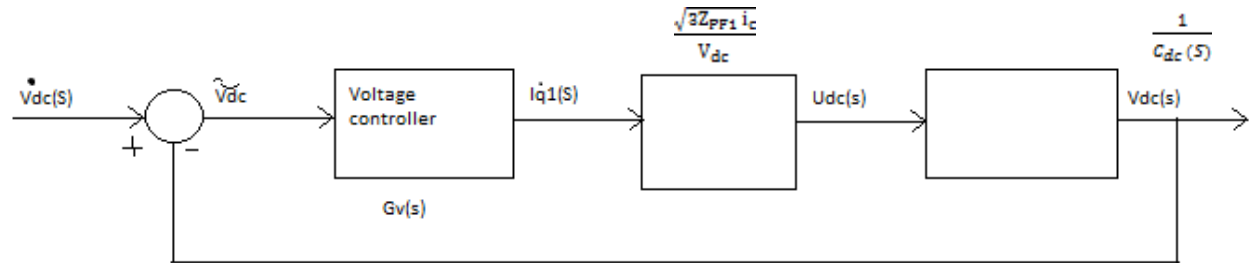


Fig.3 Control loop of the voltage

From (24) we can deduced to

$$C_{dc} \frac{dV_{dc}}{dt} = q_{nq} i_q \quad (31)$$

An equivalent u_{dc} is defined as

$$u_{dc} = q_{nq} i_q \quad (32)$$

Hence the reactive current of the active filter is

$$i_q = \frac{u_{dc}}{q_{nq}} - \frac{u_{dc} V_{dc}}{q_{nq} V_{dc}} \quad (33)$$

Now assume $q_{nq} V_{dc} \approx V_{Mq}$ and $q_{nd} V_{dc} \approx V_{Md}$ hence

$$i_q = \frac{u_{dc} V_{dc}}{V_{m q}} \quad (34)$$

the q axes active filter voltage V_{Mq} is given by

$$V_{Mq} = -Z_{PF1} i_q^*$$

Where Z_{PF1} is the impedance of the passive filter at 50 Hz and i_q^* is a dc component.

The control effort of the dc-voltage loop is

$$i_{q1}^* = \frac{u_{dc} V_{dc}}{-Z_{PF1} i_q} \quad (35)$$

The three phase filter current are expressed as

$$\begin{bmatrix} i_{c1} \\ i_{c2} \\ i_{c3} \end{bmatrix} = \sqrt{\frac{2}{3}} i_q \begin{bmatrix} -\sin\theta \\ -\sin(\theta - 2\pi/3) \\ -\sin(\theta - 4\pi/3) \end{bmatrix} \quad (36)$$

The fundamental filter rms current I_c is given by

$$I_c = \frac{i_q}{\sqrt{3}} \quad (37)$$

The laplace form of the control effort can be derived as follows:

$$i_{q1}^* = \frac{V_{dc}}{\sqrt{3} Z_{PF1} I_c} u_{dc}(s) \quad (38)$$

The outer control loop of the dc voltage is shown in Fig. To regulate dc voltage V_{dc} , the error

$V_{dc}^* - V_{dc}$ is passing through a P-I type controller given by

$$u_{dc} = K_1 V_{dc}^* + K_2 \int V_{dc}^* dt \quad (39)$$

hence the closed loop transfer function is

$$\frac{V_{dc}(s)}{V_{dc}^*(s)} = \frac{2\varepsilon\omega_{nv}}{S^2 + 2\varepsilon\omega_{nv}S + \omega^2} \quad (40)$$

Where ω_{nv} is the outer loop natural angular frequency and ζ is the damping factor.

The transfer functions of Fig. is

$$\frac{V_{dc}(s)}{V_{dc}^*(s)} = \frac{\frac{\sqrt{3} Z_{PF1} K_1 I_c}{V_{dc} C_{dc}}(s) + \frac{\sqrt{3} Z_{PF1} K_2 I_c}{V_{dc} C_{dc}}}{S^2 + \frac{\sqrt{3} Z_{PF1} K_1 I_c}{V_{dc} C_{dc}}(s) + \frac{\sqrt{3} Z_{PF1} K_2 I_c}{V_{dc} C_{dc}}} \quad (41)$$

The proportional k_1 and integral k_2 gains are then obtained as:

$$\begin{aligned} K_1 &= 2\varepsilon\omega_{nv} \frac{V_{dc} C_{dc}}{\sqrt{3} Z_{PF1} I_c} \\ K_2 &= \omega_{nv}^2 \frac{V_{dc} C_{dc}}{\sqrt{3} Z_{PF1} I_c} \end{aligned} \quad (42)$$

III. SIMULATION RESULT

The shunt hybrid power filter which is connected to a non-linear load is simulated by using MATLAB/SIMULINK environment. The scheme is first simulated without any filter to find out the THD of the supply current. Then it is simulated with the hybrid filter to observe the difference in THD of supply current.

3.1 Simulation response without filter

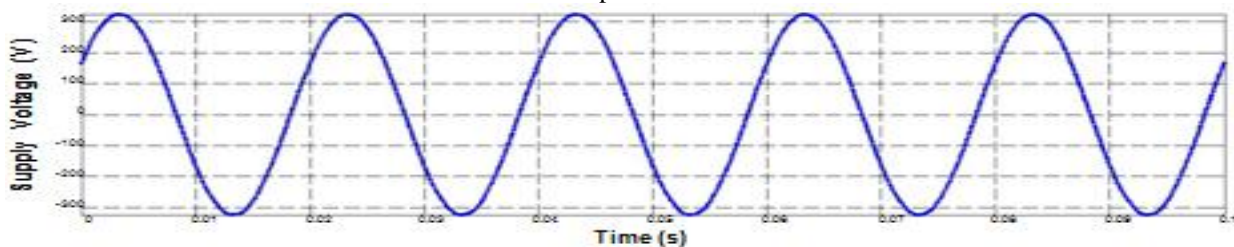


Fig.4 Wave forms of Supply Voltage (V) without filter.

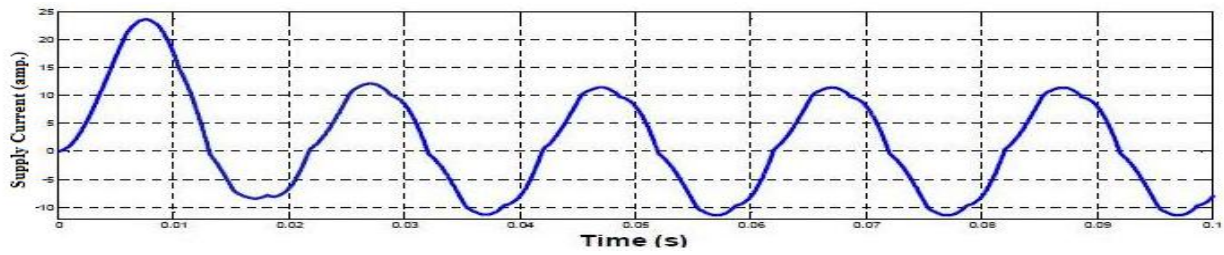


Fig.5 Wave forms of Supply Current (A) without filter

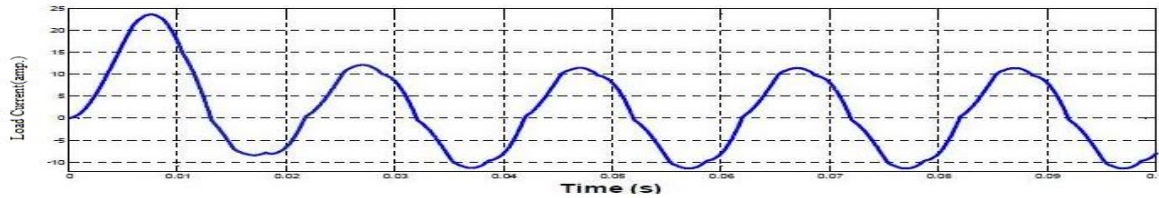


Fig.6 Wave forms of Load current (A) without filter.

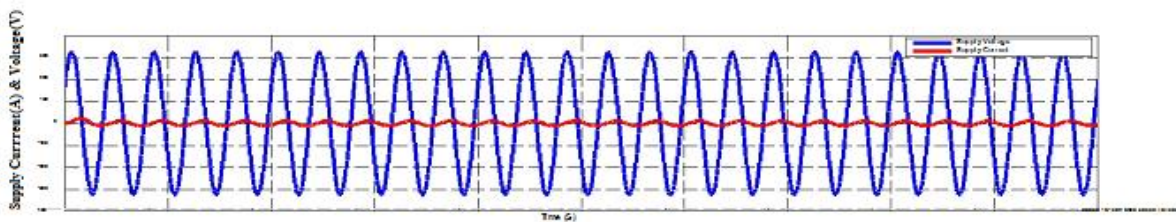


Fig.7 Wave forms of Supply Voltage (V) and Current (A) without filter.

Fig.7 shows the supply voltage and current without filter, we can see that the current is not in phase with the voltage.

3.2 Simulation response with shunt hybrid power filter

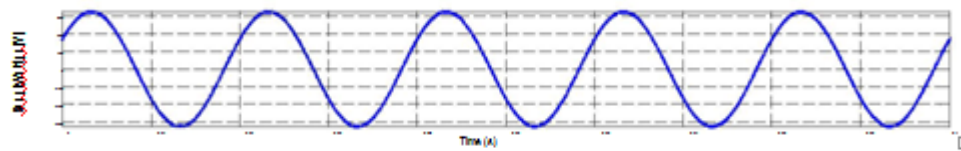


Fig.8 Wave forms of Supply Voltage (V) with hybrid filter.

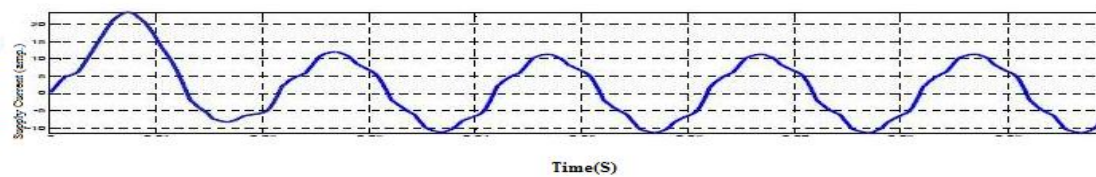


Fig.9 Wave forms of Supply Current (A) with hybrid filter.

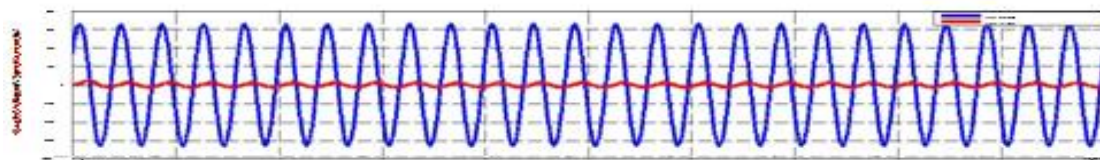


Fig.10 Wave forms of Supply Voltage and Current with hybrid filter.

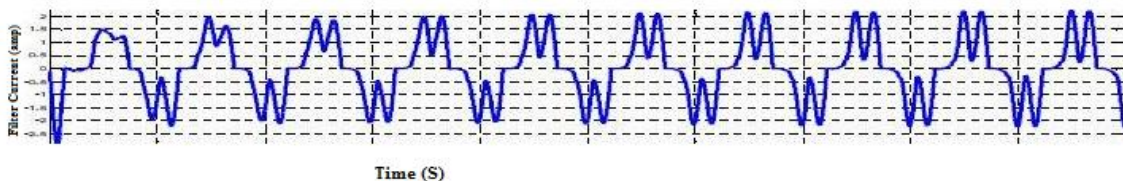


Fig.11 Wave forms of filter Current (A) With hybrid Filter

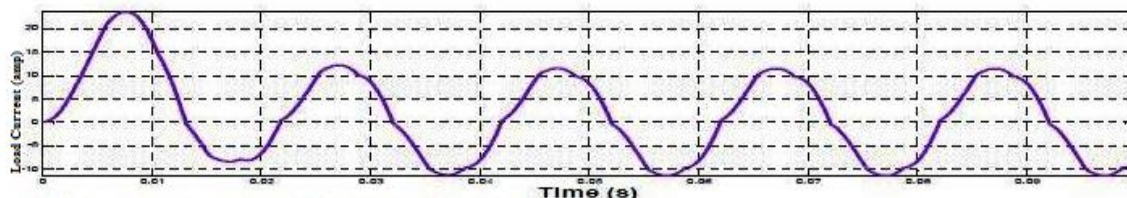


Fig.12 Wave forms of Load Current (A) with hybrid filter.

Fig.8-Fig.12 represents the simulation responses by using hybrid filter. Here we can see that in Fig.9 the supply current harmonic is quite reduced, but in the current is in phase with the voltage.

IV. CONCLUSION

This project work presents design of shunt hybrid power filter for a distribution system. The hybrid filter reduces the harmonics as compare to open loop response. This hybrid filter is tested and verified using MATLAB program. The implemented for three phase shunt hybrid power filter. Here non-linear load implemented. The harmonic current control and DC-capacitor voltage can be regulated under-linear loads. We obtained it from the simulation responses. The shunt hybrid power filter is verified with the simulation results. Hence we obtained comparative results by using these SHPF and without filter. The comparative simulation result presented in the table-1 and simulation parameter represented in table-2

Table-1
Nonlinear Load

Currents	THD(%) before compensation Without filter	THD(%) before compensation With hybrid filter
Supply Current	23.24	8.51
Load Current	23.24	11.11
Filter Current	NIL	43.14

Hence we got the simulation responses for nonlinear load. In nonlinear load the THD is compensated from 23.24% to 8.51SHPF which is represented in Table 1.

Table-2
Specification Parameters

Phase voltage and frequency	$V_s=230v(\text{rms}), f_s=50\text{Hz}$
Supply /line inductance	$L_{sa}=L_{sb}=L_{sc}=4 \text{ mH}$
Rectifier front-end inductance	$L_{ra}=L_{rb}=L_{rc}=30 \text{ mH}$
For V-S Type Load resistance, load capacitance	$R_L=20 \Omega, C_L=500 \mu F$
Passive filter parameters	$L_{pf}=14 \text{ mH}, C_{pf}=24 \mu F$
Inverter dc- bus voltage and capacitance	$V_{dc}=50v, C_{dc}=3000 \mu F$
Controller Parameter	$K_p=300, K_i=0.007$

V. 5 SCOPE OF FUTURE WORK

- Experimental investigations can be done on shunt hybrid power filter by developing a prototype model in the laboratory to verify the simulation results for P-I Controller.
- Experimental investigations can be done on shunt hybrid power filter by developing a prototype model in the laboratory to verify the simulation results for hysteresis controllers.
- For the further experiment a smith controller used for the best result.
- Again For the further experiment a PID Controller used for the best result.
- In this thesis not consideration of the signal time delay, now Further investigation of the consideration of the signal time delay.
-

REFERENCES

- [1]. T. Nageswara Prasad , V. Chandra Jagan Mohan, Dr. V.C. Veera Reddy, Harmonic reduction in hybrid filters for power quality improvement in distribution system, Journal of theoretical and applied information technology 15th jan. 2012 Vol. 35 No.-1
- [2]. Luis A. Morán, Juan W. Dixon, José R. Espinoza, Rogel R. Wallace, Using Active power filters to improve power quality, FNDECYT 1990.
- [3]. Bhim Singh, Kamal Al-Haddad, Senior Member, IEEE, and Amrbrish Chandra, Member, IEEE, A Review of Active Filters for Power Quality Improvement, IEEE Transactions on Industrial Electronic, Vol.-46, No.5 October 1999.
- [4]. Karuppanan P and Kamala Kanta Mahapatra, PI, PID and Fuzzy logic controller for Reactive Power and Harmonic Compensation, ACEEE Int. J. on Electrical and Power Engineering, Vol. 01, No. 03, Dec 2010.

- [5]. Prashanta Kumar Das, B. Srikanth, Gayatri Vidya, Modeling, Analysis and Simulation of Three Phase Hybrid Power Filter for Power Quality Improvement, International Journal of Engineering Research and Applications (IJERA) ISSN: 2248-9622 Vol. 2, Issue 3, May-Jun 2012.
- [6]. C.Nalini Kiran, Subhransu Sekhar Dash, S.Prema Latha, International Journal of Scientific & Engineering Research Volume 2, Issue 5, May-2011.
- [7]. V. Koteswara Rao, K. Sujesh, S. Radha Krishna Reddy, Y. Naresh Kumar, CH. Kamal A Novel Approach on Harmonic Elimination in Single Phase Systems by Means of a Hybrid Series Active Filter (HSAF). International Journal of Engineering and Advanced Technology (IJEAT) ISSN: 2249 – 8958, Volume-1, Issue-4, April 2012.
- [8]. P. Kishore Kumar, M.Sharanya, Design Of Hybrid Series Active Filters for Harmonic Reduction in Single Phase Systems, International Journal of Modern Engineering Research (IJMER) Vol. 3, Issue. 5, Sep - Oct. 2013 pp-3170-3176 ISSN: 2249-6645.
- [9]. T.Mahalekshmi, Mepco Schlenk, Current Harmonic Compensation and Power Factor Improvement by Hybrid Shunt Active Power Filter International Journal of Computer Applications (0975 – 8887) Volume 4 – No.3, July 2010.
- [10]. L. Asiminoaei, E. Aeloiza, P. N. Enjeti, and F. B laabjerg, Shunt active-power- filter topology based on parallel interleaved inverters, IEEE Trans.Ind. Electron. vol. 55, no. 3, pp. 1175–1189, Mar. 2008.
- [11]. B. Singh, V. Verma, A. Chandra, K. Al-Haddad, Hybrid filters for power quality improvement. IEEE Proc. on Generation, Transmission and Distribution, Vol. 152, pp. 365-378, 2005.
- [12]. Salem Rahmani, Abdelhamid Hamadi, Nassar Mendalek, and Kamal Al-Haddad. A New Control Technique for Three-Phase Shunt Hybrid Power Filter. IEEE Transactions on industrial electronics, vol. 56, no. 8,pp. 606-805, august 2009.
- [13]. H. Fujita, H. Akagi, Hybrid A practical approach to harmonic compensation in power systems; series connection of passive and active filters, IEEE Trans. on Industry Applications, Vol. 27, pp. 1020-1025, 1991.
- [14]. Akagi, H. (2005). "Active harmonic filters", Proceedings of the IEEE, Vol. 93, No. 12, pp. 2128 - 2141, December, 2005.
- [15]. Aredes, M., Hafner, J. & Heumann, K., "Three- phase four-wire shunt active filter control strategies", IEEE Transactions on Power Electronics, Vol. 12, No. 2, pp. 311 -318, March 1997.
- [16]. Bollen, M.H., "Understanding Power Quality Problems: Voltage Sags and Interruptions", Wiley-IEEE Press, Piscataway, New Jersey.
- [17]. Buso, S., Malesani, L. & Mattavelli P., "Comparison of current control techniques for active filter applications", IEEE Transactions on Industrial Electronics, Vol. 45, No. 5, pp. 722 -729, October, 1998.
- [18]. E. F. Fuchs, M. A. S. Masoum, "Power Quality in Electrical Machines and Power Systems," Academic Press, USA, 2008.
- [19]. J. C. Das, "Passive filters; potentialities and limitations," *IEEE Trans. on Industry Applications*, Vol. 40, pp. 232- 241, 2004.
- [20]. S. Rahmani, K. Al-Haddad, and H. Y. Kanaan, "A comparative study of two PWM techniques for single-phase shunt active power filtersem-ploying direct current control strategy," *J. IET Proc.—Elect. Power Appl.*, Vol. 1, no. 3, pp. 376–385, Sep. 2008.
- [21]. N. Mendalek, K. Al-Haddad, L.-A. Dessaint, and F. Fnaiech, "Nonlinear control technique to enhance dynamic performance o f a shunt active power filter," *Proc. Inst. Elect. Eng.—Elect. Power Appl.*, vol. 150, no. 4,pp. 373–379, Jul. 2003.
- [22]. L. Yacoubi, K. Al-Haddad, L. A. Dessaint, and F. Fnaiech, "A DSP-based implementation o f a nonlinear model reference adaptive control f or a three-phase three-level NPC boost rectifier prototype," *IEEE Trans. Power Electron.*, vol. 20, no. 5, 1084–1092, Sep. 2005.
- [23]. F. Defay, A. M. Llor, and M. Fadel, "A predictive control with flying capacitor balancing of a multicell active power filter," *IEEE Trans. Ind. Electron.*, vol. 55, no. 9, 3212–3220, Sep. 2008.
- [24]. R. S. Herrera, P. Salmeron, and H. Kim, "Instantaneous reactive power theory applied to active power filter compensation: Different approaches, assessment, and experimental results," *IEEE Trans. Ind. Electron.*, vol. 55, no. 1, pp. 184–196, Jan. 2008.
- [25]. R. Grino, R. Cardoner, R. Costa-Castello, and E. Fossas, "Digital repetitive control of a three-phase four-wire shunt active filter," *IEEE Trans. Ind. Electron.*, vol. 54, no. 3, pp. 1495–1503, Jun. 2007.
- [26]. [Akagi, H., Kanazawa, Y. & Nabae, A., "Instantaneous reactive power compensators comprising switching devices without energy storage components", IEEE Transactions on Industry Applications, Vol. 20, No. 3, pp. 625 - 630, May / June, 1984.
- [27]. Akagi, H., Watanabe, E.H. & Aredes, M. "Instantaneous Power Theory and Applications to Power Conditioning", IEEE Press, ISBN 978-0-470-10761-4, Piscataway, New Jersey.
- [28]. Bhattacharya, S., Veltman, A., Divan, D.M. & Lorenz, R.D., "Flux-based active filter controller", IEEE Transactions on Industry Applications, Vol. 32, No. 3, pp. 491-502, May / June 1996.
- [29]. Cavallini, A. & Montanari, G. R., "Compensation strategies for shunt active filter control", IEEE Transactions on Power Electronics, Vol. 9, No. 6, pp. 587 - 593, November, 1994.
- [30]. Chen, B.S., & Joós, G., "Direct power control of active filters with averaged switching frequency regulation", IEEE Transactions on Power Electronics, Vol. 23, No. 6, pp. 2729- 2737, November, 2008.
- [31]. Chen, C.L., Lin, C.E. & Huang, C.L., "Reactive and harmonic current compensation for unbalanced three-phase systems using the synchronous detection method", Electric Power Systems Research, Vol. 26, No. 3, pp. 163-170, April, 1993.
- [32]. Furuhashi, T., Okuma, S. & Uchikawa, Y., "A study on the theory of instantaneous reactive power", IEEE Transactions on Industrial Electronics, Vol. 37, No. 1, pp. 86 - 90, January / February, 1990.
- [33]. Hingorani, N. G. & Gyugyi, L., "Understanding Facts: Concepts and Technology of Flexible AC Transmission Systems", Wiley-IEEE Press, Piscataway, New Jersey.
- [34]. Holmes, D.G. & Lipo, T.A., "Pulse Width Modulation for Power Converters - Principles and Practice", IEEE Press, Piscataway, New Jersey. [15] Hsu, J.S., "Instantaneous phasor method for obtaining instantaneous balanced fundamental
- [35]. Journal of Theoretical and Applied Information Technology 15 th January 2012. Vol. 35 No.1 © 2005 - 2012 JATIT & LLS. All rights reserved.
- [36]. components for power quality control and continuous diagnostics", IEEE Transactions on Power Delivery, Vol. 13, No. 4, pp. 1494 - 1500, October, 1998.
- [37]. Komurcugil, H. & Kukrer, O., "A new control strategy for single-phase shunt active power filters using a Lyapunov function", IEEE Transactions on Industrial Electronics, Vol. 53, No. 1, pp. 305 - 312, February, 2006.
- [38]. Lascu, C., Asiminoaei, L., Boldea, I. & Blaabjerg, F., "High performance current controller for selective harmonic compensation in active power filters", IEEE Transactions on Power Electronics, Vol. 22, No. 5, pp. 1826 - 1835, September, 2007.
- [39]. Lin, B. R. & Yang, T. Y., "Three-level voltage-source inverter for shunt active filter", IEEE Proceedings Electric Power Applications, Vol. 151, No. 6, pp. 744 - 751, November, 2004.
- [40]. Marconi, L., Ronchi, F. & Tilli, A., "Robust non-linear control of shunt active filters for harmonic current compensation", Automatica, Vol. 43, No.2, pp. 252 - 263, February, 2007.

Determination of Optimal Account and Location of Series Compensation and SVS for an AC Transmission System

B.Suresh Kumar

Asst.Professor-CBIT-Hyderabad

ABSTRACT:

The paper mainly concentrates on the latest development of compensation using Series Capacitor and SVS (Static VAR System).

The above concept to full extent in terms of advantages of the above mentioned compensation and to express the disadvantages of the concept along with the remedies. The paper involves universal software (C Language) programming developed for finding the optimal amount and location of compensation and SVS for an AC transmission system for any length of AC transmission line of any extra high tension voltages.

In this work optimal location of the series compensation and SVS has been determined for a given transmission system. We derived the generalized expressions for Maximum receiving end power, Compensation efficiency and Optimal value of series compensation have been developed in terms of the line constants and capacitive reactance used for different schemes of series compensation. Based upon steady state performance analysis, it is determined that the compensation scheme in which series compensation and SVS are located at the mid point of the transmission line yields Maximum receiving end power and Maximum Compensation Efficiency.

Comparison criteria based upon the Maximum Power Transfer $P_{R(max)}$ over the line has been developed. The generalized expressions for the optimum value of series compensation has been derived and hence the optimum value of series compensation has been determined for various cases of Series Compensation the criteria of $P_{R(max)}$ and compensation efficiency η_c have been utilized for assessing the optimal location of series and shunt compensation. Based upon the studies performed in case 5, mid point location of Series Compensation and SVS which yields the Maximum Receiving end Power $P_{R(max)}$ and Compensation Efficiency η_c .

I. INTRODUCTION

LONG DISTANCE TRANSMISSION LINES: In early days, the electric power was mainly used for electric lighting and the power was obtained from the steam power stations which are located very close to the load centers. Later, with the development of industry, demand for large amounts of power grew. Bulk power stations had to be constructed in order to meet the growing demand for large amounts of power. As the capacity of the steam power station grew, it became necessary, from the point of view of economy, to erect them where the fuel and water were most easily obtained. Therefore, the site of power stations was, sometimes far away from the load centers and the necessity of transmission lines for carrying power thus came into existence.

As the distance of transmission became high, various factors affecting transmission capacity arose. The important ones amongst them are:

1. Active loss in the transmission line
2. Reactive loss and the voltage drop in the line
3. Stability

1.2 COMPENSATION OF TRANSMISSION LINES:

“Compensation” means the modification of the electrical characteristics of a transmission line in order to increase its power transmission capacity while satisfying the fundamental requirements for transmission namely, stability and flat voltage profile.

1.3 TYPES OF COMPENSATIONS:

The compensation of transmission system is broadly classified as follows:

1. Surge impedance compensation
2. Line length compensation
3. Compensation by sectioning

1.3.1 SURGE IMPEDANCE COMPENSATION:

A flat voltage profile can be obtained if the surge impedance of the line is changed, by suitable compensation, to a value Z_0 so that the surge impedance loading, then is equal to the actual load. This type of compensation should be ideally capable of variation with quick response. This type of compensation, whose primary function is to modify the value of the surge impedance, is called the surge impedance compensation.

1.3.2 LINE LENGTH COMPENSATION:

Controlling the virtual surge impedance to match a given load is not sufficient by itself to ensure stability of transmission over longer distance hence line length compensation is used to improve the stability.

For a loss less line, the sending end and receiving end quantities are related by the following equation.

$$V_s = V_r \cos\theta + jZ_0 \frac{(P_r - jQ_r)}{V_r} \sin\theta$$

Equating imaginary parts of the above equation, we get

$$P_r = \frac{V_s V_r}{Z_0 \sin\theta} \sin\delta$$

Where ‘ δ ’ is the power angle of the line. From the above equation, it can be seen that the stability can be improved by decreasing either the surge impedance (Z_0) or the electrical length ‘ θ ’. Usually ‘ θ ’ is decreased to improve stability. The value of ‘ θ ’ is decreased by using series capacitor. This type of compensation is called “line length compensation” or “ θ compensation”.

1.3.3 COMPENSATION BY SECTIONING:

The line is divided into a number of sections by connecting constant voltage compensations at intervals along the line. Constant voltage compensators are compensating equipment which attempt to maintain voltage constant at their location. The maximum transmissible power is that of the weakest section. However, this section being shorter than the whole line, an increase in maximum power and stability results. The type of compensation is called compensation by sectioning or dynamic compensation.

II. TYPES OF COMPENSATORS

2.1 PASSIVE AND ACTIVE COMPENSATORS :

“Passive Compensators” include shunt reactors, shunt capacitors and series capacitors. These devices may be either permanently connected or switched, but in their usual forms they are in capable of continuous (i.e., steeples) variation. They operate is essentially static. Apart from switching they are uncontrolled.

“Active compensators” are usually shunt connected devices which have the property of tending to maintain a substantially constant voltage at their terminals. They do this by generating or absorbing precisely the required amount of corrective reactive power in response to any small variation of voltage at their point of connection. They are usually capable of continuous variation and rapid response. Control may be inherent, as in the saturated, reactor compensator, or by means of a control system, as in the synchronous condenser and thyristor controlled compensators.

2.2 SERIES COMPENSATION:

The series compensation will reduce the reactance of the line by means of series capacitors. This increases the maximum Power, reduces the transmission angle at given level of power transfer and increase the virtual natural load. The line reactance now absorbs less of the line charging reactive power, often necessitating some form of shunt inductive compensation.

$$P = \frac{V^2}{X} \sin\delta$$

The voltage drop ΔV due to series compensation is given by $\Delta V = IR \cos\Phi_r + I (X_L - X_C) \sin\Phi_r$

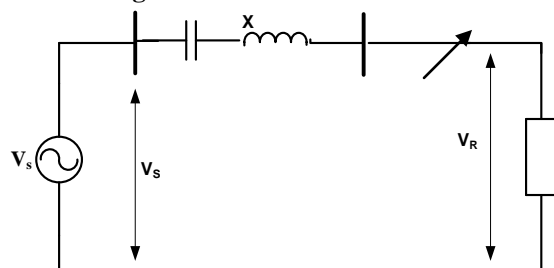
Here X_C = Capacitive reactance of the series capacitor bank per phase and X_L is the total inductive reactance of the line per phase. In practice, X_C may be so selected that the factor $(X_L - X_C) \sin\Phi_r$ becomes negative and equals $R \cos\Phi_r$ so that ΔV becomes zero. The ratio X_L/X_C is called “compensation factor” and expressed in percentage known as the “Percentage Compensation” or Degree of compensation”.

2.2.2 VOLTAGE STABILITY:

A simple radial system with feeder line reactance 'X', series compensation reactance X_C and load impedance Z is shown in figure below. The corresponding normalized terminal voltage ' V_r ' versus power 'P' plots, with unity PF load at 0%, 50% and 75% series capacitive compensation.

$$P = \frac{V^2}{X_L - X_c} \sin\delta$$

Circuit Diagram :



2.2.3 LOCATION OF SERIES CAPACITORS:

The effect of series capacitor on a circuit is from its point of location towards load end. Hence on a radial feeder, series capacitor must be located at source and load whose voltage is to be improved. If there are number of tapped loads distributed throughout, the rule of thumb for the best location of series capacitors is at, about one third of electrical impedance of the feeder from source bus.

2.2.4 RATING OF SERIES CAPACITORS:

The rating have to determined for series capacitors i.e., KVAR, voltage and current. As series capacitor has to carry full line current in the circuit where it is inserted, its continuous current rating should be at least equal to peak line current and preferably greater than the peak line current for the purpose of catering further load growth. The value of X_c depends upon the percentage of compensation required. The voltage rating is (IX_c) and KVAR rating per phase is $(3I^2X_c)$.

2.2.5 APPLICATIONS:

1. Improved system steady state stability.
2. Improved system transient stability.
3. Better load division on parallel circuits.
4. Reduce voltage drops in load areas during severe disturbances.
5. Reduced transmission losses.
6. Better adjustment of line loading.

7.2.3 SHUNT COMPENSATION:

For shunt compensation, shunt reactors, synchronous condensers and shunt capacitors are extensively used. In addition to these, a thyristor controlled static shunt compensator to meet reactive power generation and absorption demand has appeared in recent years. The most typical reasons for shunt compensation in EHV lines are explained below.

One primary reason for using shunt reactors or reactive control devices on EHV lines is to control steady state over voltage when energizing the long EHV lines or when operating under light load conditions. If shunt reactors are not used, the reactive power generated by line capacitance can cause high voltages at the receiving end of the line. However, to restrict insulation stresses caused by over voltage following sudden load rejection a substantial part of the shunt reactive compensation is usually left permanently connected.

**2.3.1 PASSIVESHUNTCOMPENSATION:
CONTROL OF O.C VOLTAGE WITH SHUNT REACTORS**

Passive shunt reactors are used to control the voltage at the receiving end of open circuited line. If these reactors could be uniformly distributed along the length of the line, then it is possible to get a flat voltage profile, with reduced surge impedance loading. However in practice, they cannot be uniformly distributed. Instead, they are connected at the end of line and at intermediate points, usually at intermediate switching stations. In case of very long line, some of the shut reactors are permanently connected to the line in order to provide maximum security against over voltage problem is less severe and the reactors are switched in or out frequently as the load varies. Shunt capacitors are usually switched type. If there is a sudden load rejection or open circuiting of the line, it may be necessary to disconnect them quickly to prevent them from increasing the voltage further and also to reduce the likelihood of ferroresonance where transformers remain connected.

2.4 STATIC VAR SYSTEM (SVS):

A static VAR system as per IEEE definition is a combination of static compensators and mechanically switched capacitors and reactors whose operation is coordinated. A static VAR system is thus not a well defined compensating arrangement because it does not have a uniform V-I characteristics and its overall response time is greatly dependent on the mechanical switching devices used.

2.4.1 CONFIGURATION OF SVS:

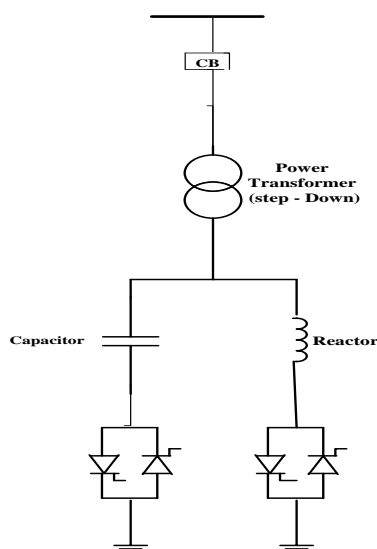
In conventional shunt compensation schemes shunt reactor is switched on during low loads and shunt capacitors are switched on during heavy loads or low lagging power factor loads.

In SVS, the compensation is controlled by any of the following:

1. Thyristor Switched Capacitors (TSC)
2. Thyristor Controlled Reactors (TCR)
3. Thyristor Switched Capacitors combined with Thyristor Controlled Reactors (TSC/TCR)

III. COMBINED TSC/TCR SVS:

In case of EHV transmission systems, the compensation requirements demand shunt capacitors during high loads and shunt reactors during low loads. Depending upon the desired control range of reactive power compensation required, thyristor controlled compensation is built up using a suitable combination of “Thyristor Switched Capacitors (TSC)” and “Thyristor Controlled Reactors (TCR)”.



2.4.4 CONTROL SYSTEM FOR SVS:

The amount of sophistication required for control system of SVS depends on application.

1. Voltage control
2. VAR flow control

Referring to figure below, the bus bar voltage (V) and current flowing into the compensator (I) are both sensed by means of VT and CT. Both these values are fed to the Automatic Voltage Regulator (VAR).

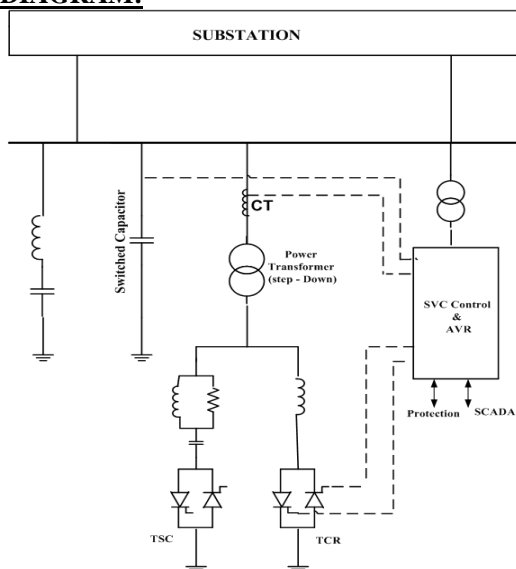
AVR in SVS is programmed to regulate transmission bus voltage with preselected tolerances and time delays.

The AVR and

Automatic VAR compensator performs the following tasks:

1. Controls phase angle of thyristor in SVS. SVS control is integrated with substation protection and SCADA system (Supervisory Control And Data Acquisition)
2. As the transmission voltage varies with load, the AVR performs the function of current control of flowing through the reactor R during each half cycle via the thyristor (Th). Smoothing Reactors (SR) provides a smoothing effect for current flowing through capacitor branches.

DIAGRAM:



GENERALISED EXPRESSION

3.1 REPRESENTATION OF LINES:

A transmission line is a set of conductors being run from one place to another supported on transmission towers. Such lines have four distributed parameters series resistance, inductance, shunt capacitance and conductance. It is observed that is very important in representing the lines of different lengths. It is to be noted that the electrical power is being transmitted over the overhead lines at approximately the speed of light. In order to get one full wave variation of voltage or current on the line the length of the line for 50Hz supply will be given by

$$f \cdot \lambda = v$$

Where f is frequency of supply, λ is the wave length.

Transmission lines are normally operated with a balanced three phase load. The analysis can therefore proceed on a per phase basis. A transmission line on a per phase basis can be regarded as a two part network, where in the sending end voltage V_s and current I_s are related to the receiving end voltage V_R and I_R through ABCD constants as

$$\begin{bmatrix} V_s \\ I_s \end{bmatrix} = \begin{bmatrix} A & B \\ C & D \end{bmatrix} \begin{bmatrix} V_R \\ I_R \end{bmatrix}$$

Also the following identity holds for ABCD constants:

$$AD - BC = 1$$

These constants can be determined easily for short and medium length lines by suitable approximations lumping the line impedance and shunt admittance. For long lines exact analysis has to be carried out by considering the distribution of resistance, inductance and capacitance parameters and the ABCD constants of the line are determined.

3.2 ABCD LINE PARAMETERS OF TRANSMISSION LINE:

For long transmission lines sending end and receiving end relations given by

$$\begin{bmatrix} V_s \\ I_s \end{bmatrix} = \begin{bmatrix} \cosh \gamma l & Z_c \sinh \gamma l \\ \frac{1}{Z_c} \sinh \gamma l & \cosh \gamma l \end{bmatrix} \begin{bmatrix} V_R \\ I_R \end{bmatrix}$$

$$A = D = \text{Cosh} \gamma l$$

$$B = Z_C \text{ Sinh} \gamma l$$

$$C = (1/Z_C) \text{ Sinh} \gamma l$$

Where $Z_C = \sqrt{\frac{Z}{Y}}$

$$\gamma = \sqrt{YZ} = \text{Propagation constant}$$

$$= \alpha + j\beta$$

$\alpha = \text{Attenuation constant}$
 $\beta = \text{Phase constant}$

$$A = \text{Cosh} \gamma l = 1 + \frac{\gamma^2 l^2}{2} + \frac{\gamma^4 l^4}{24} + \dots \approx \left(1 + \frac{YZ}{2}\right)$$

$$\text{Sinh} \gamma l = \left[\gamma l + \frac{\gamma^3 l^3}{6} + \frac{\gamma^5 l^5}{120} + \dots \right] \approx \sqrt{YZ} \left(1 + \frac{YZ}{6}\right) \quad B = Z_C \text{ Sinh} \gamma l = Z \left(1 + \frac{YZ}{6}\right)$$

$$C = \frac{1}{Z_C} \text{ Sinh} \gamma l \approx Y \left(1 + \frac{YZ}{6}\right)$$

3.3 MAXIMUM RECEIVING END POWER :

The receiving end complex power in terms of generalized $A_0 B_0 C_0 D_0$ line parameters. Where A_0, B_0, C_0, D_0 are the ABCD parameter of the line after the compensation.

$$P_R = \frac{|V_S| |V_R|}{|B_0|} \cos(\beta - \delta) - \frac{|A_0|}{|B_0|} |V_R|^2 \cos(\beta - \alpha) \dots \dots \dots (3.1)$$

Where $A_0 = |A_0| \angle \alpha$ and $B_0 = |B_0| \angle \beta$

P_R will be maximum at $\delta = \beta$

Such that,

$$P_{R(max)} = \frac{|V_S| |V_R|}{|B_0|} - \frac{|A_0|}{|B_0|} |V_R|^2 \cos(\beta - \alpha) \dots \dots \dots (3.2)$$

In practical situations α is very small

Therefore, neglecting α

$$P_{R(max)} = \frac{|V_S| |V_R|}{|B_0|} - \frac{|A_0|}{|B_0|} |V_R|^2 \cos \beta \dots \dots \dots (3.3)$$

Substituting $|V_S| = K |V_R|$

$$P_{R(max)} = \frac{|V_R|^2}{|B_0|} \{K - |A_0| \cos \beta\} \dots \dots \dots (3.4)$$

3.4 OPTIMUM VALUE OF CAPACITIVE REACTANCE :

The generalized expression based upon the equation (3.4) derived in terms of the series capacitive reactance (X_C) used in each case. The optimum value of series capacitive reactance $X_{C(opt)}$ is determined by:

$$\frac{dP_{R(max)}}{dX_C}$$

3.5 COMPENSATION EFFICIENCY:

The compensation efficiency η_C is defined as the ratio of net reduction in transfer reactance to the series capacitive reactance used. Thus the effective series capacitive reactance X'_C (as compared to the actual value of X_C) is given by

$$X'_c = \eta_c X_c$$

Therefore,

$$\eta_c = \frac{\text{Net reduction in transfer reactance}}{\text{Series capacitive reactance used}} \dots \dots \dots (3.6)$$

Based upon the equation (3.6) the generalized expressions for the compensation efficiency are derived for series and shunt compensation location.

3.5 DEGREE OF COMPENSATION:

Degree of compensation is defined as it is the ration of capacitive reactance and the line inductive reactance it given by

$$K = \frac{X_c}{X}$$

For better understanding we re-call the formula

$$P_1 = \frac{|V_1| |V_2|}{X} \text{ SIN } \delta$$

With series capacitor, we get

$$P'_{1} = \frac{|V_1| |V_2|}{(X - X_c)} \text{ SIN } \delta$$

from the above equations we get increase in power transmission $P_{increase}$

$$P_{increase} = P'_{1} - P_1 = \frac{K}{1 - K} P_1$$

Increase in the lengths of transmission lines and in transmission voltages, decrease in series capacitor costs.

Series capacitors can be located either in the lines or intermediate sub-stations or switching stations. Line location has many advantages such as better voltage profile along the line and reduced short circuit current contributes to a much simpler protection of the capacitors.

5.3 RESULTS:

(1)IE (I) DATA:

Case number	$P_{R(max)}$	$\eta_{c(opt)\%}$	$X_{c(opt)(p.u)}$	$S_{(opt)\%}$
1	18.48	78.47	0.108	88.76
2	21.52	89.52	0.099	81.84
3	23.56	78.47	0.116	95.64
4	14.62	92.44	0.096	79.42
5	17.53	95.50	0.096	80.00
6	16.52	84.82	0.108	90.00
7	13.25	90.00	0.096	80.00

(2)KHAMMUM-VIZAG LINE DATA:

Case number	$P_{R(max)}$	$\eta_{c(opt)\%}$	$X_{c(opt)(p.u)}$	$S_{(opt)\%}$
1	34.38	93.52	0.055	81.28
2	36.76	96.78	0.054	80.18
3	37.73	93.52	0.056	83.60
4	37.73	98.14	0.051	76.02
5	61.47	99.11	0.059	88.29
6	48.32	96.32	0.062	86.12
7	37.73	95.23	0.043	72.31
8	37.38	93.53	0.055	81.28

CONCLUSIONS

In the presented paper, comparison criteria based upon the Maximum Power Transfer $P_{R(\max)}$ over the line has been developed. The generalized expressions for $P_{R(\max)}$ in terms of A,B,C,D constants and capacitive reactance (X_C) are derived for the series compensated line. The generalized expressions for the optimum value of series compensation have been derived and hence the optimum value of series compensation has been determined for various cases of series compensation. The criteria of $P_{R(\max)}$ and compensation efficiency have been utilized for assessing the optimal location of series and shunt compensation. Based upon the studies performed (case 5) midpoint location of series compensation and SVS is recommended which yields the Maximum Receiving end Power $P_{R(\max)}$ and Compensation Efficiency η_c

REFERENCES

- [1]. T.J.E.Miller, "Reactive Power Control Electrical Systems", John Wiley & Sons Publishers, 1982
- [2]. Narain G. Hingorani & Laszlo Gyugyi, "Understanding FACTS", Standard Publishers & Distributors, New Delhi.
- [3]. N.Kumar & M.P.Dave, "Applications of an Auxilliary Controlled Static System for Damping Subsynchronous Resonance in power System", Power System Research, Vol.37, 1996, P.189.
- [4]. S.Rao, "EHV-AC, HVDC Transmission & Distribution Engineering", Khanna Publishers.A.P.Transco., "Technical Reference Book".
- [5]. I.J. Nagarath & D.P. Kothari, "Modern Power System Analysis", TATA McGraw Hill Publishers.
- [6]. C.L. Wadhwa, "Electrical Power System", New Age International (P) Ltd., Publishers.

Strength and Durability of Fly Ash, Cement and Gypsum Bricks

Nitin S. Naik¹, B.M.Bahadure², C.L.Jeurkar³

1 Assistant Professor, Department of Civil Engineering, College of Engineering, Kopargaon (M.S.)

2 Assistant Professor, Department of Civil Engineering, K.B.P.Polytechnic, Kopargaon (M.S.)

3 Associate Professor, Department of Civil Engineering, College of Engineering, Kopargaon (M.S.)

Abstract:

Burnt clay brick is an age old building material which is used for housing in urban area as well as rural part of India. These bricks are manufactured from good plastic clay, which is obtained from agricultural land. Excess use of agricultural land for this clay results in loss of good fertile soil and diversion of agricultural land for brick manufacturing. Manufacturing of bricks involved burning of bricks using coal. Burning of bricks using coal produces green house gases leading to environmental pollution. Fly Ash bricks are an alternative for the conventional bricks which can be used effectively to replace the conventional bricks. Various properties of these bricks were studied by different researchers and they found that these bricks can be used for construction of low cost houses in the area in the vicinity of thermal power plant. This paper is an attempt to study the strength and durability aspect of bricks prepared using Fly Ash, Cement and Phosphogypsum

Key Words: Bricks, Fly Ash, Cement, Gypsum, Durability, Sulphate resistance.

I. INTRODUCTION

In our country we are using ordinary burnt clay bricks. These bricks are having numerous disadvantages such as environmental pollution i.e. air pollution and land pollution. Air pollution takes place due to burning of bricks using coal as a fuel for burning. Burning of coal produces green house gases leading to environmental pollution. For manufacturing of these bricks huge amount of clay is required. This clay is obtained from agricultural land. Thus it causes land pollution through loss of good fertile soil. The manufacturing of bricks in our country is over 60 billion clay bricks annually (1) causing a strong impact on soil erosion and unprocessed emissions. For production of these bricks about 160 million tones of top soil is required which converts about 7500 acres of fertile land in to barren land (1). Manufacturing of conventional bricks is also associated with various social issues related to labours. To overcome these issues and problems now a day various attempts was done by various researchers to study various properties of bricks prepared using various by products and waste materials such as fly ash, lime and gypsum. Through their study they found that these bricks can be used as replacement or an alternative material to burnt clay bricks (2) (3) (4). Such bricks can be manufactured at lower cost and having good compressive strength. In case of lime is not available in the vicinity, OPC can be used as a source of lime.

This paper discusses the durability and strength aspect of the bricks prepared using fly ash, cement and phosphogypsum.

II. MATERIAL USED

For the present study fly ash used is obtained from thermal power plant located at Eklehara, Nasik. A good quality of lime is not available in the vicinity hence OPC is used as a source of lime. Phosphogypsum ($\text{CaSO}_4 \cdot 2 \text{H}_2\text{O}$) is obtained from a local agricultural products manufacturing company.

III. MIX PROPORTIONS

In the first part of this study various mix proportions of fly ash, cement and Phosphogypsum were studied for their compressive strength and it was found that bricks prepared with fly ash, cement and Phosphogypsum give sufficient compressive strength. Water absorption of these bricks was found to be on higher side as compared to the conventional burnt clay bricks. The object of this study is to discuss the durability and strength of these bricks, hence both the durability and strength aspect is discussed in this paper.

Table No.1 shows various mix proportions used for the present study.

Table 1: ix proportions

Sr. No.	Mix Proportions	Constituents (%)		
		Fly ash	Cement	Phosphogypsum
01	M-1	25	50	25
02	M-2	30	40	30
03	M-3	35	30	35
04	M-4	40	20	40
05	M-5	45	10	45

IV. METHODOLOGY

a) Mixing of Raw Material: The weighed quantity of Phosphogypsum, Cement and fly ash was thoroughly mixed in dry state in a pan with the help of a trowel. The mixture in dry state is mixed till it attains a uniform colour. When the mixture attains uniform colour weighed quantity of water is added in the mixture of fly ash, cement and phosphogypsum. After addition of the required quantity of water the mixture is thoroughly mixed with the help of trowel in a pan. After mixing the mix initially with the trowel the mixture is again mixed thoroughly by kneading until the mass attained a uniform consistency. To calculate the quantity of water to be added Standard normal consistency test was performed and the water content for the normal consistency was determined. The water content used in the mix for strength tests was 90% of that required to produce the standard normal consistency (4).

b) Preparation of mortar blocks: Standard cement mortar cube moulds of size 70.7mm x70.7mm x 70.7mm were used for preparation of blocks. The mixed binder was placed in the cube mould and was compacted properly by rod. Excess paste was hand finished. The mould was filled in three layers and each layer was compacted properly.

b) Method of Curing: The blocks were taken out from the moulds after 24 hours. After removal from the moulds the blocks were kept for air drying for 2 days. After sufficient strength was gained these blocks were transferred to water filled curing tanks. The durability of blocks was investigated by curing these blocks in the aggressive environments of sulfate solution. The sulfate solution having sulfate concentration equal to 10,000 ppm was prepared in the laboratory by mixing 14.79 g of Na₂ SO₄ in one liter of water.

V. EXPERIMENTAL WORK

Number of cubes was prepared using the mix proportions mentioned in Table 1 above and tested for their compressive strength and water absorption, after testing cubes it was found that M-5 can be used for bricks and hence bricks were prepared using M-5 proportions and tested for their compressive strength and water absorption. Since this paper discusses the durability and strength aspect only the results of compressive strength and water absorption test conducted on bricks are given in Table 3 while table 2 shows the results of tests conducted on cubes.

Table 2: Compressive strength and water absorption of cubes

Mix Designation	Compressive Strength in MPa			Water Absorption (%)
	7 days	14 days	28 days	
M-1	12.93	17.80	23.56	29.29
M-2	10.00	17.00	20.67	30.37
M-3	9.88	14.26	18.23	24.91
M-4	5.63	9.96	17.46	20.25
M-5	3.16	7.96	12.00	28.22

Table 3: Compressive strength and water absorption of bricks for M-5 mix proportion

Mix Designation	Compressive Strength in MPa			Water Absorption (%) after 28 days
	7 days	14 days	28 days	
M-5	2.254	6.360	9.420	28.44

After performing compressive strength test and water absorption test on bricks prepared using M-5 mix proportion it was found that mix M-5 is suitable to be used as brick material instead of clay.

To check the durability aspect of the mix i.e. fly ash, cement and phosphogypsum durability test was conducted on all the five mix proportions. For durability test Sulphate solution of concentration 10000 ppm is prepared in the laboratory by mixing 14.79 g of Sodium Sulphate in one litre of water. Three cubes from each type of mix are immersed in Sulphate solution. These cubes will be tested for their compressive strength after 28 days (3). Table 4 shows test results of durability test on fly ash, cement and phosphogypsum cubes.

Table 4: Compressive strength of cubes after curing in Sulphate solution

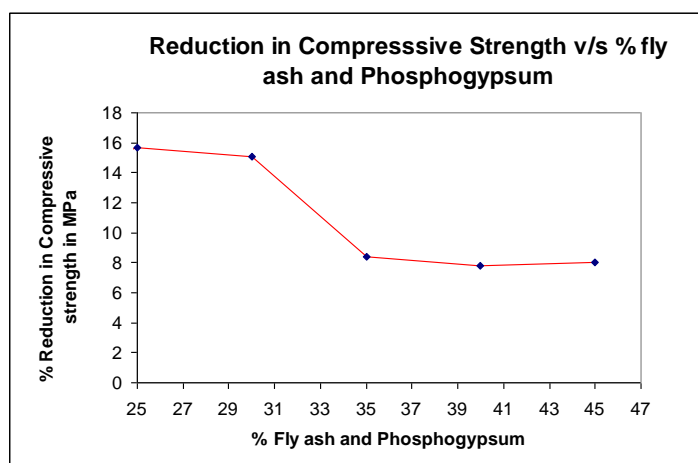
Mix Designation	Compressive Strength in MPa
	28 days
M-1	19.86
M-2	17.56
M-3	16.60
M-4	16.10
M-5	11.036

After testing the cubes for sulphate attack it was found that their strength decreases due to exposure to sulphate solution. Table 5 shows summary of all tests i.e. compressive strength of cubes with curing in potable water, compressive strength after curing in sulphate solution and water absorption test of cubes.

Table 5: Summary of results

Mix Designation	Compressive Strength in MPa		% loss of compressive strength due to sulphate attack.	Water Absorption (%)
	28 days curing in water	28 days curing in sulphate solution		
M-1	23.56	19.86	15.70	29.29
M-2	20.67	17.56	15.04	30.37
M-3	18.23	16.60	8.94	24.91
M-4	17.46	16.10	7.78	20.25
M-5	12.00	11.036	8.033	28.22

Graph 1 shows reduction in compressive strength due to sulphate attack v/s % of fly ash and phosphogypsum



Graph 1 Reduction in compressive strength v/s percentage of fly ash and phosphogypsum

VI. TEST RESULTS AND DISCUSSION

The results of compressive strength on cubes of fly ash, cement and phosphogypsum when cured in potable water are shown in table 2 along with results of water absorption of the cubes. While the results of compressive strength of cubes cured in sulphate solution are presented in table 4. Table 3 shows results of compressive strength and water absorption of bricks prepare with mix M-5. Summary of results for all the tests performed on the fly ash, cement and phosphogypsum binder is shown in table 5. Graph 1 shows effect of curing of the cubes in sulphate solution on compressive strength.

Table 2 shows compressive strength of fly ash, cement and phosphogypsum cubes for different mix proportions. From the table it is clear that the said binder gives good compressive strength though the water absorption is slightly on higher side of the I.S. requirements. When bricks are prepared with mix M-5 and tested for compressive strength and water absorption, it has been found that the bricks are having good compressive strength of 6.360MPa at the age of 14 days and 9.420 MPa at the age of 28 days, which is well above the I.S. requirement of 3.5 MPa. The water absorption of the bricks is found to be 28.44 % after submergence in water for 28 days which is above the I.S. requirement. The results are shown in table 3.

Table 4 shows compressive strength of cubes of all mix proportions when exposed to sulphate solution for 28 days. If it is compared with compressive strength of cubes given in table 2, it can be observed that curing in sulphate solution has resulted in reduction in compressive strength. Graph 1 shows the reduction in compressive strength against the percentage of fly ash and phosphogypsum. The graph shows that for higher percentage of fly ash and phosphogypsum the percentage reduction in compressive strength isles, thus if the percentage of fly ash and phosphogypsum increases durability of the mix increases. Thus the bricks prepared from fly ash, cement and phosphogypsum can offer good resistance to sulphate attack. For higher percentage of cement in the mix the percentage reduction in compressive strength is very high i.e. up to 16%. Due to action of fly ash with sulphate solution and due to increased percentage of phosphogypsum resistance of the mix against sulphate attack increases. From the above results and discussion following conclusions can be drawn.

VII. CONCLUSIONS.

Based on the experimental investigation reported in this study, following conclusions are drawn:

1. Unique possibility exists for the bulk utilization of fly ash in producing bricks in the proximity of thermal power plants, phosphoric acid and fertilizer industries.
2. The test cubes are having sufficient strength and have potential as a replacement for conventional burnt clay bricks.
3. Cementitious binder with fly ash and phosphogypsum content equal to 90% gives better compressive strength and 28.22 % water absorption and thus suitable for use in construction industry.
4. Being lighter in weight, it will reduce the dead weight and material handling cost in multi storied constructions.
5. When subjected to higher Sulphate concentration, the cementitious binders which gave low water absorption exhibited a very low strength loss.
6. From the testing of bricks for compression and water absorption it can be concluded that such bricks are having sufficient strength to be used as a replacement for traditional bricks. The water absorption of fly ash, cement and phosphogypsum bricks is found more than 20%, but such bricks can be used at places where water absorption is not a problem. i.e. for curtain walls.

REFERENCES

- [1] N. Bhanumathidas and N. Kalidas, "The role of Fal-G", The Indian Concrete Journal, July 1992, pp.389-391.
- [2] R. Ambalavanam and A. Roja, "Feasibility studies on utilization of waste lime and gypsum with fly ash", The Indian Concrete Journal, Nov.1996,pp.611-616.
- [3] Kumar Sunil, "Utilization of Fal-G bricks in buildings", The Indian Concrete Journal, July 2001, pp.463-466.
- [4] Kumar Sunil, "Utilization of Fal-G bricks and blocks", Construction and Building Materials,.
- [5] Dr. D. Sree Rama Chandra Murthy et. Al., "Conventionally reinforced concrete beams with Fal-G cement in flexure", CE and CR, Sept.2006, pp.47-53.
- [6] Luciano Santoro and Ignazio Aletta, "Hydration of mixtures containing Fly ash, lime and phosphogypsum", Thermochimia Acta,98 ,1986, pp.71-80.
- [7] A.K.Sabat, "Utilization of industrial wastes in Geotechnical construction- An overview", proceeding of National conference at Ludhiana, CEMCT-2006, Nov.2006, pp.228-231G.J. Borse. Numerical Methods with Matlab. PWS, 1997.
- [8] Jagroop Singh, "Effect of fly ash, cement and randomly distributed fibers on compressive strength of Kaolinite", proceeding of National conference at Ludhiana, CEMCT-2006, Nov.2006, pp.207-210.
- [9] Ismail Demir et al., " Effect of Silica fume and expanded perlite addition on the technical properties of the fly ash-lime-gypsum mixture", construction and Building Materials, 2007
- [10] Stefania Grzeszczyk et al., "Effect of Super Plasticizers on the rheological properties of fly ash suspensions containing activators of the pozzolanic reaction", Cement and Concrete Research, June 2000, pp.1263-1266.
- [11] Amit Mittal et al., "Parametric Study on Use of Pozzolanic Materials in Concrete", New Building Materials and Construction World, October 2006, pp94-112.

An Extensive Hypothetical Review on Call Handover Process in Cellular Network

Vaibhav V.Kamble¹, Shubhangi G. Salvi², Bharatratna P. Gaikwad³,
Rahul B. Gaikwad⁴

^{1,2}PG Student, Government College of Engineering, Aurangabad (M.S.),

³Research student, Dept. of CS & IT, Dr.B.A.M. University Aurangabad, (M.S.), India

⁴PG Student, Marathwada Institute of Technology, Aurangabad, (M.S.), India

Abstract:

This paper gives an overview on call handover process in cellular communication network. Mobility is key issue in current and future cellular networks such as GSM, UMTS and LTE. The handover process impacts on Quality of Service for network provider. If this process accomplishes inaccurately handover can result in loss of call. Handover is the process in which active call is transferred from one cell to another cell as the subscriber moves all over the coverage area of cellular network. Received signal level, received signal quality etc. parameters play vital role in handover decision process. MS station detects the signal level of current serving BTS along with surrounding BTS. The type of handover occurrence depends on cellular network structure. In this paper we revised the concept of handover process, different handover schemes and types then we briefly illustrate inter BSC handover sequence process.

Keywords: Cellular network, call handover process, received signal level, received signal quality, Quality of service, GSM, UMTS, LTE.

I. INTRODUCTION

One of the important parts of the cellular or mobile communication system like GSM (Global system for mobile communication) is network which is split in several radio cells. To provide frequency and coverage to these cells from limited available frequency (spectrum) and from these limited frequency operator have to cover all cellular network. So operators reuse these available frequencies to cover all over network by taking care of adjacent and co-channel interference should be less. The subscriber when moves from one cell to another cell without breaking call this process is known as handover. On the performance of handover process the (quality of service) QoS of operator is dependent. Handover is also known as Handoff. The term handover is more used within Europe, while handoff term uses more in North America [2].

Handover schemes are categories by hard, soft and seamless handoffs. They are also characterized by “break before make” and “make before break.” In hard handover, current radio link are released before new resources are used; in soft handover, both existing and new radio link are used during the handover process [5]. Different cellular generations handle handover in slightly different ways. This paper explains way of handovers in GSM. Figure 1 shows the basic call handover process.

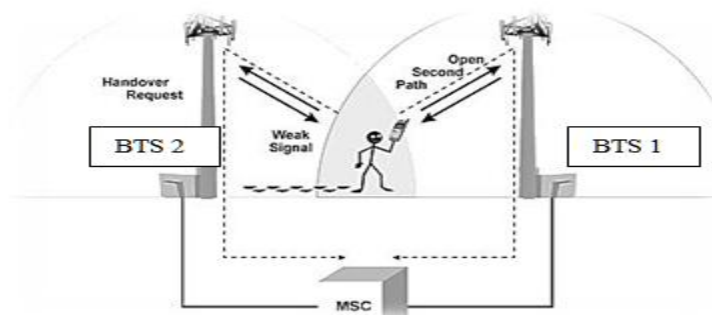


Figure 1. Basic Call Handover Process

Figure 1 shows the basic call handover process. In this diagram, a mobile subscriber is communicating with (Base Trans receiver Station) BTS1. BTS 1 provides a list of radio channels to measure nearby BTS. After the cellular phone measures the quality of the radio channels, it returns this information to the serving BTS. Using this information from neighboring BTS, the serving BTS sends a handover message which instructs the cellular phone to tune to a new radio channel of the adjacent BTS 2. The cellular phone begins transmission on the new channel by sending a short burst. The new BTS uses this information to send a command to adjust the relative timing of the cellular phone. After the cellular phone adjusted, the voice channel from the MSC is switched from BTS 1 to BTS 2 and voice conversation can continue [10].

There are number of parameters that needed to know to determine whether a handover is required. These parameters are RXQUAL (received signal quality), RXLEV (received signal strength), and DISTANCE (Distance of MS from BTS), PBGT (Drops below power budget margin). The mobile scans radio channels and reports back the quality of the link to the BTS. In this way the mobile assists in the handover decision and as a result this from of GSM handover is known as MAHO (Mobile Assisted Hand Over). The cellular network system known the quality of the link between the mobile and the BTS as well as the strength of local BTSs as reported back by the mobile. It also knows the availability of channels in the nearby cells. As a result it has all the information it needs to be able to make decision about whether it needs to hand the mobile to hand the mobile over from one BTS to another [11][13].

If the network decides that it is necessary for the mobile to handover. It assigns a new channel and time slot to the mobile. It informs the BTS and the mobile of the change. The mobile then retunes during the period it is not transmitting or receiving, i.e. in an idle period. A key element of the GSM handover is timing and synchronization. There are a number of possible scenarios that may occur dependent upon the level of synchronization [11].

This paper is organized as follows. Section I gives introduction of this paper. Types of handovers are described in section II. Sections III describe handover mechanism. Section IV concluded this paper.

II. GSM HANDOVER TYPES

Handover types can be distinguished depending on the cellular network structure. In the GSM cellular system there are four types of handover which are as follows [13].

2.1 Intra BSC handover

This type of handovers is occurs when subscriber moves from one cell to another cell of the coverage area of one BTS to another belonging to the same BSC (Base Station Controller).

2.2 Inter BSC handover

When subscriber moves from one cell to another cell of the coverage area of one BTS to another belonging to the one BSC to another but within the same MSC (Mobile Switching Center). This type of handover is called as Inter BSC handover.

2.3 Inter MSC handover

This form of handover occurs within two different MSC. When subscriber moves from one cell to another cell of the coverage area of one BTS to another belonging to the one BSC to another within two different MSC.

2.4 Intra BTS handover

In this type of handover subscriber remains attached to the same BTS but only cell can be changed.

With advanced the evolution in cellular system. Technology migrates from GSM to UMTS/WCDMA (Universal Mobile Telecommunication System/ Wideband Code Division Multiple Access) as well then LTE (Long Term Evolution). So there is a need of handover from one technology to another technology. These handovers are called as intersystem handover or inter-RAT (Radio Access Technologies) handover. The two most common inter system handovers are as follows

2.5 UMTS/WCDMA to GSM

While in UMTS, i) if the currently assigned UMTS cell falls below the UMTS threshold (implying that the connected UMTS cell is not 'strong-enough'), and ii) if there is no other UMTS neighboring cell whose threshold is larger, then the algorithm looks for GSM cells to handover. If conditions i) and ii) above are met, and if the RSSI of the strongest GSM cell is above the GSM threshold, then the mobile is instructed to do an inter-system handover from UMTS to GSM; otherwise the mobile continues with UMTS (in which case the call quality, in terms of received threshold may get worse, eventually leading to a call drop if no suitable GSM cell or better UMTS cell is found) [8].

2.6 GSM TO UMTS/WCDMA

While in GSM, i) if the RSSI (Received Signal Strength Indicator) of the currently assigned GSM cell falls below the GSM threshold (implying that the connected GSM cell is not ‘strong-enough’), and ii) if there is no other GSM neighboring cell whose RSSI is larger, then algorithm looks for UMTS cells to handover. If conditions i) and ii) above are met, and if the strongest UMTS cell is above the UMTS threshold then the mobile is instructed to do an inter-system handover from GSM-UMTS; otherwise the mobile continues with GSM (in which case the call quality, in terms of received RSSI may get worse, Eventually leading to a call drop)[8].

III. HANDOVER MECHANISM

In this section we are focusing on the handover procedure. For understanding handover procedure sequence in detail we see the mechanism of inter BSC handover sequence stepwise. The procedure is described as follows. Figure 2 shows handover mechanism and figure 3 illustrates diagram of inters BSC handover sequence with commands [14].

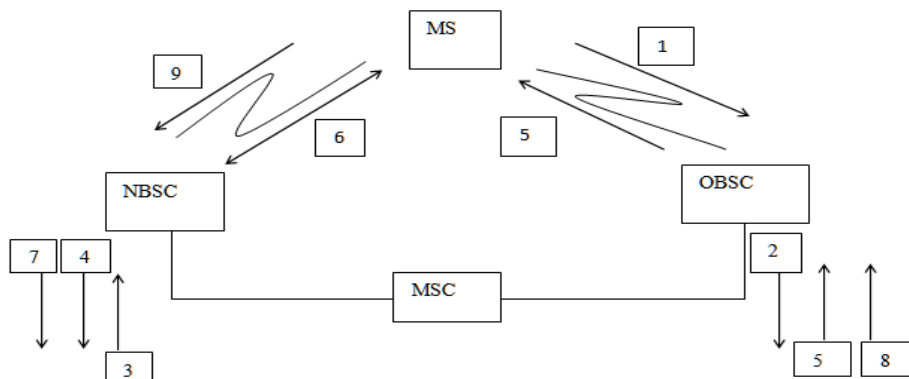


Figure 2. Handover mechanism.

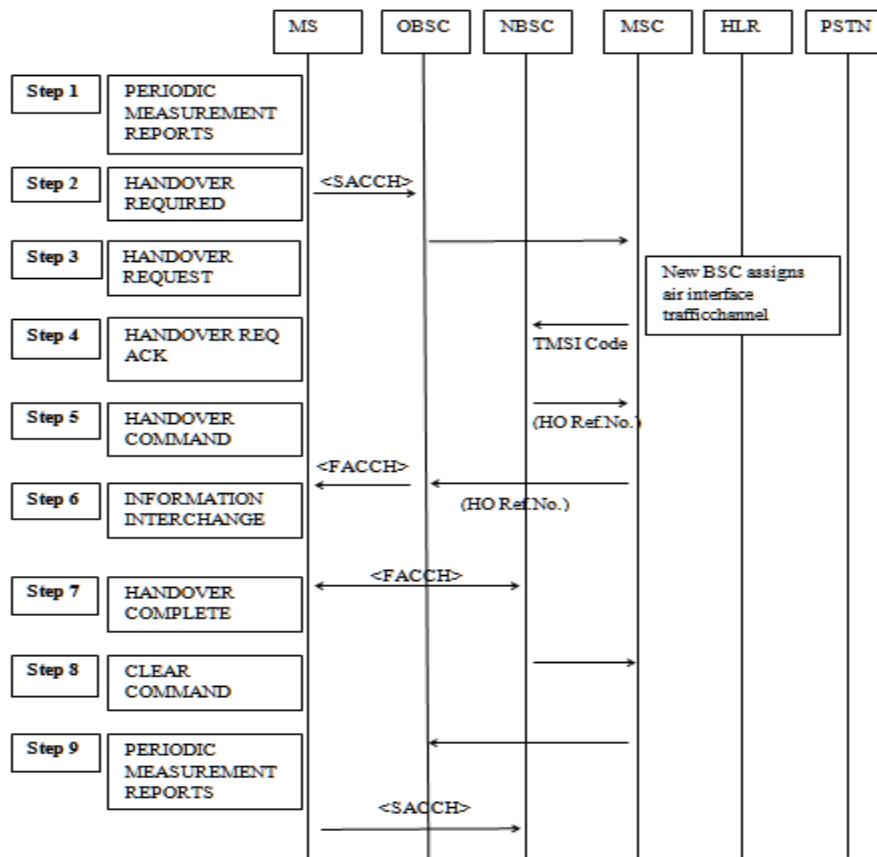


Figure3. Inter BSC Call Handover Sequence.

Step1: The MS is in the conversation state and is continuously compiling measurement both of the current transmission and the broad control channels of up to the thirty two surrounding cells. The measurements from the six best cells are reported back to the BSC, every480ms.

Step2: When the handover is required, due to low receive signal strength indication (RSSI) or poor signal quality the existing “originating” BSC (oBSC) notifies the MSC (“handover required”).

Step3: The target or “new” BSC (nBSC) is alerted with the message “handover request” tagged with the TMSI (Temporary mobile subscriber identity).

Step4: The new BSC allocates a handover reference number which it uses to determine whether the correct MS gains access to the air interface channel which it allocates, and acknowledges the MSC’s request with “handover request Ack”. This tagged with the HO reference number. The nBSC assigns a traffic channel.

Step5: The MSC, via the oBSC orders the MS to change to the new channel with the message “handover” commands on FACCH (Fast associated control channel).

Step6: There is an information interchange between nBSC and MS. This the FACCH channel but an access burst is used. The messages and information carried depend upon the type of the handover being performed.

Step7: Once all necessary information has been transferred the message “handover complete” is sent to the MSC.

Step8: The MSC now sends a “clear commands” to the oBSC; this frees the radio resources for another MS. The channel is not cleared until this point in case the new BSC cannot accommodate the MS being handed over.

Step9: The MS, still in the conversation mode, then continues to prepare periodic measurement reports and sends them to the new BSC.

IV. CONCLUSION

In this paper we extensively revised call handover process in GSM cellular network. The different call handover schemes and types are discussed and gives focused on the Received signal level, received signal quality etc. parameters that are involved in call handover decision. Finally we gives theoretical demonstration of inter BSC call handover sequence.

REFERENCES

- [1] YaseeinSoubhi Hussein1*, BorhanuddinMohd Ali1, 2 Pooria Varahram1 and Aduwati Sali1, Enhanced handover mechanism in long term evolution (LTE) networks, ISSN 1992-2248 ©2011 Academic Journals Scientific Research and Essays Vol. 6(24), pp. 5138-5152, 23 October, 2011.
- [2] Gregory P. Pollini, Bell Communications Research, Inc., Trends in Handover Design, IEEE Communications Magazine March 1996, 0163-6804/96/\$05.00 © 1996 IEEE.
- [3] NasifEkiz, Tara Salih, SibelKüçüköner, and Kemal Fidanboyulu, An Overview of Handoff Techniques in Cellular Networks, World Academy of Science, Engineering and Technology 6 2007.
- [4] A.Gueroui and S.Boumerdassi_LaboratoirePRISM, Université de Versailles, A Handover Optimisation Scheme in Cellular Networks.
- [5] Carolin I. Bauer1, Dr. S. John Rees2, CLASSIFICATION OF HANDOVER SCHEMES WITHIN A CELLULAR ENVIRONMENT, PIMRC 2002, 0-7803-7589-0/02/\$17.00 ©2002 IEEE.
- [6] S. Malathy, Improving Handoff Call Connectivity in CellularNetwork by Predicting its Future Move, European Journal of Scientific Research, ISSN 1450-216X Vol.78 No.1 (2012), pp.57-64 © EuroJournals Publishing, Inc. 2012.
- [7] Cristóvão Oliveira, GSM System – Handover, ref. IST-2001-32747 Global Computing Initiative.
- [8] N. Saravanan†, N. Sreenivasulu†, D. Jayaram†, and A. Chockalingam‡, Design and Performance Evaluation of an Inter-System Handover Algorithm in UMTS/GSM Networks.
- [9] Tripathi, N., Nortel, Jerry, R and Vanlandingham. (1998) Handoff in Cellular Systems. IEEE Personal Communications • December 1998, 1070-9916/98/\$10.00 © 1998 IEEE.
- [10] Google search, <<http://www.wirelessdictionary.com/Wireless-Dictionary-Handover-HANDO-Definition.html>>
- [11] Googlesearch,http://www.radioelectronics.com/info/cellulartelecomms/cellular_concepts/handover_handoff.php
- [12] Google search, <http://en.wikipedia.org/wiki/Handover>
- [13] Optimization and Log File Analysis in GSM, by SomerGOKSEL, January 26, 2003.
- [14] MOTOROLA, Call and Handover Sequences (ppt), Appendix 2.
- [15] AkhilaS, Suthikshn Kumar, Handover in GSM Networks, 2009 Fifth International Conference on MEMS NANO, and Smart Systems, 978-0-7695-3938-6/09 \$25.00 © 2009 IEEE.
- [16] Frank A. Zdarsky and Jens B. Schmitt, Handover in Mobile Communication Networks: Who is in Control Anyway?, Proceedings of the 30th EUROMICRO Conference (EUROMICRO’04)1089-6503/04 \$ 20.00 IEEE.

Extensions of Enestrom-Kakeya Theorem

M. H. Gulzar

*Department of Mathematics
University of Kashmir, Srinagar 190006*

ABSTRACT:

In this paper we give an extension of the famous Enestrom-Kakeya Theorem, which generalizes many generalizations of the said theorem as well.

Mathematics Subject Classification: 30 C 10, 30 C 15

Keywords and Phrases: Coefficient, Polynomial, Zero

I. INTRODUCTION AND STATEMENT OF RESULTS

A famous result giving a bound for all the zeros of a polynomial with real positive monotonically decreasing coefficients is the following result known as Enestrom-Kakeya theorem [8]:

Theorem A: Let $P(z) = \sum_{j=0}^n a_j z^j$ be a polynomial of degree n such that

$$a_n \geq a_{n-1} \geq \dots \geq a_1 \geq a_0 > 0.$$

Then all the zeros of $P(z)$ lie in the closed disk $|z| \leq 1$.

If the coefficients are monotonic but not positive, Joyal, Labelle and Rahman [6] gave the following generalization of Theorem A:

Theorem B: Let $P(z) = \sum_{j=0}^n a_j z^j$ be a polynomial of degree n such that

$$a_n \geq a_{n-1} \geq \dots \geq a_1 \geq a_0.$$

Then all the zeros of $P(z)$ lie in the closed disk $|z| \leq \frac{a_n - a_0 + |a_0|}{|a_n|}$.

Aziz and Zargar [1] generalized Theorem B by proving the following result:

Theorem C: Let $P(z) = \sum_{j=0}^n a_j z^j$ be a polynomial of degree n such that for some $k \geq 1$,

$$ka_n \geq a_{n-1} \geq \dots \geq a_1 \geq a_0.$$

Then all the zeros of $P(z)$ lie in the closed disk

$$|z + k - 1| \leq \frac{ka_n - a_0 + |a_0|}{|a_n|}.$$

Gulzar [4,5] generalized Theorem C to polynomials with complex coefficients and proved the following results:

Theorem D: Let $P(z) = \sum_{j=0}^n a_j z^j$ be a polynomial of degree n with $\operatorname{Re}(a_j) = \alpha_j$,

$\operatorname{Im}(a_j) = \beta_j, j = 0, 1, \dots, n$ such that for some $k \geq 1, 0 < \tau \leq 1$,

$$k\alpha_n \geq \alpha_{n-1} \geq \dots \geq \alpha_1 \geq \tau\alpha_0.$$

Then all the zeros of $P(z)$ lie in the closed disk

$$\left| z + (k-1) \frac{\alpha_n}{a_n} \right| \leq \frac{k\alpha_n + 2|\alpha_0| - \tau(\alpha_0 + |\alpha_0|) + 2\sum_{j=0}^n |\beta_j|}{|a_n|}.$$

Theorem E: Let $P(z) = \sum_{j=0}^n a_j z^j$ be a polynomial of degree n with $\text{Re}(a_j) = \alpha_j$,

$\text{Im}(a_j) = \beta_j, j = 0, 1, \dots, n$ such that for some $k \geq 1, 0 < \tau \leq 1$,

$$k\beta_n \geq \beta_{n-1} \geq \dots \geq \beta_1 \geq \tau\beta_0.$$

Then all the zeros of $P(z)$ lie in the closed disk

$$\left| z + (k-1) \frac{\beta_n}{a_n} \right| \leq \frac{k\beta_n + 2|\beta_0| - \tau(\beta_0 + |\beta_0|) + 2\sum_{j=0}^n |\alpha_j|}{|a_n|}.$$

Theorem F : Let $P(z) = \sum_{j=0}^n a_j z^j$ be a polynomial of degree n such that for some

real $\alpha, \beta; \left| \arg a_j - \beta \right| \leq \alpha \leq \frac{\pi}{2}, j = 0, 1, 2, \dots, n$, and for some $k \geq 1, 0 < \tau \leq 1$,

$$k|a_n| \geq |a_{n-1}| \geq \dots \geq |a_1| \geq \tau|a_0|.$$

Then all the zeros of $P(z)$ lie in the closed disk

$$|z| \leq \frac{k|a_n|(1 + \cos \alpha + \sin \alpha) - |a_n| + 2|a_0| - \tau|a_0|(\cos \alpha - \sin \alpha + 1) + 2 \sin \alpha \sum_{j=1}^{n-1} |a_j|}{|a_n|}.$$

Some questions which have been raised by some researchers in connection with the Enestrom-Kakeya Theorem are[2]:

What happens, if (i) instead of the leading coefficient a_n , there is some a_j with

$a_{j+1} \geq a_j < a_{j-1}$ such that for some $k \geq 1, a_n \geq a_{n-1} \geq \dots \geq a_{j+1} \geq ka_j \geq a_{j-1} \dots \geq \alpha_1 \geq \alpha_0$, $j=1, 2, \dots, n$ and (ii) for some $k_1 \geq 1, k_2 \geq 1; k_1 a_n \geq k_2 a_{n-1} \geq \dots \geq a_1 \geq a_0$.

In this direction, Liman and Shah [7, Cor.1] have proved the following result:

Theorem G: Let $P(z) = \sum_{j=0}^n a_j z^j$ be a polynomial of degree n such that for some $k \geq 1$,

$$a_n \geq a_{n-1} \geq \dots \geq a_{\lambda+1} \geq ka_\lambda \geq a_{\lambda-1} \dots \geq a_1 \geq a_0.$$

Then $P(z)$ has all its zeros in

$$|z| \leq \frac{a_n - a_0 + |a_0| + (k-1) \left\{ \sum_{j=\lambda}^n (a_j + |a_j|) - |a_n| \right\}}{|a_n|}.$$

Unfortunately, the conclusion of the theorem is not correct and their claim that it follows from Theorem 1 in [7] is false. The correct form of the result is as follows:

Theorem H: Let $P(z) = \sum_{j=0}^n a_j z^j$ be a polynomial of degree n with $\text{Re}(a_j) = \alpha_j$,

$\text{Im}(a_j) = \beta_j, j = 0, 1, \dots, n$ such that for some $k \geq 1$,

$$a_n \geq a_{n-1} \geq \dots \geq a_{\lambda+1} \geq ka_\lambda \geq a_{\lambda-1} \dots \geq a_1 \geq a_0.$$

Then $P(z)$ has all its zeros in

$$|z| \leq \frac{a_n - a_0 + |a_0| + 2(k-1)|a_\lambda|}{|a_n|}.$$

In this paper, we are going to prove the following more general result:

Theorem 1: Let $P(z) = \sum_{j=0}^n a_j z^j$ be a polynomial of degree n such that for some $k \geq 1, 0 < \tau \leq 1$,

$$a_n \geq a_{n-1} \geq \dots \geq a_{\lambda+1} \geq ka_\lambda \geq a_{\lambda-1} \dots \geq a_1 \geq \tau a_0.$$

Then $P(z)$ has all its zeros in

$$|z| \leq \frac{a_n + 2(k-1)|a_\lambda| - \tau(a_0 + |a_0|) + 2|a_0|}{|a_n|}.$$

Remark 1: For $\tau = 1$, Theorem 1 reduces to Theorem H.

Taking in particular $k = \frac{a_{\lambda-1}}{a_\lambda} \geq 1$ in Theorem 1, we get the following

Corollary 1: Let $P(z) = \sum_{j=0}^n a_j z^j$ be a polynomial of degree n with $\text{Re}(a_j) = \alpha_j$,

$\text{Im}(a_j) = \beta_j, j = 0, 1, \dots, n$ such that

$$a_n \geq a_{n-1} \geq \dots \geq a_{\lambda+1} \geq a_\lambda \leq a_{\lambda-1} \geq \dots \geq a_1 \geq \tau a_0.$$

Then $P(z)$ has all its zeros in

$$|z| \leq \frac{a_n + 2\left(\frac{a_{\lambda-1} - a_\lambda}{a_\lambda}\right)|a_\lambda| - \tau(a_0 + |a_0|) + 2|a_0|}{|a_n|}.$$

For $\tau = 1$, Cor. 1 reduces to the following

Corollary 2: Let $P(z) = \sum_{j=0}^n a_j z^j$ be a polynomial of degree n with $\text{Re}(a_j) = \alpha_j$,

$\text{Im}(a_j) = \beta_j, j = 0, 1, \dots, n$ such that

$$a_n \geq a_{n-1} \geq \dots \geq a_{\lambda+1} \geq a_\lambda \leq a_{j-1} \geq \dots \geq a_1 \geq a_0.$$

Then $P(z)$ has all its zeros in

$$|z| \leq \frac{a_n + \left(\frac{a_{\lambda-1} - a_\lambda}{a_\lambda}\right)(|a_\lambda| - a_0 + |a_0|)}{|a_n|}.$$

Theorem 1 is a special case of the following more general result:

Theorem 2: Let $P(z) = \sum_{j=0}^n a_j z^j$ be a polynomial of degree n with $\text{Re}(a_j) = \alpha_j$,

$\text{Im}(a_j) = \beta_j, j = 0, 1, \dots, n$ such that for some $k \geq 1$,

$$\alpha_n \geq \alpha_{n-1} \geq \dots \geq \alpha_{\lambda+1} \geq k\alpha_\lambda \geq \alpha_{\lambda-1} \dots \geq \alpha_1 \geq \tau\alpha_0.$$

Then $P(z)$ has all its zeros in

$$|z| \leq \frac{\alpha_n + 2(k-1)|\alpha_\lambda| - \tau(\alpha_0 + |\alpha_0|) + 2|\alpha_0| + 2\sum_{j=0}^n |\beta_j|}{|a_n|}.$$

Remark 2: If $\beta_j = 0, \forall j = 0, 1, 2, \dots, n$ i.e. a_j is real, then Theorem 2 reduces to Theorem 1.

Applying Theorem 2 to the polynomial $-iP(z)$, we get the following result:

Theorem 3: Let $P(z) = \sum_{j=0}^n a_j z^j$ be a polynomial of degree n with $\text{Re}(a_j) = \alpha_j$,

$\text{Im}(a_j) = \beta_j, j = 0, 1, \dots, n$ such that for some $k \geq 1, 0 < \tau \leq 1$,

$$\beta_n \geq \beta_{n-1} \geq \dots \geq \beta_{j+1} \geq k\beta_j \geq \beta_{j-1} \dots \geq \beta_1 \geq \tau\beta_0.$$

Then $P(z)$ has all its zeros in

$$|z| \leq \frac{a_n + 2(k-1)|\beta_n| - \tau(\beta_0 + |\beta_0|) + 2|\beta_0| + 2\sum_{j=0}^n |\alpha_j|}{|a_n|}.$$

For polynomials with complex coefficients, we have the following form of Theorem 1:

Theorem 4: Let $P(z) = \sum_{j=0}^n a_j z^j$ be a polynomial of degree n such that for some $k \geq 1, 0 < \tau \leq 1$,

$$|a_n| \geq |a_{n-1}| \geq \dots \geq |a_{\lambda+1}| \geq k|a_\lambda| \geq |a_{\lambda-1}| \dots \geq |a_1| \geq \tau|a_0|.$$

Then $P(z)$ has all its zeros in

$$|z| \leq \frac{1}{|a_n|} [|a_n|(\cos \alpha + \sin \alpha) - k|a_\lambda|(\cos \alpha - \sin \alpha - 1) + 2|a_\lambda|(k + k \sin \alpha - 1) - \tau|a_0|(\cos \alpha - \sin \alpha + 1) + 2|a_0|]$$

Remark 3: For $k=1$, Theorem 4 reduces to Theorem F with $k=1$.

Next, we prove the following result:

Theorem 5: Let $P(z) = \sum_{j=0}^n a_j z^j$ be a polynomial of degree n with $\text{Re}(a_j) = \alpha_j$,

$\text{Im}(a_j) = \beta_j, j = 0, 1, \dots, n$ such that for some $k_1 \geq 1, k_2 \geq 1, 0 < \tau \leq 1$,

$$k_1\alpha_n \geq k_2\alpha_{n-1} \geq \alpha_{n-2} \dots \alpha_1 \geq \tau\alpha_0.$$

Then $P(z)$ has all its zeros in

$$|z| \leq \frac{(k_1|a_n| + k_2|a_{n-1}|) + (k_1\alpha_n - k_2\alpha_{n-1}) + \alpha_{n-1} - (|a_n| + |a_{n-1}|) + 2|a_0| + 2\sum_{j=0}^n |\beta_j|}{|a_n|}.$$

Remark 4: If $\beta_j = 0, \forall j = 0, 1, 2, \dots, n$ i.e. a_j is real, we get the following result:

Corollary 3: Let $P(z) = \sum_{j=0}^n a_j z^j$ be a polynomial of degree n such that for some

$k_1 \geq 1, k_2 \geq 1, 0 < \tau \leq 1$,

$$k_1 a_n \geq k_2 a_{n-1} \geq a_{n-2} \dots a_1 \geq \tau a_0.$$

Then $P(z)$ has all its zeros in

$$|z| \leq \frac{(k_1|a_n| + k_2|a_{n-1}|) + (k_1 a_n - k_2 a_{n-1}) + a_{n-1} - (|a_n| + |a_{n-1}|) + 2|a_0|}{|a_n|}.$$

Applying Theorem 2 to the polynomial $-iP(z)$, we get the following result from Theorem 4:

Theorem 6: Let $P(z) = \sum_{j=0}^n a_j z^j$ be a polynomial of degree n with $\text{Re}(a_j) = \alpha_j$,

$\text{Im}(a_j) = \beta_j, j = 0, 1, \dots, n$ such that for some $k_1 \geq 1, k_2 \geq 1, 0 < \tau \leq 1$,

$$k_1 \beta_n \geq k_2 \beta_{n-1} \geq \beta_{n-2} \dots \geq \beta_1 \geq \tau \beta_0 .$$

Then P(z) has all its zeros in

$$|z| \leq \frac{(k_1 |\beta_n| + k_2 |\beta_{n-1}|) + (k_1 \beta_n - k_2 \beta_{n-1}) + \beta_{n-1} - (|\beta_n| + |\beta_{n-1}|) + 2|\beta_0| + 2 \sum_{j=0}^n |\alpha_j|}{|a_n|} .$$

Theorem 7: Let $P(z) = \sum_{j=0}^n a_j z^j$ be a polynomial of degree n such that for some

real α, β ; $|\arg a_j - \beta| \leq \alpha \leq \frac{\pi}{2}$, $j = 0, 1, 2, \dots, n$, and for some $k_1 \geq 1, k_2 \geq 1, 0 < \tau \leq 1$,

$$k_1 |a_n| \geq k_2 |a_{n-1}| \geq |a_{n-2}| \dots \geq |a_1| \geq \tau |a_0| .$$

Then P(z) has all its zeros in

$$|z| \leq \frac{1}{|a_n|} \left[k_1 |a_n| (1 + \cos \alpha + \sin \alpha) + k_2 |a_{n-1}| (1 - \cos \alpha + \sin \alpha) - |a_n| - |a_{n-1}| (1 - \cos \alpha) + 2 |a_0| \right] - \tau |a_0| (\cos \alpha - \sin \alpha + 1) + 2 \sin \alpha \sum_{j=1}^{n-2} |a_j| .$$

Remark 4: For $k_1 = k, k_2 = 1$, Theorem 6 reduces to Theorem F.

Taking $\tau = 1$ in Theorem 7, we get the following

Corollary 4: Let $P(z) = \sum_{j=0}^n a_j z^j$ be a polynomial of degree n such that for some

real α, β ; $|\arg a_j - \beta| \leq \alpha \leq \frac{\pi}{2}$, $j = 0, 1, 2, \dots, n$, and for some $k_1 \geq 1, k_2 \geq 1$,

$$k_1 |a_n| \geq k_2 |a_{n-1}| \geq |a_{n-2}| \dots \geq |a_1| \geq |a_0| .$$

Then P(z) has all its zeros in

$$|z| \leq \frac{1}{|a_n|} \left[k_1 |a_n| (1 + \cos \alpha + \sin \alpha) + k_2 |a_{n-1}| (1 - \cos \alpha + \sin \alpha) - |a_n| \right. \\ \left. - |a_{n-1}| (1 - \cos \alpha) - \tau |a_0| (1 + \cos \alpha - \sin \alpha) + 2 |a_0| + 2 \sin \alpha \sum_{j=1}^{n-1} |a_j| \right] .$$

II. LEMMA

For the proof of Theorem 6, we need the following lemma:

Lemma: Let a_1 and a_2 be any two complex numbers such that $|a_1| \geq |a_2|$ and for some real numbers α and

β , $|\arg a_j - \beta| \leq \alpha \leq \frac{\pi}{2}$, $j = 1, 2$, then

$$|a_1 - a_2| \leq (|a_1| - |a_2|) \cos \alpha + (|a_1| + |a_2|) \sin \alpha .$$

The above lemma is due to Govil and Rahman [3].

3. Proofs of Theorems

Proof of Theorem 2: Consider the polynomial

$$F(z) = (1 - z)P(z) = (1 - z)(a_n z^n + a_{n-1} z^{n-1} + \dots + a_1 z + a_0) \\ = -a_n z^{n+1} + (a_n - a_{n-1})z^n + (a_{n-1} - a_{n-2})z^{n-1} + \dots + (a_{\lambda+1} - a_\lambda)z^{\lambda+1} \\ + (a_\lambda - a_{\lambda-1})z^\lambda + \dots + (a_1 - a_0)z + a_0$$

$$\begin{aligned}
 &= -a_n z^{n+1} + (\alpha_n - \alpha_{n-1})z^n + (\alpha_{n-1} - \alpha_{n-2})z^{n-1} + \dots \\
 &\quad + \{(\alpha_{\lambda+1} - k\alpha_\lambda) + (k\alpha_\lambda - \alpha_{\lambda-1})\} z^{\lambda+1} + \{(k\alpha_\lambda - \alpha_{\lambda-1}) - (k\alpha_\lambda - \alpha_\lambda)\} z^\lambda + \dots \\
 &\quad + \{(\alpha_1 - \tau\alpha_0) + (\tau\alpha_0 - \alpha_0)\} z + \alpha_0 + i\{(\beta_n - \beta_{n-1})z^n + \dots + (\beta_1 - \beta_0)z + \beta_0\}
 \end{aligned}$$

For $|z| > 1$, we have, $\frac{1}{|z|^j} < 1, \forall j = 1, 2, \dots, n$ so that, by using the hypothesis,

$$\begin{aligned}
 |F(z)| &\geq |a_n| |z|^{n+1} - [|\alpha_n - \alpha_{n-1}| |z|^n + |\alpha_{n-1} - \alpha_{n-2}| |z|^{n-1} + \dots + |\alpha_{\lambda+1} - k\alpha_\lambda| |z|^{\lambda+1} \\
 &\quad + (k-1)|\alpha_\lambda| |z|^{\lambda+1} + |k\alpha_\lambda - \alpha_{\lambda-1}| |z|^\lambda + (k-1)|\alpha_\lambda| |z|^\lambda + \dots + |\alpha_1 - \tau\alpha_0| |z| \\
 &\quad + (1-\tau)|\alpha_0| |z| + |\alpha_0| + \sum_{j=1}^n |\beta_j - \beta_{j-1}| |z|^j + |\beta_0|] \\
 &= |z|^n [|a_n| |z| - \{ |\alpha_n - \alpha_{n-1}| + |\alpha_{n-1} - \alpha_{n-2}| \frac{1}{|z|} + \dots + |\alpha_{\lambda+1} - k\alpha_\lambda| \frac{1}{|z|^{n-\lambda-1}} \\
 &\quad + (k-1)|\alpha_\lambda| \frac{1}{|z|^{n-\lambda-1}} + |k\alpha_\lambda - \alpha_{\lambda-1}| \frac{1}{|z|^{n-\lambda}} + (k-1)|\alpha_\lambda| \frac{1}{|z|^{n-\lambda}} + \dots + |\alpha_1 - \tau\alpha_0| \frac{1}{|z|^{n-1}} \\
 &\quad + (1-\tau)|\alpha_0| \frac{1}{|z|^{n-1}} + |\alpha_0| \frac{1}{|z|^n} + \sum_{j=1}^n |\beta_j - \beta_{j-1}| \frac{1}{|z|^{n-j}} + |\beta_0| \frac{1}{|z|^n} \}] \\
 &> |z|^n [|a_n| |z| - [|\alpha_n - \alpha_{n-1}| + |\alpha_{n-1} - \alpha_{n-2}| + \dots + |\alpha_{\lambda+1} - k\alpha_\lambda| + (k-1)|\alpha_\lambda| \\
 &\quad + |k\alpha_\lambda - \alpha_{\lambda-1}| + (k-1)|\alpha_\lambda| + \dots + |\alpha_1 - \tau\alpha_0| + (1-\tau)|\alpha_0| + |\alpha_0| \\
 &\quad + \sum_{j=1}^n (|\beta_j| + |\beta_{j-1}|) + |\beta_0|] \\
 &= |z|^n [|a_n| |z| - [|\alpha_n + 2(k-1)|\alpha_\lambda| - \tau(\alpha_0 + |\alpha_0|) + 2|\alpha_0| + 2\sum_{j=0}^n |\beta_j|] \\
 &> 0
 \end{aligned}$$

if

$$|z| > \frac{|\alpha_n + 2(k-1)|\alpha_\lambda| - \tau(\alpha_0 + |\alpha_0|) + 2|\alpha_0| + 2\sum_{j=0}^n |\beta_j|}{|a_n|} .$$

This shows that the zeros of F(z) having modulus greater than 1 lie in

$$|z| \leq \frac{|\alpha_n + 2(k-1)|\alpha_\lambda| - \tau(\alpha_0 + |\alpha_0|) + 2|\alpha_0| + 2\sum_{j=0}^n |\beta_j|}{|a_n|} .$$

But the zeros of F(z) whose modulus is less than or equal to 1 already satisfy the above inequality. Hence, it follows that all the zeros of F(z) lie in

$$|z| \leq \frac{|\alpha_n + 2(k-1)|\alpha_\lambda| - \tau(\alpha_0 + |\alpha_0|) + 2|\alpha_0| + 2\sum_{j=0}^n |\beta_j|}{|a_n|} .$$

Since the zeros of $P(z)$ are also the zeros of $F(z)$, the result follows.

Proof of Theorem 4: Consider the polynomial

$$\begin{aligned} F(z) &= (1-z)P(z) = (1-z)(a_n z^n + a_{n-1} z^{n-1} + \dots + a_1 z + a_0) \\ &= -a_n z^{n+1} + (a_n - a_{n-1})z^n + (a_{n-1} - a_{n-2})z^{n-1} + \dots + \{(a_{\lambda+1} - ka_\lambda) + (ka_\lambda - a_\lambda)\} z^{\lambda+1} \\ &\quad + \{(ka_\lambda - a_{\lambda-1}) - (ka_\lambda - a_\lambda)\} z^\lambda + (a_{\lambda-1} - a_{\lambda-2})z^{\lambda-1} + \dots \\ &\quad \{(a_1 - \tau a_0) + (\tau a_0 - a_0)\} z + a_0. \end{aligned}$$

For $|z| > 1$, we have, $\frac{1}{|z|^j} < 1, \forall j = 1, 2, \dots, n$, so that, by using the hypothesis and the Lemma,

$$\begin{aligned} |F(z)| &\geq |a_n| |z|^{n+1} - [|a_n - a_{n-1}| |z|^n + |a_{n-1} - a_{n-2}| |z|^{n-1} + \dots + |a_{\lambda+1} - ka_\lambda| |z|^{\lambda+1} \\ &\quad + (k-1)|a_\lambda| |z|^{\lambda+1} + |ka_\lambda - a_{\lambda-1}| |z|^\lambda + (k-1)|a_\lambda| |z|^\lambda + \dots + |a_1 - \tau a_0| |z| \\ &\quad + (1-\tau)|a_0| |z| + |a_0|] \\ &= |z|^n [|a_n| |z| - \{|a_n - a_{n-1}| + |a_{n-1} - a_{n-2}| \frac{1}{|z|} + \dots + |a_{\lambda+1} - ka_\lambda| \frac{1}{|z|^{n-\lambda-1}} \\ &\quad + (k-1)|a_\lambda| \frac{1}{|z|^{n-\lambda-1}} + |ka_\lambda - a_{\lambda-1}| \frac{1}{|z|^{n-\lambda}} + (k-1)|a_\lambda| \frac{1}{|z|^{n-\lambda}} + \dots + |a_1 - \tau a_0| \frac{1}{|z|^{n-1}} \\ &\quad + (1-\tau)|a_0| \frac{1}{|z|^{n-1}} + |a_0| \frac{1}{|z|^n} \}] \\ &> |z|^n [|a_n| |z| - \{|a_n - a_{n-1}| + |a_{n-1} - a_{n-2}| + \dots + |a_{\lambda+1} - ka_\lambda| \\ &\quad + (k-1)|a_\lambda| + |ka_\lambda - a_{\lambda-1}| + (k-1)|a_\lambda| + \dots + |a_1 - \tau a_0| \\ &\quad + (1-\tau)|a_0| + |a_0| \}] \\ &\geq |z|^n [|a_n| |z| - \{(|a_n| - |a_{n-1}|) \cos \alpha + (|a_n| + |a_{n-1}|) \sin \alpha + (|a_{n-1}| - |a_{n-2}|) \cos \alpha \\ &\quad + (|a_{n-1}| + |a_{n-2}|) \sin \alpha + \dots + (|a_{\lambda+1}| - k|a_\lambda|) \cos \alpha + (|a_{\lambda+1}| + k|a_\lambda|) \sin \alpha \\ &\quad + (k-1)|a_\lambda| + (k|a_\lambda| - |a_{\lambda+1}|) \cos \alpha + (k|a_\lambda| + |a_{\lambda+1}|) \sin \alpha + (k-1)|a_\lambda| \\ &\quad + (|a_{\lambda+1}| - |a_{\lambda-2}|) \cos \alpha + (|a_{\lambda+1}| + |a_{\lambda-2}|) \sin \alpha + \dots + (|a_1| - \tau|a_0|) \cos \alpha \\ &\quad + (|a_1| + \tau|a_0|) \sin \alpha + (1-\tau)|a_0| + |a_0| \}] \\ &= |z|^n [|a_n| |z| - \{|a_n| (\cos \alpha + \sin \alpha) - k|a_\lambda| (\cos \alpha - \sin \alpha - 1) + 2|a_\lambda| (k + k \sin \alpha - 1) \\ &\quad - \tau|a_0| (\cos \alpha - \sin \alpha + 1) + 2|a_0| \}] \\ &> 0 \end{aligned}$$

if

$$\begin{aligned} |z| &> \frac{1}{|a_n|} [|a_n| (\cos \alpha + \sin \alpha) - k|a_\lambda| (\cos \alpha - \sin \alpha - 1) + 2|a_\lambda| (k + k \sin \alpha - 1) \\ &\quad - \tau|a_0| (\cos \alpha - \sin \alpha + 1) + 2|a_0|] \end{aligned}$$

This shows that the zeros of $F(z)$ having modulus greater than 1 lie in

$$|z| \leq \frac{1}{|a_n|} [|a_n| (\cos \alpha + \sin \alpha) - k |a_\lambda| (\cos \alpha - \sin \alpha - 1) + 2 |a_\lambda| (k + k \sin \alpha - 1) - \tau |a_0| (\cos \alpha - \sin \alpha + 1) + 2 |a_0|]$$

But the zeros of $F(z)$ whose modulus is less than or equal to 1 already satisfy the above inequality. Hence, it follows that all the zeros of $F(z)$ lie in

$$|z| \leq \frac{1}{|a_n|} [|a_n| (\cos \alpha + \sin \alpha) - k |a_\lambda| (\cos \alpha - \sin \alpha - 1) + 2 |a_\lambda| (k + k \sin \alpha - 1) - \tau |a_0| (\cos \alpha - \sin \alpha + 1) + 2 |a_0|]$$

Since the zeros of $P(z)$ are also the zeros of $F(z)$, the result follows.

Proof of Theorem 5: Consider the polynomial

$$\begin{aligned} F(z) &= (1-z)P(z) = (1-z)(a_n z^n + a_{n-1} z^{n-1} + \dots + a_1 z + a_0) \\ &= -a_n z^{n+1} + (a_n - a_{n-1})z^n + (a_{n-1} - a_{n-2})z^{n-1} + \dots + (a_1 - a_0)z + a_0 \\ &= -a_n z^{n+1} + \{ (k_1 \alpha_n - k_2 \alpha_{n-1}) - (k_1 \alpha_n - \alpha_n) + (k_2 \alpha_{n-1} - \alpha_{n-1}) \} z^n + (\alpha_{n-1} - \alpha_{n-2})z^{n-1} \\ &\quad + \dots + \{ (\alpha_1 - \tau \alpha_0) + (\tau \alpha_0 - \alpha_0) \} z + \alpha_0 + i \{ (\beta_n - \beta_{n-1})z^n + \dots \\ &\quad + (\beta_1 - \beta_0)z + \beta_0 \} \end{aligned}$$

For $|z| > 1$, we have, $\frac{1}{|z|^j} < 1, \forall j = 1, 2, \dots, n$, so that, by using the hypothesis,

$$\begin{aligned} |F(z)| &\geq |a_n| |z|^{n+1} - [|k_1 \alpha_n - k_2 \alpha_{n-1}| |z|^n + |k_1 \alpha_n - \alpha_n| |z|^n + |k_2 \alpha_{n-1} - \alpha_{n-1}| |z|^n + |\alpha_{n-1} - \alpha_{n-2}| |z|^{n-1} \\ &\quad + \dots + |\alpha_1 - \tau \alpha_0| |z| + (1-\tau) |\alpha_0| |z| + |\alpha_0| + \sum_{j=1}^n |\beta_j - \beta_{j-1}| |z|^j + |\beta_0|] \\ &= |z|^n [|a_n| |z| - [|k_1 \alpha_n - k_2 \alpha_{n-1}| + |k_1 \alpha_n - \alpha_n| + |k_2 \alpha_{n-1} - \alpha_{n-1}| + |\alpha_{n-1} - \alpha_{n-2}| \frac{1}{|z|} \dots \\ &\quad + |\alpha_1 - \tau \alpha_0| \frac{1}{|z|^{n-1}} + (1-\tau) |\alpha_0| \frac{1}{|z|^{n-1}} + |\alpha_0| \frac{1}{|z|^n} + \sum_{j=1}^n |\beta_j - \beta_{j-1}| \frac{1}{|z|^{n-j}} + |\beta_0| \frac{1}{|z|^n}]] \\ &> |z|^n [|a_n| |z| - \{ |k_1 \alpha_n - k_2 \alpha_{n-1}| + (k_1 - 1) |\alpha_n| + (k_2 - 1) |\alpha_{n-1}| + \alpha_{n-1} - \alpha_{n-2} + \dots \\ &\quad + \alpha_1 - \tau \alpha_0 + (1-\tau) |\alpha_0| + |\alpha_0| + \sum_{j=1}^n (|\beta_j| + |\beta_{j-1}|) + |\beta_0| \}] \\ &= |z|^n [|a_n| |z| - \{ |k_1 \alpha_n - k_2 \alpha_{n-1}| + (k_1 - 1) |\alpha_n| + (k_2 - 1) |\alpha_{n-1}| + \alpha_{n-1} + \dots \\ &\quad - \tau (\alpha_0 + |\alpha_0|) + 2 |\alpha_0| + 2 \sum_{j=0}^n |\beta_j| \}] \\ &= |z|^n [|a_n| |z| - \{ (k_1 |\alpha_n| + k_2 |\alpha_{n-1}|) + (k_1 \alpha_n - k_2 \alpha_{n-1}) + \alpha_{n-1} - (|\alpha_n| + |\alpha_{n-1}|) \\ &\quad + 2 |\alpha_0| + 2 \sum_{j=0}^n |\beta_j| \}] \end{aligned}$$

> 0

if

$$|z| > \frac{1}{|a_n|} [(k_1|\alpha_n| + k_2|\alpha_{n-1}|) + (k_1\alpha_n - k_2\alpha_{n-1}) + \alpha_{n-1} - (|\alpha_n| + |\alpha_{n-1}|) + 2|\alpha_0| + 2\sum_{j=0}^n |\beta_j|]$$

This shows that the zeros of F(z) having modulus greater than 1 lie in

$$|z| \leq \frac{1}{|a_n|} [(k_1|\alpha_n| + k_2|\alpha_{n-1}|) + (k_1\alpha_n - k_2\alpha_{n-1}) + \alpha_{n-1} - (|\alpha_n| + |\alpha_{n-1}|) + 2|\alpha_0| + 2\sum_{j=0}^n |\beta_j|].$$

But the zeros of F(z) whose modulus is less than or equal to 1 already satisfy the above inequality. Hence, it follows that all the zeros of F(z) lie in

$$|z| \leq \frac{1}{|a_n|} [(k_1|\alpha_n| + k_2|\alpha_{n-1}|) + (k_1\alpha_n - k_2\alpha_{n-1}) + \alpha_{n-1} - (|\alpha_n| + |\alpha_{n-1}|) + 2|\alpha_0| + 2\sum_{j=0}^n |\beta_j|]$$

Since the zeros of P(z) are also the zeros of F(z), Theorem 4 follows.

Proof of Theorem 6. Consider the polynomial

$$\begin{aligned} F(z) &= (1-z)P(z) = (1-z)(a_n z^n + a_{n-1} z^{n-1} + \dots + a_1 z + a_0) \\ &= -a_n z^{n+1} + (a_n - a_{n-1})z^n + (a_{n-1} - a_{n-2})z^{n-1} + \dots + (a_1 - a_0)z + a_0 \\ &= -a_n z^{n+1} + \{(k_1 a_n - k_2 a_{n-1}) - (k_1 a_n - a_n) + (k_2 a_{n-1} - a_{n-1})\} z^n + (a_{n-1} - a_{n-2}) z^{n-1} \\ &\quad + \dots + \{(a_1 - \tau a_0) + (\tau a_0 - a_0)\} z + a_0 \end{aligned}$$

For $|z| > 1$, we have, $\frac{1}{|z|^j} < 1, \forall j = 1, 2, \dots, n$, so that, by using the hypothesis and the Lemma,

$$\begin{aligned} |F(z)| &\geq |a_n||z|^{n+1} - [k_1 a_n - k_2 a_{n-1}||z|^n + |k_1 a_n - a_n||z|^n + |k_2 a_{n-1} - a_{n-1}||z|^n + |a_{n-1} - a_{n-2}||z|^{n-1} \\ &\quad + \dots + |a_1 - \tau a_0||z| + (1-\tau)|a_0||z| + |a_0|] \\ &= |z|^n [|a_n||z| - [k_1 a_n - k_2 a_{n-1}| + |k_1 a_n - a_n| + |k_2 a_{n-1} - a_{n-1}| + |a_{n-1} - a_{n-2}| \frac{1}{|z|} + \dots \\ &\quad + |a_1 - \tau a_0| \frac{1}{|z|^{n-1}} + (1-\tau)|a_0| \frac{1}{|z|^{n-1}} + |a_0| \frac{1}{|z|^n}] \\ &> |z|^n [|a_n||z| - \{ |k_1 a_n - k_2 a_{n-1}| + |k_1 a_n - a_n| + |k_2 a_{n-1} - a_{n-1}| + |a_{n-1} - a_{n-2}| + \dots \\ &\quad + |a_1 - \tau a_0| + (1-\tau)|a_0| + |a_0| \}] \\ &\geq |z|^n [|a_n||z| - \{ (k_1|a_n| - k_2|a_{n-1}|) \cos \alpha + (k_1|a_n| + k_2|a_{n-1}|) \sin \alpha + (k_1 - 1)|a_n| \\ &\quad + (k_2 - 1)|a_{n-1}| + (|a_{n-1}| - |a_{n-2}|) \cos \alpha + (|a_{n-1}| + |a_{n-2}|) \sin \alpha + \dots \\ &\quad + (|a_1| - \tau|a_0|) \cos \alpha + (|a_1| + \tau|a_0|) \sin \alpha + (1-\tau)|a_0| \}] \\ &= |z|^n [|a_n||z| - \{ k_1|a_n|(1 + \cos \alpha + \sin \alpha) + k_2|a_{n-1}|(1 - \cos \alpha + \sin \alpha) - |a_n| \\ &\quad - |a_{n-1}|(1 - \cos \alpha) - \tau|a_0|(1 + \cos \alpha - \sin \alpha) + 2|a_0| + 2 \sin \alpha \sum_{j=1}^{n-1} |a_j| \}] \end{aligned}$$

>0

if

$$|z| > \frac{1}{|a_n|} [k_1 |a_n| (1 + \cos \alpha + \sin \alpha) + k_2 |a_{n-1}| (1 - \cos \alpha + \sin \alpha) - |a_n| - |a_{n-1}| (1 - \cos \alpha) - \tau |a_0| (1 + \cos \alpha - \sin \alpha) + 2|a_0| + 2 \sin \alpha \sum_{j=1}^{n-1} |a_j|].$$

This shows that the zeros of F(z) having modulus greater than 1 lie in

$$|z| \leq \frac{1}{|a_n|} [k_1 |a_n| (1 + \cos \alpha + \sin \alpha) + k_2 |a_{n-1}| (1 - \cos \alpha + \sin \alpha) - |a_n| - |a_{n-1}| (1 - \cos \alpha) - \tau |a_0| (1 + \cos \alpha - \sin \alpha) + 2|a_0| + 2 \sin \alpha \sum_{j=1}^{n-1} |a_j|].$$

But the zeros of F(z) whose modulus is less than or equal to 1 already satisfy the above inequality. Hence, it follows that all the zeros of F(z) lie in

$$|z| \leq \frac{1}{|a_n|} [k_1 |a_n| (1 + \cos \alpha + \sin \alpha) + k_2 |a_{n-1}| (1 - \cos \alpha + \sin \alpha) - |a_n| - |a_{n-1}| (1 - \cos \alpha) - \tau |a_0| (1 + \cos \alpha - \sin \alpha) + 2|a_0| + 2 \sin \alpha \sum_{j=1}^{n-1} |a_j|].$$

Since the zeros of P(z) are also the zeros of F(z), the result follows.

REFERENCES

- [1] A.Aziz and B.A.Zargar, Some Extensions of Enestrom-Kakeya Theorem, Glasnik Math. 31(1996), 239-244.
- [2] N. K. Govvil, International Congress of ASIAM, Jammu University, India March 31-April 3, 2007.
- [3] N. K. Govil and Q.I. Rahman, On the Enestrom-Kakeya Theorem, Tohoku Math.J.20 (1968), 126-136.
- [4] M. H. Gulzar, Some Refinements of Enestrom-Kakeya Theorem, Int. Journal of Mathematical Archive -2(9, 2011),1512-1529.
- [5] M. H. Gulzar, Ph.D thesis, Department of Mathematics, University of Kashmir Srinagar, 2012.
- [6] A. Joyal, G. Labelle and Q. I. Rahman, On the Location of Zeros of Polynomials, Canad. Math. Bull., 10(1967), 53-66.
- [7] A. Liman and W. M. Shah, Extensions of Enestrom-Kakeya Theorem, Int. Journal of Modern Mathematical Sciences, 2013, 8(2), 82-89.
- [8] M. Marden, Geometry of Polynomials, Math. Surveys, No.3; Amer. Math. Soc. Providence R.I. 1966.

Analysis of Vulnerability Assessment in the Coastal Dakshina Kannada District, Mulki to Talapady Area, Karnataka

S. S. Honnanagoudar¹, D. Venkat Reddy¹ and Mahesha. A²

¹Department of Civil Engineering and ²Department of Applied Mechanics and Hydraulics
National Institute of Technology Karnataka, Surathkal, Mangalore - 575025, Karnataka.

ABSTRACT

The areal extent of the study area is about 40 kms. The wells were located on the map using GPS values obtained after conducting GPS survey in the field. Environmental preservation of the coastal regions constitutes a socioeconomic element of major importance for both the present and the future. The term vulnerability refers to the potential degree of damage that can be expected depending on the characteristics of an element risk with respect to a certain hazard. Seawater intrusion is a global issue, by increasing demand for freshwater in coastal zones. Based on GALDIT Index, the aquifer vulnerability index mapping was carried out. The distributions of vulnerability areas are high, medium and low class are 7.5, 5 and 2.5 respectively. The main purpose of the study is to determine the vulnerability of the groundwater in the south western part of the Dakshina Kannada coast against seawater intrusion to the current sea level. The methodology used in the study consists of assessment of vulnerability to groundwater contamination using GALDIT method, identification of saltwater intruded area using indicators of saltwater intrusion like $Cl/(HCO_3+CO_3)$ ratio and NA/Cl ratio etc.

KEYWORDS: Coastal aquifer, GALDIT index, saltwater intrusion, vulnerability assessment, GIS, overlay.

I. INTRODUCTION

Environmental preservation of the coastal regions constitutes a socioeconomic element of major importance for both the present and the future. These areas have been weakened because of various pressures exerted including over exploitation of groundwater for agricultural purposes and intensive domestic use of soil and fertilizer. This resulted in decline of resources such as soil and groundwater resources and in their quality and also in the increase of their vulnerability to different impact factor.

Generally, the term of vulnerability refers to the potential degree of damage that can be expected depending on the characteristics of an element at risk with respect to a certain hazard (Varnes, 1984; Georgescu, et al., 1993). Relating to groundwater, the vulnerability is defined by Lobo-Ferreira and Cabral (1991) as “the sensitivity of groundwater quality to an imposed contaminant load, which is determined by the intrinsic characteristics of the aquifer”. Thus the vulnerability of groundwater to different pollutants or to seawater intrusion constitutes a subject of analysis in several studies (Chachadi et al., 2002; Cardona et al., 2004; Lobo-Ferreira et al., 2005). Also the vulnerability of soil to salinization is demonstrated in many studies (George et al., 1997; Kotb et al., 2000; De Paz et al., 2004; Asa Rani et al., 2008; Zhang et al., 2011). The main purpose of the study is to determine the vulnerability of the groundwater in the south western part of the Dakshina Kannada coast against seawater intrusion to the current sea level.

Study area

The study area is located in the south western part of Karnataka, adjoining the Arabian sea. Its geographical area is about 4770 sq. km and the study area for the investigation is the coastal basin between Talapady and Mulki (Honnaganoudar et al., 2012). The areal extent of the study area is about 40 kms. The wells were located on the map using GPS values obtained after conducting GPS survey in the field. The elevation of the locations, lithology, depth to water table (later reduced to mean sea level), and distance of the well from the shore and river were noted. Water samples were collected from each well during September 2011 to August 2013 (two years) and subjected to chemical analysis by following standard procedures (APHA, 1998; Trivedi and Goel, 1986). The most important factors controlling the saltwater intrusion are considered in determination of vulnerability of aquifers. Elevations of water levels and well locations were determined with respect to mean sea level by conducting field survey.

Methodology

The methodology used in the study consists of assessment of vulnerability to groundwater contamination using GALDIT method, identification of saltwater intruded area using indicators of saltwater intrusion like $Cl/(HCO_3+CO_3)$ ratio and NA/Cl ratio etc.

Assessment of ranks to various parameters required for GALDIT

The Parameter such as GALDIT was weighted depending on the suggestions of local knowledge and the field conditions for assessing the vulnerability of the groundwater aquifer. The weight and the ranks for GALDIT parameters are given in the Table 1.

Table 1 GALDIT Parameter

	G	A	L	D	I	T
Parameters	Groundwater Occurrence	Aquifer Conductivity	Height of the ground water level	Distance from the shore	Impact of existing status	Aquifer Thickness
Weight Rates	1	3	4	4	1	2
2.5	Bounded aquifer	Very Low < 5m	Very Low > 2 m	>1000 m	<1	< 5
5.5	Leaky confined aquifer	Low 5 -10 m	Low 1.5 -2 m	750 -1000	1 -1.5	5-7.5
7.5	Unconfined aquifer	Medium 10-40 m	Medium 10-40 m	500-750	1.5 -2	7.5-10
10	Confined aquifer	High >40m	High >40m	<500	>2	>10

Vulnerability Evaluation and Ranking

The most important factors that control the saltwater intrusion are found to be the following.

- Groundwater occurrence (aquifer type; unconfined, confined and leaky confined).
- Aquifer hydraulic conductivity.
- Height of groundwater Level above sea level.
- Distance from the shore (distance inland perpendicular from shoreline).
- Impact of existing status of saltwater intrusion in the area.
- Thickness of the aquifer which is being mapped.

The acronym GALDIT is formed from the highlighted letters of the parameters for ease of reference. These factors, in combination, are used to assess the general saltwater intrusion potential of each hydro-geologic setting. The GALDIT factors represent measurable parameters for which data are generally available from a variety of sources without detailed reconnaissance.

The system contains three significant components - weights, ranges and importance ratings. Each GALDIT factor has been evaluated with respect to the other to determine the relative importance of each factor. The basic assumption made in the analysis is that the bottom of the aquifer lies below the mean sea level.

Mapping of GALDIT Index

Mapping of GALDIT index gives its variation in the study area, which is done by Arc GIS 9.5 software. Location of sampling stations and the water GALDIT index at each sampling site is required for mapping. The important steps involved for mappings are georeferencing, digitization and spatial interpolation. Georeferencing is the process of fixing of the locations of the real world features within the framework of a particular coordinate system. A series of concepts and techniques are used that progressively transforms the measurements that are carried out on the field to the map. Digitization usually begins with a set of control points, which are used for converting the digitized map to real world coordinates. Spatial interpretation is the process of using points with known values to estimate values at other points. Spatial interpretation is therefore a means of creating surface data from sample points so that the surface data can be used for analysis.

II. RESULTS AND DISCUSSION

Groundwater occurrence, G

From the pump test data it is evident that the aquifer is unconfined in nature with rich groundwater potential and hence a rating of 7.5 is adopted as per the specifications. Also, from the field observations it is evident that the aquifer is shallow and unconfined in nature.

Aquifer hydraulic conductivity, A

Finally from all the studies conducted to evaluate the hydraulic conductivity in the study area, we can conclude that the hydraulic conductivity varies from 5.43 m/day to 85.59 m/day and hence a common GALDIT rating of 10 can be assigned for the entire study area.

Height of water above the sea level, L

The groundwater levels were measured every month at the monitoring wells identified. The parameter required for the present study, ‘L’ is obtained by reducing the water level with respect to mean sea level and is presented in Table 2.

Table 2 Height of water above mean sea level

Well No.	Sept. 2011	Sept.2012	Well No.	Sept. 2011	Sept.2012
1	0.44	0.34	16	10.04	9.64
2	11.44	10.44	17	5.04	5.14
3	10.64	11.94	18	7.14	7.04
4	14.64	15.54	19	12.74	15.74
5	6.04	6.34	20	14.54	14.24
6	3.06	3.34	21	18.04	18.24
7	3.69	4.14	22	10.94	11.04
8	4.00	3.94	23	6.74	7.24
9	5.14	5.44	24	-2.86	-1.46
10	7.34	7.44	25	6.34	6.54
11	26.06	26.24	26	4.44	4.84
12	26.24	26.44	27	5.34	5.54
13	5.04	5.14	28	10.64	11.94
14	-1.06	-1.34	29	6.64	6.94
15	10.09	10.54	30	21.74	22.44

In the study area coastal wells are sunk in the porous soil. The water level gradually declines after the rains. As evident from Table 2; we can see some negative values indicating the possibility of salt water intrusion. The water table distribution of the area is presented in Fig 1 and Fig 2. Wells 14 and 24 have water level below ground level i.e. less than 1m throughout the year and well no. 1 is less than 1m i.e. 0.44 m to 0.34 m. The rating given for the above class is 10, remaining wells are more than 2 m and ratings are 2.5.

Distance from the shore/river, D

The magnitude of the saltwater intrusion is directly related to the perpendicular distance from the coast. Out of the monitoring network of wells, the nearest location to the saline source is well no.15 (Distance, D=27.70 m) and the farthest location is well no.19 (D=5035m).

Impact of existing status of saltwater intrusion, I

The chloride concentration of groundwater defines the extent of saltwater intrusion. The chloride concentration in the range of 40 to 300 mg/l is indicative of saltwater intrusion. (Edet et al., 2011). The present results in Table 3 infer that the aquifer water is contaminated with saltwater as Cl⁻, the most abundant ion in saltwater, is in higher proportions. The HCO₃⁻ ion which is the most dominant ion in fresh groundwater occurs generally in small amounts in saltwater. Chloride concentration greater than 250 mg/l is considered unfit for drinking purpose.

Table 3 Ratio of Cl/HCO₃ for the samples taken from monitoring wells

Well No.	Sept. 2011	Sept. 2012	Well No.	Sept. 2011	Sept. 2012
1	1.22	1.19	16	1.41	0.64
2	1.15	1.20	17	0.32	0.70
3	0.71	0.68	18	0.49	0.70
4	0.29	0.5	19	0.84	0.75
5	0.29	0.47	20	1.81	2.28
6	0.33	0.26	21	1.59	1.48
7	0.43	0.26	22	0.53	0.70
8	0.14	0.78	23	0.94	3.24
9	0.17	0.15	24	2.17	2.08
10	0.79	0.75	25	0.84	0.82
11	0.15	0.16	26	0.70	0.67
12	2.15	1.37	27	0.41	0.32
13	0.25	0.23	28	0.14	1.45
14	1.39	2.78	29	4.51	0.26
15	0.43	0.35	30	0.53	0.88

From Table 3 we can observe that in monsoon season well no.12, 24 and 29 are high in saltwater intrusion Fig. 3 and Fig. 4. Well no. 14, 20, 23 and 24 are high in saltwater intrusion for the month of September 2012.

Thickness of the aquifer, T

The thickness of the aquifer is obtained from the electrical resistivity survey conducted in the study area at 14 locations. The resistivity survey indicated that the area consists of shallow unconfined aquifer with the thickness ranging from 18 m to 30 m. From the resistivity survey we can observe that all the values are greater than 10 m, and hence the GALDIT rating of 10 is adopted throughout the study area.

III. VULNERABILITY ANALYSIS AND VULNERABILITY ZONING

The GALDIT scores for all parameters were obtained by analysing the generated data and it has been done for monsoon session is given in Table 4. The GALDIT index has also been calculated. The spatial variation of GALDIT index is depicted in Fig.5 and Fig.6, the vulnerability of aquifers of the study area is divided into 3 classes such as highly vulnerable, moderately vulnerable and low vulnerable with respect to saltwater intrusion. Most of the study area comes under moderately vulnerable and highly vulnerable.

Table 4 GALDIT index during monsoon, from Sept. 2011 and Sept. 2012

Well No.	Sept. 2011	Sept. 2012	Well No.	Sept. 2011	Sept. 2012
1	9.5	9.50	16	5.50	5.33
2	5.5	5.50	17	5.33	5.33
3	5.33	5.33	18	5.33	5.33
4	5.33	5.33	19	5.33	5.33
5	5.33	5.33	20	5.66	5.83
6	6.00	6.00	21	5.66	5.50
7	7.33	7.33	22	6.00	6.00
8	6.66	6.00	23	7.33	7.83
9	6.00	6.00	24	9.83	9.83
10	5.33	5.33	25	7.33	7.33
11	5.33	5.33	26	5.33	5.33
12	5.83	5.50	27	5.33	5.33
13	7.33	7.33	28	5.33	5.50
14	8.16	8.50	29	7.16	6.66
15	7.33	7.33	30	5.33	5.33

It was found that in monsoon coastal that stretches at well no 1, 14 and 24 are highly vulnerable to saltwater intrusion as shown in Fig. 5 and Fig. 6. Thus the present study indicates that the coastal groundwater system within the study area is under the threat of seawater intrusion.

IV. CONCLUDING REMARKS

GALDIT Model shows that

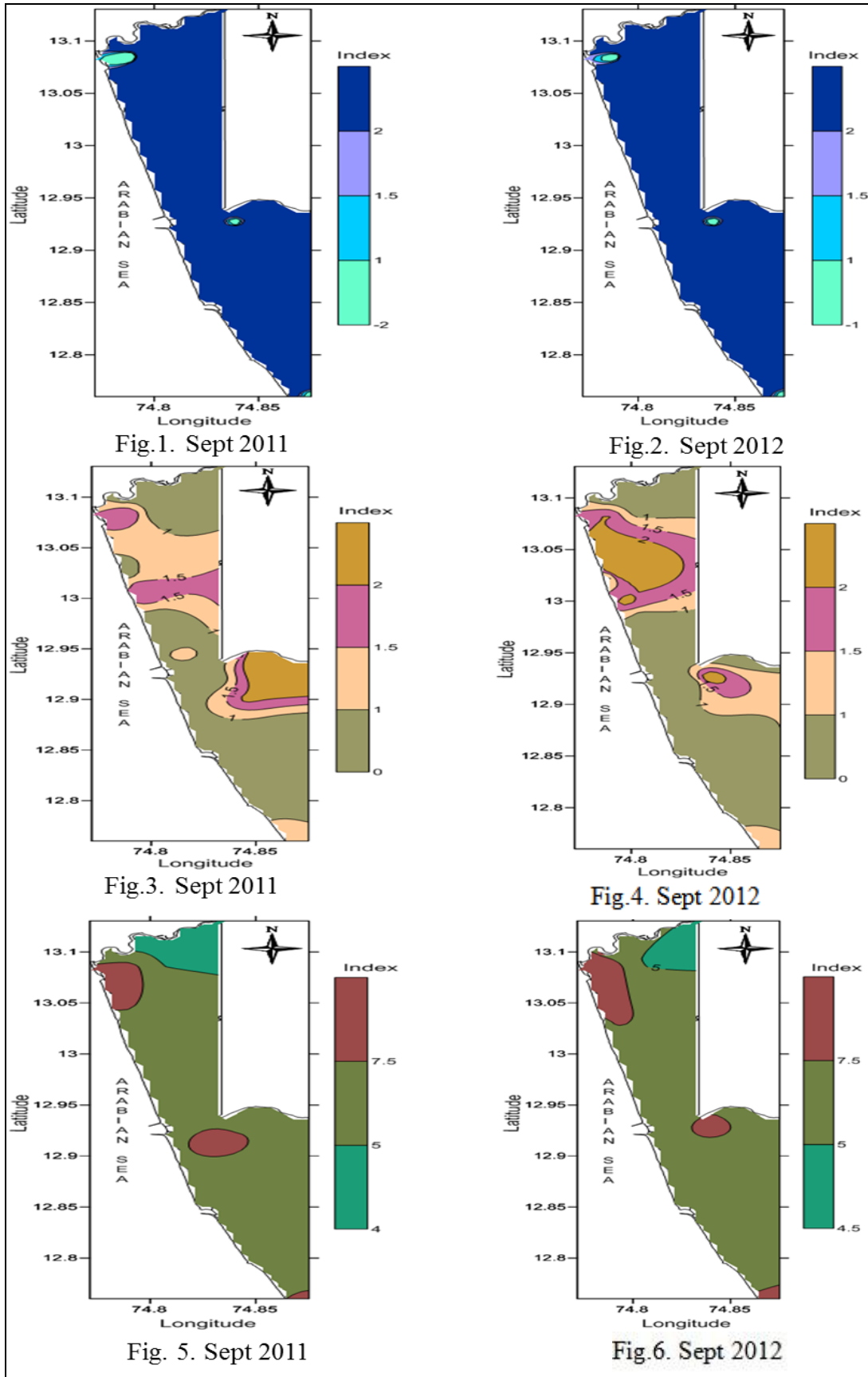
- In pre monsoon coastal stretches are viz., Mulki, Pavanje, Mukka and Haleyangadi are highly vulnerable to saltwater affected area.
- In post monsoon the coastal stretches of the study area Talapady and Kavoor are also highly affected area on southern side in the month of April and December.

Based on indicators of saltwater intrusion

- $Cl/(HCO_3 + CO_3)$: In monsoon season, contamination due to saltwater intrusion is found high at Kavoor, Haliyangadi and Mulki for the month of September 2011. In the month of September 2012, the saltwater intrusion is found at Kavoor, Surathkal, Mukka and Pavanje.
- In the post monsoon season, contamination due to saltwater intrusion at Talapady, Uchilla, Kavoor, Surathkal, Mukka and Pavanje for the month of December 2012.
- In the pre monsoon season, contamination due to high saltwater intrusion at Talapady, Kavoor, Thokuru, Mukka and Pavanje for the month of April 2012. In the month of April 2013 the saltwater intrusion is found high at Talapady, Ullal and Pavanje.
- The tidal nature of the river is affecting the adjoining well fields up to a distance of about 22 km. along the river course from the sea during April –May.
- Over all the values of Cl/HCO_3 ranges 0.14 to 7.41. Well no. 12 located close to Gurupur, Pavanje and Mulki are very near to Pavanje river.
- From the GALDIT analysis, it is found that the wells located within 250 m on either side of the river are highly vulnerable during Feb – May. The wells located at farther locations (250-700 m) are found to be moderately vulnerable and beyond 700 m, low vulnerable.

REFERENCES

- [1]. APHA, (1998), "Standard Methods for the Examination of water and wastewater", 20th Edition, American Public Health Association Washington D.C., USA., 1-1220.
- [2]. Asa Rani L. and Suresh Babu D.S. (2008). "A statistical evaluation of ground water chemistry for the westcoast of Tamilnadu, India", *Indian J. Marine Sciences*, 37(2),186 -192.
- [3]. Cabral, J. J. S. P., Wroble, L. C. and Brebbia, C. A. (1991). "A beam formulation using B-spines:II-multiple knots and non-uniform blending functions", *Eng. Analysis with boundary Elements*, 8,51-55.
- [4]. Chachadi, A. G., Lobo Ferreira J. P, Noronha, L. and Choudri B. S. (2002). "Assessing the impact of the sea level rise on saltwater intrusion in coastal aquifers using GALDIT model", *NIH, Roorkee, A Coastal policy Research Newsletter*, 7, 27-31.
- [5]. De Paz, J. M., Visconti, F., Zapata, R. and Sanchez, J. (2004). "Integration of two simple models in a geographical information system to evaluate salinization risk in irrigated land of the valencian community", *Spain soil use manage.*, 20, 332-342.
- [6]. George, R. J. McFarlane, D. J. and Nulsen, R. A. (1997). "Salinity threatens the viability of agriculture and ecosystems in western Australia", *J. Hydrogeol.* 5, 6-21.
- [7]. Georgescu, P., Dinu, C., Niculescu V. and Ion D. (1993). "Some applications of VES to groundwater exploration in the vicinity of Romanian coast of the black sea", *Revue Roumaine de Geophysique*, 37, 113-121.
- [8]. Cardona, A., Carrillo-Rivera, J., Huizar-Alvarez, R. and Gamiel, C. E. (2004). "Salinization in coastal aquifers of arid zones: an example from Santo Domingo, Baja California Sur, Mexico", *Env. Geo.*, 45, 350-366.
- [9]. Honnanagoudar, S.S., Venkata Reddy, D and Mahesha, A. (2012), 'Aquifer Characterization and Water quality Investigations of Tropical Aquifer of West Coast of India.' *International Journal of Earth Sciences and Engineering*. Vol. 5, No. 6, pp. 1619 -1629.
- [10]. Kotb, T. H. S., Watanabe, T. Y. Ogino. And Tanji, K. K., (2000). "Soil salinization in the Nile Delta and related policy issues in Egypt", *Agri. Water Mangt.* 43 (2), 239-261.
- [11]. Lobo Ferreira. andChachadi, A. G. (2005). "Assessing aquifer vulnerability to saltwater intrusion using GALDIT method: Part 1 – Application to the portuguese aquifer to Monte Gordo", *Proceedings of this 4th InterselticColloquim on Hydrol. Mangt. Water Resor., Portugal.*1-12.
- [12]. Trivedi, R. K., Khatavkar, S. B. and Goel, P. K. (1986). "Characterization, treatment and disposal of waste water in a textile industry", *Ind. Poll. Cont.* 2 (1), 1-12.
- [13]. Zhang, X., Wang, Q., Liu, Y., Wu, J., & Yu, M., (2011), "Application of multivariate statistical techniques in the assessment of water quality in the Southwest New Territories and Kowloon, Hong Kong", *Environmental Monitoring and Assessment*, 173, pp.17–27.



Robotics Helicopter Control and its Applications in Engineering

Prof.Dr.Eng.PVL Narayana Rao¹, Mr.Jemal Ahmed Andeta²,
Mr.Habte Lejebo Leka³, Mr.AbrahamAssefa Simmani⁴,
Er.Pothireddy Siva Abhilash⁵

¹Professor of Computer Science Engineering, Dept. of Information System, College of Computing & Informatics, Wolkite University, Ethiopia

²Dean of the College of Computing and Informatics, Wolkite University, Ethiopia

³Head of the Dept. of Information Systems, Wolkite University, Ethiopia

⁴Head of the Dept. of Information Technology, Wolkite University, Ethiopia

⁵Software Engineer, Staffordshire University, Staffordshire, United Kingdom

ABSTRACT

The Robot assembly comprises of one robot helicopter and two unmanned ground vehicles, they are AT Robots. The AVATAI (Aerial Vehicle Autonomous Tracking and Inspection) is based upon the Bergen Industrial RC model helicopter. The following sensors/electronics are onboard all robots; GPS, color CCD camera, wireless video and embedded PC/104 boards running QNX (a realtime OS). Wireless Ethernet provides a 2.0 Mbps multiway communication link between all robots and the operator. The AVATAI also has an Inertial Navigation System and the Pioneers have seven ultrasound sensors for obstacle detection. The helicopter is controlled partly by the onboard control system and in part by a human pilot. The Pioneers are fully autonomous. To date we have demonstrated 1) High-level tasking by a human operator of the robot group to cooperatively patrol a designated area and 2) Automatic retasking of the robots by simulated "alarms" on the area perimeter. The robots navigate to the alarm scene to provide live video while maintaining basic patrolling functionality.

KEY WORDS: GPS, AVATAI, Pioneer, OCU, QNX, Navigation System

I. INTRODUCTION

Our experimental test bed (Figure 1) is composed of a robot helicopter and two mobile ground robots thus making it a morphologically heterogeneous group. The advantages of using a group of robots to execute coordinated activity have been discussed extensively in the literature. However heterogeneous groups typically involve higher overhead in terms of system maintenance and design. The USC Robotics Research Laboratory designed a heterogeneous group consists of a robot helicopter and several mobile robots for inspection and observation applications.



Figure 1: The experimental testbed consisting of the AVATAI (Autonomous Vehicle Aerial Tracking and Inspection) robot helicopter and two Pioneer AT mobile robots.

In the work described here, we focus on an experimental task motivated by an application where a single person has control and tasks the robot group at a high level. A possible application is alarmed with security in urban areas where a single guard would need to control and monitor several (possibly heterogeneous) robots. In the application described here the robot group patrols an outdoor open area (a few obstacles are present on the ground) defined by a perimeter. The boundary is defined by a set of vertices (in GPS coordinates) which when connected by line segments form the boundary of a closed convex irregular polygon. In the work reported here the robot helicopter is flown by a human pilot for purposes of safety and speed. However we rely on a human pilot to transition from a stable hover at one point in space to another. Both ground robots are fully autonomous in the experiments reported here.

The robots in the experiments cover the area bounded by the perimeter and send imagery back to a human operator via a wireless video downlink. The operator is able to set high level goals for the ground robots. An example of a high level goal is "follow the helicopter." If a particular ground robot is given this high level goal it will stop patrolling and will follow the helicopter as it moves. The motivation behind this is to allow the ground robots to "take a closer look" at areas which the operator finds interesting based on aerial imagery. The operator can designate points of interest within the perimeter which serve as area markers for robots to periodically explore. The basic idea behind the implementation of the control programs is however to achieve robust functionality without explicit top-down planning. Rather the overall behavior of the group is the result of interacting control systems that run on the individual robots which essentially allow each robot a high degree of autonomy.

II. HARDWARE AND SOFTWARE DESCRIPTION

2.1 AVATAI Hardware

The current AVATAI, shown in Figure 1, is based upon the Bergen Industrial Helicopter, a radio controlled (RC) model helicopter. It has a two meter diameter main rotor, is powered by a 4.0 horsepower twin cylinder gas engine and has a payload capability of approximately 10 kilograms. The helicopter has five degrees of control: main rotor lateral and longitudinal cyclic pitch, tail rotor pitch, main rotor collective pitch and engine throttle. The first three control the roll, pitch and yaw of the helicopter while the last two control its thrust. The helicopter can be controlled by a human pilot using a hand held transmitter which relays pilot control inputs to an onboard radio receiver using the 72 MHz frequency band. The receiver is connected to five actuators, one for each degree of control on the helicopter. For autonomous operation, these pilot control inputs are replaced by computer generated control inputs. A block diagram of the AVATAI system; including sensors, onboard and off board computing resources, wireless communication links and electrical power sources, is given in Figure 2. A variety of sensors are mounted on the AVATAI that provide information about the state of the helicopter as well as the environment in which it operates. An integrated Global Positioning System/Inertial Navigation System (GPS/INS) device, consisting of a GPS receiver and an Inertial Measurement Unit (IMU), is the primary sensor used for low-level control of the helicopter. The GPS/INS provides position (latitude, longitude and altitude), velocity (horizontal and vertical), attitude (roll and pitch), heading (yaw), delta theta and delta velocity information. This particular GPS receiver can only track 4 satellites at once and consequently provides a relatively poor estimate of current latitude and longitude as compared to other available receivers. So, a second standalone GPS receiver is used that can track up to 12 satellites at once.

This improves the standard deviations of the estimates of latitude and longitude from 4.5 meters for the 4-channel GPS unit down to 20 centimeters for the 12-channel unit. This GPS receiver is used for the high-level (guidance and navigation) control of the helicopter. A downward facing ultrasonic (sonar) transducer provides altitude information and a RPM sensor mounted on the main rotor mast measures engine speed. A downward looking color CCD camera provides visual information of the area below the AVATAI.

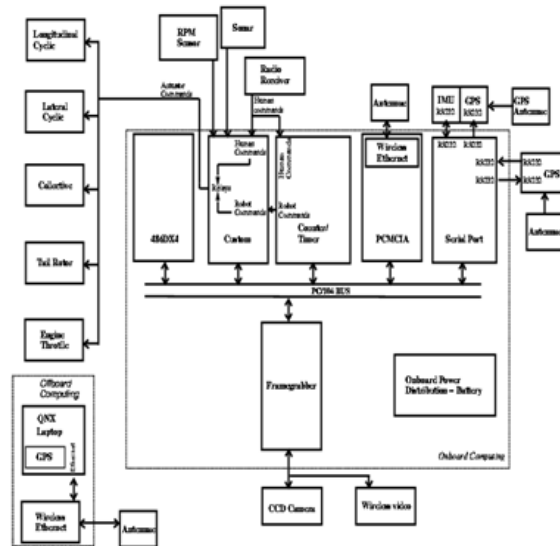


Figure 2: AVATAI system block diagram

Onboard computing needs are met using a number of commercial off the shelf (COTS) PC/104 boards and one additional custom built PC/104 board. The main processor board contains a 486DX4 CPU which runs at 133 MHz, has 16 Mbytes of RAM and 40 Mbytes of solid state disk on chip (DOC). The DOC contains both the realtime operating system (RTOS) and flight software. The 486DX4 boots up the RTOS at system power up, executes all flight control and image processing software and provides an interface to other PC/104 boards. These boards include a timer/counter board used both to generate actuator commands and read pilot commands, a custom built PC/104 board that allows switching between human generated and robot generated commands on an actuator by actuator basis as well as acting as an interface to the RPM sensor and sonar, a serial port board for interfacing to the GPS/INS and standalone GPS, a color video frame grabber for the CCD camera and a PC/104 to PCMCIA interface board to allow the use of PCMCIA cards onboard the AVATAI. A 2.4 GHz wireless Ethernet PCMCIA card provides a multiway 2.0 Mbps communication link between the AVATAI, other robots and a human using an operator control unit (OCU). (The OCU comprises the off board computing resources and will be described in detail later). The human receives grabbed video frame information and other telemetry from the AVATAI and sends high-level tasking commands to the AVATAI via this link. In addition, differential GPS corrections are sent from the OCU to the GPS receivers onboard the AVATAI through the wireless Ethernet to improve the GPS performance. A live video feed, provided by a one way 1.3 GHz wireless video link from the CCD camera, is displayed on a monitor. Nickel-metal hydride (NiMH) and lithium-ion (Li-Ion) batteries supply power to the electronics. The GPS/INS is relatively power hungry, requiring 0.8 amps at +24 volts and so a dedicated 12-volt, 3.5 amp-hour NiMH battery is connected to a DC/DC converter to produce +24 volt power. The electronics can operate for roughly an hour with this battery supply. Mission length is limited by the flight time of the helicopter on a single tank of gasoline, which is approximately 30 minutes in duration.

2.2 AVATAI Software

The operating system used is QNX; a UNIX-like, hard real time, multitasking, extensible POSIX RTOS with a small, robust microkernel ideal for embedded systems. The flight software encompasses all remaining software running onboard the AVATAI. This currently includes (or is planned to include):

1. low-level software drivers for interfacing with sensors and actuators
2. Flight control software for guidance, navigation, and control.
3. learning software
4. self-test software including built in test (BIT) and health checks software for increasing robot fault tolerance
5. vision processing software running on the frame grabber

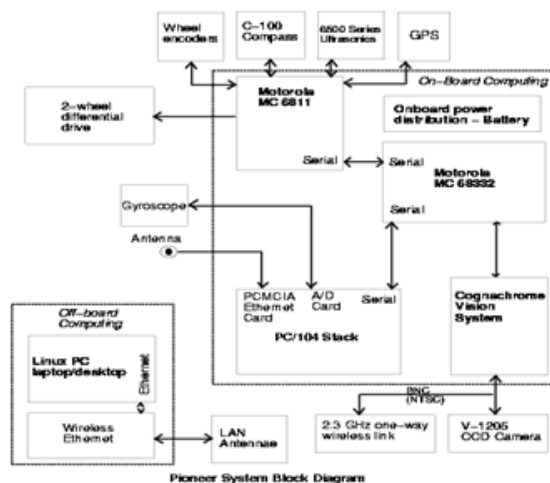


Figure 3: Pioneer system block diagram

All software is written primarily in C/C++, with assembly used only when required for speed of execution. Custom drivers have been written for the timer/counter card, the GPS/INS and GPS units, the frame grabber and the wireless Ethernet PCMCIA card. The remaining software is still under development.

2.3 Pioneer Hardware

The Pioneer AT robots used in this work is identical to each other. Each robot is four-wheeled base with skid steering. The wheels on the left are coupled mechanically as are the wheels on the right resulting in two degrees of freedom in the drive. Turning is accomplished by a speed differential between the left and right sides. Each robot has a Lithium-Ion (Li-Ion) battery pack (Two 10.8 volt, 4.05 amp-hour Li-Ion) for the electronics. The motors are powered by a lead acid battery that allows up to 4 hours of operation on hard surfaces and approximately one hour on grass. Each robot is equipped with a ring of seven front looking sonars which are controlled by a low-level Motorola 6811 microcontroller. The wheel speeds are available through encoders. The low-level 6811 board is connected to a PC/104 stack via a serial connection. The Pioneer also has a vision system comprised of a camera on a pan-tilt head controlled by a Motorola 68332 board running the Congnachrome color vision system. The main PC/104 processor board contains a 486DX4 133MHz CPU, 4 Mbytes of RAM and 40 Mbytes of solid state disk on chip which contains both the real time operating system (RTOS) and control software. Each robot is equipped with a NovaTel GPS system connected to the PC/104 processor via a serial port. Additional sensors include a compass and a gyroscope. The gyroscope is connected to a A/D card on the PC/104 stack. A 2.4 GHz wireless Ethernet PCMCIA card provides a multiway 2.0 Mbps communication link between each Pioneer and the other robots. A live video feed, provided by a one-way 2.3 GHz wireless video link from the CCD camera, is displayed on a monitor. A block diagram of the Pioneer hardware is given in Figure 3.

2.4 Pioneer Software

The control system for the Pioneer AT (described in the next section) is all written in C and runs under QNX on the PC/104 stack described above. The software includes

1. Low-level software drivers for interfacing with sensors specifically software for the wireless Ethernet driver and the GPS driver.
2. control software for obstacle detection and avoidance, navigation and mapping

2.5 OCU Hardware

The operator control unit is implemented using a Toshiba Tecra 510CDT laptop PC based upon a 133 MHz Pentium CPU. It has 144 Mbytes of RAM, a 4.3 Gbyte hard drive, a 12.1 inch high-res color monitor, a CD-ROM and an Ethernet connection. The QNX operating system is installed as well as the Watcom C/C++ compiler. A docking station expands the capabilities of the laptop by providing two full-length expansion slots for standard ISA and 32-bit PC Expansion Cards and onehalf-length 32-bit PC expansion slot. It also has a selectable bay for installing additional hardware such as CD-ROM drives or floppy drives. A 1.44M byte floppy drive has been installed in the slot. The 510CDT has multiple functions and is used during all phases of the project; including development, integration and test. The primary purpose of the laptop is to function as a wireless OCU for communication and tasking of the robots. A 2.4 GHz wireless Ethernet device is connected to the Toshiba, providing a multiway connection between the human at the OCU and the wireless PCMCIA cards

onboard the robots. Additional functions of the 510CDT include the following: First, it provides a software development environment through the use of the QNX operating system and the Watcom C/C++ Compiler. Using this environment code is developed and tested. Also, using RCS, a QNX software version control utility, software configuration management is implemented. Second, the 4.3 Gbyte hard drives provide long-term storage capability for mission data. Third, the docking station provides an ISA slot for a GPS receiver used to produce differential GPS corrections for use by the mobile robots.

III. USER INTERFACE

The user interface for the system is implemented under QNX using the Phab GUI development system. The basic layout of the interface is deliberately kept simple so as to allow an inexperienced operator to quickly learn how to use it. A screenshot of the interface is shown in Figure 4. The user interface allows the operator to examine telemetry from any robot, task individual robots to do specific activities (such as following, patrolling etc.) and monitor the location of the robots in a 2D plan view. In addition, TV monitors show the operator a live wireless video feed from each of the individual robots. Tasking is done by selecting a robot with the mouse and clicking on one of the tasks available in the form of the task list popup menu.

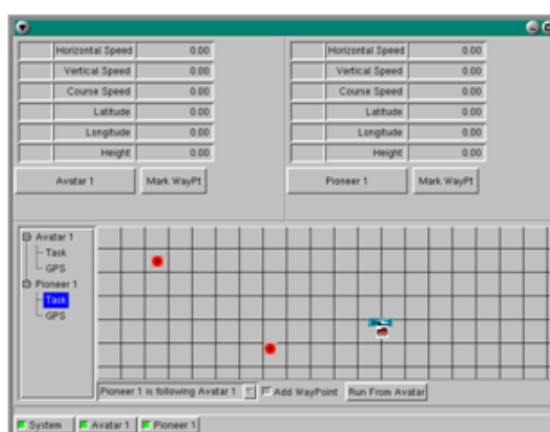


Figure 4: A screenshot of the user interface

IV. RESULTS WITH TEST TASKS

The system described here has been tested with two simple tasks to date. The operator initializes the system with a set of GPS coordinates that define the perimeter of interest. The robot locations are registered to a common coordinate frame which is displayed to the operator on the user interface. The first task used for testing was a cooperative patrolling activity by the robots. The helicopter was flown by the human pilot and the Pioneer ground vehicles followed it on the ground using GPS. The only input from the operator is at the start of the task. When the helicopter is fully autonomous we expect to be able to load a flight plan into it (in the form of several via points) and have the rest of the robots follow in loose formation.

The second task we have used for testing involves the automatic retasking of the robots by simulated "alarms" on the area perimeter. The robots navigate to the alarm scene to provide live video while maintaining basic patrolling functionality. When an alarm goes off (alarms are simulated by user keyboard input to the system), the robot nearest to the alarm disengages the patrolling behavior and navigates to the site of the alarm. Since this is a reconnaissance style scenario the robot simply returns a close-up view of the scene of the alarm to the operator in the form of a live video feed. The other robot continues patrolling. A detailed analysis of the behavior of the group as a whole is the subject of a forthcoming paper [Sukhatme 99]. Videotapes of the system are available at <http://robotics.usc.edu/brochure/afv.html>.

REFERENCES

- [1] Amidi, O. (1996), An Autonomous Vision-Guided Helicopter, PhD thesis, Department of Electrical and Computer Engineering, Carnegie Mellon University.
- [2] Arbib, M.A. (1995), Schema theory, in M.Arbib, ed., 'The Handbook of Brain Theory and Neural Networks', MIT Press, Cambridge, MA, pp.830--834.
- [3] Arkin, R.C. (1990), 'Integrating behavioral, perceptual, and world knowledge in reactive navigation', *Robotics and Autonomous Systems* 6,105--122.
- [4] Arkin, R.C. (1992), 'Cooperation without communication: Multiagent schema based robot navigation', *Journal of Robotic Systems*.
- [5] Arkin, R.C. (1998), *Behavior-Based Robotics*, The MIT Press, Cambridge, MA.
- [6] Brooks, R.A. (1986), 'A robust layered control system for a mobile robot', *IEEE Journal Robotics and Automation* 2(1),14--23.
- [6] Cavalcante, C., Cardoso, J., Ramos, J. J.G. & Neves, O.R. (1995), Design and tuning of a helicopter fuzzy controller, in 'Proceedings of 1995 IEEE International Conference on Fuzzy Systems', Vol.3, pp.1549--1554.
- [7] DeBitetto, P., Johnson, E.N., Lanzilotta, E., Trott, C. & Bosse, M. (1996), The 1996 MIT/Boston University/Draper Laboratory autonomous helicopter system, in 'Proceedings of 1996 Association for Unmanned Vehicle Systems 23rd Annual Technical Symposium and Exhibition', Orlando, pp.911--920.
- [8] Dedeoglu, G., Mataric, M. & Sukhatme, G.S. (1999), Cooperative robot mapping, in 'Proceedings of the 1999 SPIE Conference'.
- [9] Fukuda, T., Nadagawa, S., Kawachi, Y. & Buss, M. (1989), Structure decision for self-organizing robots based on cell structures - cebot, in 'IEEE International Conference on Robotics and Automation', IEEE Computer Society Press, Los Alamitos, CA, Scottsdale, Arizona, pp.695--700.

V. BIOGRAPHIES

P.V.L. NARAYANA RAO was born in Vijayawada, Krishna District, Andhra Pradesh, India. He completed M.Tech. from Sam Higginbottom Institute of Agriculture, Technology and Sciences Deemed University (Formerly Allahabad Agricultural Institute), UP, India and PhD in Computer Science Engineering from Lingaya's University, Faridabad, Haryana State, India. He has 8 years of National Teaching experience in reputed India Post Graduation Engineering Colleges, 14 years of International Teaching experience in different Universities of Foreign Country Ethiopia, East Africa and 4 years National Industrial Experience in India as a System Analyst, Systems Developer. He is currently working as Professor (CSE), Wolkite University, SNNPR, P.O.Box No.7, Wolkite, Ethiopia, and East Africa. He is a member of various professional societies like WASET, USA, IAEng, Hongkong and CSE, Ethiopia. He has various publications in the National and International Journals.

JEMAL AHMEDANDETA was born in Arekite, SNNPR, Ethiopia, and East Africa. He completed his graduation in Information Science from Haremaya University, Ethiopia, East Africa and presently working as the Dean of the college of Computing and Informatics in Wolkite University, Wolkite, Ethiopia.

HABTE LEJEBOLEKA was born in Arba Minch, SNNPR, Ethiopia, and East Africa. He completed his graduation in Information System from Addis Ababa University, Ethiopia and now he is working as Head of the Department of Information System in Wolkite University, Wolkite, Ethiopia.

ABRAHAM ASSEFA SIMMANI was born in Wolkite, SNNPR, Ethiopia, and East Africa. He completed his graduation in Information Technology from Wollega University, Ethiopia and now he is working as Head of the Department of Information Technology in Wolkite University, Wolkite, Ethiopia.

POTHIREDDY SIVA ABHILASH was born in Vijayawada, Krishna District, Andhra Pradesh, India. He completed M.S degree in Tele Communication Engineering from Staffordshire University, Staffordshire, United Kingdom in 2013. He is working as Software Engineer in Hyderabad, Telangana State, India. He has various publications in the International Journals.

Design And Implementation Of A Microcontroller-Based Keycard

Aneke Chikezie*, Ezenkwu Chinedu Pascal**, Ozuomba Simeon***

Department of Electrical/Electronics and Computer Engineering, University of Uyo, Uyo, Akwa Ibom State,
Nigeria

ABSTRACT:

The advent of Information and Communication Technology (ICT) has improved organizations' approach to achieving security. In this paper, a microcontroller-based security door system is proposed to automate and computerize keycard for access control in both private and public offices in an organisation. The system is designed to serve the purpose of security. To operate this door, a welcome screen is shown on the microcomputer which serves as the visual interface. The user is required to insert a smart card which serves the purpose of a key into the card reader on the door. The controller holds the codes which drives the card reader. On validating the smart card, it loads and shows another screen on the monitor asking for user password. This is used to ensure that the user is actually an authenticated user of the card. A buzzer is also added to the system to alert the security personnel in the security unit if an unauthorized user attempts to gain access to the room three times.

KEYWORDS: microcontroller, microcomputer, card reader, keycard, security, security door system, visual interface

I. INTRODUCTION:

Inderpreet Kaur (2010) opined that “ with advancement of technology things are becoming simpler and easier for us. Automation is the use of control systems and information technologies to reduce the need for human work in the production of goods and services. In the scope of industrialization, automation is a step beyond mechanization.” According to Oke et al(2009) , “most doors used in some organisations are controlled manually especially by security personel employed by these organisations, through the use of handles and locks with key to operate the locks. Examples are banks, hotels, motels and so on; some are controlled by switches while others are controlled by the biometrics technique.”

The thrust of this work, is to develop a Micro-controller based keycard and interactive lock that provides access permission into restricted area(s) in an organization to only authorized persons who possess valid keycard and also have a correct pass code which has been legalized by the Administrator's computer which has a software program interfaced with the project circuitry. This program handles the validation of the card and the authentication of the password. The program also triggers the door to automatically lock after 30 seconds of opening.

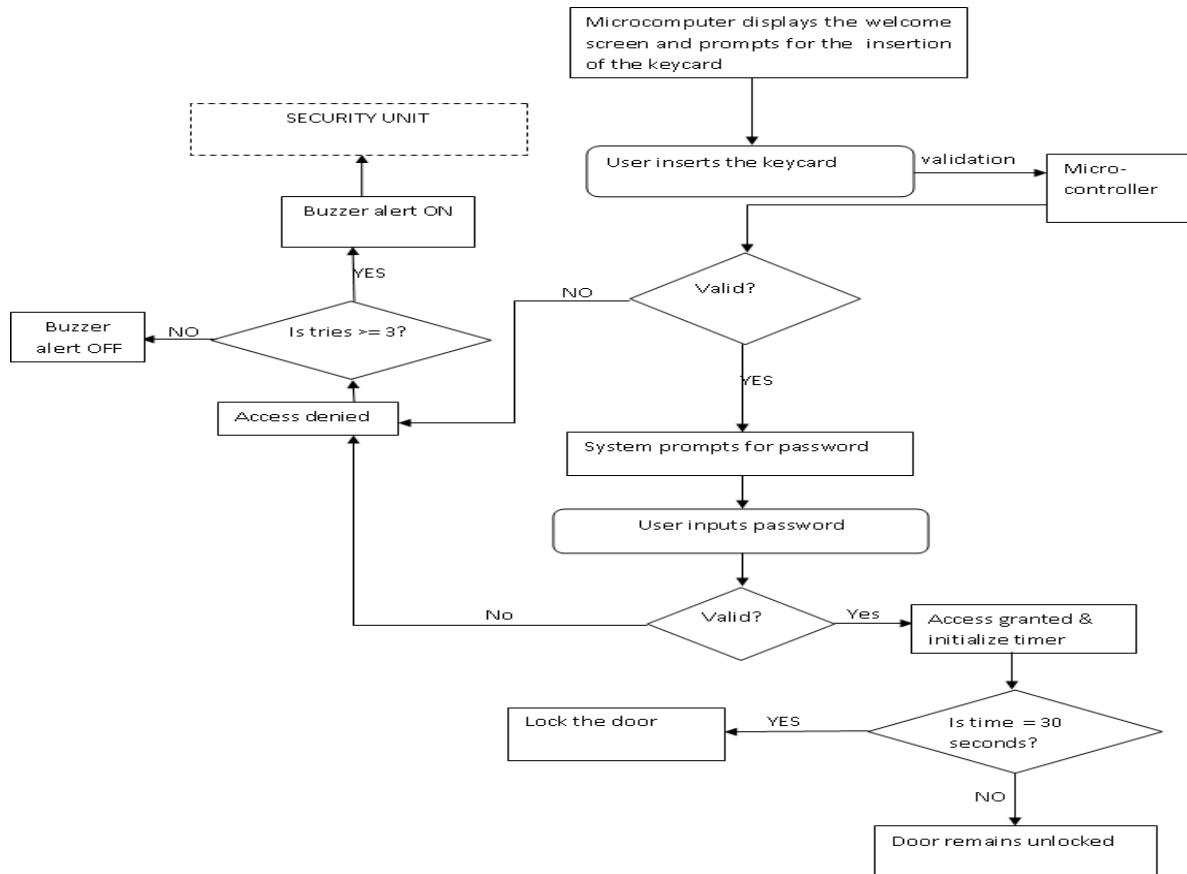


Fig1: The process flow diagram of the system

To gain access to the restricted area, a smart card (keycard) should be inserted into the card bay incorporated in the door. The microcontroller validates this card by ensuring that it conforms to the requirement. If the card is valid, the user is prompted for a password which is keyed in from the keypad also incorporated on the door. The microcontroller again validates this password and if correct, unlocks the door for access. The controller times down to 30 seconds and relocks the door. Once access has been gained, door can be mechanically opened from inside without any form of security. A buzzer is also added to the system to alert the security personnel in the security unit of an unauthorized attempt to gain access to the room. The process flow diagram illustrating the operation of the system is presented in Fig. 1.

The whole operation is designed to serve the purpose of security. To gain access to the room;

- Firstly, for any system to function, it needs power supply. The power source is the AC from the wall socket which is been stepped down to 12V DC and then regulated to 5V DC which most of the system components requires. Components like relays and motor that need 12V tap power before the voltage regulator.
- To operate this door, a welcome screen is shown on the microcomputer which serves as the visual interface. It is required to insert a smart card which serves the purpose of a key. The card is of resistive type having a 6.6K Ω resistor embedded into it thus any smart card that does not provide this value is seen as invalid and this is what I used to differentiate between the card keys. It has just two pins heads/eyes which the reader uses to identify the card.
- Next is to insert the card into the card reader on the door. The card reader is designed using a 555 timer configured in its monostable mode where the card acts as the R2 of the 555 timer circuit. It compares the resistance of the card inserted into it with the internal resistance which has been set to be 1K Ω and if equal sends a signal to the microcontroller for validity. The reader is designed to be installed on the door and reads the card. The 555 Timer or card reader unit is connected to the microcomputer.

- The microcontroller is an AT89C51 controller which is made up of 40 pins which has four ports of eight pins each thus 32 I/O pins. The controller holds the codes which drives the card reader. On validating the smart card, it loads and shows another screen on the monitor asking for user password. This is used to ensure that the user is actually an authenticated user of the card.

Block Diagram

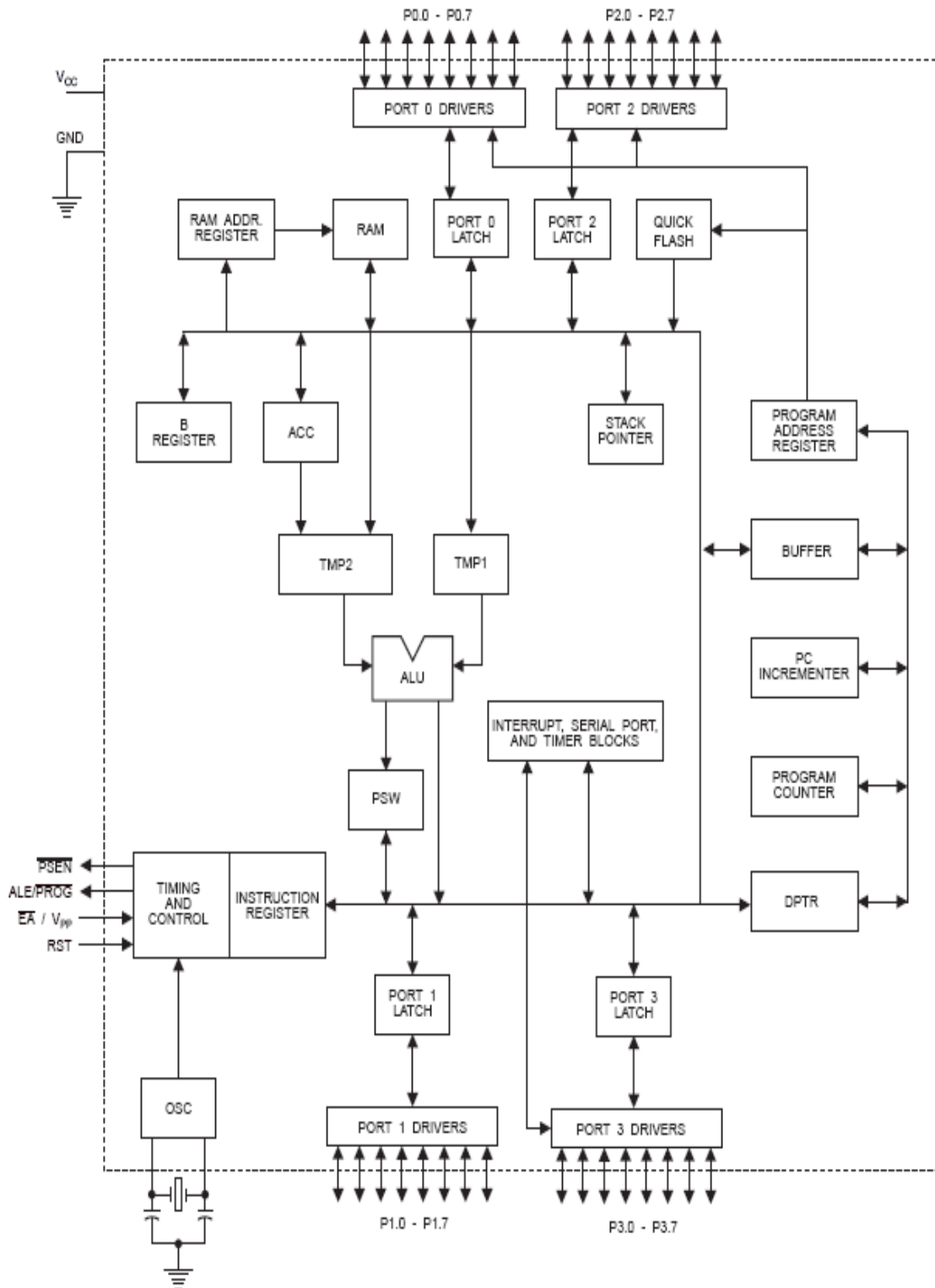


Fig 2: Block Diagram of AT89C51 Microcontroller

- The next step is to key in the password using a 12key keyboard designed for this purpose. The keyboard is of dot matrix configuration. It is made of 12 switches arranged in a 3 x 4 matrix format. The rows elements are connected to port 1 of the controller while the column elements to port 3. For the controller to detect a depressed key, it places a Logic 0 on the first row and Logic 1 on all other rows. It places a logic 1 on all the columns thus if any switch on the first row is depressed, the logic state of that row/column intersect is altered the numeric value for that intersect is registered. This is applicable to other intersects.
- If the password is valid, the microcontroller sends a Logic 1 to forward bias transistor1 which in turn causes relay1 to force the door’s motor to move in the forward direction (by electromagnetism) thus opening the door. The controller also after 30 seconds sends Logic 0 to transistor1 to reverse bias it while forward biasing transistor2 to cause relay2 to force the motor to move in the opposite direction thus closing the door.
- The controller is connected to the microcomputer through a DB 25 LTP cable for visual interface using two data lines and one status line; D0, D1, S3. The controller also is connected to a buzzer through a transistor. It sends a Logic 1 to this transistor which on forward biasing, triggers off the buzzer if an invalid smart card is tried three consecutive times or if an invalid code is used three consecutive times within a space of 5 minutes. This is to alert security of intrusion.

II. SYSTEM DESIGN APPROACH

The design of this system incorporates both the top-down and bottom up design approach. In the top-down design category the designer starts from the input and achieves the objective section by section down to the output of the work Inyiama(2007). This category of design deals with designing from the output of the system down or back to the input of the system Inyiama(2007). The two were deployed since some sections of the system that operate with the output result in reference to the input require the bottom up design approach while other sections that depend on the input for their output are designed using the top down approach.

2.1 System sub-system

The design of the microcontroller based keycard is modularized into Sub-systems:

- Hardware Sub-system
- Software Sub-system

Hardware Sub-System

This describes the sequence involved in the step by step unit design of the system, the detail of the components fixtures and soldering of the sub units as well as the block schematics design of each unit starting from the power supply to the door latch and computer interface, taking each of the steps sequentially. The block diagram showing the system hardware sub-systems is shown in fig.2.

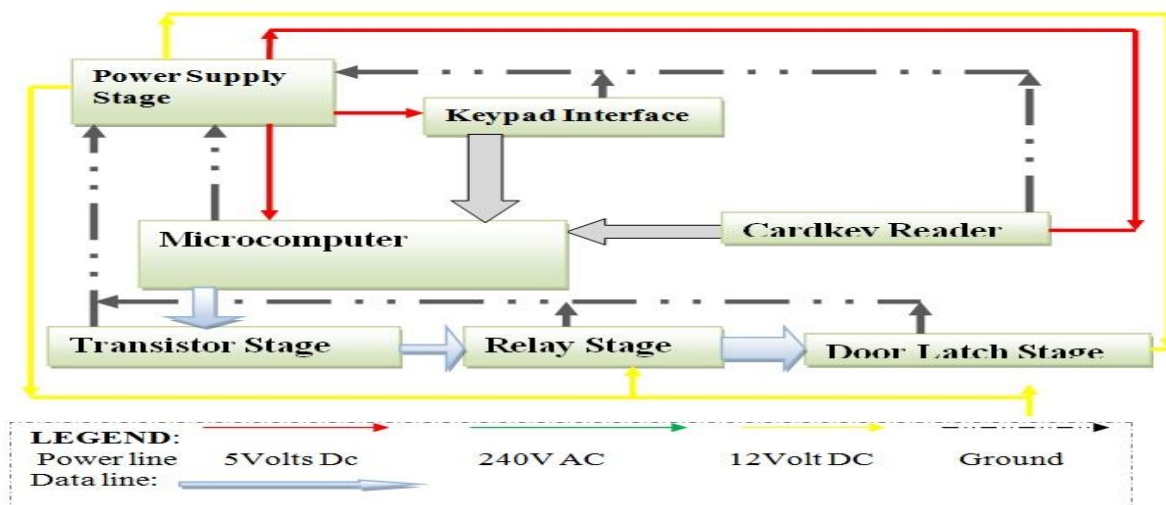


Fig.2: Block diagram showing the system hardware sub-components

- **Card Reader Module**

This module is divided into two main sub unit which are the card key, a resistive circuit embedded into a card which when installed into the reader, instructs or identify a specific operation to the reader and the reader circuit. 555 Timer is a timer chip/integrated circuit which is universally used in IC timing circuitries.

The resistive voltage divider is used to set the voltage comparator threshold. All resistors are of equal value thus the upper comparator has a reference of $\frac{2}{3}V_{CC}$ and lower comparator has a reference of $\frac{1}{3}V_{CC}$. The comparator output controls the state of the flip-flop. When the trigger voltage goes below $\frac{1}{3}V_{CC}$, the flip-flop is set and the output jumps to its HIGH level. The threshold input is normally connected to an external RC timing network. In this work, the timer in monostable mode was used.

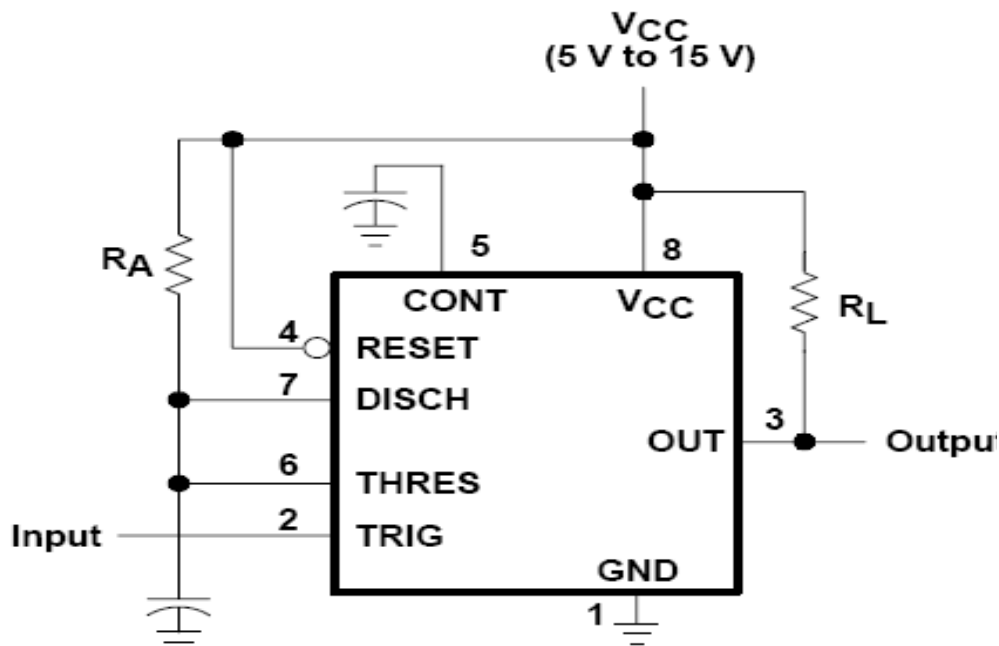


Fig 3: Circuit for a Monostable Configuration of 555 Timer Chip

- **Interface Module:**

This is the connection of the hardware and the computer system using a DB25 printer cable through a parallel port. The DB25 cable has the following specifications; 25 pins, pin 2 to 9 are labeled D0 through D7; Pins 10, 11, 12, 13 and 15 are used for acknowledgement and handshakes labeled Š3, S4, S5, Š6, S7 respectively. They are very important pin sets used in printer to system communications.



Fig 4 Photo OF A LTP Db25 Printer Parallel Port Head Device

Another set of pins used for control and state changes are pins 1, 14, 16 and 17 labeled Č3 C2 Č1 and Č0 respectively. They are hence used for basic controls of the interface. The remaining pins are ground pins; they are pins 18, 19, 20, 21, 22, 23, 24, and 25. Each of these pins are labeled or identified with different and unique cable colours. Hence the colour of each cable of each pin is not exactly the same with the neighboring pin, in practical this unique colour identification is used in installing the port. Bit to Pin Mapping for the Standard Parallel Port (SPP):

Table 1: Tabulated Presentations of the Types of Port on the Cable

Address		<u>MSB</u>							<u>LSB</u>
	Bit:	7	6	5	4	3	2	1	0
Base (Data port)	Pin:	9	8	7	6	5	4	3	2
Base+1 (Status port)	Pin:	11	10	12	13	15			
Base+2 (Control port)	Pin:					~17	16	~14	~1

Generally, the port is divided into three major sections; the data interface section, the control and the common connection interface. The Data interface contains the parallel Data connection (D0 to D7), the control section has two main sub section, the status and the control section, the status common contains the S3 to S7 and the control section contains the Co to C3 pins .

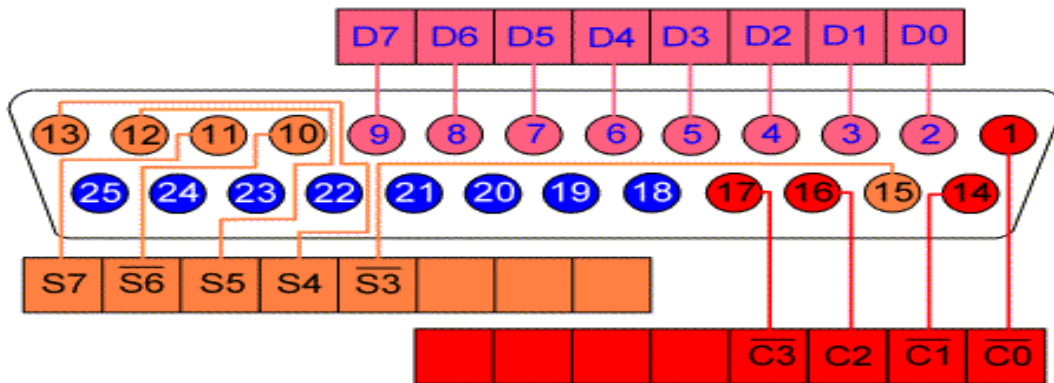


Fig 5: Photo of the Connection Db25 Pin Assignment

The common is used to ground all the bytes addressed pins. Again it is noticed that the two main sections (Data and Control) are all 1 bytes in size rating.

Table 2: Table Showing Db Pin Assignment and Comparison

Pin No (DB25)	Pin No (36 pin)	Signal name	Direction	Register – bit	Inverted
1	1	nStrobe	Out	Control-0	Yes
2	2	Data0	In/Out	Data-0	No
3	3	Data1	In/Out	Data-1	No
4	4	Data2	In/Out	Data-2	No
5	5	Data3	In/Out	Data-3	No
6	6	Data4	In/Out	Data-4	No
7	7	Data5	In/Out	Data-5	No

8	8	Data6	In/Out	Data-6	No
9	9	Data7	In/Out	Data-7	No
10	10	nAck	In	Status-6	No
11	11	Busy	In	Status-7	Yes
12	12	Paper-Out	In	Status-5	No
13	13	Select	In	Status-4	No
14	14	Linefeed	Out	Control-1	Yes
15	32	nError	In	Status-3	No
16	31	nInitialize	Out	Control-2	No
17	36	nSelect-Printer	Out	Control-3	Yes
18-25	19-30,33,17,16	Ground	-	-	-

In the design interface, only pins 2, 3 are used for data and 12 for status. The rest of the pins were not used (not connected). Resistors were used at the base of this connection to prevent surge from damaging the port of the computer.

• **The Cardkey Reader and the LTP Interface Connection:**

This is the connection of 555 timer reader circuits which is configured in the monostable mode and the LTP cable to the controller chip through the basic parallel printer ports as described by the diagram below.

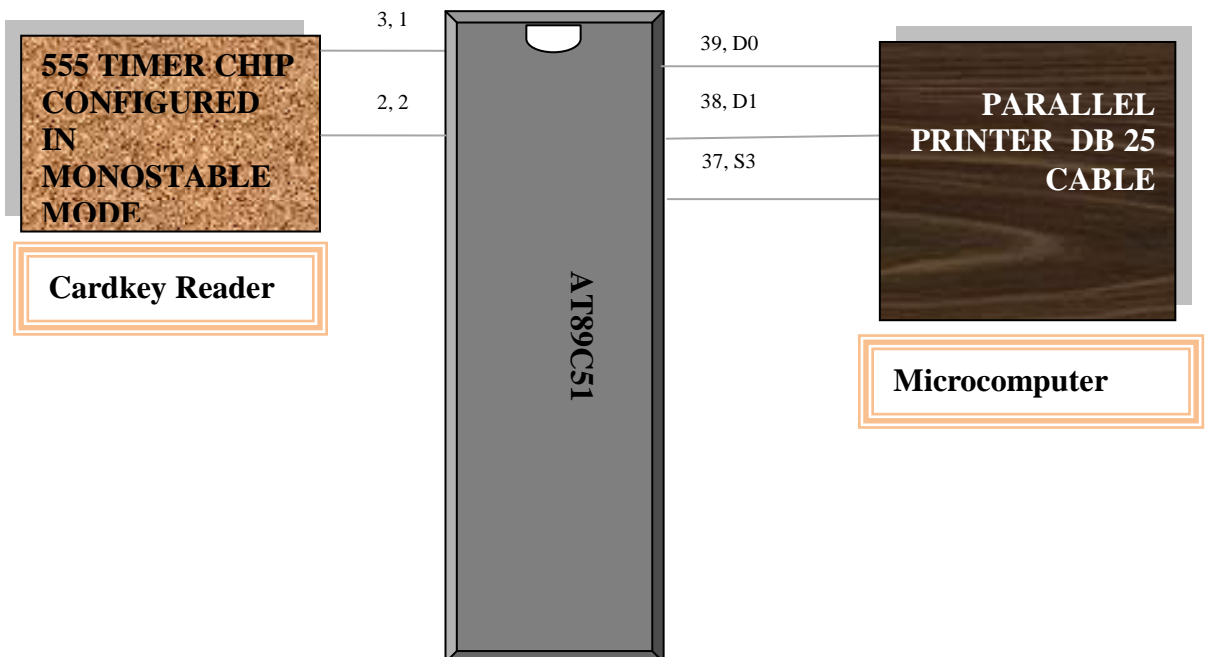


Fig 6: The Cardkey Reader and the LTP Interface Connection

The circuits described with the aid of diagrams and circuit components above are the basic connections made with the microcontroller chip and other circuit components. From a summary of the circuits it can be seen that very small size of the memory will be running hence the controller will be very smart and have free calculations of its operation.

- **The Keyboard Interface:**

This is the interface to the dot matrix keyboard. The 3 x 4 dot matrix keyboard is designed to connect to the microcontroller through port 1 and port 3. The row elements of the keyboard are connected to port 1; P1.4, P1.5, P1.6 while the column elements are connected to port 3; P3.0, P3.1, P3.2, P3.3.

Software Sub-System

- **C Programming Design for the Atmel AT89C51 Controller**

The software was designed using CRIMSON EDITOR C compiler and SDCC (small device C compiler) which contains the header file of the Microcontroller (AT89C51). It used virtual conventional C programming language keywords and syntax. The program environment is where the codes are written, compiled and debugged .It will generate an Intel hex file which is transferred into the microcontroller via a computer interfaced programming device. The codes are written to send a Logic 1 to forward bias transistors and Logic 0 for reverse; for the timer to ensure that door closes after 30 seconds of opening; to accept only a 6.6KΩ smart card and accept only a correct password.

- **Designing the Visual Basic Interface**

The visual basic interface was designed in a way that it can be easily and securely used to validate the cardkey and password. There are various steps taken in the course of this design which are;

- Securing the form from unauthorized access
- Outlining the aim of the interface for simple usage
- Arranging forms, labels and textbox for the VB form or window design
- Writing the VB basic codes for the form which accepts card and validates it.
- Writing the VB basic codes for user password authentication.

Taking the above in turns would probably result to the interface form that will be used for card validations.

When the start button is clicked, user can now insert card and key in password which if valid the controller displays “ACCESS GRANTED” on the label and opens the door.

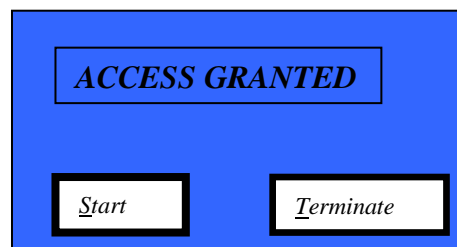


Fig 7. VB Interface

CONCLUSION

The thrust of this work is the design and implementation of a microcontroller-based keycard tailored to improve security in both private and public offices in an organization. In this work, the mode of operation of the system has been explicitly presented. The system sub-systems; both hardware and software have been presented and details of their designs also discussed. To improve the security of the organization, a buzzer is added to the system in order to alert the security personnel if three wrong consecutive tries are made on the system.

REFERENCES

- [1] Douglas Hall "Microprocessor and Interfacing". (pg 20-24, 32), 1996.
- [2] ELECTRONIC CIRCUITS (Fundamentals of Transistor Applications in Digital Circuit designing By Prof. G. N. Onoh. 2005.
- [3] Practical Approach to Corporate Data Processing by Prof H.C Inyama, 2007
- [4] Microchip Technology, Inc. 2009. "PIC16F84A Data Sheet". (Retrieved May 30, 2009).
<http://ww1.microchip.com/downloads/en/devicedoc/39582b.pdf>
- [5] Oke, A.O., O.M. Olaniyi, O.T. Arulogun, and O.M. Olaniyan. 2009. "Development of a Microcontroller-Controlled Security Door System". *Pacific Journal of Science and Technology*. 10(2):398-403.
- [6] Inderpreet Kaur. "Microcontroller Based Home Automation System With Security". *International Journal of Advanced Computer Science and Applications*, Vol. 1, No. 6, December 2010

A Review on Parallel Scheduling of Machines and AGV'S in an FMS environment

Prof.Mallikarjuna¹, Vivekananda², Md.Jaffar², Jadesh², Hanumantaraya²

¹(Assistant Professor, Dept of ME, Ballari Institute Of technology & Management, Bellary, India)

²(Dept of ME, Ballari Institute Of technology & Management, Bellary, India)

ABSTRACT:

This paper focuses on the problem of parallel scheduling of machines and automated guided vehicles (AGV's) in a flexible manufacturing system (FMS) so as to minimize the make span. Here several algorithms were employed to solve this combinatorial optimization problem. In this paper the authors have attempted to schedule both the machines and AGV's parallelly for which Differential Evolution (DE) and Simulated annealing (SA) techniques are applied. The impact of the major contribution is indicated by applying these techniques to a set of standard benchmark problems. For this particular problem coding has been developed, which gives the optimum sequence with make span value and AGV's schedule for number of job sets. Finally a comparison of DE and SA applied to a highly generalized class of job shop scheduling problems is to be done and results to be concluded

KEYWORDS: AGV's, Benchmark problem, Combinatorial optimization problem, Differential Evolution, Flexible manufacturing system, Job shop scheduling, Simulated Annealing.

I. INTRODUCTION

A flexible manufacturing system is that kind of manufacturing system in which there is some amount of flexibility that allows the system to react in the case of changes, whether predicted or unpredicted.

The main purpose of the FMS to combine the job shop and productive of flow line

For this purpose it possesses 2 kinds of flexibility

- (1) Machine flexibility
- (2) Routing flexibility

Machine flexibility covers the system ability to be changed to produce new product types and ability to change the order of operations executed on a part. Routing flexibility consists of ability to use multiple machines to perform the same operation on a part as well as the system ability to absorb large scale changes such as in volume, capacity or capability.

FMS system comprises of 3 main systems those are :

- [1] The machines which are often automated to CNC machines
- [2] Material Handling system to which the CNC machines are connected in order to optimize the parts flow.
- [3] And the Central Control Computer which controls material movement and machine flow.

This paper has mainly considered with an FMS that is required to process various types of job loaded in a least possible time at different processing stations. Each job requires a definite sequence of operations that indicates the order in which the operations are to be performed. The production demands a flexible MHS to move the parts to various processing stations during a production run. Automated Guided Vehicles [AGV's] are used in many material handling situations involving large, heavy loads over flexible routes. AGV's are the most flexible of the floor cart system and follow electromagnetic impulses transmitted from a guided wire embedded in the plant floor. Configuration and operating environment of FMS involving AGV's and CNC Machines is as shown in the below figure

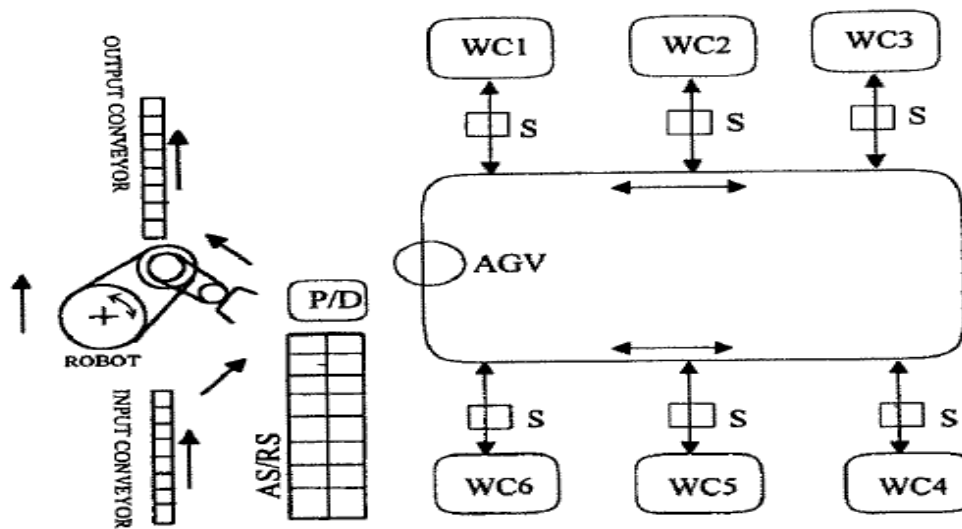


Fig. 2. Configuration of a flexible manufacturing system. WC,work cell; AGV, automated guided vehicle; P/D, pick and deposit; AS/RS, automated storage/retrieval system; S, shuttle.

The main advantage of an FMS are its high flexibility in managing manufacturing resources like Time and Effort in order to manufacture a new product. The best application of an FMS is found in the production of small sets of products like those from a mass production.

II. OBJECTIVES OF SCHEDULING :

The scheduling is made to meet specific objectives. The objectives are decided upon the situation, market demands, company demands and the customer's satisfaction. There are two types for the scheduling objectives :

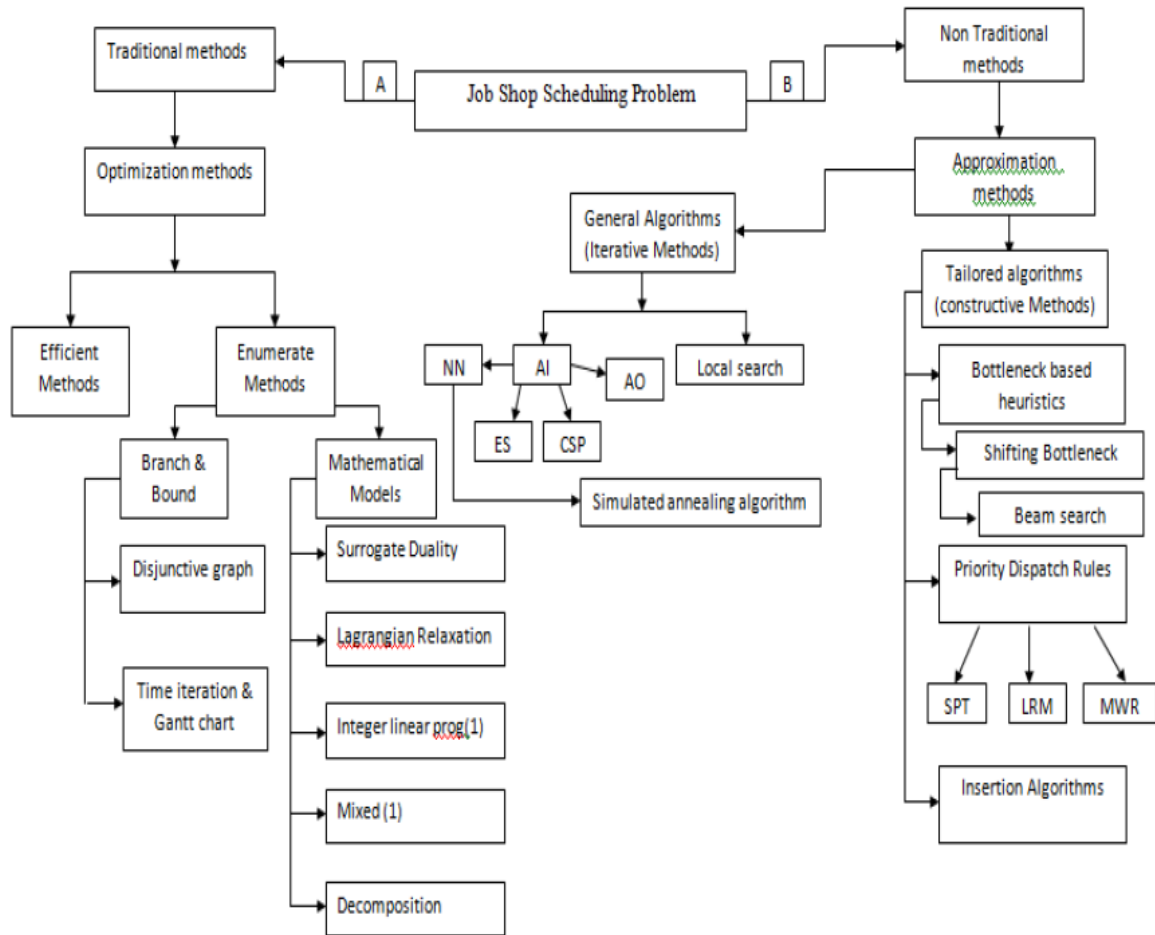
- [1] Minimizing the make span
- [2] Due date based cost minimization

The objectives considered under the minimizing the make span are,

- (a) Minimize machine idle time
- (b) Minimize the in process inventory costs
- (c) Finish each job as soon as possible
- (d) Finish the last job as soon as possible

The objectives considered under the due date based cost minimization are,

- (a) Minimize the cost due to not meeting the due dates
- (b) Minimize the maximum lateness of any job
- (c) Minimize the total tardiness
- (d) Minimize the number of late jobs



III. LITERATURE REVIEW:

Sl no.	Authors	Technique used	Remarks
1.	C.S.P Rao, M.V.Satish kumar, G.Rangajanardhan	Hybrid Differential Evolution	In this by the application of differential evolution, the simultaneous scheduling of machines and AGV's has been done. In this, operation based coding system is employed to represent the solution vector, which is further modified to suit the DE application
02.	B.S.P.Reddy, C.S.P. Rao	Hybrid Multi Objective Genetic Algorithm	In this the authors have made an attempt to consider simultaneously the machine and the vehicle scheduling aspects in an FMS and addressed the combined problem for the minimization of make span, mean flow time and mean tardiness objectives.
03.	S. V. Kamble & K. S. Kadam	Particle Swarm Optimization	Minimizing the idle time of the m/c and minimizing the total penalty cost for not meeting the deadline concurrently. To achieve this it is necessary to determine the routing for jobs processing sequence of operation on m/c and the starting time for operation on m/c and starting time for operation in order to balance the workload of machine.

04.	Ghada El Khayat, Andre Langevin, Diane Riopel	Mathematical Programming and Constraint Programming	Machines and MHE are considered as the constraining resources. A mathematical programming model and a constraint programming model presented for the problem and solved optimally on test problems used for modeling, testing and integrating both models in a decision support system. The performance of two methods is comparable when using the data from the literature.
05.	Muhammad Hafidz Fazli bin Md Fauadi and Tomohiro Murata	Binary Particle Swarm Optimization	It exploits a population of particles to search for promising regions of the search space (swarm). While each particle randomly moves within the search space with a specified velocity. It stores data of the best position it ever encountered. This is known as personal best (pbest) position. Upon finishing each iteration, the pbest position obtained by all individuals of the swarm is communicated to all of the particles in the population. The best value of pbest will be selected as the global best position (Gbest) to represent the best position within the population.
06.	K.V.Subbaiah, M.Nageswara Rao and K. Narayana Rao	Sheep Flock Heredity Algorithm	For this particular problem, coding has been developed, which gives optimum sequence with makespan value and AGV'S schedule for ten job sets and four layouts. Most of the time, results of sheep flock algorithm are better than other algorithm and traditional methods.
07.	Paul Pandian,P, S. Saravana Sankar,S.G.Ponnambalam and M. Victor Raj	Jumping Genes Genetic Algorithm	The one of best evolutionary approach i.e., genetic algorithm with jumping genes operation is applied in this study, to optimize AGV flow time and the performance measures of Flexible Job shop manufacturing system. The non dominated sorting approach is used.Genetic algorithm with jumping genes operator is used to evaluate the method.
08.	J.Jerald,P.Asokan, R. Saravanan ,A. Delphin Carolina Rani	Adaptive Genetic Algorithm	Two contradictory objectives are to be achieved simultaneously by scheduling parts and AGVs using the adaptive genetic algorithm. The results are compared to those obtained by conventional genetic algorithm.
09.	M.K.A.Ariffin, M.Badakhshian, S.B.Sulaiman, A.A.Faeiza	Fuzzy Genetic Algorithm	Fuzzy logic controller (FLC) is proposed to control the behaviour of genetic algorithm (GA) to solve the scheduling problem of AGVs. This paper presents an FLC to control the crossover and mutation rate for controlling the GA

IV. SCHEDULING TECHNIQUES :

These techniques are mainly divided into two categories i.e. Traditional and Non Traditional. A brief introduction of these techniques are given below.

(a) Traditional techniques:

- ❖ These techniques are slow and guarantee of global convergence as long as problems are small. Traditional Techniques are also called as Optimization Techniques. They are
- Mathematical programming like Linear programming, Integer programming, Dynamic programming, Transportation etc.
- Enumerate Procedure Decomposition like Lagrangian Relaxation.

(b) Non traditional techniques:

- ❖ These methods are very fast but they do not guarantee for optimal solutions. Non Traditional Techniques are also called as Approximation Methods. They involve
- Constructive Methods like Priority dispatch rules, composite dispatching rules.
- Insertion Algorithms like Bottleneck based heuristics, Shifting Bottleneck Procedure.
- Evolutionary Programs like Genetic Algorithm, Particle Swarm Optimization.
- Local Search Techniques like Ants Colony Optimization, Simulated Annealing, adaptive Search, Tabu Search, Problem Space methods
- Iterative Methods like Artificial Intelligence Techniques, Artificial Neural Network, Heuristics Procedure, Beam-Search, and Hybrid Techniques.

V. SOME NON TRADITIONAL TECHNIQUES :

Genetic algorithm:

A Genetic Algorithm is an 'intelligent' probabilistic search algorithm that simulates the process of evolution by taking a population of solutions and applying genetic operators in each reproduction. Each solution in the population is evaluated according to some fitness measure. Fitter solutions in the population are used for reproduction. New 'off spring' solutions are generated and unfit solutions in the population are replaced.

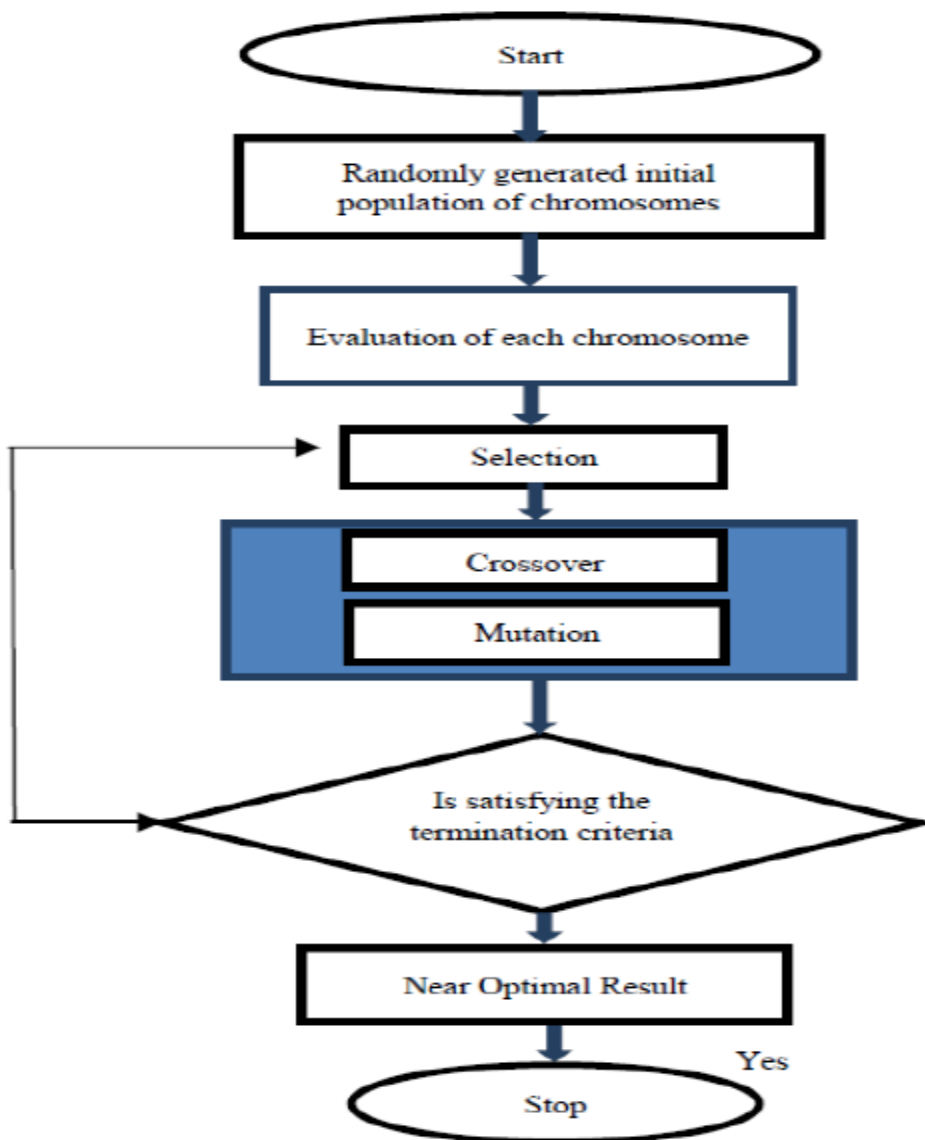
GA coding scheme:

As GA works on coding of parameters, the feasible job sequences (the parameter of the considered problems) are coded in two different ways.

- (i) Pheno style coding
- (ii) Binary coding

Algorithm:

- Step 1: Generate random population of n chromosomes(suitable solution for problem)
- Step 2: Evaluate the fitness $f(x)$ of each chromosome x in the population.
- Step 3: Create a new population by repeating following steps until the new population is complete
- Step 4: Select two parent chromosomes from a population according to their fitness (the better fitness, the bigger chance to be selected)
- Step 5: With a crossover probability crossover the parents to form a new offspring(children). If no crossover was performed, offspring is an exact copy of parents.
- Step 6: with a mutation probability mutate new offspring at each locus(position in chromosome)
- Step 7: place new offspring in a new population
- Step 8: use new generated population for a further run of algorithm.
- Step 9: if the end condition is satisfied, stop, and returns the best solution in current population and Go to step 2.



Simulated Annealing:

The simulated annealing algorithm resembles the cooling process of molten metals through annealing. At high temperature, the atoms in the molten metal can move freely with respect to each another. But, as the temperature is reduced, the movement of the atoms gets reduced. The atoms start to get ordered and finally form crystals having the minimum possible energy. However, the formation of the crystal depends on the cooling rate. If the temperature is reduced at a fast rate, the crystalline state may not be achieved at all; instead the system may end up in a polycrystalline state, which may have a higher energy state than the crystalline state. Therefore, to achieve the absolute minimum state, the temperature needs to be reduced at a slow rate. The process of slow cooling is known as annealing in metallurgical parlance. SA simulates this process of slow cooling of molten to achieve the minimum function value in a minimization problem. The cooling phenomenon is simulated by controlling a temperature – like parameter introduced with the concept of the Boltzmann probability distribution.

Algorithm:

- Step 1: Choose an initial point $X^{(0)}$, a termination criterion $\hat{\epsilon}$. Set T as a sufficiently high value number of iterations to be performed at a particular temperature n , and set $t=0$.
- Step 2: Calculate the neighbouring point $X^{(t+1)} = N(x^{(t)})$. Usually, a random point in the neighbourhood is created.
- Step 3: If $DE = E(x^{(t+1)}) - E(x^{(t)}) < 0$, set $t=t+1$; Else create a random number (r) in the range $(0,1)$. If $r_{\text{exp}}(DE/T)$, set $t=t+1$; Else go to Step 2.
- Step 4: if $(x^{(t+1)} - x^{(t)}) < \hat{\epsilon}$ and T is small, Terminate. Else go to Step 2.

VI. DIFFERENTIAL EVOLUTION:

Evolutionary Algorithms (EA) which simulates evolution process in computer have created lot of interest among the researchers, which led to their application in a variety of fields. Genetic Algorithms, GA (Holland, J.H., 1975) are popular among the EAs and they were used to address scheduling problems by many researchers. Even though GA can be considered as a better searching algorithm and many versions of GA were developed by several researchers, still developed a hybrid GA procedure, which uses operation based coding for scheduling machines. They have also developed a heuristic to solve the vehicle scheduling, because of which they have reduced the length of the chromosome to half that created by Ulusoy. Lacomme et al., (2005) addressed the job input sequencing and vehicle dispatching in a single vehicle automated guided vehicle system. They have coupled the heuristic branch and bound approach with discrete event simulation model. Siva P.Reddy et al., (2006) have attempted the same problem set as that of Ulusoy and Tamer with a modified GA approach. Jerald et al.,(2006) have used an adoptive genetic algorithm for solving the simultaneous scheduling of parts and AGVs problem.

Mutation

Unlike GA, where mutation follows crossover, in DE mutation will be performed first. Three vectors $xr1$, $xr2$, $xr3$ which are different from the current vector will be randomly selected and the weighted difference of two vectors in the population is added to a third vector to get the resultant vector known as mutant vector ($v_i, g+1$), as given below

$$V_i, g+1 = xr1, g + F(xr2, g - xr3, g)$$

Where $F > 0$ is scaling factor, which controls the magnitude of the differential variation of $(xr2, g - xr3, g)$.

VII. TABU SEARCH:

The basic idea of Tabu search (Glover 1989, 1990) is to explore the search space of all feasible scheduling solutions by a sequence of moves. A move from one schedule to another schedule is made by evaluating all candidates and choosing the best available, just like gradient-based techniques. Some moves are classified as tabu (i.e., they are forbidden) because they either trap the search at a local optimum, or they lead to cycling (repeating part of the search). These moves are put onto something called the Tabu List, which is built up from the history of moves used during the search. These tabu moves force exploration of the search space until the old solution area (e.g., local optimum) is left behind. Another key element is that of freeing the search by a short term memory function that provides "strategic forgetting". Tabu search methods have been evolving to more advanced frameworks that includes longer term memory mechanisms. These advanced frameworks are sometimes referred as Adaptive Memory Programming (AMP, Glover 1996). Tabu search methods have been applied successfully to scheduling problems and as solvers of mixed integer programming problems. Nowicki and Smutnicki (Glover 1996) implemented tabu search methods for job shop and flow shop scheduling problems. Vaessens (Glover 1996) showed that tabu search methods (in specific job shop scheduling cases) are superior over other approaches such as simulated annealing, genetic algorithms, and neural networks.

Algorithm :

Begin

T:=[];

S:=initial solution;

S*:=s

Repeat

Find the best admissible $s' \in N(s)$;

If $f(s') > f(s^*)$ then $s^* := s'$

S:=s';

Update tabu list T;

Until stopping criterion:

End;

Particle swarm Optimization :

One of the latest evolutionary techniques for unconstrained continuous optimization is particle swarm optimization (PSO) proposed by Kennedy and Eberhart (1995), inspired by social behaviour of bird flocking or fish schooling. PSO learned from these scenarios are used to solve the optimization problems. In PSO, each single solution is a "bird" in the search space.[37],[38],& [39]. We call it "particle". All of particles have fitness values, which are evaluated by the fitness function to be optimized, and have velocities, which direct the flying

of the particles. The particles are “flown” through the problem space by following the current optimum particles. PSO is initialized with a group of random particles (solutions) and then searches for optima by updating generations. In each iteration, each particle is updated by following two “best” values. The first one is the best solution (fitness) it has achieved so far. (The fitness value is also stored.) this value is called ‘pbest’. Another “best” value that is tracked by the particle swarm optimizer is the best value, obtained so far by any particle in the population. This best value is a global best and called ‘gbest’.

Algorithm :

Step 1: initialize a population on n particles randomly.

Step 2: Calculate fitness value for each particle. If the fitness value is better than the best fitness value (pbest) in history. Set current value as the new *pbest*.

Step 3: Choose particle with the best fitness value of all the particles as the *gbest*.

Step 4: for each particle, calculate particle velocity according to the equation

$$V[] = c1 * rand() * (pbest[] - present[]) + c2 * rand() * (gbest[] - present[])$$

Where $present[] = present[] + v[]$

$V[]$ is the particle velocity, $present[]$ is the current particle(solution),

$rand()$ is random functions in the range [0,1].

$c1, c2$ are learning factors=0.5.

step 5: particle velocities on each dimension are clamped to a maximum velocity V_{max} . If the sum of acceleration would cause the velocity on that dimension to exceed V_{max} (specified by user), the velocity on the dimension is limited to V_{max} .

Step 6: Terminate if maximum of iterations is reached. Else, goto Step2

The original PSO was designed for a continuous solution space. In original PSO we can't modify the position representation, particle velocity, and particle movement. Then another heuristic is made to modify the above parameters, called Hybrid PSO. So they work better with combinational optimization problems. This Hybrid PSO was designed for a discrete solution space.

VIII. CONCLUSION :

Flexibility is unavoidable in manufacturing sector now a days, which can be achieved by Flexible Manufacturing System (FMS). Many researchers concentrated on scheduling of FMS only but few of them focused on problems of scheduling of AGV's as well as machines. This paper introduces most important non traditional optimization algorithms to integrate both scheduling of AGV'S and Machines simultaneously. While they are difficult to solve, parallel scheduling problems are among the most important because they impact the ability of manufacturers to meet customer demands and make a profit. They also impact the ability of autonomous systems to optimize their operations, the deployment of intelligent systems, and the optimizations of communications systems. For this reason, operations research analysts and engineers will continue this pursuit well in the next coming centuries.

REFERENCES:

- [1]. Hymavathi Madivada and C.S.P. Rao. A Review Of Non Traditional Algorithm for Job Shop Scheduling
- [2]. K. V. Subbaiah, M. Nageswara Rao and K. Narayana Rao. Scheduling of AGVs and machines in FMS with makespan criteria using sheep flock heredity algorithm.
- [3]. N.Jawahar, P.Aravindan, S.G.Ponnambalam and R.K.Suresh. AGV Schedule Integrated with Production In Flexible Manufacturing Systems.
- [4]. M.V. Satish Kumar, KITS, Singapur, A.P, INDIA C.S.P Rao, NIT, Warangal, A.P, INDIA G.Rangajanardhan, JNTU, Kakinada, A.P, INDIA. A Hybrid Differential Evolution Approach for Simultaneous Scheduling Problems in a Flexible Manufacturing Environment.
- [5]. Paul Pandian, P. Saravana Sankar, S.G. Ponnambalam and M. Victor Raj. Scheduling of Automated Guided Vehicle and Flexible Jobshop using Jumping Genes Genetic Algorithm.
- [6]. Pramot Srinoi, A/Prof. Ebrahim Shayan and Dr. Fatemeh Ghotb. Scheduling of Flexible Manufacturing Systems Using Fuzzy Logic.
- [7]. S. V. Kamble & K. S. Kadam. A Particle Swarm Optimization –Based Heuristic for Scheduling in FMS Review.
- [8]. M. V. Satish Kumar, Ranga Janardhana & C. S. P. Rao. Simultaneous scheduling of machines and vehicles in an FMS environment with alternative routing.
- [9]. B. Siva Prasad Reddy and C.S.P. Rao. Simultaneous Scheduling of Machines and Material Handling System in an FMS.
- [10]. J. Jerald · P. Asokan · R. Saravanan · A. Delphin Carolina Rani. Simultaneous scheduling of parts and automated guided vehicles in an FMS environment using adaptive genetic algorithm.
- [11]. Moacir Godinho Filho, Clarissa Fullin Barco and Roberto Fernandes Tavares Neto. Using Genetic Algorithms to solve scheduling problems on flexible manufacturing systems (FMS): a literature survey, classification and analysis.
- [12]. Muhammad Hafidz Fazli, Md Fauadi and Tomohiro Murata. Makespan Minimization of Machines and Automated Guided Vehicles Schedule Using Binary Particle Swarm Optimization.

Mapreduce Performance Evaluation through Benchmarking and Stress Testing On Multi-Node Hadoop Cluster

¹Urvashi Chaudhary , ²Harshit Singh

¹Indian Institute of Technology

²ABV-Indian Institute of Information Technology and Management

ABSTRACT

Over the past few years, many data based applications have been developed using the powerful tools provided by the World Wide Web. In today's world an organization may generate petabytes of data each second. To gain insights from this vast pool of data, applications based on data-mining and web indexing such as artificial neural networks, decision trees etc., play an important role. Such tools are tremendously helping social networking sites such as Facebook and Twitter to get meaningful information from their data. Hadoop is an open source distributed batch processing infrastructure. It works by distributing the amount of processing required by a task across a number of machines, thereby balancing the load depending on the node. Hadoop, in a very short time has gained huge popularity amongst many IT firms. Infact, many big players such as IBM, Google, Quora and Yahoo are using numerous applications based on Hadoop infrastructure.

KEYWORDS: TestDFSIO performance benchmark, MapReduce, Apache Hadoop

I. INTRODUCTION

MapReduce[7] has proven to be an efficient programming model for data processing. MapReduce programs coded in several different languages can be run on Hadoop. Since MapReduce programs run parallel, it is possible to perform analysis on large data sets simultaneously by deploying a number of machines. Although, the hadoop model appears complex initially but familiarity with its tools makes it easy to use. In the MapReduce [2] architecture there exist one master JobTracker and one slave TaskTracker in each clusternode. The master schedules and monitors the tasks of each job on the slaves. In case of a task failure the master re-executes the task. The slave simply performs the tasks assigned to it by the master.

II. RELATED WORKS

GridMix, [1] the name assigned to denote the past works on Hadoop performance benchmarking has been upgraded many times over the years. GridMix aims to symbolize real application assignments on Hadoop clusters and has been used to validate and measure optimizations across dissimilar Hadoop releases. Hadoop is a successful execution of the MapReduce model. The Hadoop framework consists of two main elements: MapReduce and Hadoop Distributed File System (HDFS).

MapReduce

It is a type of programming model and is used to process and generate huge amounts of data. Their main functions like map and reduce are supplied by the user and depend on user's intention [4]. Map: Map operates by processing a series of key/value pairs and generates zero or more key/value pairs. It is possible that the Map's input and output type are different from each other [2]. Reduce: For each unique key in the sorted order, the application's Reduce function is called. Reduce generates zero or more output by iterating through the values that are linked with that key [2].

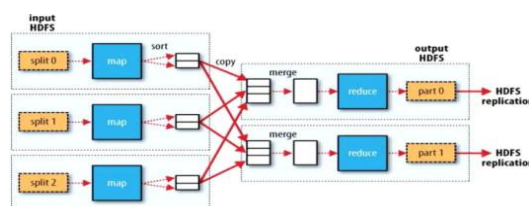


Figure 1. MapReduce Programming Model[6]

2.2 NameNode

The hierarchy of files and directories make the HDFS namespace. On the Name Node these are represented by inodes. The contents of the files are split into larger blocks (128MB standard but user selectable). Then each block of the file is replicated at multiple data nodes [3].

2.3 DataNode

It handles the task of storing the data on the Hadoop File System and responding to the requests of the file system operations. On starting the cluster the data node is connected to the name node. On providing the location of the data to the client, the client directly communicates to the data node similar to the working of the MapReduceTaskTracker [3].

2.4 Secondary NameNode

It stores the log of the corrections made to the file system additional to a native file system. The HDFS reads the state from an image file called *fsimage* on starting the name node. It then applies changes from the log file [3].

2.5 TaskTracker

It receives the tasks - Map, Reduce and Shuffle operations from a Job Tracker. It can accept a limited number of tasks configured by the set of slots. The Job-Tracker during scheduling a task looks for an empty slot on the same server that hosts the Data Node containing the data. If it is not found, an empty slot on the machine in the same rack is chosen [9].

2.6 JobTracker

It is used to track the particular nodes in the cluster i.e. the tasks of MapReduce. These nodes are mostly the nodes with the data in them or are in the same rack [8].

[1] JobTracker receives jobs from client applications.

[2] Name Node is communicated by JobTracker to find the location of the data.

[3] It then finds the TaskTracker nodes with empty slots at or cleans the data.

[4] It finally sends the work to the chosen TaskTracker node.

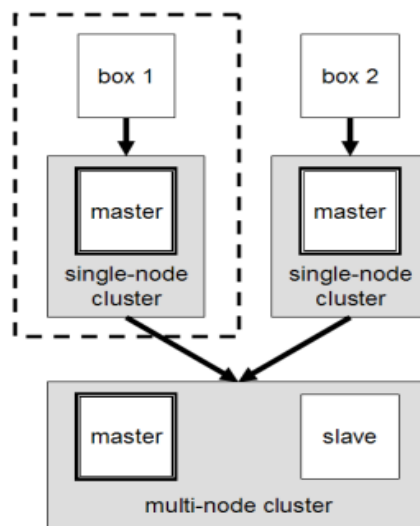


Figure 2. Multi Cluster Node

III. DESIGN AND IMPLEMENTATION

In this paper, we are deploying multi-node cluster Hadoop on two machines in which master machine with core i5 2.3 GHz processor, 2GB of RAM and slave machine with Pentium 4 3.4GHz, 1GB of RAM. Both machine has LAN network of 100 Mbps and setting up of cluster we use Hadoop 1.0.4 and UBUNTU 10.04

Before deploying Hadoop we have prerequisite as follows

Sun Java: It requires working Java 1.6.x or above installation.

Table 1. Writing Speed of Several files

Number of files	Total Megabytes processed	Throughput MB/sec	Average I/O Rate	I/O rate standard deviation	Test execution time (second)
1	1000	62.5273557181	62.52735519	0.0042950560	47.91
2	2000	37.1848583256	39.71986389	1.3875991805	65.98
3	3000	34.7567375935	37.71351623	12.865245652	65.98
5	5000	32.7102039481	33.51700210	4.9086852221	120.09
9	9000	31.2761720745	32.76895523	10.966624853	211.20
10	10000	19.5372027414	20.89837455	11.742043454	329.33

Table 2. Reading Speed of Several files

Number of files	Total Megabytes processed	Throughput MB/sec	Average I/O Rate	I/O rate standard deviation	Test execution time (second)
1	1000	62.5273557181	62.52735519	0.0042950560	47.91
2	2000	37.1848583256	39.71986389	1.3875991805	65.98
3	3000	34.7567375935	37.71351623	12.865245652	65.98
5	5000	32.7102039481	33.51700210	4.9086852221	120.09
9	9000	31.2761720745	32.76895523	10.966624853	211.20
10	10000	19.5372027414	20.89837455	11.742043454	329.33

ssh: It requires to manage its node i.e. remote machine .

Hadoop Implementation

We have implemented Hadoop on Ubuntu 10.04.

As the hadoop is written in java, we needed Sun jdk to run hadoop. This was not available on the official server of sun jdk. Now we have to install jdk to run hadoop.

- Installing the jdk 1.6 version for Ubuntu 10.04.
- apt-get install sun-java6-jdk
- IPv6 should be disabled.

For performance evaluation benchmarking and stress testing on Hadoop we use TestDFSIO tool.

IV. EXPERIMENT AND PERFORMANCE

4.1 Interpreting TestDFSIO Results

In this paper, TestDFSIO has been used to benchmark the read and write test for HDFS. This test proved to be extremely useful in determining performance blockage in the network and for conducting stress test on HDFS. This setup proved to be extremely economical in terms of hardware, OS and setup costs (specifically the Name Node and the Data Nodes) and to give us a first influence of how fast our cluster is in terms of I/O.

4.2 Data Throughput

From the table 1, 2 one can infer that throughput MB/sec and average I/O rate MB/sec emerge as the most important parameters. Both the parameters depend on the file size reading and writing speed obtained by the individual map tasks and the elapsed time to do so. Throughput MB/sec for a TestDFSIO job using N map tasks can be determined in the following manner. The index $1 \leq i \leq N$ denotes the individual map tasks:

$$\text{Throughput}(N) = \sum_{i=0}^N \text{filesize} / \sum_{i=0}^N \text{time} \quad (1)$$

Average I/O rate MB/sec is defined as

$$\text{Average Rate I/O Rate}(N) = \sum_{i=0}^N \text{rate} / N \quad (2)$$

Here the metrics “concurrent” throughput and average I/O rate in cluster’s capacity prove to be significant. Let us assume that TestDFSIO create 10 files and our cluster size is limited to 2 map slots. Hence, the number of MapReduce waves to write the full test data will be 10 (5 * 2) since the cluster will be able to run only 200 map tasks at an instant.

In this example, we multiplied the throughput and average I/O rate by the minimum of the number of files and the number of available map slots in the cluster. Here:

Concurrent throughput = $31.3 * 2 = 62.6$ MB/s

Concurrent average I/O rate at $31.49 * 2 = 62.98$ MB/s

As given in the figure 3 and figure 4 we can see that the throughput during reading is more than the throughput during writing. As the number of files is increased, the throughput of both reading and writing starts decreasing but in the reading case, throughput decreases more rapidly as compared to writing.

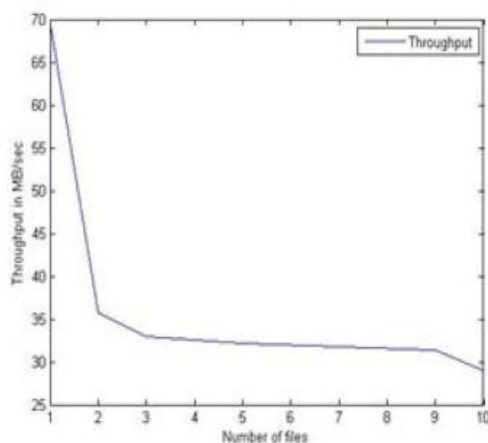


Figure 3 .Write throughput performance

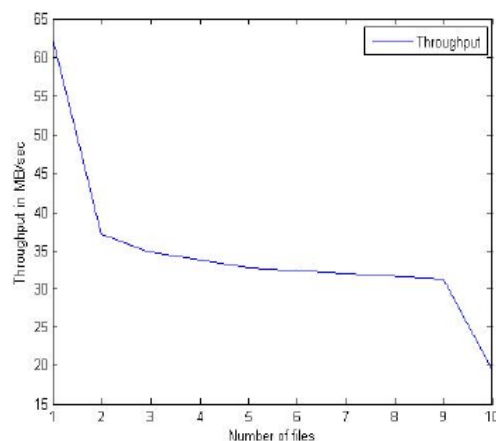


Figure 4. Read throughput performance

V. CONCLUSIONS

The HDFS reading performance of files is much faster than writing. It also shows that when number of files increases performance decreases. The evaluation of reading and writing Throughput runs on multi cluster in a particular machine. Time execution of files writing is more than reading as number of files increases it decreases. In the above figure we can easily see the throughput performance of file. Writing is more costly than reading according to the scenario.

REFERENCES

- [1] H. T. C. Douglas, "GridMix Emulating Production Workload for Apache Hadoop.", http://developer.yahoo.com/blogs/hadoop/posts/2010/04/gridmix3_emulating_production, 2010.
- [2] T. White, Hadoop The Definitive Guide 3rd Edition, O'Reilly, 2012.
- [3] M. Doug Cuttling, "Hadoop Home Page Hadoop Architecture.", http://hadoop.apache.org/docs/r1.0.4/hdfs_design.html, 2012.
- [4] Yahoo Inc., http://hadoop.apache.org/docs/stable/hdfs_user_guide.html, 2008.
- [5] M. Noll, "Michael Noll.", <http://www.michael-noll.com>.
- [6] Zhang, "MapReduce Sharing.", 2011, pp. 8-15.
- [7] J. Dean and S. Ghemawat, "MapReduce: Simplified data processing on large clusters." in *OSDI*, 2008.
- [8] H. Apache, "JobTracker.", Apache, <http://wiki.apache.org/hadoop/JobTracker>, 2008.
- [9] H. Apache, "TaskTracker.", Apache, <http://wiki.apache.org/hadoop/JobTracker>, 2008.

Characteristics of soils for underground pipeline laying in the southwest Niger Delta

Uko, E. D., Benjamin, F. S. and Tamunobereton-ari, I.
Department of Physics, Rivers State University of Science and Technology,
PMB 5080, Port Harcourt 500001, Nigeria

ABSTRACT:

Geoelectric investigation of the geophysical characteristics of the soil with depth carried out to guide against the adverse impacts that result due to soil-pipeline interaction over a long period after the burial of a pipeline. Thirty (30) stations along the proposed pipeline route were geoelectrically sounded with ABEM Terrameter SAS-300 model instrument. A maximum current electrode separation (AB) of 100m at each station was used. Resist software computer iterative procedure was used to obtain interpreted depths and resistivities from the field data. The findings revealed that the burial depth zone of the pipeline (i.e. surface 0m to a depth of about 15m) is made up of clayey and silty clay materials and highly conductive as shown by the low resistivity values ranging from 17 Ω m to 700 Ω m thereby making the soil materials of this depth domain highly corrosive. The results suggest that the best depth region for the laying of the pipeline based on the lithologic and resistivity distribution should be ≥ 25 m. These information will equip the pipeline engineers and corrosion specialist (cathodic protection engineers) with relevant data in the planning, design and proper execution of the pipeline project along the said route, by properly coating the pipes to be used, appropriate design and installation of cathodic protection kits and routine pipeline monitoring that will safeguard the environment, prevent equipment failure, preserve national assets, reduce maintenance cost and minimize or eliminate citizens/companies confrontations to create conducive operational atmosphere for mutual benefit of citizens and companies during and after the actual execution of the project.

KEYWORDS: Pipeline, corrosion, cathodic protection, lithology, electrical resistivity, Niger Delta

I. INTRODUCTION

Soil materials and properties are strongly correlated and can be quantified through the geoelectric properties. Indeed, the flux of electrical charges through soils permits metals and electrolytes in which the conductivities are high to be distinguished from insulating materials like air and plastics which have low conductivities. Soil materials exhibit intermediate electrical properties depending on their physical and chemical properties (Plummer and McGear, 1993; Kearey *et al.*, 2002; Zohdy *et al.*, 1973; Halvorson and Rhoades, 1976).

Geoelectric investigation of soils with depth is a dependable tool for lithologic characterization, the understanding of the dynamics of the subsurface with respect to the strength of the soil for construction purposes, electrical earthing, corrosion mitigation, groundwater resource exploration, management and planning. An understanding of the electrical property of the soil is also needed in the design and subsequent construction of an efficient ground bed system for cathodic protection of metallic pipelines and structures against corrosion (Telford *et al.*, 1976; Kelly, 1977; Edlefsen and Anderson, 1941; Kirkham and Taylor, 1949; Todd, 1959). Many pipelines already laid are subjected to rust and corrosion. However, a proper management programme is required. The determination of electrical characteristics is best made on data acquired in the area of study. In the present study, we attempt to determine geoelectric properties and correlate the properties with lithologic sequences, depth, conductive layers, thickness, and lateral extent (Koefoed and Dirk, 1979; Tamunobereton-ari *et al.*, 2010). The results of this study are very important because of severe and large scale oil spillages experienced in these areas and generally in the Niger Delta that had impacted and still impacting seriously on the wellbeing of the people of the areas, from which there had been blames and counter-blames of companies on equipment failures due to corrosion of the pipelines.

The work is significant because pipelines are the major medium of crude oil and gas transportation, distribution of municipal water supply and in the course of time. Metallic pipelines get corroded as a result of age, and the corrosive nature of the contacting soil and nature of fluid being transported. Once corrosion commences from a point on a pipeline an anodic-cathodic condition is created; part of the pipeline become anodic, while the other part which is not badly damaged by corrosion is cathodic, hence fast transfer of electrons takes place between cathode and anode. If this is not nipped on time, the fluid in the pipe starts sipping through the first layer lithology. If porous and permeable (sand), but if the soil is plastic clay that is well compacted/lithified, the oil passes through the surface to a gathering point or into the river, killing marine lives.

In addition to this, oil which is less dense than water, floats at the surface and marking time for ignition (fire outbreak). However, for a broken gas pipeline, the gas goes straight into the environment and very fast at igniting on exposure to heat. Once pipelines are broken, aquifers are polluted, and flora and fauna are destroyed. So in order to prevent this potential catastrophic scenario from taken place and to preserve assets, reduce maintenance and inspection costs, and preserve the environment, pipelines are to be cathodically protected and this can only be done, after electrical properties of the contacting soil have been investigated and established.

II. GEOLOGY, PHYSIOGRAPHY AND HYDROGEOLOGY OF THE AREA OF STUDY

The research was carried out in the Niger Delta, in an area encompassing two local government areas in Rivers and Bayelsa States. The map of the location of the study area is shown in Figure 1. The location is the site of the proposed Associated Gas (AG) pipeline route along the Shell Petroleum Development Company (SPDC) of Nigeria right of way (ROW) from Adibawa flow station in Rivers State through Zarama field in Bayelsa State. The general physio-graphy of the area essentially reflects the influence of movements of flood water in the Niger delta and their search for lines of flow to the sea, hence depositing their transported sediments along the paths of flow in the rivers.

Geologically, the entire site and the environs lie within freshwater zone of the Niger delta and they are of Miocene era. This zone is generally known to be characterized by considerable thickness of greyish silty-clay (mostly active) with intercalation of Coastal Plain Sand of the Benin geologic formation (Short and Stauble, 1967).

The area lies within the humid tropical climate zone due to its proximity with the Gulf of Guinea. This area has its wet season from March to November, while dry season occur from November to February. The vegetation is the evergreen thick forest type complete with raffia palms. Prominent superficial soil type is silty clay which is underlain by sand. The project route is a flat terrain with sparse undulations caused by seasonal water channels.

III. CAUSES OF PIPE CORROSION

Corrosion is the gradual destruction of a metal by a variety of slow chemical, electrochemical reactions between the metal and its environment. The major cause of the corrosion of underground pipeline is indeed the nature of the soil (Uhlig, 1973; Ekott *et al*, 2012). The best known form of corrosion is rusting, which is an oxidation reaction between iron that has dissolved in water and dissolved oxygen (all metals are to some extent soluble in water). The end-product of this reaction is ferric hydroxide, which is insoluble and may accumulate somewhere else where it can contribute to incrustation. The oxidation of dissolved iron causes more iron to go into solution, until eventually the metal is completely destroyed. The speed and degree to which iron and other metals dissolve in water is greatly affected by the water's acidity (Bouwer, 1978; Durham, and Durham, 2005).

The contact of two dissimilar chemical solutions can generate electric potential difference, which also cause corrosion described as concentration-cell corrosion. This kind of corrosion occurs on macro scale when the chemical concentration of groundwater changes with depth, and on micro scale in small pores or cracks in the metal and other hidden places like under gaskets, washers, coupling, and joints. A similar type of corrosion is the galvanic corrosion, which is caused by electric potentials generated when two dissimilar metals are in direct contact and immersed in an electrolyte to complete the electric circuit. This will cause electrolysis reaction with corrosion taking place at the anodic (most corrosive) metal and electrolysis products accumulating on the cathodic (least corrosive) metal. Galvanic corrosion will also occur when there is contact between identical metals in different stages of corrosion when new pipe is connected to an old pipe. The old pipe is usually rustier, which acts as a protective coating, the new pipe will then corrode. In alloy there exists selective corrosion, dezincification, or degraphitization form of galvanic corrosion (Bouwer, 1978).

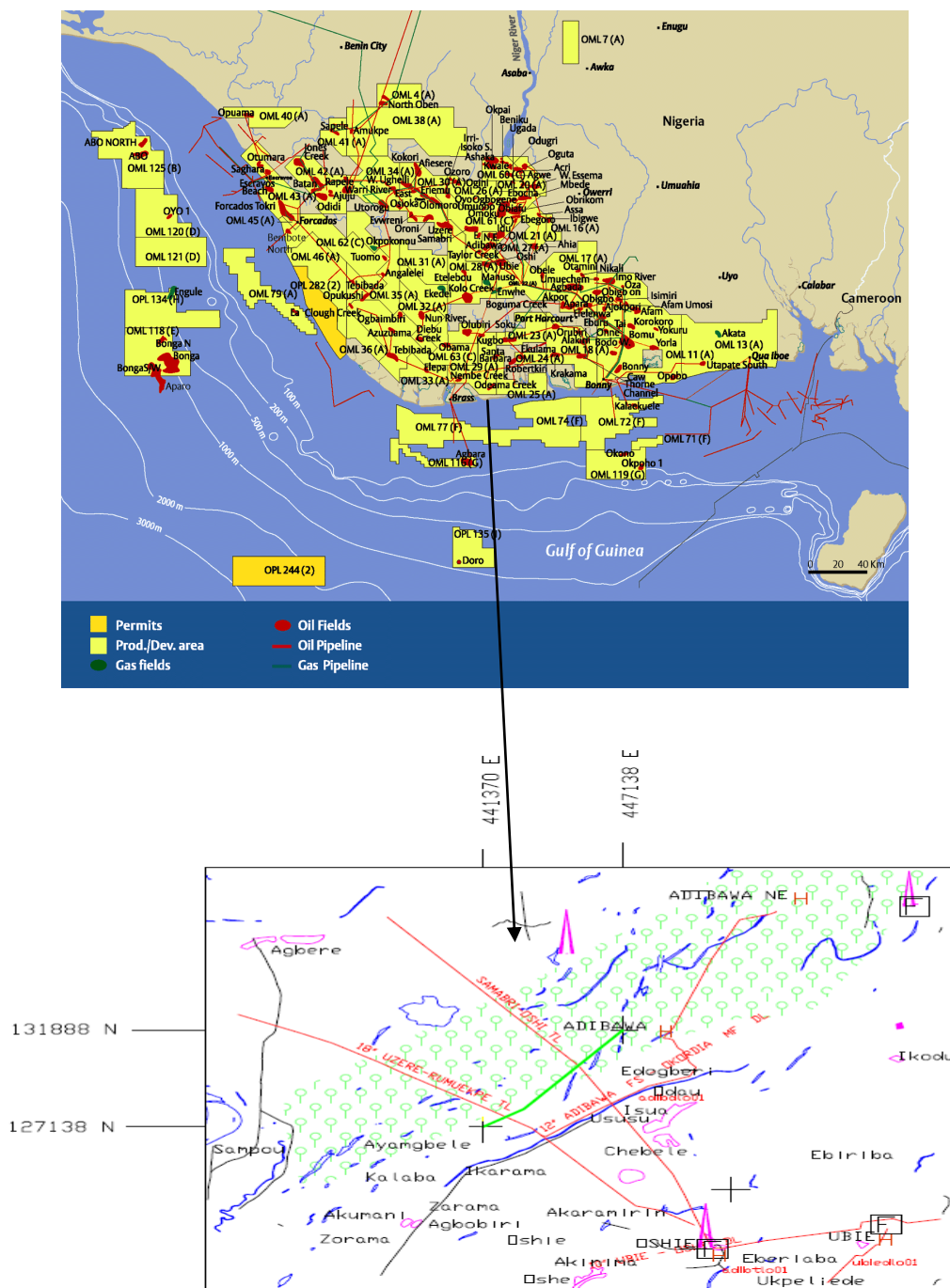


Figure 1: Map of Niger Delta showing the study area

IV. EFFECTS OF PIPELINE CORROSION

Failures of oil or gas pipelines can have severe environmental and economic consequences (Okoroafor, 2004; Rim-Rekeh and Awatefe, 2006). Protective coatings offer a first barrier against corrosion. However, damage of the coating during installation and coating degradation result in severe corrosion and necessitate the installation of properly designed cathodic protection (CP) systems. When designing a cathodic protection system, the aim is to obtain a pipe-to-soil potential along the entire length of the pipeline network that is more negative than a well-defined minimum protection level. The basic idea of a cathodic protection system is that the pipeline is cathodically protected through the use of an electrical current. This can be done with either galvanic anodes or impressed current. Because the current supplies a steady stream of free electrons along the pipeline, the hydroxyl ions do not recombine with the oxygen from the water, and corrosion is avoided or minimized (Purcar and Bortels, 2009).

The steel in the pipelines have areas that are both cathodic and anodic. The anodic areas are the places that corrode, so as part of galvanic or anodic pipeline cathodic protection, sacrificial anodes are attached or combined with the pipeline so that the pipeline itself does not corrode (Durham and Durham, 2005). Such sacrificial anodes can be made of a variety of materials, depending on the material that the pipeline is to be made from. Often, aluminum, magnesium and zinc alloys are used. This basically means that the entire pipe becomes a cathode and the sacrificial anode corrodes. There is no outside power source necessary for this type of protection because the materials themselves cause the current to flow naturally. The sacrificial anode will eventually become totally corroded and will need replacement as the pipeline structure ages.

The same elements that cause corrosion can be used to control it or to protect a different material. Aluminum, zinc, or magnesium will corrode if placed in contact with iron products. Example, Aluminum has an electronegativity of 1.61, while iron's electronegativity is 1.83. Therefore, aluminum molecules have an ionic charge that is less negative than the steel. This causes an electrochemical attraction between the two metals. Aluminum molecules will flow from the aluminum, through the electrolyte, and deposit on the iron. This fact can be used to protect steel pipe if the aluminum is sacrificed. Where the aluminum forced to a more negative potential through some outside energy, iron molecules would travel in the opposite direction and deposit on the aluminum. Cathodic protection, then, is the process of forcing a metal to be more negative (cathodic) than the natural state. If the metal is forced negative enough, then corrosion will stop.

The corrosion protection of oil and gas pipelines is mostly always concerned with the outer surface as the flow of fluid prevents or minimizes corrosion of the internal surface. Therefore, the best approaches for metallic pipeline corrosion protection are: cathodic protection, use of nonmetallic asbestos-cement and high-impact plastic casings, and also the use of corrosion-resistant metals; as listed in the decreasing corrosion resistance order: Monel metal, stainless steel, Everdur metal, silicon red brass, yellow brass, and low carbon steel (Banton *et al*, 1997; Gass, 1977; Ritchie, 1976).

V. THE PRINCIPLE OF RESISTIVITY SURVEYS

Surface electrical resistivity surveying is based on the principle that the distribution of electrical potential in the ground around a current-carrying electrode depends on the electrical resistivities and distribution of the surrounding soils and rocks. The usual practice in the field is to apply an electrical direct current (DC) between two electrodes implanted in the ground and to measure the difference of potential between two additional electrodes that do not carry current. Usually, the potential electrodes are in line between the current electrodes, but in principle, they can be located anywhere.

A geoelectric layer is described by two fundamental parameters: its resistivity ρ_i and its thickness h_i , where the subscript i indicates the position of the layer in the section ($i = 1$ for the uppermost layer). Other geoelectric parameters are derived from its resistivity and thickness. These are:

$$\text{Longitudinal unit conductance, } S_L = \frac{h_i}{\rho_i} \tag{1}$$

$$\text{Transverse unit resistance, } T_i = h_i \rho_i \tag{2}$$

$$\text{Longitudinal resistivity, } \rho_L = \frac{h_i}{s_i} \tag{3}$$

$$\text{Transverse resistivity, } \rho_t = \frac{T_i}{h_i} \tag{4}$$

$$\text{Anisotropy, } \lambda = \sqrt{\frac{\rho_t}{\rho_L}} \tag{5}$$

$$\text{For isotropic layer } \rho_t = \rho_L \text{ therefore } \lambda = 1 \tag{6}$$

These secondary geoelectric layers are essential to describing geoelectric section of several layers. For n layers, the total longitudinal unit conductance is:

$$S = \sum_{L=1}^n \frac{h_L}{\rho_L} = \frac{h_1}{\rho_1} + \frac{h_2}{\rho_2} + \dots + \frac{h_n}{\rho_n} \tag{7}$$

$$T = \sum_{t=1}^n h_t \rho_t = h_1 \rho_1 + h_2 \rho_2 + \dots + h_n \rho_n \tag{8}$$

Average longitudinal resistivity is:

$$\rho_L = \frac{H}{S} = \frac{\sum_1^n h_i}{\sum_1^n \frac{h_i}{\rho_i}} \quad (9)$$

Average transverse resistivity is:

$$\rho_t = \frac{T}{H} = \frac{\sum_1^n h_i \rho_L}{\sum_1^n h_i} \quad (10)$$

hence anisotropy is:

$$\lambda = \sqrt{\frac{\rho_t}{\rho_L}} = \frac{\sqrt{TS}}{H} \quad (11)$$

The above parameters (S, T, ρ_L , ρ_t and λ) are derived by considering a column of unit cross-sectional area (1x1 meter) cut out from a group of infinite lateral extent. If current flows vertically through the section, then the different layers in the section will behave like resistors arranged in series, and the total resistance of the layer section will be:

$$R_t = R_1 + R_2 + R_3 + \dots R_n \quad (12)$$

$$R = \rho_1 \frac{h_1}{1 \times 1} + \rho_2 \frac{h_2}{1 \times 1} + \rho_3 \frac{h_3}{1 \times 1} + \dots \rho_n \frac{h_n}{1 \times 1} \quad (13)$$

$$= \rho_1 h_1 = T \quad (14)$$

The symbol T is used instead of R to indicate that the resistance is measured in a direction transverse to the bedding and also because the dimensions of this unit resistance is usually measured in Ωm^2 instead of ohms. If current flows parallel to the bedding plane, the layers in the column will behave as resistors connected in parallel and the conductance will be:

$$S = \frac{1}{R_1} + \frac{1}{R_2} + \frac{1}{R_3} + \dots + \frac{1}{R_n} \quad (15)$$

$$S = \frac{1 \cdot h_1}{\rho_1 \cdot 1} + \frac{1 \cdot h_2}{\rho_2 \cdot 1} + \dots + \frac{1 \cdot h_n}{\rho_n \cdot 1} \quad (16)$$

$$S = \frac{h_1}{\rho_1} + \frac{h_2}{\rho_2} + \frac{h_3}{\rho_3} + \dots + \frac{h_n}{\rho_n} \quad (17)$$

$$T = \rho_1 h_1 + \rho_2 h_2 + \dots \rho_n h_n$$

where S = total longitudinal conductance,

T = total transverse resistance,

h = thickness

ρ = resistivity

VI. MATERIALS AND METHODS

The survey involved thirty VES soundings at specified locations, 250m apart and any change in lithology, along the Adibawa-Zarama-Gbaran pipeline route. Data obtained from the field include the resistance of the ground between the two inner electrodes, and the lithostratigraphic sequences of the geology of the study area.

The current and potential differences generated by the instrument were also used to calculate the resistance of the ground to the flow of electric current from which resistivities were obtained. The resistivities with corresponding C1C2/2 are uploaded into the Resist software and analyzed to generate apparent resistivity curves, from which the geoelectric layers of the area were delineated.

The VES locations were identified with the aid of global positioning satellite system (GPS) and Total Station Survey equipment. VES soundings were also done at visible changes in soil type and at the banks of rivers and creeks, this was necessary because these locations are known to have a high concentration of mineral salts or mineralized fluids like alluvial clay or mud in the pore fluids, which can give unique resistivity readings. Figures 2a and 2b show an assemblage of data acquisition equipment in the field.

Method of four-electrode probe has been used in soil practices since 1931 for evaluating soil water content and salinity under field conditions (Edlefsen and Anderson, 1941). Halvorson and Rhoades (1976) applied a four-electrode probe in the Wenner configuration to locate saline seeps on croplands in USA and Canada. Austin and Rhoades (1979) developed and introduced a compact four-electrode salinity sensor into routine agricultural practices. In this research, a total of thirty (30) resistivity soundings were carried out at 250 meters intervals along the 6.75 kilometer Adibawa-Zarama proposed pipeline route. The survey started from Adibawa towards Zarama. The field array type used in the research is the Schlumberger array, owing to its ability to effectively delineate small intervals of soil horizons with comparably less length of spread, less labour and it's relatively less cumbersome.

In this work, the electric drilling is employed for the Schlumberger layout because of its advantages over other methods. In this method the fraction of total current which flows at depth varies with the current-electrode separation. The field procedure used a fixed center with an expanding spread. The presence of horizontal or gently dipping beds of different resistivities is best detected by the expanding spread. Hence the method is useful in determination of depth of overburden, deep structure and resistivity of flat lying sedimentary beds and possibly the bedrock if not too deep (Koefoed and Dirk, 1979; Lowrie, 1997; Gupta and Hanks, 1972).

With the Schlumberger array, the potential (MN) electrodes separation is kept constant while the current electrodes AB or (L) spacing is increased in steps. A maximum current electrode separation (AB) of 100m was marked out in this work. In each measurement, the digital averaging instrument, Abem Terrameter SAS 300 Model, displayed the resistance directly. The readings are made possible as the four electrodes driven into the ground are connected to AB and MN terminals of the meter through the reels of cables. This procedure is repeated for each location along the marked profile as the depth of penetration of current into the ground is increased in the electrode separation.

VII. RESULTS AND DISCUSSION

The results of the survey work are presented by Table 1; showing thirty (30) sounding stations and their respective coordinates. Also, presented are the interpreted layers, their thicknesses and their corresponding resistivities by the Resist software program. The stations traverse through the length of the pipeline route from adibawa to Zarama. The number of layers, their thicknesses and resistivities vary from station to station with a minimum of four (4) layers to a maximum of seven (7) layers. Figure 2 shows a 2D model of the geoelectric section of the pipeline route covering the 30 sounding stations, which by colour codes reveal the resistivity values and the conductive zones with respect to depth.

VES Curves in Log-Log plots are shown by the Figures 3 to 32 below. Apparent Resistivities are plotted as ordinates while Current Electrode spacing (AB/2) as abscissas. Chart-sheet for each station; the chronological geoelectric layers and their corresponding resistivities (ohm m), and depths (m) respectively are recorded. The line plot of the Figures is a plot of apparent resistivity against AB/2 while the block or square shaped plot is a plot of apparent resistivity against layer thickness. Low resistivity values are observed in the upper three, four layers from the surface 0m to a depth of about 15m, which is within the region of the proposed burial depth of the pipeline, while the fifth to the seventh layers have higher resistivity values indicative of less conductive regions. Geological information from the pipeline route reveals that the proposed depth domain for the burial of the pipeline is made up of clayey to silty clay materials. Figures 33 to 38 are iso-resistivity maps showing the lithologic composition and resistivity distribution of the layers, while Figure 39 is a 2D Geoelectric section showing depth and lateral extent of lithologic distribution along the pipeline route.

Table 1: Table showing summary of geoelectric parameters

Survey station	Coord. (m)	P (Ωm)	Layer Thickness (m)	Total layers Thickness (m) H	P _L (Ωm)	P _t (Ωm)	Survey station	Coord. (m)	P (Ωm)	Layer Thickness (m) h	Total layers Thickness (m) H	P _L (Ωm)	P _t (Ωm)
VES 1	E446713 N131888 (0 km)	110 68 605 308 3800	1.55 3.25 9.7 7.5 **	22	215.12	389.55	VES 8	E445858 N130684 (1.75 km)	98 155 610 1450 605 4555	1.5 1.42 13.7 8 11.2 **	28.9	580.63	936.3
VES 2	E446951 N131710 (0.25 km)	104. 5 65.6 1005 304. 5 3300	1.55 0.75 4.6 14.6 **	21.5	272.88	431.62	VES 9	E445664 N130514 (2.0 km)	59 320 1250 498 3900	3 1.6 11 13.1 **	28.7	315.55	730.41
VES 3	E446765 N131541 (0.5 km)	91.2 45 570 260. 6 1996 4900	1.65 1.3 4.95 14.1 12 **	34	293.65	901.5	VES 10	E445485 N130341 (2.25 km)	79.5 315 1180 506 3996	2.94 2.02 11.0 4 9 **	25	354.43	738.05
VES 4	E446590 N131368 (0.75 km)	106. 6 37 790 505. 6 2200 4950	1.68 1.28 15.04 10 7 **	35	378.98	930.4	VES 11	E445297 N130174 (2.0 km)	182 113 600 220 1250 3997	1.5 2.2 6.8 8.1 12 **	30.6	358.05	698.81
VES 5	E446402 N131200 (1.0 km)	44.3 142 840 645 3415	1.65 1.32 5.23 19.8 **	28	362.51	465.41	VES 12	E445118 N130005 (2.25 km)	79.5 315 1400 1000 3996	2.94 4.1 5.6 15 **	27.64	425.25	597.87
VES 6	E446217 N131035 (1.25 km)	98 155 610 1450 605 4555	1.54 0.84 1.56 13.56 11.3 **	28.8	585.81	929.85	VES 13	E444935 N129836 (2.5 km)	182 113 600 220 1250 3997	1.5 2.2 6.8 8.1 12 **	30.6	412.79	565.48
VES 7	E446042 N130862 (1.5 km)	98.5 195 505 1360 498 3967	1.5 1 1.42 13.78 11.2 **	28.9	545.5	853.33	VES 14	E444745 N129660 (2.75 km)	116 53 317 640 498 3970	1.55 1.45 1.6 12 11.4 **	28	339.96	486.21

Characteristics of soils for underground pipeline laying in the southwest Niger Delta

Survey station	Coord. (m)	P (Ωm)	Layer Thick. (m)	Total layers Thickness (m) H	P _L (Ωm)	P _t (Ωm)
VES 15	E4447 N1294 96 (3.0km)	59 320 1250 678 3900	3	27.6	347.40	418.01
			1.6			
			7			
			16			
VES 16	E4443 N1293 20 (3.25km)	111 55 320 610 240 1500	1.5	28	226.50	357.27
			1.9			
			1.6			
			10			
VES 17	E4442 N1291 49 (3.4km)	113 55 320 615 320 1612	1.66	24.87	185.09	208.15
			3.44			
			1.67			
			3.1			
VES 18	E4440 N1289 70 (3.6km)	100 54.4 416 614 489 1760	1.5	30.39	257.63	315.33
			3.5			
			1.6			
			4.89			
VES 19	E4438 N1288 05 (3.75km)	150 55 416 730 415 1536	1.5	28	207.41	366.72
			1.9			
			1.8			
			9.6			
VES 20	E4436 N1286 39 (4.0km)	176 67 499 740 410 2200	1.5	27.62	339.63	459.24
			1.9			
			1.81			
			9.41			
VES 21	E4435	178	1.55			

Survey station	Coord. (m)	P (Ωm)	Layer Thick. (m) h	Total layers Thickness (m) H	P _L (Ωm)	P _t (Ωm)
VES 23	E443112 N128120 (4.75 km)	104.7 55 410 49 220 600	1.4	29	82.56	168.66
			8			
			2.2			
			9			
			6.0			
			3			
VES 24	E442909 N127824 (5.0 km)	98 50 402 150 820	1.4	29.5	140.83	189.38
			7			
			2.4			
			1			
			5.8			
			7			
VES 25	E442703 N127824 (5.25 km)	98 50 402 220 820	1.5	27.48	159.23	165.43
			3.5			
			3.2			
			8			
			19.			
			2			
VES 26	EE44250 N127684 (5.5 km)	453 70 130 23 650	1.5	28.7	31.37	70.49
			2.3			
			5.7			
			19.			
			2			
			**			
VES 27	E442294 N127541 (5.75 km)	135 56 220 130 2560	1.6	26	128.91	145.45
			2.1			
			6.1			
			16.			
			2			
			**			
VES 28	E442078 N127400 (6.0 km)	40 17 230 50 330	1.5	33	50.11	80.49
			2.2			
			2			
			6.0			
			8			
			23.			
VES 29	E441866 N127133 (6.25 km)	60 46 235 118 1450	1.4	25	111.34	141.
			5			
			2.3			
			5			
			7.2			
			14			

Characteristics of soils for underground pipeline laying in the southwest Niger Delta

S	11	55	1.75			
21	N1284	416	11.3			
	97	730	12.4			
		415	**	27	318.83	523.13
	(4.25 km)					
E4432						
VE	96					
S	N1282	178	1.56			
22	96	55.7	2.19			
	(4.5 km)	902	10.85			
		400	13.4			
		1998	**	28	299.11	555.23

			**			56
			2.9			
VES 30	E441370	79.5	4			
	N127138	315	2.0			
	(6.5 km)	506	2			
		3996	9	13.96	228.	38
			**		18	8.
						54

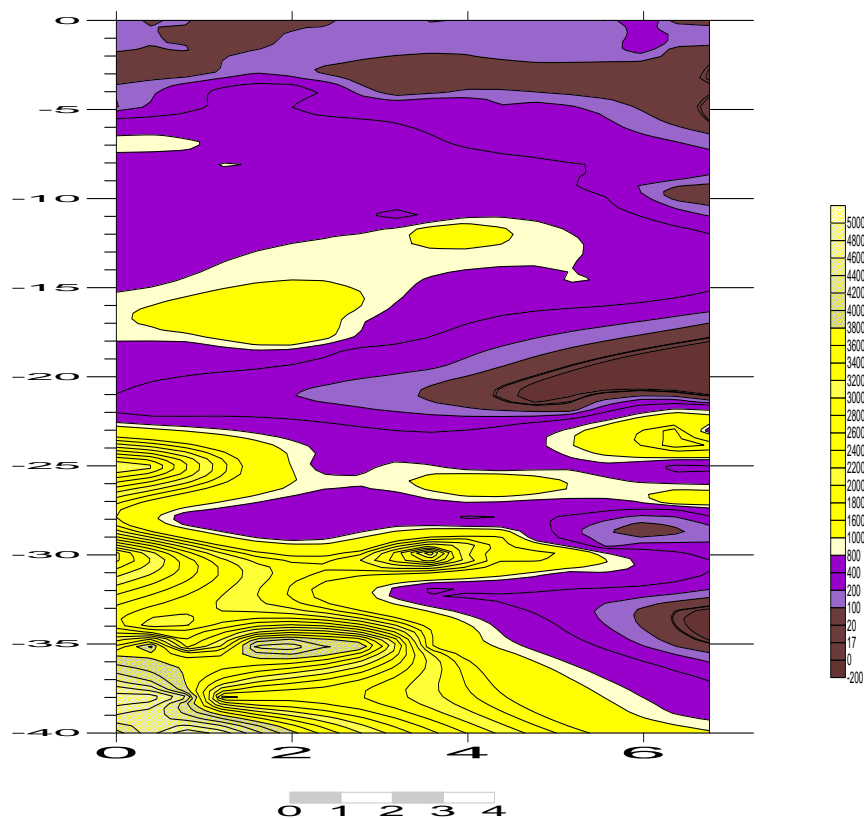


Figure 2: 2D model of the geoelectric section showing depth and resistivity values

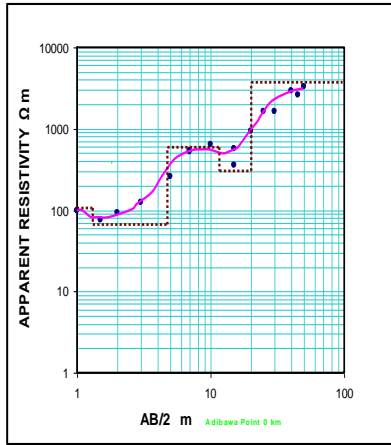


Figure 3: Resistivity Curve for VES 1

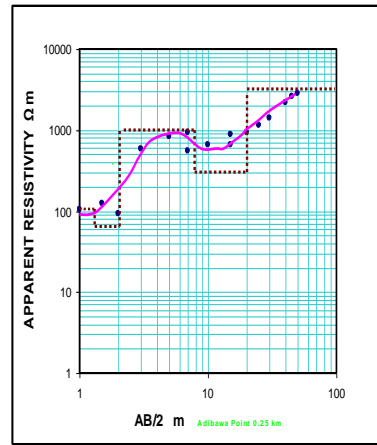


Figure 4: Resistivity Curve for VES 2

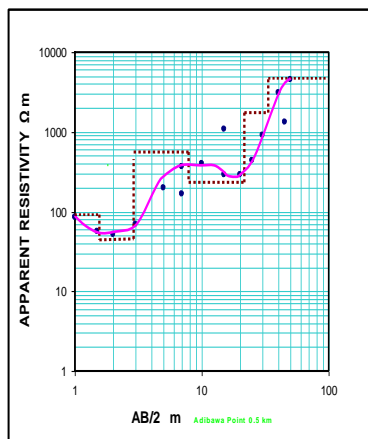


Figure 5: Resistivity Curve for VES 3

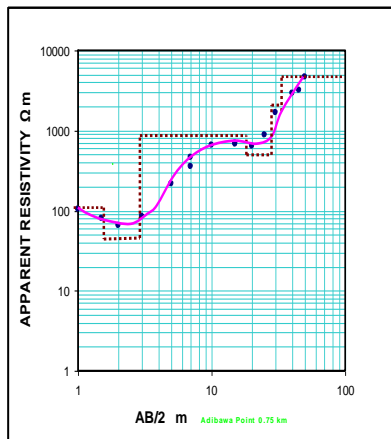


Figure 6: Resistivity Curve for VES 4

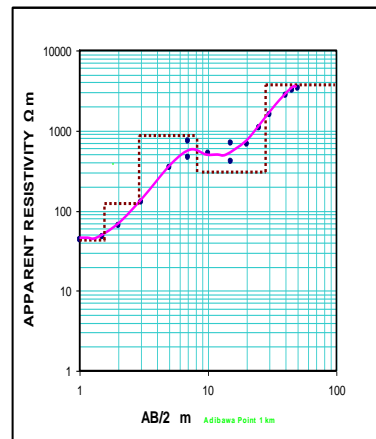


Figure 7: Resistivity Curve for VES 5

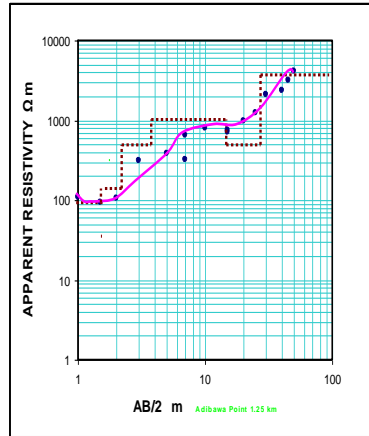


Figure 8: Resistivity Curve for VES 6

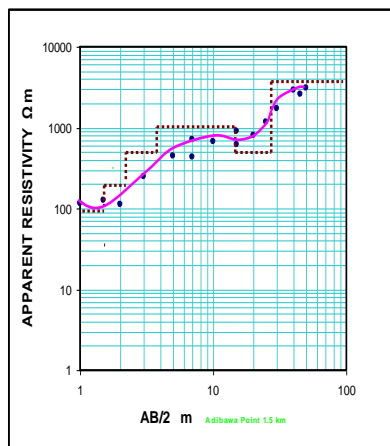


Figure 9: Resistivity Curve for VES 7

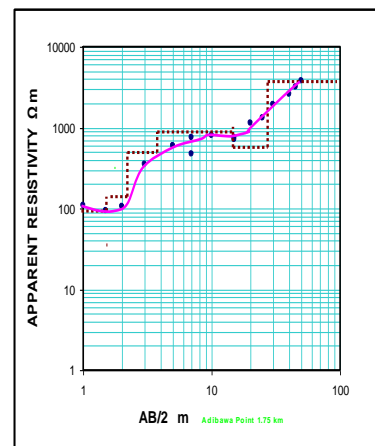


Figure 10: Resistivity Curve for VES 8

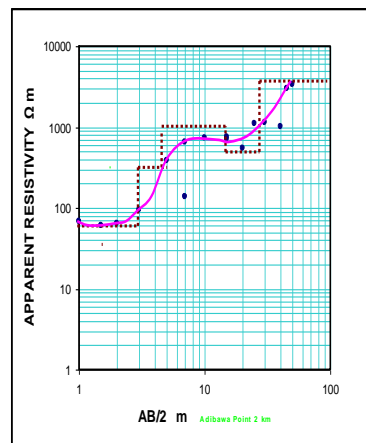


Figure 11: Resistivity Curve for VES 9

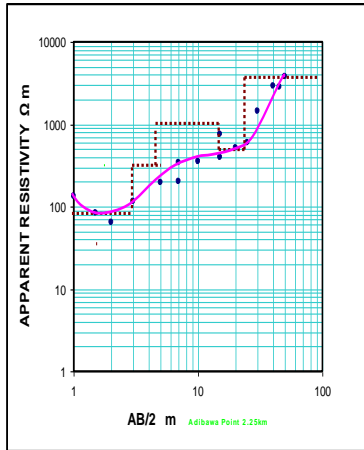


Figure 12: Resistivity Curve for VES 10

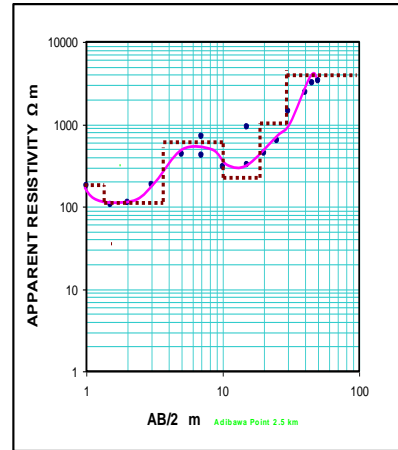


Figure 13: Resistivity Curve for VES 11

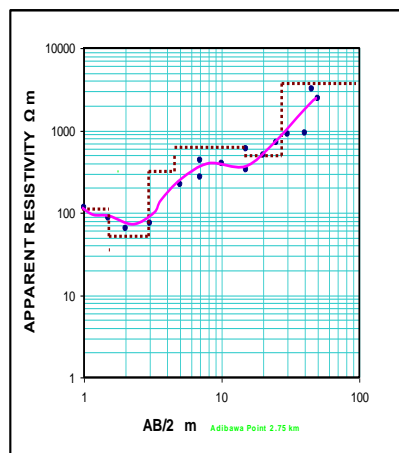


Figure 14: Resistivity Curve for VES 12

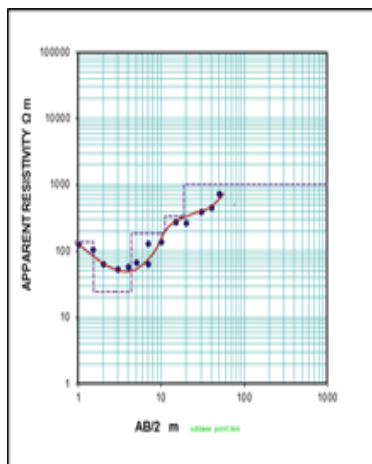


Figure 15: Resistivity Curve for VES 13

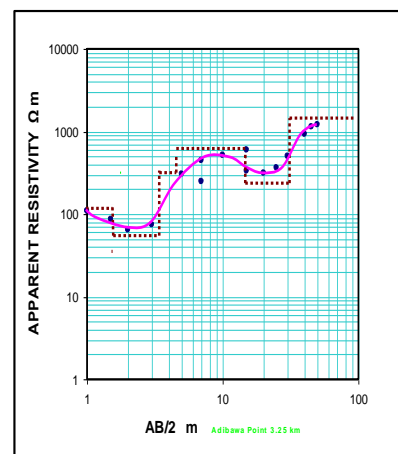


Figure 16: Resistivity Curve for VES 14

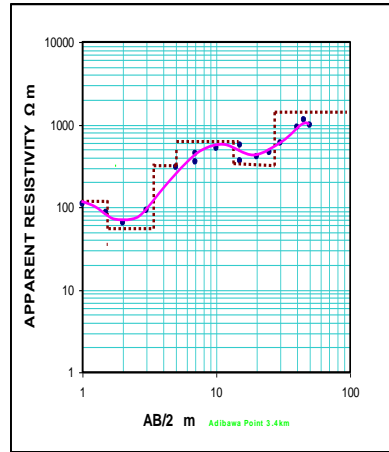


Figure 17: Resistivity Curve for VES 15

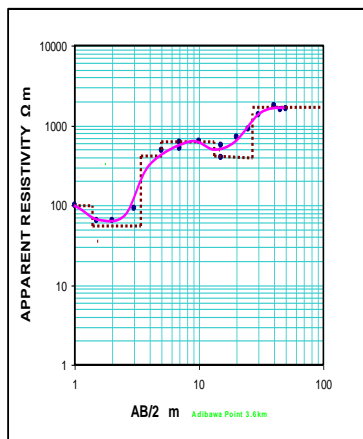


Figure 18: Resistivity Curve for VES 16

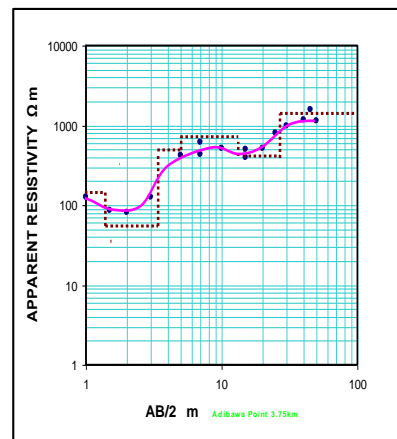


Figure 19: Resistivity Curve for VES 17

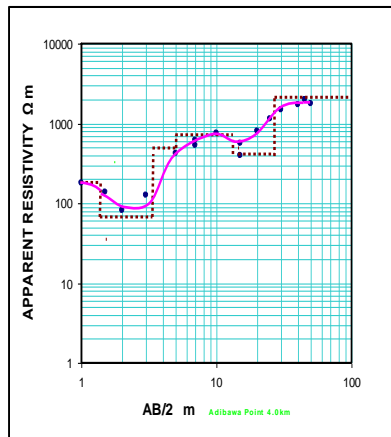


Figure 20: Resistivity Curve for VES 18

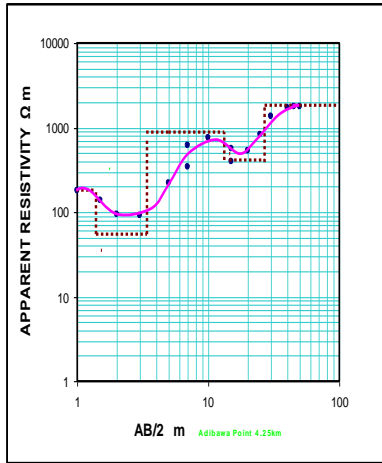


Figure 21: Resistivity Curve for VES 19

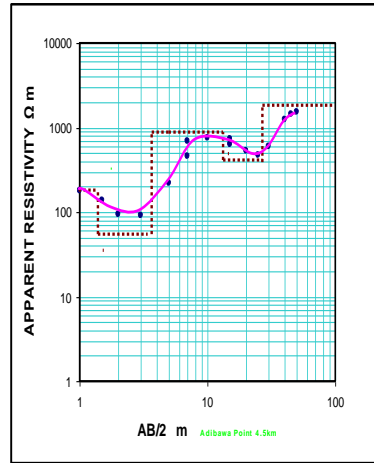


Figure 22: Resistivity Curve for VES 20

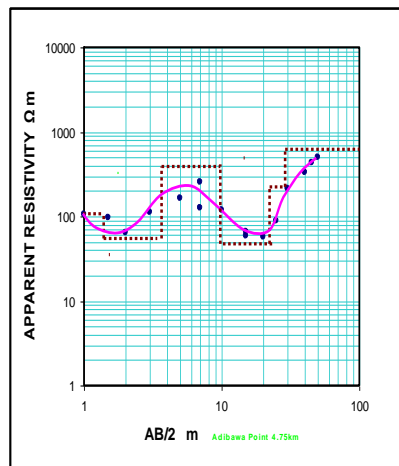


Figure 23: Resistivity Curve for VES 21

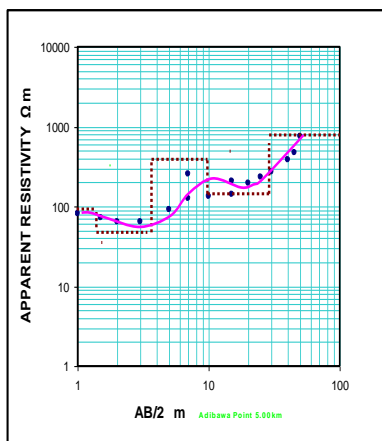


Figure 24: Resistivity Curve for VES 22

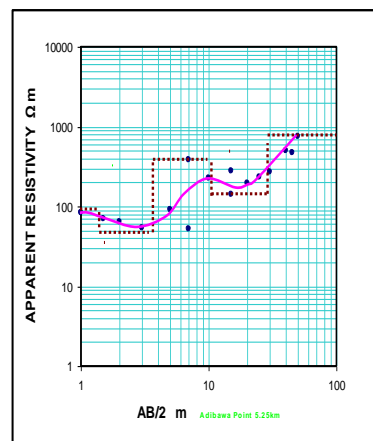


Figure 25: Resistivity Curve for VES 23

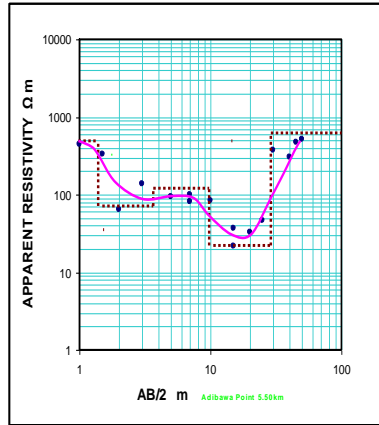


Figure 26: Resistivity Curve for VES 24

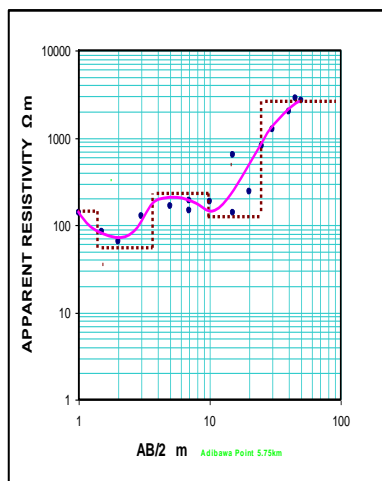


Figure 27: Resistivity Curve for VES 25

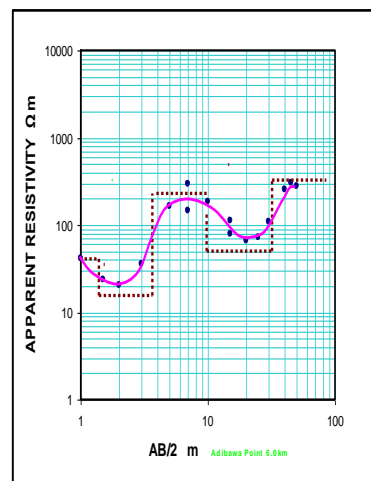


Figure 28: Resistivity Curve for VES 26

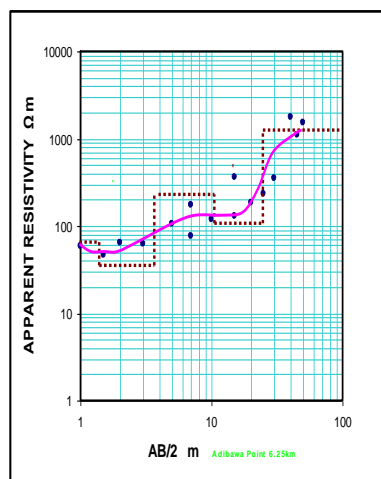


Figure 29: Resistivity Curve for VES 27

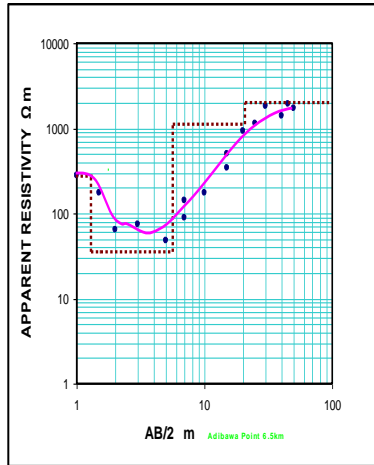


Figure 30: Resistivity Curve for VES 28

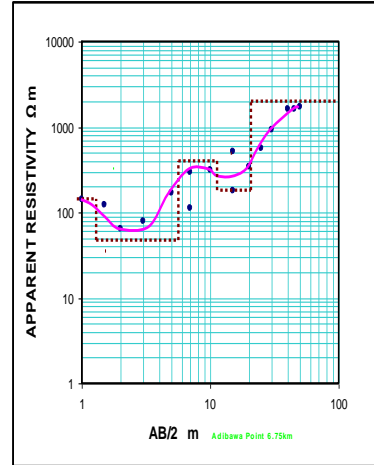


Figure 31: Resistivity Curve for VES 29

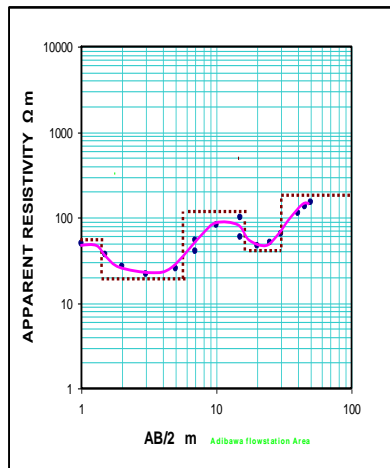
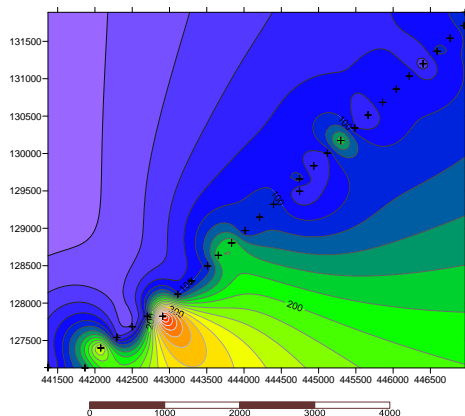
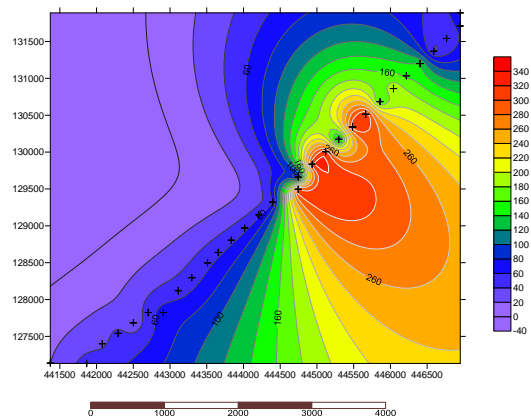


Figure 32: Resistivity Curve for VES 30



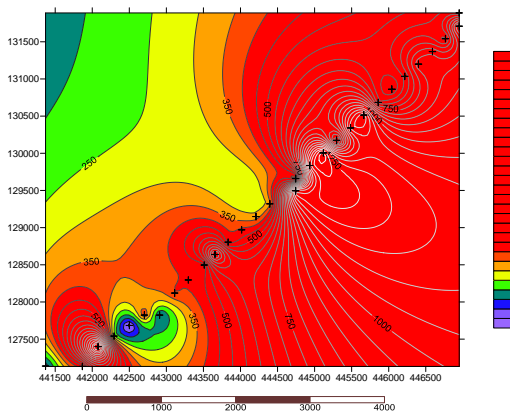
+ VES POINTS

Figure 33: 1st geoelectric layer (Clay) iso-resistivity Map



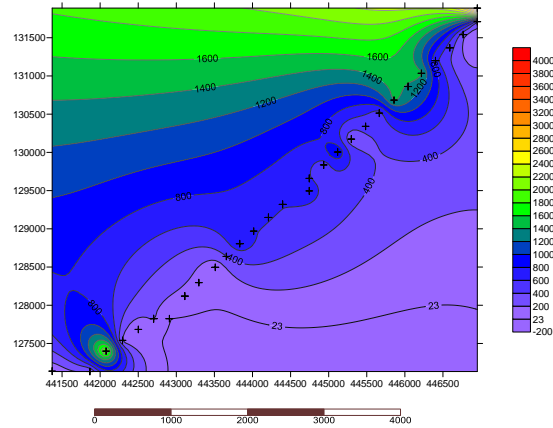
+ VES POINTS

Figure 34: 2nd geoelectric layer (sandy Clay) iso-resistivity Map



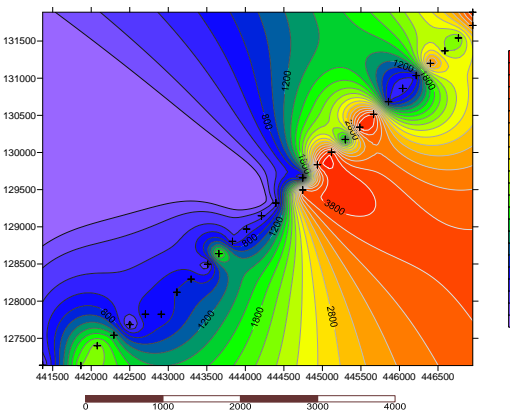
+ VES POINTS

Figure 35: 3rd geoelectric layer (sandy Clay) iso-resistivity Map



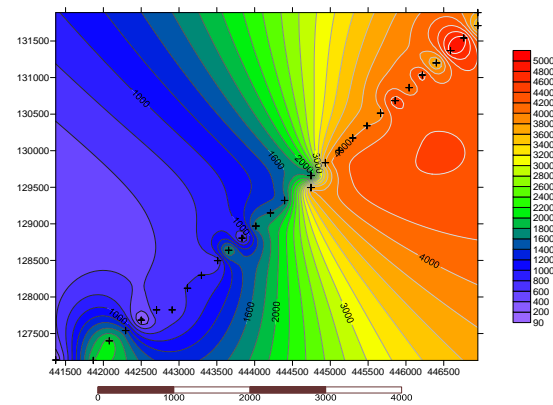
+ VES POINTS

Figure 36: 4th geoelectric layer (mainly sand and clayey sand, few clay) iso-resistivity Map



+ VES POINTS

Figure 37: 5th geoelectric layer (basically sand, little clayey to silty sand and little very few clay band) iso-resistivity Map



+ VES POINTS

Figure 38: 6th geoelectric layer (basically sand, only one to two clay band was captured here) iso-resistivity Map

40

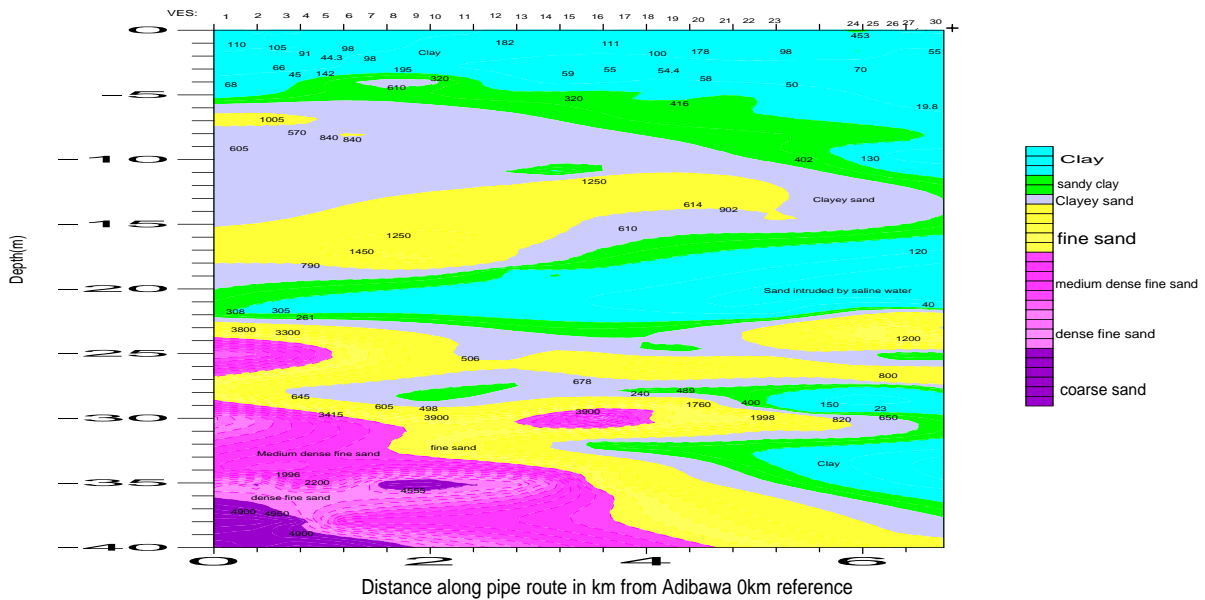


Figure 39: 2D Geoelectric section showing depth and lateral extent of lithologic distribution.

VIII. CONCLUSIONS

From the results of this work, it is very clear of the importance of gathering such sensitive data of an area before the commencement of the actual project to guide against environmental disaster from equipment failure due to soil-pipeline interaction after the execution of such project that will pose serious danger to the well-being of man. The findings also reveal that the proposed burial depth zone of the pipeline (i.e. surface 0m to a depth of about 15m) is made up of clayey and silty clay materials and also being highly conductive as shown by the low resistivity values ranging from 17 Ω m to 700 Ω m thereby making this depth range highly corrosive. The results suggest that the best depth region for the laying of the pipeline based on the lithologic and resistivity distribution should be ≥ 25 m. These information will equip the pipeline engineers and corrosion specialist (cathodic protection engineers) with relevant data in the planning, design and proper execution of the pipeline project along the said route (Adibawa-Zarama), by properly coating the pipes to be used, application of cathodic protection and routine pipeline monitoring that will safeguard the environment, prevent equipment failure, preserve national assets, reduce maintenance cost and minimize or eliminate citizens/companies confrontations to create conducive operational atmosphere for mutual benefit of citizens and companies.

It is also very much evident from the findings of the reliability of the survey method (resistivity method, Schlumberger array, the software program) used in this work, which made it possible to precisely determine the required parameters, interpreted to establish the desired results within the shortest possible time and space.

IX. ACKNOWLEDGEMENT

The authors are thankful to Mr. F. S. Benjamin for provision of data, data processing and supports.

REFERENCES

- [1] R. S. Austin and J. D. Rhoades. A compact, low-cost circuit for reading four-electrode salinity sensors. *Soil Sci. Soc. Am. J.* 43:808 – 809, 1979.
- [2] O. Banton, M. K. Seguin and M. A. Cimon. Mapping field-scale physical properties of soil with electrical resistivity. *Soil Sci. Soc. Am. J.* 61:1010 – 1017, 1997.
- [3] H. Bouwer. *Groundwater Hydrology*, McGraw-Hill, Kogakusha, Ltd. Tokyo, 1978.
- [4] M. O. Durham and R. A. Durham. Consequences and Standards from using Cathodic Protection Systems to Prevent Corrosion, *IEEE Industry Applications Magazine*, 41 - 47, 2005.
- [5] N. E. Edlefsen and A. B. C. Anderson. The four-electrode resistance method for measuring soil-moisture content under field conditions. *Soil Sci.* 51:367-376, 1941.
- [6] E. J. Ekott, E. J. Akpabio and U. I. Etukudo. Cathodic protection of buried steel oil pipeline in Niger Delta. *Environmental Research Journal.* 6(4): 304 – 307, 2012.
- [7] T. E. Gass. Installing Thermoplastic water well casing. *Water Well Journal* 31 (7): 34-35, 1977.
- [8] Gupta, S. C. and R. J. Hanks. 1972. Influence of water content on electrical conductivity of the soil. *Soil Sci. Soc. Am. Proc.* 36:855-857.
- [9] A. D. Halvorson and J. D. Rhoades. Field mapping soil conductivity to delineate dryland saline seeps with four-electrode technique. *Soil Sci. Soc. Am. J.* 40:571 - 574, 1976.
- [10] P. Kearey, M. Brooks and I. Hill. *An Introduction to Geophysical Exploration*, 3rd ed. T. J. International, Padstow, Cornwall, 2002.
- [11] E. W. Kelly. Geoelectric sounding for estimating aquifer hydraulic conductivity, *Ground Water.* 15: 420 – 424, 1977.
- [12] D. Kirkham and G. S. Taylor. Some tests of a four-electrode probe for soil moisture measurements. *Soil Sci. Soc. Proc.* 14:42 - 46, 1949.
- [13] W. Lowrie. *Fundamentals of Geophysics*. Cambridge University Press, Edinburgh, 1997.
- [14] C. Okoroafor. Cathodic protection as a means of saving national asset. *J. Corrosion Sci. Tech.*, 1: 1 – 6, 2004.
- [15] C. C. Plummer and D. McGeary. *Physical Geology*, 6th Ed. Wm.C. Brown Publishers, England, 1993.
- [16] M. Purcar and L. Bortels. Design and optimization of pipeline cathodic protection systems. *Fiscicula de Energetica*, 15: 289 – 294, 2009.
- [17] A. Rim-Rekeh and J. K. Awatefe. Investigation of soil corrosivity in the corrosion of low carbon steel pipe in soil environment. *J. Applied Sci. Res.* 2: 466 – 469, 2006.
- [18] E. A. Ritchie. Cathodic protection wells and groundwater pollution. *Ground Water* 14(3): 146 – 149, 1976.
- [19] K. C. Short and A. Stauble. *Outline of Geology of Niger Delta*, America Association of Petroleum Geologists Bull. 51: 761 – 779, 1967.
- [20] I. Tamunobereton-ari, E. D. Uko and V.B. Omubo-Pepple. Anthropogenic activities-Implications for groundwater resource in Okrika, Rivers State, Nigeria. *Research Journal of applied Sciences.* 5 (3): 204 – 211, 2010.
- [21] W. M. Telford, L. P. Geldart, P. E. Sheriff and D. A. Keys. *Applied Geophysics*, Cambridge University Press, London, 1978.
- [22] D. K. Todd. *Groundwater Hydrology*, John Wiley and Sons, Inc. New York, 1959.
- [23] H. Uhlig. *Corrosion and corrosion control*, 2nd Ed. John Wiley and Sons Inc. Canada, 1973.
- [24] A. A. R. Zohdy, L. A. Anderson and L. P. J. Muffler. Resistivity, self-potential, and induced polarization surveys of a vapor dominated geothermal system: *Geophysics*, 38, 1130 - 1144, 1973.

Efficient Ranking and Suggesting Popular Itemsets In Mobile Stores Using Fp Tree Approach

¹B.Sujatha Asst prof, ²Shaista Nousheen Asst.prof, ³Tasneem rahath Asst prof,
⁴ Nikhath Fatima Asst.prof

Abstract

We considered the problem of ranking the popularity of items and suggesting popular items based on user feedback. User feedback is obtained by iteratively presenting a set of suggested items, and users selecting items based on their own preferences either the true popularity ranking of items, and suggest true popular items. We consider FP tree approach with some modifications overcoming the complexity that has been seen in other randomized algorithms. The most effective feature of this approach is that it reduces the number of database scans and complexity.

I. INTRODUCTION

1.1 TERMINOLOGY:

In this section we first want to introduce the different terms that we were going to use in our paper as follows.

1.1.1 Ranking: Ranking is giving rank scores to the most popular item by taking user feedback. The most frequently occurring item is given the highest rank score.

1.1.2 Selection: We focus on the ranking of items where the only available information is the observed selection of items. In learning of the users preference over items, one may leverage some side information about items, but this is out of the scope of this paper.

1.1.3 Imitate: The user study was conducted in very famous mobile stores and which has been used to set of mobiles. The user may check the list and select the set of mobiles which they like most and depending on those like results the new suggestion list has been developed by the algorithm.

1.1.4 Popular: In practice, one may use prior information about item popularity. For example, in the survey the user may select the suggested mobile or they may also select the others. If they selected the already suggested items they will become more popular and if he don't they may get out of the popular list.

1.1.5 Association Rule: Association Rules are if/then statements that help uncover relationships between seemingly unrelated data in the relational database or other information repository. An example of an association rule would be **if a customer buys a nokia mobile, he is 70% interested in also purchasing nokia accessories.**

II. THEORETICAL STUDY

We consider the mobile phone selection and suggesting the best sold mobile and their combinations that were most liked by most of the users. Consider a set of mobiles $M: (m_1, m_2, m_3, m_4, \dots, m_n)$ where $n > 1$. Now we were calculating the set of items in C where were mostly sold and mostly liked by the users, as S

$S: (s_1, s_2, s_3, s_4, \dots, s_g)$ where $g > 1$.

We need to consider an item I , we interpret s_i as the portion of users that would select item i if suggestions were not made. We assume that the popularity rank scores s as follows:

- Items of set S were estimated to is as $s_1 \geq s_2 \geq s_3 \geq \dots, s_c$,
- s is completely normalized such that it is a probability distribution, i.e., $s_1 + s_2 + s_3 + \dots + s_c = 1$.
- s_i is always positive for all items i .

III. PROPOSED ALGORITHM AND STUDY

We have some of the systems already existing in the same field and we have also identified some of the disadvantages in them as follows:

- the popularity for any item is given based on the production of that item. This may not give good result because customers may not have the knowledge of true popularity they needed and depend on the results given by the producer.
- the updates are performed regardless of the true popularity by virtual analysis.
- Producer have to analyse things manually and complexity involves in this. Due to this time consumption may be high.
- the algorithms used in this system may fail to achieve true popularity.

We consider the problem learning of the popularity of items that is assumed to be unknown but has to be learned from the observed user's selection of items. We have selected a mobile market and mobile distribution outlets as our data set and examined them completely in all areas where we can give the list of items suggested by the users and we have made web-application to make an survey at real-time and considered the data given by more that 1000 members of different categories of people and applied our proposed Fp tree approach on the set of data and started suggesting the item in the mobile outlets for the actual users, which had helped the mobile phone companies and also the outlet in-charges. We have implemented the same in some of the mobile outlets in INDIA where we got very good results. The actual goal of the system is to efficiently learn the popularity of items and suggest the popular items to users. This was done to the user to suggest them the mostly used mobiles and their accessories, such that they also buy the best and at the same time the outlet owner will also get benefited. The most important feature in our project is suggesting the users by refreshing the latest results every time the user gives the input and changes his like list.

Now we have overcome many of the disadvantages of the existing systems and achieved many advantages with the proposed algorithm and method as follows:

- In our approach, we consider the problem of ranking the popularity of items and suggesting popular items based on user feedback.
- User feedback is obtained by iteratively presenting a set of suggested items, and users selecting items based on their own preferences either from this suggestion set or from the set of all possible items.
- The goal is to quickly learn the true popularity ranking of items and suggest true popular items.
- In this system better algorithms are used. The algorithms use ranking rules and suggestion rules in order to achieve true popularity.

IV. PROPOSED APPROACHFP-TREE

Like most traditional studies in association mining, we define the frequent pattern mining problem as follows. Definition 1 (Frequent pattern) Let $I = \{a_1, a_2, \dots, a_m\}$ be a set of items, and a transaction database $DB = \{T_1, T_2, \dots, T_n\}$, where T_i ($i \in [1:n]$) is a transaction which contains a set of items in I . The support (or occurrence frequency) of a pattern A , which is a set of items, is the number of transactions containing A in DB . A , is a frequent pattern if A 's support is no less than a predefined minimum support threshold, σ . Given a transaction database DB and a minimum support threshold, σ , the problem of finding the complete set of frequent patterns is called the frequent pattern mining problem.

2.1 Frequent Pattern Tree

To design a compact data structure for efficient frequent pattern mining, let's first examine a tiny example. Example 1 Let the transaction database, DB , be (the first two columns of) Table 1 and the minimum support threshold be 3.

TID	Items bought	(Ordered)frequent items
100	f, a, c, d, g, i,m,p	f, c, a,m, p
200	a, b, c, f, l,m,o	f, c, a, b,m
300	b, f, h, j,o	f, b
400	b, c, k, s,p	c, b, p
500	a, f, c, e, l, p,m,n	f, c, a,m, p

A compact data structure can be designed based on the following observations:

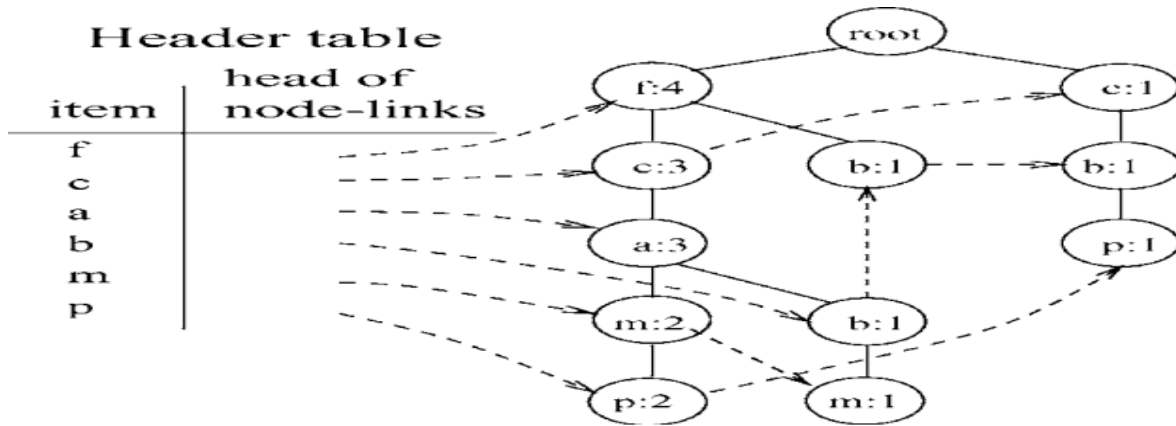
- [1]. Since only the frequent items will play a role in the frequent-pattern mining, it is necessary to perform one scan of transaction database *DB* to identify the set of frequent items (with *frequency count* obtained as a by-product).
- [2]. If the *set* of frequent items of each transaction can be stored in some compact structure, it may be possible to avoid repeatedly scanning the original transaction database.
- [3]. If multiple transactions share a set of frequent items, it may be possible to merge the shared sets with the number of occurrences registered as *count*. It is easy to check whether two sets are identical if the frequent items in all of the transactions are listed according to a fixed order.
- [4]. If two transactions share a common prefix, according to some sorted order of frequent items, the shared parts can be merged using one prefix structure as long as the *count* is registered properly. If the frequent items are sorted in their *frequency descending order*, there are better chances that more prefix strings can be shared. With the above observations, one may construct a frequent-pattern tree as follows.

First, a scan of *DB* derives a *list* of frequent items, $_f:4, (c:4), (a:3), (b:3), (m:3), (p:3)$ (the number after “:” indicates the support), in which items are ordered in frequency descending order. This ordering is important since each path of a tree will follow this order. For convenience of later discussions, the frequent items in each transaction are listed in this ordering in the rightmost column of Table 1. Second, the root of a tree is created and labeled with “*null*”. The FP-tree is constructed as follows by scanning the transaction database *DB* the second time.

- [1]. The scan of the first transaction leads to the construction of the first branch of the tree:
- [2]. $_f:1, (c:1), (a:1), (m:1), (p:1)$. Notice that the frequent items in the transaction are listed according to the order in the *list* of frequent items.
- [3]. For the second transaction, since its (ordered) frequent item list $_f, c, a, b, m$ shares a
- [4]. common prefix $_f, c, a$ with the existing path $_f, c, a, m, p$, the count of each node along the prefix is incremented by 1, and one new node $(b:1)$ is created and linked as a child of $(a:2)$ and another new node $(m:1)$ is created and linked as the child of $(b:1)$.
- [5]. For the third transaction, since its frequent item list $_f, b$ shares only the node $_f$ with
- [6]. the *f*-prefix subtree, *f*'s count is incremented by 1, and a new node $(b:1)$ is created and linked as a child of $(f:3)$.
- [7]. The scan of the fourth transaction leads to the construction of the second branch of the tree, $_(c:1), (b:1), (p:1)$.
- [8]. For the last transaction, since its frequent item list $_f, c, a, m, p$ is identical to the first one, the path is shared with the count of each node along the path incremented by 1.
- [9]. To facilitate tree traversal, an item header table is built in which each item points to its first occurrence in the tree via a node-link. Nodes with the same item-name are linked in sequence via such *node-links*. After scanning all the transactions, the tree, together with the associated node-links, are shown in figure 1.

Based on this example, a *frequent-pattern tree* can be designed as follows. *Definition 1 (FP-tree)*. A *frequent-pattern tree* (or *FP-tree* in short) is a tree structure defined below.

- [1]. It consists of one root labeled as “*null*”, a set of item-prefix sub trees as the children of the root, and a frequent-item-header table.
- [2]. Each node in the item-prefix sub tree consists of three fields: *item-name*, *count*, and *node-link*, where *item-name* registers which item this node represents, *count* registers the number of transactions represented by the portion of the path reaching this node, and



node-link links to the next node in the FP-tree carrying the same item-name, or null if there is none.

[3] Each entry in the frequent-item-header table consists of two fields, (1) *item-name* and (2) *head of node-link* (a pointer pointing to the first node in the FP-tree carrying the *item-name*).Based on this definition, we have the following FP-tree construction algorithm.

Algorithm 1 (FP-tree construction).

Input: A transaction database *DB* and a minimum support threshold ζ .

Output: FP-tree, the frequent-pattern tree of *DB*.

Method: The FP-tree is constructed as follows.

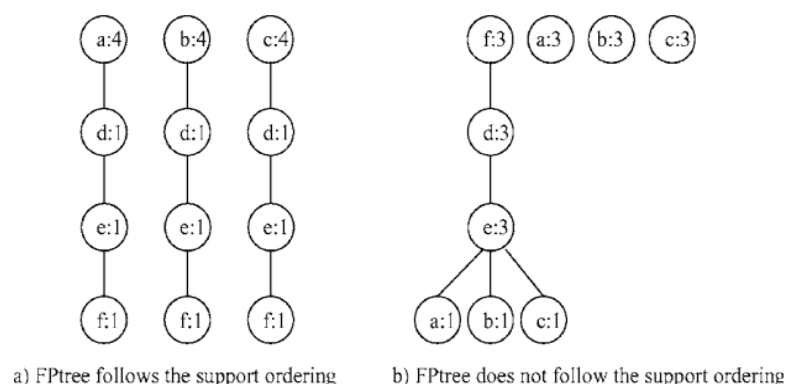
1. Scan the transaction database *DB* once. Collect *F*, the set of frequent items, and the support of each frequent item. Sort *F* in support-descending order as *FList*, the list of frequent items.
2. Create the root of an FP-tree, *T*, and label it as “null”. For each transaction *Trans* in *DB* do the following. Select the frequent items in *Trans* and sort them according to the order of *FList*. Let the sorted frequent-item list in *Trans* be $[p | P]$, where *p* is the first element and *P* is theremaining list. Call *insert tree*($[p | P], T$). The function *insert tree*($[p | P], T$) is performed as follows. If *T* has a child *N* such that *N.item-name* = *p.item-name*, then increment *N*'s count by 1; else create a new node *N*, with its count initialized to 1, its parent link linked to *T*, and its node-link linked to the nodes with the same *item-name* via the node-link structure. If *P* is nonempty, call *inserttree*(*P*, *N*) recursively. Analysis. The FP-tree construction takes exactly two scans of the transaction database: The first scan collects the set of frequent items, and the second scan constructs the FP-tree. The cost of inserting a transaction *Trans* into the FP-tree is $(|freq(Trans)|)$, where *freq*(*Trans*) is the set of frequent items in *Trans*. We will show that the FP-tree contains the complete information for frequent-pattern mining.

Completeness and compactness of FP-tree

There are several important properties of FP-tree that can be derived from the FP-tree construction process. Given a transaction database *DB* and a support threshold ζ . Let *F* be the frequent items in *DB*. For each transaction *T*, *freq*(*T*) is the set of frequent items in *T*, i.e., $freq(T) = T \cap F$, and is called the *frequent item projection* of transaction *T*. According to the *Apriori* principle, the set of frequent item projections of transactions in the database is sufficient for mining the complete set of frequent patterns, because an infrequent item plays no role in frequent patterns.

Lemma 1. *Given a transaction database DB and a support threshold ζ , the complete set of frequent item projections of transactions in the database can be derived from DB's FP-tree.* Rationale. Based on the FP-tree construction process, for each transaction in the *DB*, its frequent item projection is mapped to one path in the FP-tree. For a path $a_1 a_2 \dots a_k$ from the root to a node in the FP-tree, let *c_{ak}* be the count at the node labeled *ak* and *c_{_ak}* be the sum of counts of children nodes of *ak*. Then, according to the construction of the FP-tree, the path registers frequent item projections of $c_{ak} - c_{_ak}$ transactions. Therefore, the FP-tree registers the complete set of frequent item projections without duplication. Based on this lemma, after an FP-tree for *DB* is constructed, it contains the complete information for mining frequent patterns from the transaction database. Thereafter, only the FP-tree is needed in the remaining mining process, regardless of the number and length of the frequent patterns.

Lemma 2. Given a transaction database DB and a support threshold ξ . Without considering the (null) root, the size of an FP-tree is bounded by $\sum_{T \in DB} |freq(T)|$, and the height of the tree is bounded by $\max_{T \in DB} \{|freq(T)|\}$, where $freq(T)$ is the frequent item projection of transaction T . Rationale. Based on the FP-tree construction process, for any transaction T in DB , there exists a path in the FP-tree starting from the corresponding item prefix subtree so that the set of nodes in the path is exactly the same set of frequent items in T . The root is the only extra node that is not created by frequent-item insertion, and each node contains one node-link and one count. Thus we have the bound of the size of the tree stated in the Lemma. The height of any p -prefix subtree is the maximum number of frequent items in any transaction with p appearing at the head of its frequent item list. Therefore, the height of the tree is bounded by the maximal number of frequent items in any transaction in the database, if we do not consider the additional level added by the root. Lemma 2.2 shows an important benefit of FP-tree: the size of an FP-tree is bounded by the size of its corresponding database because each transaction will contribute at most one path to the FP-tree, with the length equal to the number of frequent items in that transaction. Since there are often a lot of sharings of frequent items among transactions, the size of the tree is usually much smaller than its original database. Unlike the *Apriori*-like method which may generate an exponential number of candidates in the worst case, under no circumstances, may an FP-tree with an exponential number of nodes be generated. FP-tree is a highly compact structure which stores the information for frequent-pattern mining. Since a single path " $a_1 \rightarrow a_2 \rightarrow \dots \rightarrow a_n$ " in the a_1 -prefix subtree registers all the transactions whose maximal frequent set is in the form of " $a_1 \rightarrow a_2 \rightarrow \dots \rightarrow a_k$ " for any $1 \leq k \leq n$, the size of the FP-tree is substantially smaller than the size of the database and that of the candidate sets generated in the association rule mining. The items in the frequent item set are ordered in the support-descending order: More frequently occurring items are more likely to be shared and thus they are arranged closer to the top of the FP-tree. This ordering enhances the compactness of the FP-tree structure. However, this does not mean that the tree so constructed *always* achieves the maximal compactness. With the knowledge of particular data characteristics, it is sometimes possible to achieve even better compression than the frequency-descending ordering. Consider the following example. Let the set of transactions be: $\{adef, bdef, cdef, a, a, a, b, b, b, c, c, c\}$, and the minimum support threshold be 3. The frequent item set associated with support count becomes $\{a:4, b:4, c:4, d:3, e:3, f:3\}$. Following the item frequency ordering $a \rightarrow b \rightarrow c \rightarrow d \rightarrow e \rightarrow f$, the FP-tree constructed will contain 12 nodes, as shown in figure 2(a). However, following another item ordering $f \rightarrow d \rightarrow e \rightarrow a \rightarrow b \rightarrow c$, it will contain only 9 nodes, as shown in figure 2(b). The compactness of FP-tree is also verified by our experiments. Sometimes a rather small FP-tree is resulted from a quite large database. For example, for the database *Connect-4* used in *MaxMiner* (Bayardo, 1998), which contains 67,557 transactions with 43 items in each transaction, when the support threshold is 50% (which is used in the *MaxMiner* experiments (Bayardo, 1998)), the total number of occurrences of frequent items is 2,219,609, whereas the total number of nodes in the FP-tree is 13,449 which represents a reduction ratio of 165.04, while it still holds hundreds of thousands of frequent patterns! (Notice that for databases with mostly short transactions, the reduction ratio is not that high.)



Therefore, it is not surprising some gigabyte transaction database containing many long patterns may even generate an FP-tree that fits in main memory. Nevertheless, one cannot assume that an FP-tree can always fit in main memory no matter how large a database is. Methods for highly scalable *FP-growth* mining will be discussed in Section 5.

4.1 Mining frequent patterns using FP-tree: Construction of a compact FP-tree ensures that subsequent mining can be performed with a rather compact data structure. However, this does not automatically guarantee that it will be highly efficient since one may still encounter the combinatorial problem of candidate generation if one simply uses this FP-tree to generate and check all the candidate patterns. In this section, we study how to explore the compact information stored in an FP-tree, develop the principles of frequent-pattern growth by examination of our running example, explore how to perform further optimization when there exists a single prefix path in an FP-tree, and propose a frequent-pattern growth algorithm, *FP-growth*, for mining the *complete set of frequent patterns* using FP-tree. **4.1.1 Principles of frequent-pattern growth for FP-tree mining** In this subsection, we examine some interesting properties of the FP-tree structure which will facilitate frequent-pattern mining.

Property 1 (Node-link property). For any frequent item a_i , all the possible patterns containing only frequent items and a_i can be obtained by following a_i 's node-links, starting from a_i 's head in the FP-tree header. This property is directly from the FP-tree construction process, and it facilitates the access of all the frequent-pattern information related to a_i by traversing the FP-tree once following a_i 's node-links. To facilitate the understanding of other properties of FP-tree related to mining, we first go through an example which performs mining on the constructed FP-tree (figure 1) in Example 1. *Example 2.* Let us examine the mining process based on the constructed FP-tree shown in figure 1. Based on Property 3.1, all the patterns containing frequent items that a node a_i participates can be collected by starting at a_i 's node-link head and following its node-links.

We examine the mining process by starting from the bottom of the node-link header table. For node p , its immediate frequent pattern is $(p:3)$, and it has two paths in the FP-tree: $_f:4, c:3, a:3, m:2, p:2_$ and $_c:1, b:1, p:1_$. The first path indicates that string “ (f, c, a, m, p) ” appears twice in the database. Notice the path also indicates that string $_f, c, a_$ appears three times and $_f_$ itself appears even four times. However, they only appear twice *together* with p . Thus, to study which string appear together with p , only p 's prefix path $_f:2, c:2, a:2, m:2_$ (or simply, $_f\ cam:2_$) counts. Similarly, the second path indicates string “ (c, b, p) ” appears once in the set of transactions in *DB*, or p 's prefix path is $_cb:1_$. These two prefix paths of p , “ $\{(f\ cam:2), (cb:1)\}$ ”, form p 's subpattern-base, which is called p 's conditional pattern base (i.e., the subpattern-base under the condition of p 's existence). Construction of an FP-tree on this conditional pattern-base (which is called p 's conditional FP-tree) leads to only one branch ($c:3$). Hence, only one frequent pattern ($cp:3$) is derived. (Notice that a pattern is an itemset and is denoted by a string here.) The search for frequent patterns associated with p terminates. For node m , its immediate frequent pattern is $(m:3)$, and it has two paths, $_f:4, c:3, a:3, m:2_$ and $_f:4, c:3, a:3, b:1, m:1_$. Notice p appears together with m as well, however, there is no need to include p here in the analysis since any frequent patterns involving p has been analyzed in the previous examination of p . Similar to the above analysis, m 's conditional pattern-base is $\{(fca:2), (fcab:1)\}$. Constructing an FP-tree on it, we derive m 's conditional FP-tree, $_f:3, c:3, a:3_$, a single frequent pattern path, as shown in figure 3. This conditional FP-tree is then mined recursively by calling $mine(_f:3, c:3, a:3_ | m)$. Figure 3 shows that “ $mine(_f:3, c:3, a:3_ | m)$ ” involves mining three items (a), (c), (f) in sequence. The first derives a frequent pattern ($am:3$), a conditional pattern-base $\{(f:3)\}$, and then a call “ $mine(_f:3, c:3_ | am)$ ”; the second derives a frequent pattern ($cm:3$), a conditional pattern-base $\{(f:3)\}$, and then a call “ $mine(_f:3_ | cm)$ ”; and the third derives only a frequent pattern ($fm:3$). Further recursive call of “ $mine(_f:3, c:3_ | am)$ ” derives two patterns ($cam:3$) and ($fam:3$), and a conditional pattern-base $\{(f:3)\}$, which then leads to a call “ $mine(_f:3_ | cam)$ ”, that derives the longest pattern ($fcam:3$). Similarly, the call of “ $mine(_f:3_ | cm)$ ” derives one pattern ($fc:3$). Therefore, the set of frequent patterns involving m is $\{(m:3), (am:3), (cm:3), (fm:3), (cam:3), (fam:3), (fcam:3), (fc:3)\}$. This indicates that a single path FP-tree can be mined by outputting all the combinations of the items in the path. Similarly, node b derives $(b:3)$ and it has three paths: $_f:4, c:3, a:3, b:1_$, $_f:4, b:1_$, and $_c:1, b:1_$. Since b 's conditional pattern-base $\{(fca:1), (f:1), (c:1)\}$ generates no frequent item, the mining for b terminates. Node a derives one frequent pattern $\{(a:3)\}$ and one subpattern base $\{(f\ c:3)\}$, a single-path conditional FP-tree. Thus, its set of frequent pattern

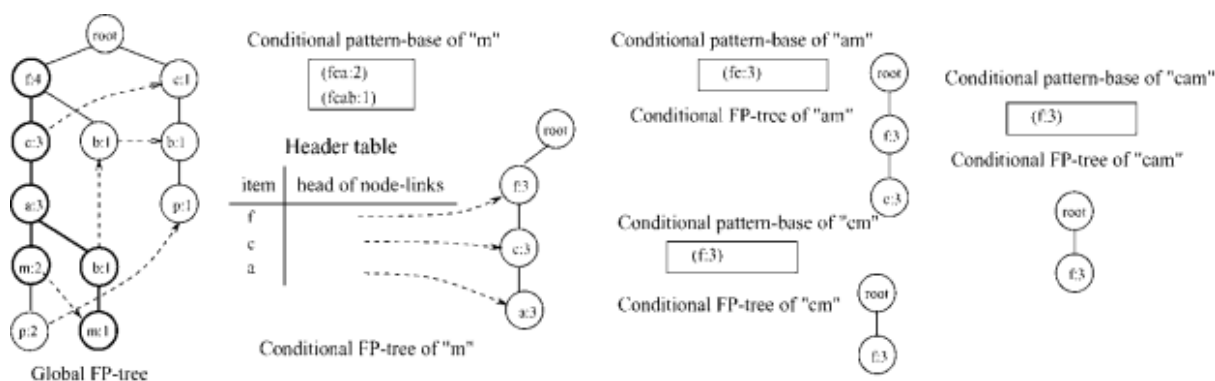


Table 2. Mining frequent patterns by creating conditional (sub)pattern-bases.

Item	Conditional pattern-base	Conditional FP-tree
P	{(fcam:2), (cb:1)}	{(c:3)} p
M	{(fca:2), (fcab:1)}	{(f:3, c:3, a:3)} m
b	{(fca:1), (f:1), (c:1)}	∅
a	{(fc:3)}	{(f:3, c:3)} a
c	{(f:3)}	{(f:3)} c
f	∅	∅

can be generated by taking their combinations. Concatenating them with (a:3), we have {(f a:3), (ca:3), (fca:3)}. Node c derives (c:4) and one subpattern-base {(f:3)}, and the set of frequent patterns associated with (c:3) is {(fc:3)}. Node f derives only (f:4) but no conditional pattern-base. The conditional pattern-bases and the conditional FP-trees generated are summarized in Table 2. The correctness and completeness of the process in Example 2 should be justified. This is accomplished by first introducing a few important properties related to the mining process.

Property 2 (Prefix path property). To calculate the frequent patterns with suffix ai , only the prefix subpaths of nodes labeled ai in the FP-tree need to be accumulated, and the frequency count of every node in the prefix path should carry the same count as that in the corresponding node ai in the path. Rationale. Let the nodes along the path P be labeled as a_1, \dots, a_n in such an order that a_1 is the root of the prefix subtree, a_n is the leaf of the subtree in P , and ai ($1 \leq i \leq n$) is the node being referenced. Based on the process of FP-tree construction presented in Algorithm 1, for each prefix node ak ($1 \leq k < i$), the prefix subpath of the node ai in P occurs together with ak exactly $ai.count$ times. Thus every such prefix node should carry the same count as node ai . Notice that a postfix node am (for $i < m \leq n$) along the same path also co-occurs with node ai . However, the patterns with am will be generated when examining the suffix node am , enclosing them here will lead to redundant generation of the patterns that would have been generated for am . Therefore, we only need to examine the prefix subpath of ai in P . For example, in Example 2, node m is involved in a path $_f:4, c:3, a:3, m:2, p:2$, to calculate the frequent patterns for node m in this path, only the prefix subpath of node m , which is $_f:4, c:3, a:3$, need to be extracted, and the frequency count of every node in the prefix path should carry the same count as node m . That is, the node counts in the prefix path should be adjusted to $_f:2, c:2, a:2$. Based on this property, the prefix subpath of node ai in a path P can be copied and transformed into a count-adjusted prefix subpath by adjusting the frequency count of every node in the prefix subpath to the same as the count of node ai . The prefix path so transformed is called the *transformed prefix path* of ai for path P . Notice that the set of transformed prefix paths of ai forms a small database of patterns which co-occur with ai . Such a database of patterns occurring with ai is called ai 's *conditional pattern-base*, and is denoted as "pattern base | ai ". Then one can compute all the frequent patterns associated with ai in this ai -conditional pattern-base by creating a small FP-tree, called ai 's *conditional FP-tree* and denoted as "FP-tree | ai ". Subsequent mining can be performed on this small conditional FP-tree. The processes of construction of conditional pattern-bases and conditional FP-trees have been demonstrated in Example 2. This process is performed recursively, and the frequent patterns can be obtained by a pattern-growth method, based on the following lemmas and corollary.

Lemma 1 (Fragment growth). Let α be an itemset in DB , B be α 's conditional patternbase, and β be an itemset in B . Then the support of $\alpha \cup \beta$ in DB is equivalent to the support of β in B . Rationale. According to the definition of conditional pattern-base, each (sub)transaction in B occurs under the condition of the occurrence of α in the original transaction database DB . If an itemset β appears in B ψ times, it appears with α in DB ψ times as well. Moreover, since all such items are collected in the conditional pattern-base of α , $\alpha \cup \beta$ occurs exactly ψ times in DB as well. Thus we have the lemma. From this lemma, we can directly derive an important corollary.

Corollary 1 (Pattern growth). Let α be a frequent itemset in DB , B be α 's conditional pattern-base, and β be an itemset in B . Then $\alpha \cup \beta$ is frequent in DB if and only if β is frequent in B . Based on Corollary 3.1, mining can be performed by first identifying the set of frequent 1-itemsets in DB , and then for each such frequent 1-itemset, constructing its conditional pattern-bases, and mining its set of frequent 1-itemsets in the conditional pattern-base, and so on. This indicates that the process of mining frequent patterns can be viewed as first mining frequent 1-itemset and then progressively growing each such itemset by mining its conditional pattern-base, which can in turn be done similarly. By doing so, a frequent k -itemset mining problem is successfully transformed into a sequence of k frequent 1-itemset mining problems via a set of conditional pattern-bases. Since mining is done by pattern growth, there is no need to generate any candidate sets in the entire mining process. Notice also in the construction of a new FP-tree from a conditional pattern-base obtained during the mining of an FP-tree, the items in the frequent itemset should be ordered in the frequency descending order of node occurrence of each item instead of its support (which represents item occurrence). This is because each node in an FP-tree may represent many occurrences of an item but such a node represents a single unit (i.e., the itemset whose elements always occur together) in the construction of an item-associated FP-tree.

3.2. Frequent-pattern growth with single prefix path of FP-tree

The frequent-pattern growth method described above works for all kinds of FP-trees. However, further optimization can be explored on a special kind of FP-tree, called *single prefixpathFP-tree*, and such an optimization is especially useful at mining long frequent patterns. A single prefix-path FP-tree is an FP-tree that consists of only a single path or a single prefix path stretching from the root to the first branching node of the tree, where a *branching node* is a node containing more than one child. Let us examine an example.

Example 3. Figure 4(a) is a single prefix-path FP-tree that consists of one prefix path, $_ (a:10) \rightarrow (b:8) \rightarrow (c:7) _$, stretching from the root of the tree to the first branching node $(c:7)$. Although it can be mined using the frequent-pattern growth method described above, a better method is to split the tree into two fragments: the single prefix-path, $_ (a:10) \rightarrow (b:8) \rightarrow (c:7) _$, as shown in figure 4(b), and the multipath part, with the root replaced by a pseudoroot R , as shown in figure 4(c). These two parts can be mined separately and then combined together. Let us examine the two separate mining processes. All the frequent patterns associated with the first part, the single prefix-path $P = _ (a:10) \rightarrow (b:8) \rightarrow (c:7) _$, can be mined by enumeration of all the combinations of the subpaths of P with the support set to the minimum support of the items contained in the subpath. This is because each such subpath is distinct and occurs the same number of times as the *minimum occurrence frequency among the items in the subpath* which is equal to the support of the last item in the subpath. Thus, path P generates the following set of frequent patterns, $freq\ pattern\ set(P) = \{(a:10), (b:8), (c:7), (ab:8), (ac:7), (bc:7), (abc:7)\}$. Let Q be the second FP-tree (figure 4(c)), the multipath part rooted with R . Q can be mined as follows. First, R is treated as a null root, and Q forms a multipath FP-tree, which can be mined using a typical frequent-pattern growth method. The mining result is: $freq\ pattern\ set(Q) = \{(d:4), (e:3), (f:3), (df:3)\}$. Figure

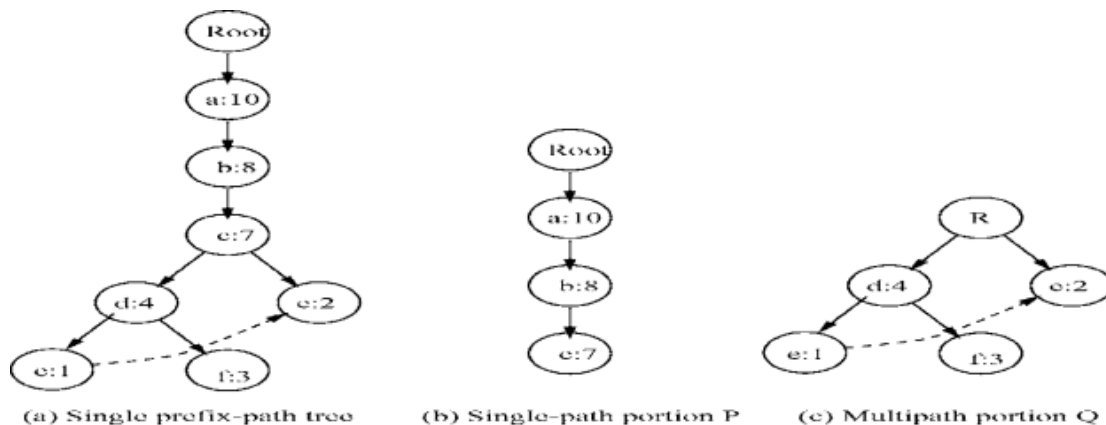


Figure 4. Mining an FP-tree with a single prefix path.

Second, for each frequent itemset in Q , R can be viewed as a conditional frequent pattern-base, and each itemset in Q with each pattern generated from R may form a distinct frequent pattern. For example, for $(d:4)$ in $freq\ pattern\ set(Q)$, P can be viewed as its conditional pattern-base, and a pattern generated from P , such as $(a:10)$, will generate with it a new frequent itemset, $(ad:4)$, since a appears together with d at most four times. Thus, for $(d:4)$ the set of frequent patterns generated will be $(d:4) \times freq\ pattern\ set(P) = \{(ad:4), (bd:4), (cd:4), (abd:4), (acd:4), (bcd:4), (abcd:4)\}$, where $X \times Y$ means that every pattern in X is combined with everyone in Y to form a “cross-product-like” larger itemset with the support being the minimum support between the two patterns. Thus, the complete set of frequent patterns generated by combining the results of P and Q will be $freq\ pattern\ set(Q) \times freq\ pattern\ set(P)$, with the support being the support of the itemset in Q (which is always no more than the support of the itemset from P). In summary, the set of frequent patterns generated from such a single prefix path consists of three distinct sets: (1) $freq\ pattern\ set(P)$, the set of frequent patterns generated from the single prefix-path, P ; (2) $freq\ pattern\ set(Q)$, the set of frequent patterns generated from the multipath part of the FP-tree, Q ; and (3) $freq\ pattern\ set(Q) \times freq\ pattern\ set(P)$, the set of frequent patterns involving both parts. We first show if an FP-tree consists of a single path P , one can generate the set of frequent patterns according to the following lemma.

Lemma 2 (Pattern generation for an FP-tree consisting of single path). Suppose an FP-tree T consists of a single path P . The complete set of the frequent patterns of T can be generated by enumeration of all the combinations of the subpaths of P with the support being the minimum support of the items contained in the subpath. Rationale. Let the single path P of the FP-tree be $_a1:s1 \rightarrow a2:s2 \rightarrow \dots \rightarrow ak :sk$. Since the FP-tree contains a single path P , the support frequency s_i of each item a_i (for $1 \leq i \leq k$) is the frequency of a_i co-occurring with its prefix string. Thus, any combination of the items in the path, such as $_a1, \dots, a_j$ (for $1 \leq i, j \leq k$), is a frequent pattern, with their cooccurrence frequency being the minimum support among those items. Since every item in each path P is unique, there is no redundant pattern to be generated with such a combinational generation. Moreover, no frequent patterns can be generated outside the FP-tree. Therefore, we have the lemma. We then show if an FP-tree consists of a single prefix-path, the set of frequent patterns can be generated by splitting the tree into two according to the following lemma.

Lemma 3 (Pattern generation for an FP-tree consisting of single prefix path). Suppose an FP-tree T , similar to the tree in figure 4(a), consists of (1) a single prefix path P , similar to the tree P in figure 4(b), and (2) the multipath part, Q , which can be viewed as an independent FP-tree with a pseudo-root R , similar to the tree Q in figure 4(c). The complete set of the frequent patterns of T consists of the following three portions:

1. The set of frequent patterns generated from P by enumeration of all the combinations of the items along path P , with the support being the minimum support among all the items that the pattern contains.
2. The set of frequent patterns generated from Q by taking root R as “null.”
3. The set of frequent patterns combining P and Q formed by taken the cross-product of the frequent patterns engerated from P and Q , denoted as $freq\ pattern\ set(P) \times freq\ pattern\ set(Q)$, that is, each frequent itemset is the union of one frequent itemset from P and one from Q and its support is the minimum one between the supports of the two itemsets. Rationale. Based on the FP-tree construction rules, each node a_i in the single prefix path of the FP-tree appears only once in the tree. The single prefix-path of the FP-tree forms a new FP-tree P , and the multipath part forms another FP-tree Q . They do not share nodes representing the same item. Thus, the two FP-trees can be mined separately. First, we show that each pattern generated from one of the three portions by lloving the pattern generation rules is distinct and frequent. According to Lemma 3.2, each pattern generated from P , the FP-tree formed by the single prefix-path, is distinct and frequent. The set of frequent patterns generated from Q by taking root R as “null” is also distinct and frequent since such patterns exist without combining any items in their conditional databases (which are in the items in P). The set of frequent patterns generated by combining P and Q , that is, taking the cross-product of the frequent patterns generated from P and Q , with the support being the minimum one between the supports of the two itemsets, is also distinct and frequent. This is because each frequent pattern generated by P can be considered as a frequent pattern in the conditional pattern-base of a frequent item in Q , and whose support should be the minimum one between the two supports since this is the frequency that both patterns appear together. Second, we show that no patterns can be generated out of this three portions. Since according to Lemma 3.1, the FP-tree T without being split into two FP-trees P and Q generatesthe complete set of frequent patterns by pattern growth. Since each pattern generated from T will be generated from either the portion P or Q or their combination, the method generates the complete set of frequent patterns. *The frequent-pattern growth algorithm* Based on the above lemmas and properties, we have the following algorithm for mining frequent patterns using FP-tree.

Algorithm 2 (FP-growth: Mining frequent patterns with FP-tree by pattern fragment growth).

Input: A database DB , represented by FP-tree constructed according to Algorithm 1, and a minimum support threshold ξ .

Output: The complete set of frequent patterns.68 HAN ET AL.

Method: call *FP-growth*(FP-tree, null).

Procedure *FP-growth*(Tree, α)

```

{
(1) if Tree contains a single prefix path // Mining single prefix-path FP-tree
(2) then {
(3) let P be the single prefix-path part of Tree;
(4) let Q be the multipath part with the top branching node replaced by a null root;
(5) for each combination (denoted as  $\beta$ ) of the nodes in the path P do
(6) generate pattern  $\beta \cup \alpha$  with support = minimum support of nodes in  $\beta$ ;
(7) let freq pattern set(P) be the set of patterns so generated; }
(8) else let Q be Tree;
(9) for each item  $ai$  in Q do { // Mining multipath FP-tree
(10) generate pattern  $\beta = ai \cup \alpha$  with support =  $ai$ .support;
(11) construct  $\beta$ 's conditional pattern-base and then  $\beta$ 's conditional FP-tree  $Tree\beta$ ;
(12) if  $Tree\beta = \emptyset$ 
(13) then call FP-growth( $Tree\beta$ ,  $\beta$ );
(14) let freq pattern set(Q) be the set of patterns so generated; }
(15) return(freq pattern set(P)  $\cup$  freq pattern set(Q)  $\cup$  (freq pattern set(P)
 $\times$ freq pattern set(Q)))
}

```

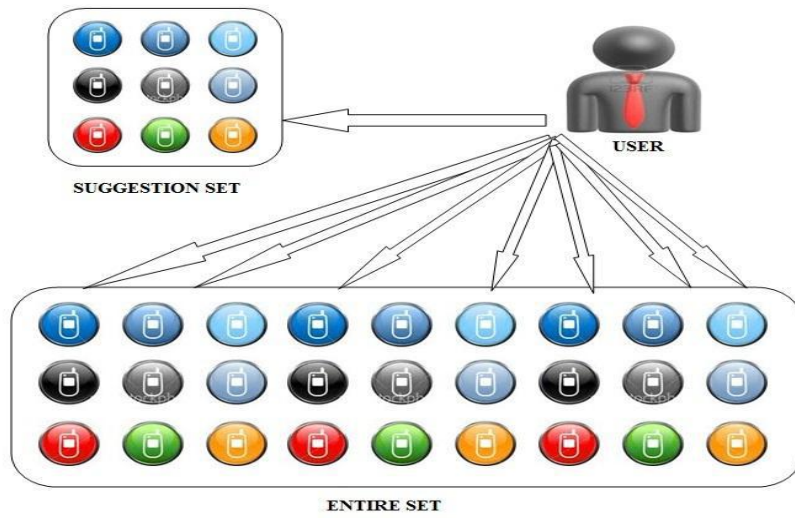
Analysis. With the properties and lemmas in Sections 2 and 3, we show that the algorithm correctly finds the complete set of frequent itemsets in transaction database *DB*. As shown in Lemma 2.1, FP-tree of *DB* contains the complete information of *DB* in relevance to frequent pattern mining under the support threshold ζ . If an FP-tree contains a single prefix-path, according to Lemma 3.3, the generation of the complete set of frequent patterns can be partitioned into three portions: the single prefix-path portion *P*, the multipath portion *Q*, and their combinations. Hence we have lines (1)-(4) and line (15) of the procedure. According to Lemma 3.2, the generated patterns for the single prefix path are the enumerations of the subpaths of the prefix path, with the support being the minimum support of the nodes in the subpath. Thus we have lines (5)-(7) of the procedure.

After that, one can treat the multipath portion or the FP-tree that does not contain the single prefix-path as portion *Q* (lines (4) and (8)) and construct conditional pattern-base and mine its conditional FP-tree for each frequent itemset ai . The correctness and completeness of the prefix path transformation are shown in Property 3.2. Thus the conditional pattern-bases store the complete information for frequent pattern mining for *Q*. According to Lemmas 3.1 and its corollary, the patterns successively grown from the conditional FP-trees are the set of sound and complete frequent patterns. Especially, according to the fragment growth property, the support of the combined fragments takes the support of the frequent itemsets generated in the conditional pattern-base. Therefore, we have lines (9)-(14) of the procedure. Line (15) sums up the complete result according to Lemma 3.3. Let's now examine the efficiency of the algorithm. The *FP-growth* mining process scans the FP-tree of *DB* once and generates a small pattern-base Bai for each frequent item ai , each consisting of the set of transformed prefix paths of ai . Frequent pattern mining is then recursively performed on the small pattern-base Bai by constructing a conditional FP-tree for Bai . As reasoned in the analysis of Algorithm 1, an FP-tree is usually much smaller than the size of *DB*. Similarly, since the conditional FP-tree, "FP-tree | ai ", is constructed on the pattern-base Bai , it should be usually much smaller and never bigger than Bai . Moreover, a pattern-base Bai is usually much smaller than its original FP-tree, because it consists of the transformed prefix paths related to only one of the frequent items, ai . Thus, each subsequent mining process works on a set of usually much smaller pattern-bases and conditional FP-trees. Moreover, the mining operations consist of mainly prefix count adjustment, counting local frequent items, and pattern fragment concatenation. This is much less costly than generation and test of a very large number of candidate patterns. Thus the algorithm is efficient.

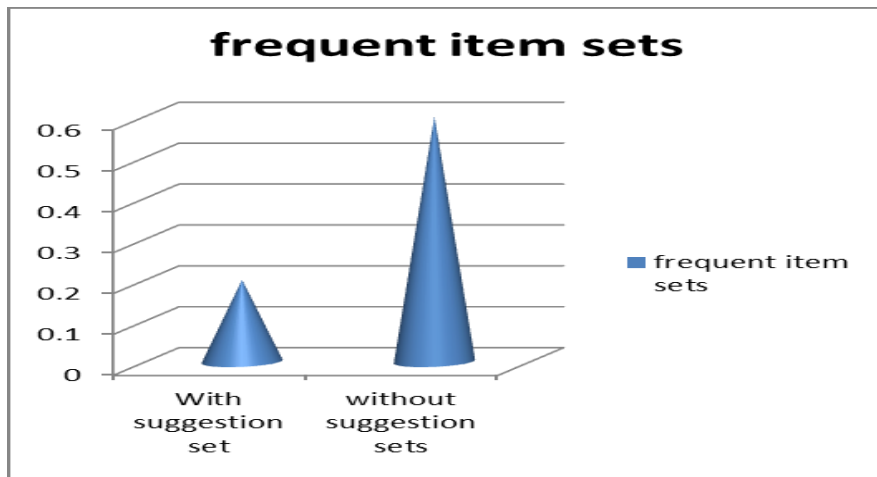
From the algorithm and its reasoning, one can see that the *FP-growth* mining process is a divide-and-conquer process, and the scale of shrinking is usually quite dramatic. If the shrinking factor is around 20-100 for constructing an FP-tree from a database, it is expected to be another hundreds of times reduction for constructing each conditional FP-tree from its already quite small conditional frequent pattern-base. Notice that even in the case that a database may generate an exponential number of frequent patterns, the size of the FP-tree is usually quite small and will never grow exponentially. For example, for a frequent pattern of length 100, " a_1, \dots, a_{100} ", the FP-tree construction results in only one path of length 100 for it, possibly " $_a_1, \rightarrow \dots \rightarrow a_{100}_$ " (if the items are ordered in the list of frequent items as a_1, \dots, a_{100}). The *FP-growth* algorithm will still generate about 1030 frequent patterns (if time permits!!), such as " $a_1, a_2, \dots, a_1a_2, \dots, a_1a_2a_3, \dots, a_1 \dots a_{100}$." However, the FP-tree contains only one frequent pattern path of 100 nodes, and according to Lemma 3.2, there is even no need to construct any conditional FP-tree in order to find all the patterns.

V. RESULTS

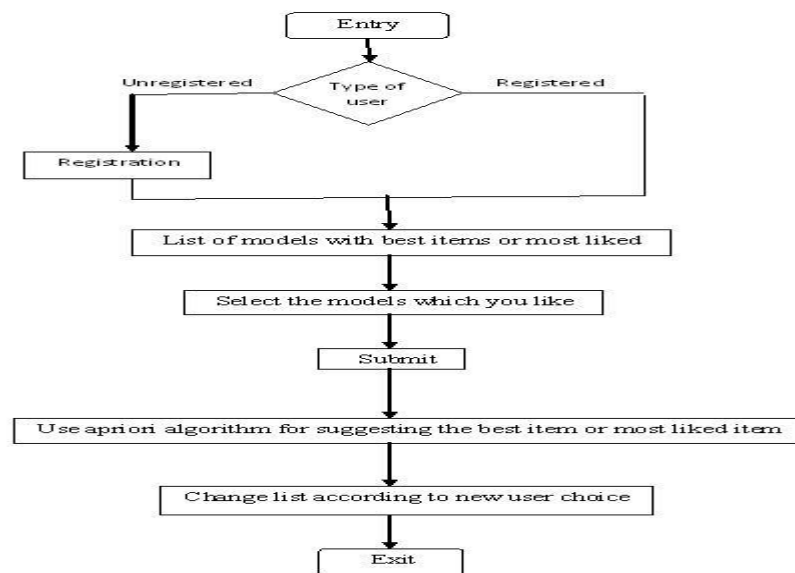
The above is the best method of ranking and suggesting the best methods in the scenario of mobile phone outlets in INDIA, which is shown in the following diagram:



As it was shown in the above diagram we were going to take the most liked items from the users and suggesting the best mobiles or the best set of suggestions that the most of the users liked or ordered.



The confidence of the suggestions were also proved by an traditional confidence calculations as follows In this section we are going to discuss about algorithms. Till now we have discussed some ranking rules , suggestion rules and Frequency move2set algorithm. We have some problems with these, so we go for an algorithm which suits our requirements well. The algorithm is Apriori algorithm. In order to know these algorithms we need to know some concepts of data mining.



Frequent itemsets: Let $I = \{I_1, I_2, I_3, \dots, I_m\}$ be a set of items. Let D , the task-relevant data, be a set of database transactions where each transaction T is a set of items such that T is a subset of I . Each transaction is associated with an identifier, called TID. Let A be a set of items. A transaction T is said to contain A if and only if A is a subset of T . An association rule is an implication of the form $A \rightarrow B$, where A is subset of I , B is subset of I and $A \cap B = \emptyset$. The rule $A \rightarrow B$ holds in the transaction set D with support s , where s is the percentage of transactions in D that contain $A \cup B$. This is taken to be the probability, $P(A \cup B)$. The rule $A \rightarrow B$ has confidence c in the transaction set D , where c is the percentage of transactions in D containing A that also contain B . This is taken to be the conditional probability, $P(B/A)$. That is, $\text{Support}(A \rightarrow B) = P(A \cup B)$ $\text{Confidence}(A \rightarrow B) = P(B/A)$ Rules that satisfy both a minimum support threshold (min_sup) and a minimum confidence threshold (min_conf) are called strong. The occurrence frequency of an itemset is the number of transactions that contain the itemset. This is also known, simply as the frequency, support count, or count of the itemset. The set of frequent k -itemset is commonly denoted by L_k . $\text{confidence}(A \rightarrow B) = P(A \cup B) / \text{support}(A) = \text{supportcount}(A \cup B) / \text{supportcount}(A)$.

Mining frequent itemsets: In general, association rule mining can be viewed as a two-step process: 1. Finding all frequent itemsets: By definition, each of these itemsets will occur at least as frequently as a predetermined minimum support count, min_sup . 2. Generate strong association rules from the frequent itemsets: By definition, these rules must satisfy minimum support and minimum confidence

VI. CONCLUSION

All the previous process already proposed were very complex and contains very complicated computations which made the ranking and suggesting the best and popular items have been more and more complex and not getting to the actual end users. Now we have proposed as very simple randomized algorithm for ranking and suggesting popular items designed to account for popularity bias. This was utilized by many of the mobile outlets in the country successfully.

REFERENCES

- [1]. Huidrom Romesh Chandra Singh, T. kalaikumar, Dr. S. Karthik, Suggestion of True Popular Items, IJCSE, 2010.
- [2]. Y.Maanasa, V.Kumar, P.Satish Babu, Framework for suggesting POPULAR ITEMS to users by Analyzing Randomized Algorithms, IJCTA, 2011.
- [3]. V. Anantharam, P. Varaiya, and J. Walrand, —Asymptotically Efficient Allocation Rules for the Multiarmed Bandit Problem with Multiple Plays—Part i: i.i.d. Rewards, I IEEE Trans. Automatic Control, vol. 32, no. 11, pp. 968-976, Nov. 1987.
- [4]. J.R. Anderson, —The Adaptive Nature of Human Categorization I Psychological Rev., vol. 98, no. 3, pp. 409-429, 1991.
- [5]. Yanbin Ye, Chia-Chu Chiang, A Parallel Apriori Algorithm for Frequent Itemsets Mining, IEEE, 2006.
- [6]. Cong-Rui Ji, Zhi-Hong Deng, Mining Frequent Ordered Patterns without Candidate Generation.
- [7]. Huang Chiung-Fen, Tsai Wen-Chih, Chen An-Pin, Application of new Apriori Algorithm MDNC to Exchange Traded Fund, International Conference on Computational Science and Engineering, 2009.
- [8]. Milan Vojnovi_c, James Cruise, Dinan Gunawardena, and Peter Marbach, Ranking and Suggesting Popular Items, IEEE, 2009.

Elaboration of stochastic mathematical models for the prediction of parameters indicative of groundwater quality Case of Souss Massa – Morocco

Manssouri T.¹, Sahbi H.¹, Manssouri I.²

(1) Laboratory of Geo-Engineering and Environment, Faculty of Sciences, University Moulay Ismail, BP 11201, Zitoune, Meknes, Morocco.

(2) Laboratory of Mechanics, Mechatronics and Command, ENSAM, Moulay Ismail University, BP 4042, 50000, Meknes, Morocco.

ABSTRACT:

Groundwater is a real wealth which requires rational management, monitoring and control achievable by the various methods that can classify them according to their degree of water mineralization lasting quality. Indeed, to assess the quality of groundwater, the knowledge of a certain number of indicators, such as the Electrical Conductivity EC, Organic material OM and the amount of Fecal Coliforms FC is paramount.

This work seeks to analyze the prediction indicators of quality of groundwater Souss-Massa Morocco. Initially, methods based on neural models MLP (Multi Layer Perceptron) are applied for the prediction of quality indicators of groundwater.

The choice of the architecture of the artificial neural network ANN MLP type is determined by the use of different statistical tests of robustness, i.e. the AIC criterion (Akaike Information Criteria), the test RMSE (Root-Mean-Square error) and the criterion MAPE (Maximum Average Percentage Error). Levenberg Marquardt algorithms are used to determine the weights and biases existing between the different layers of neural network.

In a second step, a comparative study was launched between the neural prediction model MLP type and conventional statistical models, including total multiple linear regression. The results showed that the performance of neural prediction model ANN - MLP is clearly superior than those established by the total multiple linear regression TMLR.

KEYWORDS: Prediction, Neural Network MLP type, robustness tests, Multiple Linear Regression, indicators of quality of groundwater.

I. INTRODUCTION

The management of water resources is nowadays one of the key global issues, both in agricultural and industrial activities and in terms of direct consumption of the population. Indeed, the regular growth in demand for water resources, for several decades, has had various problems, both qualitative and quantitative.

Water quality can be judged in relation to-three basic types of parameters which are:

- ✚ Organoleptic parameters which are designed to assess the quality if the water is pleasant to the senses of the observer either by sight or by smell or taste as well.
- ✚ Microbiological parameters: some microscopic beings live in water. Their concentration defines some quality of these waters; Fecal Coliforms (FC); Fecal streptococci (FS) can be found.
- ✚ The physico-chemical parameters: these parameters, global or specific, help to assess the ability of a water to the use for which it is destined. They can be divided into chemical parameters and physical parameters.

In addition, the quality of groundwater is defined by the components distributed and transported in the liquid medium. Concentration measurements of chemical indicators in water samples collected at various locations, positions near or distant from the source of infiltration are basic elements to establish and monitor quality.

In previous works, neural networks have found great success in the modeling and prediction, we include for example:

Perez et al (2001) [1] have proposed to predict the concentration of nitrogen NO₂ and nitric oxide NO in Santiago based on meteorological variables and using the linear regression method and the method of network neural. The results showed that neural networks are the method that performs the prediction error the lowest compared to other methods.

In 2008, Nohair et al [2] use neural networks to predict changes in a stream based on climatic variables such as the temperature of the ambient air, the water flow temperature received by the stream. Two methods were applied: the first, iterative type uses the estimated day j to predict the value of the water temperature on day $j + 1$ value, and the second method much simpler to implement, is of estimating the temperature of all the days taken at one time.

Bélanger et al (2005) [3] also use multilayer neural networks to predict the temperature of the water from the hydrometeorological parameters based on the model of artificial intelligence and the traditional method of multiple linear regression. The results of this study show that artificial neural networks seem to give a fit to the data slightly better than that offered by the multiple linear regression.

In 2010, Cheggaga et al (2010) [4] show the possibility of using neural networks to non-recurring layers for extrapolation, prediction and interpolation of the wind speed in time and in space in 3D (radius r , height h , time t), based on neural network learning for a few days. This work has shown the possibility of using neural networks to non-recurring layers for extrapolation and interpolation prediction of wind speed.

El Badawi et al. (2011) [5] carried out a comparative study of the performance of two modeling methods used for the prediction of heavy metal concentrations in Moroccan river sediments using a number of physico-chemical parameters.

This study showed that predictive models established by the recent method, which is based on the principle of artificial neural networks, are much more efficient compared to those established by the method based on multiple linear regression. The performance of the method shows the existence of a non-linear relationship between the physico-chemical characteristics studied (independent variables) and metal concentrations in sediments of the watershed of OuedBeht.

Manssouri et al. (2013) [6] use two modeling methods for the prediction of meteorological parameters in general and the humidity in particular. At first, the methods are based on the study of artificial neural networks MLP types (multi-layer Perceptron) are applied for the prediction of moisture, of the Chaouene area in Morocco. In a second step the new architecture of neural networks proposed of MLP types, was compared to the model of Multiple Linear Regression (MLR).

Predictive models established by the method of neural networks MLP, are more efficient than those established by multiple linear regression, because good correlation was obtained with the parameters from a neural approach with a quadratic error from 5%.

The main objective of this paper is to apply stochastic mathematical models as a tool for prediction of parameters (microbiological, physical and chemical) quality indicators groundwater in Souss_Massa.

II. GEOGRAPHICAL LOCATION

The Hydraulic Basin Souss Massa (BHSM) is located between the High Atlas in the north and the ancient mountains of the Anti-Atlas to the south. It includes the catchments of Souss Massa Tamri, Tamraght and Atlantic coastal basins Tiznit-Ifni. The total area of the study area is almost 27 900 km². The main plains of the region are the Souss (4500 km²), the plain Chtouka (1260 km²) and the plain of Tiznit (1200 km²) see Figure 1.

The study area falls within the Prefectures of Agadir Ida Outanane and Inezgane Ait Melloul and provinces Chtouka Ait Baha, Taroudant and Tiznit. It also includes other provinces like Chichaoua and Essaouira.

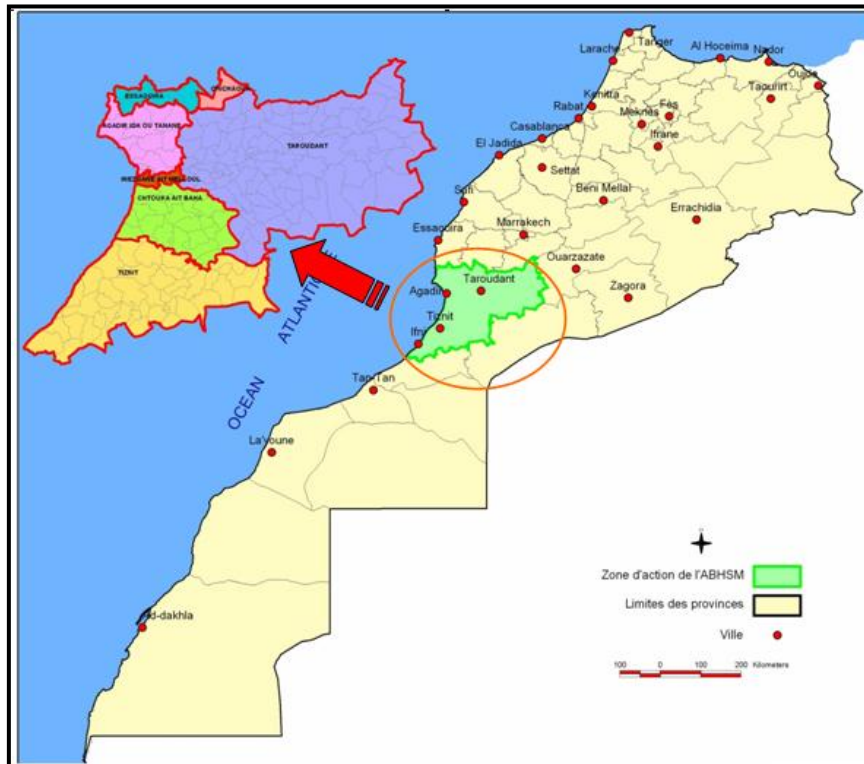


Figure 1. Location of the area of action of the Water Basin Agency of Souss Massa (ABHSM, 2004).

III. CLIMATE AND RAINFALL POTENTIAL

The climate of the region is predominantly arid, with strong sunshine (3089 hours / year). It is conditioned, including the influence of cold winds from the Atlantic Ocean (Canary Current) and Saharan latitude which gives the area a pre-Saharan climate to cool winters in the plains.

The temperatures are mild and regular, with an annual average ranging from 18.3 ° C to 20 ° C in Agadir at the dam on the Abdelmoumen river (Table 1). The maximum daily temperature reaches 49 ° C and the minimum temperature drops to 3 ° C below zero. The temperature ranges are also high and can reach 48 ° C according to a study prepared in 2004 by the Water Basin Agency of Souss Massa (BHSM Agency).

Table1. Annual average temperatures. (Agency ABHSM 2004)

Poste	Agadir	Barrage Abdelmoumen	Barrage Aoulouz	Taroudant	Barrage Youssef Ben Tachfine
T (° C)	18,3	20,6	19,9	19,7	19,9

The average annual evaporation ranges from 1400 mm in the mountains and near the Atlantic coast and 2000 mm in the plains. The minimum mean monthly evaporation is recorded in January with an average of 35 mm in the mountains and 100 mm in the plains, while the maximum was recorded in July with an average of 240 mm in the mountains and 270 mm in plain.

The humidity is quite high throughout the year on the ocean fringe, which allows maintaining a dense natural vegetative cover (effect of dew, fog and mist). The monthly average relative humidity is about 65%. Its maximum in July (73%), while the minimum occurs in December (58%).

The winds in the area are generally of two types:

Hot winds from EAST known as "Chergui" that occur in late spring to mid-autumn;

A sea breeze whose influence is felt in the coastal zone and to a depth of 25 to 30 km inland.

Rainfall is highly variable in space and time. The total number of rainy days is around 30 days per year on average, over the High Atlas is sprinkled with a number of rainy days in the order of 60 days.

Two rainfall seasons are distinguished in the region, namely:

- ✓ A wet season from November to March, during which the region receives 70-75% of the annual rainfall;
- ✓ A dry season, from April to October during which the region receives 25-30% of the annual rainfall.

The inter-average rainfall in the region varies from one watershed to another, as shown in Table 2.

	Souss	Massa	Tamraght	Tamri	Tiznit
Precipitations (mm)	280	265	390	370	145

Table2. Average annual rainfall. (Agency BHSM 2004)

I. Results and Discussion

Iv.1 Development of the Basis Learning and Test

Data Collection

The objective of this step is to collect data, both to develop different prediction models and to test them.

In the case of applications on real data, the objective is to collect a sufficient number of data to form a representative database that may occur during use of different prediction models. The data used in this study are related to the chemical analysis of parameters indicative of groundwater quality Souss Massa, made from 52 measurement points distributed over the entire groundwater heeling under the basin.

The dependent variables are the chemical characteristics determined in these water points such as Electrical Conductivity EC Organic material OM, the amount of Fecal Coliforms FC; Independent variables are sodium Na^+ , potassium K^+ , calcium Ca^{2+} the magnesium ion Mg^{2+} , the hydrogen ion HCO_3^- , sulfate ion SO_4^{2-} , the air temperature T_a ($^\circ\text{C}$), the water temperature T_e ($^\circ\text{C}$), the potential hydrogen Ph, Fecal streptococci FS, Total Coliforms TC (Figure.1)

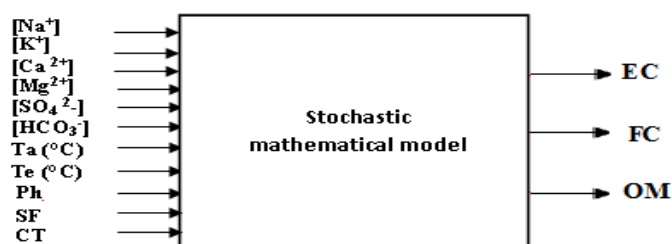


Figure.2: The inputs / outputs of the stochastic mathematical model

Data Analysis

After data collection, the analysis is necessary to determine the discriminate characteristics to detect and differentiate the data. These characteristics are the input of the neural network.

This determination of characteristics has an impact on both the size of the network (and thus the simulation time), on system performance (power separation rate prediction), and development time (learning time). Data filtering can be used to exclude those aberrant and / or redundant.

Data standardization

In general, the database must undergo pretreatment to be adapted to the inputs and outputs of stochastic mathematical models. A common pretreatment is to conduct a proper normalization that takes into account the magnitude of the values accepted by the models.

The normalization of each input x_i is given by the formula:

$$x_{i \text{ new}}^k = 0,8 * \frac{x_{i \text{ old}}^k - \min(x_i)}{\max(x_i) - \min(x_i)} + 0,1$$

A standardized data between 0.1 and 0.9 is obtained. This database consists of different variations of the independent variables (model inputs) and dependents (model output).

Iv. 2. Total Multiple Linear Regression

To construct the linear mathematical model, the database should be divided into two bases: the learning that reflects 60% of the total database and the test-validation that reflects 40% of the total data base. To build the first model we used the TLMR (Total Multiple Linear Regression).

The analysis by this method consists in finding a polynomial function, ie the value of each indicator given as a linear function of all the independent variables.

By performing the analysis by multiple linear regression with all the variables, we have obtained the equations 1, 2 and 3 respectively on the Electrical Conductivity EC, Organic Material OM and the amount of Fecal Coliforms FC from independent variables which are sodium Na^+ , potassium K^+ , calcium Ca^{2+} , magnesium ion Mg^{2+} , hydrogen ion HCO_3^- , ion SO_4^{2-} , sulfate air Temperature Ta (° C) water temperature Te (° C), hydrogen potential Ph, Fecal Streptococci FS and Total Coliforms TC.

$$CE = -2,48716025993775E-02+0,333562079485328*[Na^+]+0,269703130591743*[K^+]-4,80221916946264E-02*[Ca^{2+}]-8,76866239678415E-02*[Mg^{2+}]-0,140917153044832*[HCO_3^-]+0,165424140021363*[SO_4^{2-}]-0,17659530501312* Ta +1,32439297208373E-02* Te +3,95855888033802E-02* Ph -1,67707116677135E-03* SF +0,557636121731416* CT \quad (1)$$

$$R^2 = 0,844 \quad p < 0,0001$$

$$MO = -0,467919439118611+1,2145039855662*[Na^+]-1,20427213233719E-02*[K^+] - 0,292644994647529*[Ca^{2+}]-0,564030336075162*[Mg^{2+}]+0,370232286748363*[HCO_3^-]-0,049368993591269*[SO_4^{2-}]+1,95020345380644E-02* Ta +3,59121215403218E-02* Te +6,57040240587299E-03* Ph -5,11243331413514E-02* SF +0,661995092580923* CT \quad (2)$$

$$R^2 = 0,584 \quad p = 0,057$$

$$CF = 0,302564389883223-0,124689894191023*[Na^+] +1,26022839275979E-02*[K^+] +9,11518997299649E-02*[Ca^{2+}] +4,67050632639108E-02*[Mg^{2+}]-1,85733043744043E-02*[HCO_3^-] -2,09539963169211E-02*[SO_4^{2-}] +3,26042977324909E-02* Ta +4,75125209774659E-02* Te +6,20911785378519E-02* Ph +0,172064089619721* SF +0,418787632774451* CT \quad (3)$$

$$R^2 = 0,541 \quad p = 0,067$$

The model on the Electrical Conductivity EC (1) is highly significant based on the fact that the probability is less than 0.0001. However other models are less significant than the first-mentioned model.

For the model (2) which connects the Organic Matter MO with all the independent variables, it is less significant since its probability is 0.057 and for the model (3) which connects the amount of Fecal Coliforms FC with all the independent variables as less significant because its probability is 0.067.

We conclude that the model (1) seems the most effective compared to the other two models. Indeed, the coefficients of determination of the first model is 0, 844, while for model (2) and (3) the coefficient of determination is 0.584 and 0.541.

IV.3-The Development Of Models Of Artificial Neural Network Mlp

Neural networks are powerful techniques of nonlinear data processing, which have proven themselves in many domains. Therefore, the artificial neural networks have been applied in various domains of prediction.

The various models of artificial neural network used in this work have been developed and implemented with the programming language C++ on an I3 PC machine 2.4 GHz and 3 Go of RAM.

The artificial neural network consists of an input layer, a hidden layer and an output layer. Input variables $x = (x_1, x_2, \dots, x_{11})$ and independent normalized between 0.1 and 0.9 and then presented to the input layer of the neural network which contains eleven neurons.

They are first multiplied by the weight IW, and then added to bias IB through the input layer and the hidden layer. Neurons in the hidden layer receive the weighted signals. After addition, they transform them using a nonlinear sigmoid function $S(\cdot)$. Given by the equation:

$$S(n) = \frac{1}{1 + \exp(-n)}$$

The following mathematical model $S(IW * X + IB)$ is presented to the input of the output layer. This model will be multiplied by the weight WL then added to the bias LB that exist between the hidden layer and the output layer and then converted by a nonlinear sigmoid function $S(\cdot)$.

Finally, we obtain the mathematical model of artificial neural network as follows:

$$S \{ LW * S (IW * X + IB) + LB \}.$$

The back propagation algorithm was used to form the artificial neural network in a fast and robust manner.

The analysis was restricted to networks that contain a single hidden layer, since this architecture is able to predict all outputs.

IV.4. Test Of Robustness

To select the "best" architecture of neural network, several statistical tests are commonly used; in our case we used statistical tests Root Mean Square Error RMSE, Maximum Average Percentage Error MAPE and Akaike Information Criteria AIC.

This last criterion we try to minimize, is proposed by Akaike [7], it is derived from the information theory, and relies on the measurement of Kullback and Leibler. It is a model selection criterion that penalizes models for which the additions of new variables do not provide enough information to the model. These tests are given respectively by the following equations:

$$RMSE = \sqrt{\frac{\sum_{i=1}^{i=N} (E_{pi} - E_{ai})^2}{N}}$$

$$MAPE = \frac{1}{N} \sum_{i=1}^N \frac{|E_{pi} - E_{ai}|}{E_{ai}} * 100$$

$$AIC = \ln \left(\frac{N}{2} * L_F \right) + \frac{2N_w}{N}$$

With L_F is the cost function (mean square errors).

$$L_F = \frac{1}{N} \sum_{i=1}^{i=N} (E_{pi} - E_{ai})^2$$

E_a and E_p are the values of the target vector and vector for predicting output neuron of the network. N represents the number of samples studied tests and N_w is the total weight and bias used for each architecture.

Figures (2-4) RMSE, MAPE and AIC-after 1500 iterations for different number of neurons in the hidden layer, give the opportunity to choose 19 neurons in the hidden layer. We then get the architecture [11-19-3] as "best" configuration of the neural network Due to its good predictive ability.

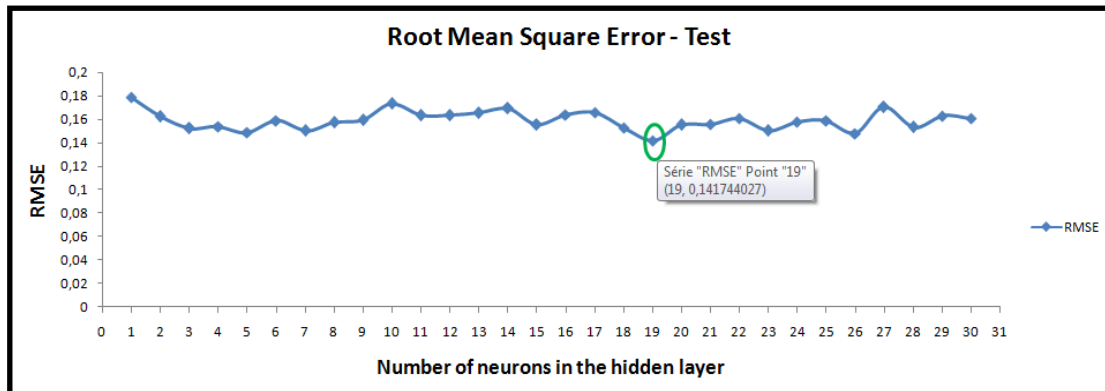


Figure 3. Robustness test: Root Mean Square Error

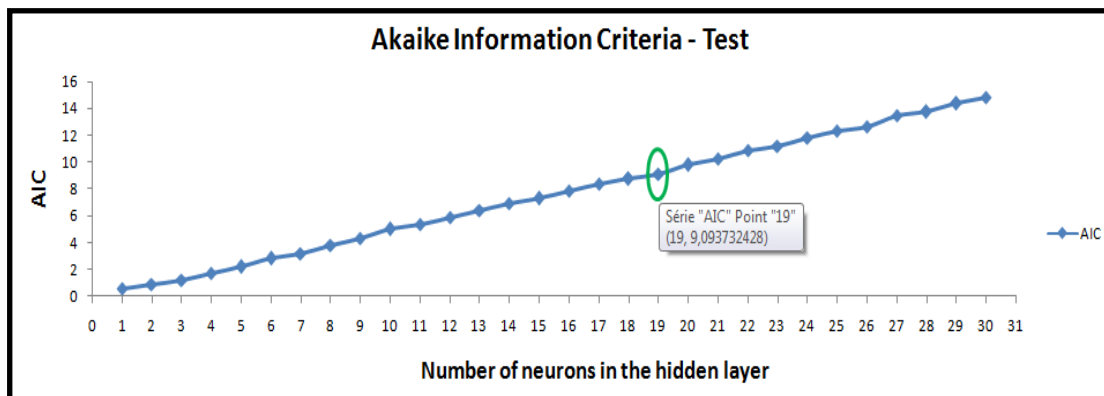


Figure 4. Robustness test: Maximum Average Percentage Error

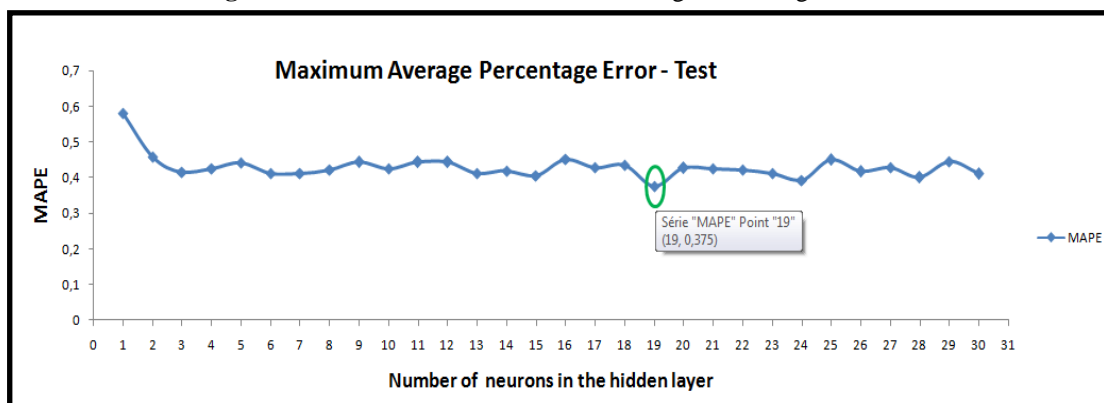


Figure 5. Robustness test: Akaike Information Criterion

IV.5-Learning And Validation

The artificial neural network MLP "Multi Layer Perceptron" consists of an input "input layer" containing eight neurons, a hidden layer "hidden layer" containing eight neurons and an output layer "output layer" containing three neurons (Figure 5).

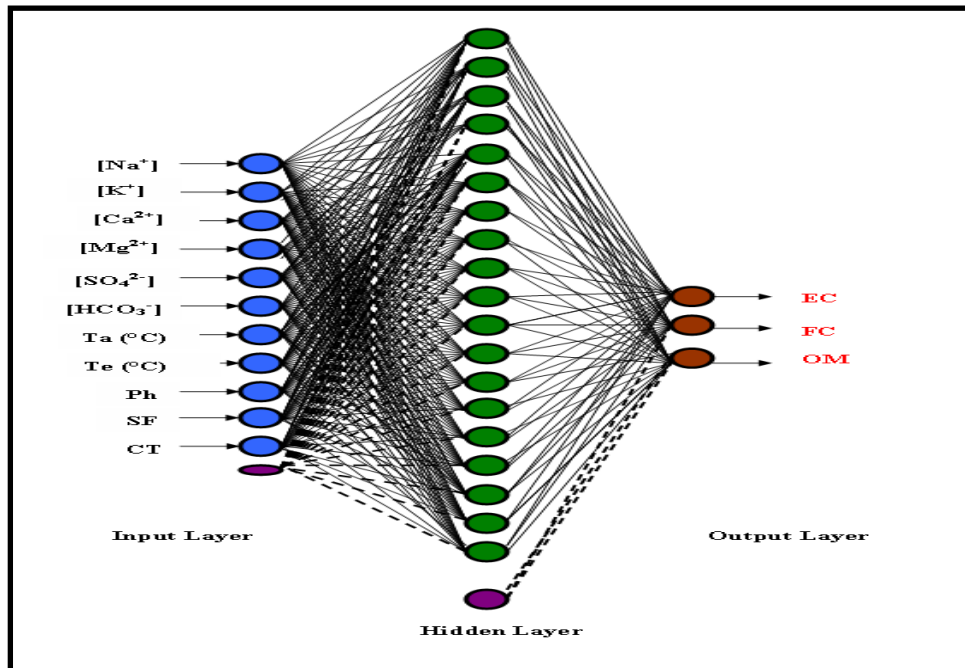


Figure 6: Neural Network architecture.

The basis learning consists of eleven vectors x_1, x_2, \dots, x_{11} , independent and normalized between 0.1 and 0.9 are: sodium Na^+ , potassium K^+ , calcium Ca^{2+} , magnesium ion Mg^{2+} , bicarbonate ion HCO_3^- , sulfate ion SO_4^{2-} , air temperature T_a ($^\circ\text{C}$), water temperature T_e ($^\circ\text{C}$), potential hydrogen Ph, Fecal Streptococci FS and Total Coliforms TC.

The basis learning, of the neural network consists of 32 samples. The weights and biases of the network were adjusted using the Levenberg Marquardt.

Once the architecture, weights and biases of the neural network have been set, we must know if this neural model is likely to be generalized.

The validation of neural architecture [11-19-3] is therefore to assess its ability to predict parameters indicating groundwater quality Souss Massa (EC, OM and FC) using the weights and biases calculated during learning to apply to another database of 20 samples test compounds, that is to say 40% of the total data.

The ANN model [11-19-3] gave a correlation coefficient for the testing and validation of 0.913117, which is equivalent to a mean square error of 0.14174, 0.375 for the average of the absolute errors and relative percentage of 9.09373 for the AIC.

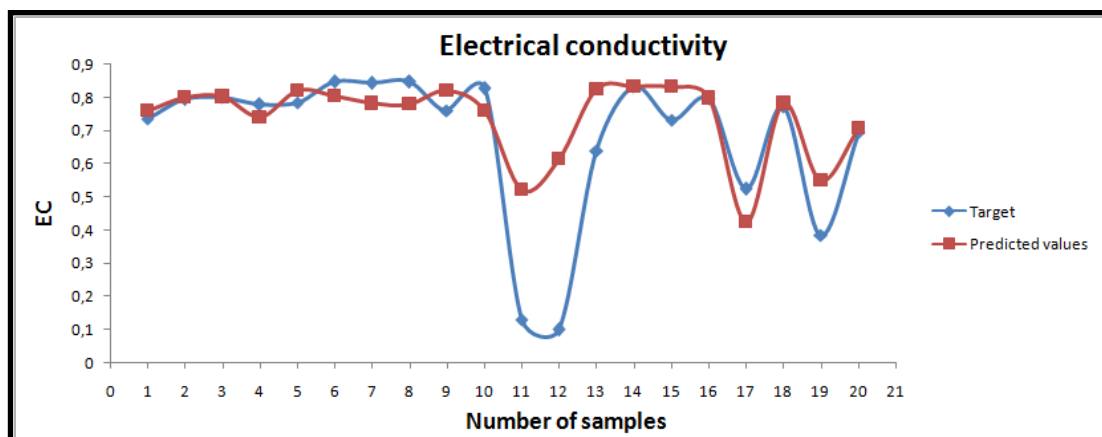


Figure 7: Result of test for predicting the Electrical Conductivity EC of the model ANN-MLP [11-19-3]

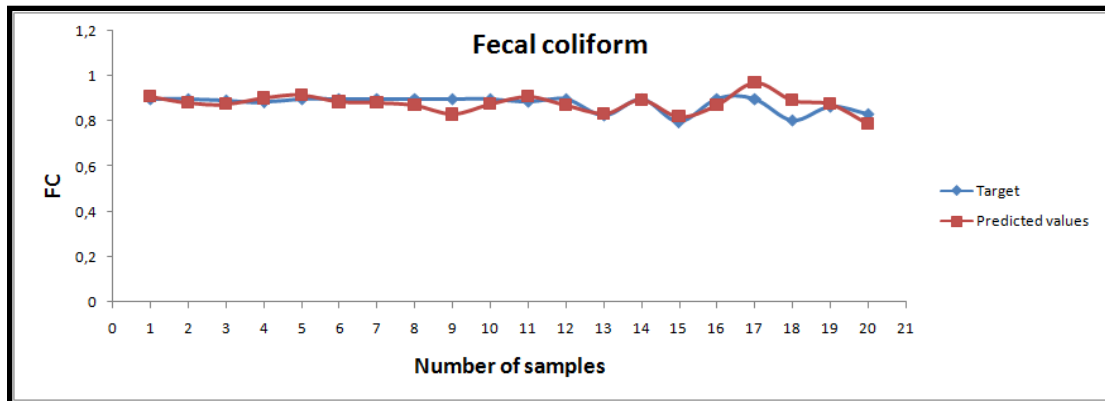


Figure 8: Results of prediction test the amount of Fecal Coliforms FC of the model ANN-MLP [11-19-3]

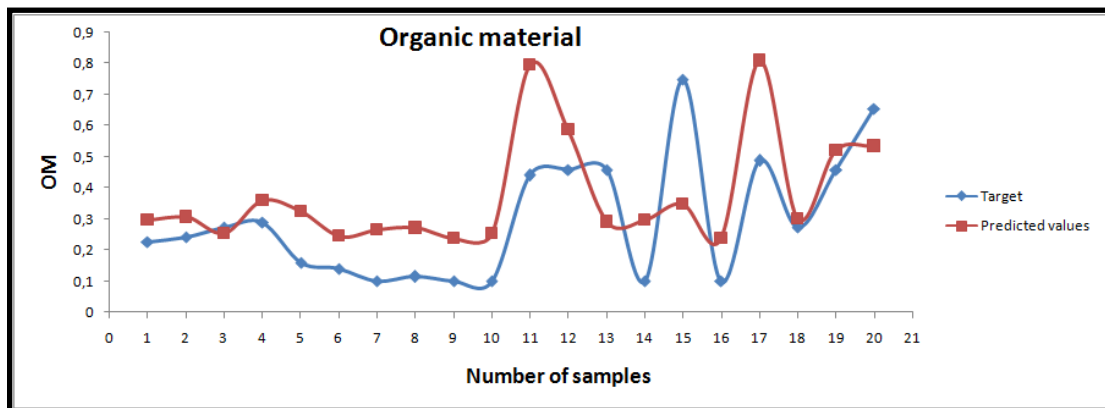


Figure 9: Test Result for predicting Organic Matter OM of the model ANN-MLP [11-19-3]

We evaluate the quality of prediction of the neural architecture [11-19-3] by the correlation coefficient. In our case the correlation coefficient is 91.3117%.

IV.5-Comparisons And Discussions

To assess the performance of the ANN-MLP method [11-19-3], we compared this method with other methods namely Multiple Linear Regression MLR.

The correlation coefficient calculated by ANN-MLP [11-19-3] is significantly higher (91.3117%), unlike the correlation coefficients calculated by the MLR are lower (between 0.541 and 0.844). On the other hand, the correlation coefficients obtained by testing the validity of the models established by the ANN (91.3117%) are significantly similar to those related to learning (99.1858%). However, the correlation coefficients of the tests of the validity of models for the MLR, are widely different from those obtained during training (see Table 3).

Method	EC		OM		FC	
	Learning	Test	Learning	Test	Learning	Test
RLM	0,844	0,6896	0,584	0,215	0,541	0,325
RNA	0,991858	0,913117	0,991858	0,913117	0,991858	0,913117

Table 3: Correlation coefficients obtained by MLR and ANN-MLP [11-19-3] on the Electrical Conductivity, Organic Matter and the amount of Fecal Coliforms.

V. CONCLUSION

We have been interested in a comparative study of the performance of two modeling methods used for the prediction of quality indicators of groundwater with hydraulic basin Souss Massa such as Electrical Conductivity EC, OM Organic Matter and the amount of Fecal Coliforms FC from a number of physico-chemical and microbiological parameters.

Both modeling methods are used; multiple linear regression and artificial neural networks (formal). The data is used for the analysis of water samples taken at several water points, distributed in space and time, of the study area.

The results obtained in this work show a significant capacity for learning and the prediction for indicators of water quality with a coefficient of determination of 91.3117%, equivalent to a mean squared error of 0,14174. Of 0.375 for the average absolute relative errors in percentage and 9.09373 for the AIC criterion for basic testing data used in addition to a better choice of the network architecture achieved through statistical tests of robustness. In multiple linear regression, the results are less significant with a coefficient of determination between 21.5% and 68.96%. This shows that the parameters are associated with indicators of groundwater quality in a non-linear relationship.

REFERENCES

- [1]. Perez, P., Trier, A. (2001). Prediction of NO and NO₂ concentrations near a street with heavy traffic in Santiago, Atmospheric Environment, 35: 1783-1789.
- [2]. Nohair.M. (2008).Utilisation de réseaux de neurones et de la régularisation bayésienne en modélisation de la température de l'eau en rivière. Revue des sciences de l'eau / Journal of Water Science, vol. 21, n° 3, 2008, p. 373-382., Faculté des sciences et techniques de Mohammedia, Maroc.11p.
- [3]. Bélanger M. (2005). Estimation de la température de l'eau en rivière en utilisant les réseaux de neurones et la régression linéaire multiple. Revue des sciences de l'eau, Rev.sci.Eau 18/3: 403-421.
- [4]. Cheggaga N., Youcef Ettoumi F. (2010). Estimation du potentiel éolien. Revue des Energies Renouvelables SMEE'10 Bou Ismail Tipaza 99 – 105.
- [5]. Abdallaoui A., El Badaoui H. (2011). Prédiction des teneurs en métaux lourds des sédiments à partir de leurs caractéristiques physico-chimiques. Journal Physical and Chemical News. 58: 90-97.
- [6]. El Badaoui H., Abdallaoui A., Manssouri I., Ousmana H., «The prediction of moisture through the use of neural networks MLP type », IOSR Journal of Computer Engineering (IOSR-JCE) e-ISSN: 2278-0661, p- ISSN: 2278-8727Volume 11, Issue 6 (May. - Jun. 2013), pp 66-74, 2013.
- [7]. AkaikeH..Information theory and the extension of the maximum likelihood principle. In: Second International Symposium on Information Theory. (Eds: V.N.Petrov and F. Csaki). Academiai Kiadó, Budapest, (1973), pp 267-281.

Experimental Studies of the Statistical Properties of Network Traffic Based on the BDS-Statistics

Alexey Smirnov¹, Dmitriy Danilenko²

¹ Professor in the Department of Software, Kirovohrad National Technical University, Kirovohrad, Ukraine,

² Graduate student in the Department of Software, Kirovohrad National Technical University, Kirovohrad, Ukraine

Abstract:

Experiments, which outcome in the results of correlation analysis of network traffic based on the BDS-test, which may be used as part of an analytical component of modern anti-virus systems, have been conducted. In addition, the correlation analysis of network traffic may be used for organizing of one of the main elements of the system for monitoring a network activity as a touch subsystem (sensors to collect traffic information), as well as an analytical part (decision-making module component). A unit to assess the significance differences of two or more samples (series) of independent observations of network traffic (Wilcoxon criterion) is used to solve the problem of detection of individual services of a telecommunications system following the observed network traffic. It allows to set different data streams belonging to the same general totality with a given accuracy and reliability..

Keywords: telecommunication systems and networks, system of intrusion detection and prevention, BDS-statistics

I. INTRODUCTION

To ensure the safety of modern telecommunication networks the so-called intrusion detection system (IDS) and intrusion prevention systems (IPS) are used [1-14]. At the heart of their operation there is the collection, analysis and processing of information about the events related to the security perimeter of the telecommunications network, the accumulation of the collected data, monitoring of network activity of individual services, deciding on the status of the protected system, as well as identifying and countering possible unauthorized use of information and communication resources [2]. One of the directions in improving systems for intrusion detection and prevention is the study of anomalies (Anomaly-Based Intrusion Detection and Prevention Systems – AB IDPS) in telecommunication systems, which is based on statistical analysis of network traffic [2]. Within this approach, IDPS defines a "normal" network activity of individual information services of a telecommunication system, then all the traffic that is not covered under the definition of "normal" is marked as "anomalous".

The analysis of correlation methods for the identification of objects showed that one of the most effective approaches for identifying dependencies in data traffic is BDS-statistics, which is constructed based on the BDS-tests (BDS-methods). BDS-tests are effective methods to identify dependencies in the time series. Their aim is to test the null hypothesis H_0 about the independence and the identical distribution of the time series' values $\xi^r = (\xi_1, \xi_2, \dots, \xi_N)$, using for it a criterion of significance. According to this criterion, for accepting the hypothesis H_0 it is necessary to choose a critical domain G_α satisfying the condition of $P(g \in G) = \alpha$, where $g(\xi_1, \xi_2, \dots, \xi_N)$ – is the observation statistics, and α – is an adjustable level of significance [17-20].

II. BDS-STATISTICS DESCRIPTION

BDS-test is based on the statistic value of $w(\xi^r)$ (BDS-statistics) [17-20]:

$$w_{m,N}(\varepsilon) = \sqrt{N - m + 1} \frac{C_{m,N}(\varepsilon) - C_{1,N-m}(\varepsilon)^m}{\sigma_{m,N}(\varepsilon)},$$

where $C_{m,N}(\varepsilon) - C_{1,N-m}(\varepsilon)^m$ – (numerator BDS-statistics) is determined by the correlation integrals $C_{m,N}(\varepsilon)$, $C_{1,N}(\varepsilon)$ for the dimension m ; ε – is the radius of the hypersphere; $\sigma_{m,N}(\varepsilon)$ – is a standard deviation of the difference $C_{m,N}(\varepsilon) - C_{1,N-m}(\varepsilon)^m$; N – a number of elements of the time series.

A number of studies [17-20] have proposed "simplified" algorithms of BDS-statistics estimation. In them, for the calculation of $C_{m,N}(\varepsilon)$ ($m > 1$), it is necessary to perform "embedding" of the time series of m -dimensional pseudo-phase space, the elements of which, by the theorem of Takens [19], are the points $\xi_i^m = (\xi_i, \xi_{i+1}, \dots, \xi_{i+m})$ with the coordinates $\{\xi_{i+k}\}_{k=1}^m$ given by m successive values of the original time series. Correlation integral determines the frequency of contact of any pair of phase space points in the hypersphere of ε radius:

$$C_{m,N}(\varepsilon) = \frac{2}{(N-m+1)(N-m)} \sum_{s=mt=s+1}^N \sum_{j=0}^{m-1} \prod_{j=0}^{m-1} I_\varepsilon(\xi_{s-j}^m, \xi_{t-j}^m),$$

$$I_\varepsilon(\xi_i^m, \xi_j^m) = \begin{cases} 1, & \|\xi_i^m - \xi_j^m\| \leq \varepsilon \\ 0, & \|\xi_i^m - \xi_j^m\| > \varepsilon \end{cases},$$

$$\{\xi_{i+k}\}_{k=1}^m \quad 0 \leq i \leq N \text{ and } 0 \leq j \leq N,$$

where $I_\varepsilon(\xi_i^m, \xi_j^m)$ is the Heaviside function for all pairs of values i and j .

The value of the correlation integral approaches a definite limit as ε decreases. The analysis of studies [17-20] showed that there is a range of ε values, which allows performing calculations with the specified accuracy coefficient. This range depends on the number of elements of the time series N . If ε is too small, there will not be enough points to capture the statistical structure; if ε is too large, there will be too many points.

The studies [17-20] recommend to choose ε so that $\varepsilon = 0.5\sigma \div 2\sigma$, where σ – is a standard deviation of the process $\{\xi_i\}_{i=1}^N$. In accordance with the theory of statistics, the dependence of the correlation integral from ε is as follows:

$$C_{m,N}(\varepsilon) \sim \varepsilon^{D_c},$$

where D_c is a correlation dimension of the time series.

For $m = 1$ we have:

$$C_{1,N}(\varepsilon) = \frac{2}{N(N-1)} \sum_{s=1}^N \sum_{t=s+1}^N I_\varepsilon(\xi_s, \xi_t).$$

The studies performed has shown, that when $N \rightarrow \infty$, the correlation integral $C_{m,N}(\varepsilon) \Rightarrow C_{1,N}(\varepsilon)^m$, and the value $(C_{m,N}(\varepsilon) - C_{1,N}(\varepsilon)^m) \cdot \sqrt{N-m+1}$ is asymptotically normally distributed random variable with a mean zero and standard deviation $\sigma_{m,N}(\varepsilon)$, which is defined as:

$$\sigma_{m,N}(\varepsilon) = 2 \sqrt{k^m + 2 \sum_{j=1}^{m-1} k^{m-j} \cdot (C_{1,N}(\varepsilon))^{2j} + (m-1)^2 \cdot (C_{1,N}(\varepsilon))^{2m} - m^2 k (C_{1,N}(\varepsilon))^{2m-2}},$$

where

$$k = \frac{1}{(N-1)(N-2)N} \left\{ \sum_{t=1}^N \left[\sum_{s=1}^N I_\varepsilon(\xi_t, \xi_s) \right]^2 - 3 \sum_{s=1}^N \sum_{t=s+1}^N I_\varepsilon(\xi_t, \xi_s) + 2N \right\}.$$

BDS-statistics $w(\xi)$ is a normally distributed random variable with the proviso that the estimate $\sigma_{m,N}(\varepsilon)$ is close to its theoretical value $\sigma_{m,N}(\varepsilon)$.

The problem of detection of chaotic signal is considered as a non-parametric verification of one of the two hypotheses:

- 1) H_0 – the observed data (data traffic) $\xi = (\xi_1, \xi_2, \dots, \xi_N)$ are independent and identically distributed, i.e. the density (function) distribution is factored $F_N(\xi_1, \xi_2, \dots, \xi_N) = \prod_{i=1}^N F(\xi_i)$.

2) H_1 - the obtained as the result of the experiment data (traffic information) have a certain relationship (a process is structured).

According to the hypothesis H_0 the statistics $w(\xi^r)$ is asymptotically distributed as $N(0,1)$, if a number of observations asymptotically approaches the infinity. A number of studies [17-20] settle the hypothesis about the need for the pilot study of more than 500 observations. Such number of experiments will allow to argue about the reliability of the received results.

The studies have shown that the criterion of the hypothesis validity H_0 (in the absence of any data traffic dependencies) is the inequality:

$$|w_{m,N}(\varepsilon)| \leq 1,96.$$

For a value of the statistic $w_{m,N}(\varepsilon)$ the given value corresponds to the level of significance $\alpha = 0,05$ (probability of a 1st type error), and when the above inequality is the true hypothesis H_0 (I.I.D.) is accepted with the probability $P_{H_0} \approx 0,95$.

In the case where the alternative hypothesis H_1 is true, a distribution of the statistic criterion $w(\xi^r)$ is changed. Therefore, when checking statistical hypotheses it is insufficient to focus on the value of the significance level α .

A power of the criterion $1-\beta$ or probability of error of the second kind β should be determined when considering the alternative hypothesis H_1 , which implies dependence (possibly nonlinear) of a time series, if the first difference of the natural logarithms have been taken. A power of the criterion is the probability of considering the alternative hypothesis H_1 in applying the criterion $w(\xi^r)$ with the proviso that it is true, that is its ability to detect the existing deviation from the null hypothesis. Obviously, for a fixed error of the 1st kind (we set it ourselves, and it does not depend on the criterion properties) the criterion will be the better, the more its power is (i.e., the smaller is the error of the 2nd kind). For calculating the power of the criterion $1-\beta$ ($\beta = p(w(\xi^r) \in G_\alpha | H_1)$), G_α - is a critical area at a given level of significance α it is necessary to know the conditional density distribution $p(w(\xi^r) | H_1)$. The power of the criterion (test) is determined empirically.

For the experiment and improving the reliability of the results, it is necessary to choose such embedding dimension m , whereby the phase space reconstruction is neither "too rare" nor "too crowded." A number of studies [] recommends $m = 6$ in experiments.

Thus, the conducted analysis of different approaches in the statistical testing showed that the BDS-test gives a possibility to detect various types of deviations from the independence and identical distribution and can serve as a general model test of the processes classification (time series) ξ^r , especially in the presence of nonlinear dynamics.

The nonparametric nature of BDS-testing may be considered to be its main feature. This is reflected in the fact that BDS-test uses a nonlinear function $w(\xi^r)$ as the statistics from observations, the distribution of which is independent of the observed values ξ^r distribution. In this case, we are able to get some information about the multidimensional function (density) of distribution $F_N(\xi_1, \xi_2, \dots, \xi_N)$ analyzing a dimensional empirical function of distribution $p(w)$ of the statistics w .

BDS-test calculation may be carried out by various methods, many implementations are known, this technique proposes using the implementation suggested by the authors of the BDS-test (by W. A. Brock, W. D. Dechert and J. A. Sheinkman). Fast algorithms for calculating BDS statistics has been also proposed [17-20]. Below are the results of experimental studies of the network traffic statistical properties based on the correlation analysis of time series (by BDS-testing). The results include the data matching the most popular network protocols and services.

III. EXPERIMENTAL STUDIES OF THE NETWORK TRAFFIC STATISTICAL PROPERTIES BASED ON THE CORRELATION ANALYSIS OF TIME SERIES

The sample size for research based on the statistical properties of the correlation analysis of time series is $N = 1000$, the calculations has been performed with different parameters (the results are shown in the respective tables). The analysis of HTTP traffic experimental data shows that the phase portrait of network traffic for data transmission using HTTP protocols shows having some dependency, consisting in grouping the most points in a certain area. Table 1 shows the values of BDS-test with different sets of parameters. HTTP is an application level of protocol data (initially – in the form of hypertext documents). HTTP is based on the "client-server" technology, that assumes existing consumers (clients) who initiate a connection and send a request, and providers (servers) that are waiting for connection request, produce the necessary actions and return a message back with the result.

Table 1 – The results of BDS-test for experimental data of HTTP traffic with different parameters of m and ε

HTTP	m	$\varepsilon = 0.5 \sigma$	$\varepsilon = \sigma$
	4	13,52	12,69
5	13,97	11,554	
6	13,87	10,65	
7	13,58	9,92	

Thus, as it follows from the experimental data obtained for this kind of HTTP traffic, the characteristic value of the BDS-test is as follows:

- for the radius $\varepsilon = 0.5 \sigma$ when $m = 4..7$ the values range from ≈ 15 to ≈ 14 ;
- for the radius $\varepsilon = \sigma$ there exists a greater variation of values ranging from 9.92 to 12.69.

These values may be used as test (reference) values at the detection of the traffic type and the corresponding network service.

Let's process the obtained experimental data of FTP traffic. FTP is a protocol used to transfer files via computer networks. It allows connecting to FTP servers, browsing the contents of directories and downloading files from the server or uploading them to the server; moreover, a mode of transmission of files between the servers is possible. FTP protocol refers to the application layer protocols and uses the TCP transport protocol for data transfer. The commands and data, in contrast to most other protocols, are transmitted on different ports. The outbound port 20 opened on the server side is used to transmit data, and the port 21 for sending commands. The port for receiving the customer data is determined in the matching dialogue. If a file transfer is interrupted for any reason, the protocol provides a means to download the rest of the file, which is very useful when transferring large files.

In the above snippet of experimental data of network traffic using FTP protocols the transition from a small number of packets (transmission of protocol commands, retrieving a list of directories, etc.) and the beginning of active download files at a certain level of speed can be clearly seen. As the server used had a load speed limit which was significantly less than bandwidth network capabilities, the "bursts" which rapidly decrease to the threshold speed limit are sometimes observed.

A points' grouping that indicate the presence of dependencies in the source data are observed in the phase portrait. Table 2 shows the values of BDS-test with different sets of parameters.

The data of Table 2 may be used as reference values for the FTP traffic in a system of intrusion detection of telecommunications systems and networks.

Table 2 – Values of BDS-test for experimental data of FTP traffic with different parameters of m and ε

FTP	m	$\varepsilon=0.5 \sigma$	$\varepsilon= \sigma$
	4	19,5	17,69
5	17,81	16,13	
6	16,49	14,91	
7	15,437	13,95	

Let's process the obtained experimental data of Skype traffic. Skype is free software with a closed code which enables encrypted voice communications over the Internet between computers (VoIP), as well as paid services for calls to mobiles and landlines. Skype app also allows making conference calls, video calls, and also provides text messaging (chat) and file transfer. There is an opportunity to transmit an image from the screen instead of an image from a webcam.

Two areas around which the majority of the points are formed are observed in the phase portrait for «skype» traffic, which indicates the presence of dependencies in the original sequence. Table 3 shows the values of BDS-test for Skype traffic with different sets of parameters.

Table 3 – Values of BDS-test of experimental data for Skype traffic with different parameters of m and ε

Skype	m	$\varepsilon=0.5 \sigma$	$\varepsilon= \sigma$
	4	16,49	180,11
	5	15,05	163,77
	6	13,95	150,94
	7	13	140,58

The results of the Skype traffic studies obtained listed in Table 2 may be used as reference values in intrusion detection systems of communication systems and networks.

Let's process the obtained experimental data of streaming video traffic. Streaming video is multimedia data which is continuously received by a user from a provider of stream broadcasting. Currently, this service is very popular and traffic volume is about half of the transmitted traffic on the Internet.

On the corresponding fragment of network traffic many bursts and downs characteristic for streaming video is observed. Two areas may be identified in the phase portrait. The first has the distribution close to random. However, in another area of the explicit the points are grouped with sufficiently high accuracy, indicating the presence of dependencies in the original sequence. Table 4 shows the values of BDS-test with different sets of parameters for experimental data of streaming video.

Table 4 – Values of BDS-test for experimental data of stream broadcasting with different parameters of m and ε

Streaming video	m	$\varepsilon=0.5 \sigma$	$\varepsilon= \sigma$
	4	32,5	18,2
	5	32,254	19,28
	6	38,45	20,39
	7	41,42	28,49

The data analysis of Table 4 shows that the values of the BDS-test for streaming video are in a sufficiently large range, but can be used as a reference.

Thus, the results of experimental studies of the statistical properties of network traffic using correlation analysis of time series show that the specific values of the BDS-test can be "meterized" for different services of telecommunication systems and networks. The calculations confirm the theoretical assumptions that different types of traffic the result of BDS-test gives different values that can be taken as a reference.

Thus, Table 6 shows the average values corresponding to the different traffic types for different values of ε , which allows identifying the network services. For example, for the values of $\varepsilon = 0.5 \sigma$ and $\varepsilon = \sigma$ the averaged values of the BDS-tests for each type of traffic can be distinguished, and on this basis a network activity detection process of a separate service of a telecommunications network can be organized.

It should be noted that in a real telecommunication network popular services may be used simultaneously, which would change the values of the BDS-test. However, the implementation of unauthorized network intrusion will change the statistical properties of the network traffic and the corresponding values of the BDS-statistics. Furthermore, even in the combined operation, as a rule, some specific service prevails, which allows to select it. And traces of the traffic generated by malicious software, viruses, etc., modify the meaning of the test to a level sufficient to generate solutions about suspicious traffic, i.e. detection of possible traces of the virus traffic in the general flow.

Table 5 – Average values of BDS-test for different services of a telecommunication network

Average values of the BDS-tests		
Service type	$\varepsilon=0.5 \sigma$	$\varepsilon=\sigma$
HTTP	13,7	11,2
Skype	14,6	171,9
Multiservice traffic	11,5	13,5
FTP	17,3	15,7
Streaming video	36,2	21,6
Malicious software	40,7	28,5

Thus, the experimental data confirm the theoretical assumption about the possibility of using the values of the BDS-test to detect traces of malicious software in the network traffic.

On this basis, the correlation analysis of the network traffic based on the BDS-testing can be used as follows. First, as part of the analytical component of modern anti-virus systems. Second, the correlation analysis of the network traffic can be used for the organization of one of the main elements of the system for monitoring of a network activity as a touch subsystem (sensors to collect information about the traffic) and the analytical part (decision component module).

When building a system for monitoring of a network activity it is necessary to solve the problem of detection of individual services and telecommunications system from the observed network traffic. Let's consider the problem of assessing the significance of differences of two or more samples (series) of independent observations of the network traffic in order to establish (with a given accuracy and reliability) of their belonging to the same general totality. For this, let's use the mathematical formalism of statistical research and a criterion of belonging of the two samples to one and the same general totality (Wilcoxon criterion).

IV. EXPERIMENTAL STUDIES OF BELONGING OF TWO SAMPLES OF NETWORK TRAFFIC TO ONE AND THE SAME GENERAL TOTALITY

In the study of complex technical systems the problem of assessing the significance of differences in two or more samples (series) of independent observations often arises, i.e. it is necessary to install (with a given accuracy and reliability) their belonging to the general totality. Let's suppose there are two samples:

$$x_1, x_2, \dots, x_{N_1}, \tag{1}$$

and

$$y_1, y_2, \dots, y_{N_2} \tag{2}$$

of random variables X and Y, with distribution $P_X(t)$ and $P_Y(t)$, respectively.

Let's assume that the observed x_i and y_i give different values of sample means

$$x^* = (x_1 + x_2 + \dots + x_{N_1}) / N_1, \tag{3}$$

$$y^* = (y_1 + y_2 + \dots + y_{N_2}) / N_2, \tag{4}$$

$$x^* = y^*,$$

and/or sample dispersions (variances)

$$\sigma_X^2 = \frac{1}{N_1} \sum_{i=1}^{N_1} (x_i - x^*)^2, \tag{5}$$

$$\sigma_Y^2 = \frac{1}{N_2} \sum_{i=1}^{N_2} (y_i - y^*)^2, \tag{6}$$

$$\sigma_X^2 = \sigma_Y^2.$$

The solution of assessing the significance of differences in the observed values of x_i and y_i is reduced to testing the null hypothesis H_0 , consisting in the distribution functions $P_X(t)$ and $P_Y(t)$ are identical for all t. An alternative hypothesis is formulated in the form of the inequality $P_X(t) < P_Y(t)$.

The criterion of belonging of two samples to one and the same general totality (Wilcoxon's criterion) is based on counting the number of inversions. For this, the observed values of x_i and y_i are located in the general sequence of ascending order of their values. The resulting non-decreasing sequence contains $N_1 + N_2$ of the values and if the hypothesis $P_X(t) = P_Y(t)$ is correct, the values of both sequences x_1, x_2, \dots, x_{N_1} and y_1, y_2, \dots, y_{N_2} are well mixed. The degree of mixing is determined by the number of inversions of the first sequence members relatively to the second. If the overall ordered sequence one certain value of x is preceded by one value of y, which means that there is one inversion. If some values of x are preceded by k values of y, then this value of x has k inversions.

Let's denote the number of inversions for the value of x_i by u_i relatively to antecedent values of y. Then the total number of inversions (for all values of the sequence x_1, x_2, \dots, x_{N_1} relatively to the values from the sequence y_1, y_2, \dots, y_{N_2}) will be determined by the sum

$$u = u_1 + u_2 + \dots + u_{N_1}.$$

The null hypothesis H_0 is rejected if the number u exceeds the selected in accordance with the level of significance of the boundary, determined from the calculation that with the sample sizes of $N_1 > 10$ and $N_2 > 10$ the number of inversions u is approximately normally distributed with center:

$$M_u = \frac{N_1 N_2}{2}, \tag{7}$$

and the variance:

$$D_u = \frac{N_1 N_2}{12} (N_1 + N_2 + 1). \tag{8}$$

At a significance level of q and the normality of distribution of inversions number, the probability of not getting the value of u into the critical area (which means no refutation of the null hypothesis) is []:

$$P(|M_u - u| \leq \varepsilon) = 1 - q = 2\Phi\left(\frac{\varepsilon}{\sigma_u}\right), \tag{9}$$

where ε sets the value of the maximum deviation of the resulting estimate from the true value, i.e. ε represents the absolute value of the error in determining the values of the desired characteristics. At the same time, the confidence probability

$$P_d = P(|M_u - u| \leq \varepsilon)$$

indicates the probability of achieving the specified accuracy ε .

Let's fix the value of the confidence probability P_d , the values of the left and right critical boundaries will be, respectively, equal to:

$$u_1 = M_u - t_\alpha \sigma_u, \tag{10}$$

$$u_2 = M_u + t_\alpha \sigma_u, \tag{11}$$

where: $\sigma_u = \sqrt{D_u}$ – is the standard deviation of the number of inversions, t_α – is the root of the equation $2\Phi(t_\alpha) = P_d$,

$$t_\alpha = \Phi^{-1}\left(\frac{1-q}{2}\right).$$

The less is the significance level of q , the less likely is the possibility to reject the tested hypothesis when it is true, i.e., to make a mistake of the first kind. But with a decrease in the level of significance the range of admissible errors expands, which leads to the increase in the probability of making the wrong decision, i.e., committing type II errors. Typically, the significance level is selected following the considerations that the relevant events in the present situation of research are (with some risk) "practically impossible" ($q = 10\%$, 5% , 2% , 1% etc.).

Using the discussed above criterion of belonging of the two samples to the same general totality, let's carry out experimental studies of the network traffic properties of telecommunication systems and networks.

Let's carry out an experimental study of belonging of two samples of network traffic to the same general totality. For this, let's form the sample (1) – (2) at 100 time reference of randomly selected network traffic segments corresponding to different telecommunication and information services (YouTube (720p), YouTube (360p), Skype (voice), Skype (video), E-mail, HTTP, FTP), thus $N_1 = N_2 = 100$. Let's estimate selective average (3) – (4) and the dispersion (5) – (6), and expectation (7) and the dispersion (8) of the number of inversions:

$$M_u = \frac{N_1 N_2}{2} = 5000, D_u = \frac{N_1 N_2}{12} (N_1 + N_2 + 1) = 167500, \sigma_u \approx 409,3.$$

Let's suppose the significance level of $q = 10\%$. Using (9) to (10) – (11) let's calculate the values of the left and right critical borders:

$$P_d = 1 - q = 0,9,$$

$$t_\alpha = \Phi^{-1}\left(\frac{1-q}{2}\right) = \Phi^{-1}(0,45) \approx 1,65,$$

$$u_1 = M_u - t_\alpha \sigma_u \approx 4324,7,$$

$$u_2 = M_u + t_\alpha \sigma_u \approx 5675,3.$$

Let's consider the first case when the observed data of network traffic YouTube (720p) act as the sample x_1, x_2, \dots, x_{100} , and the data of network traffic YouTube (720p), YouTube (360p), Skype (voice), Skype (video), E-mail, HTTP and FTP alternatively act as the sample y_1, y_2, \dots, y_{100} .

The obtained results of the studies of belonging of the respective samples of network traffic to one and the same general totality are given in Table 7. The studies have been conducted for the different ways of representing of the network traffic, as in the form of packets' number transmitted per time unit, so as the number of bits transmitted per second.

The results of experimental studies provided in Table 6 indicate that the network traffic of YouTube (720p) service differs in its statistical properties from the network traffic of other services of a telecommunication system. By the criterion of belonging of the network traffic samples to one and the same general totality (Wilcoxon criterion) for different ways of representing of the network traffic (packet/s, bit/s) the number of the observed inversions U exceeds the selected in accordance with the level of significance border and the null hypothesis H_0 is rejected. At the same time, the Wilcoxon criterion gives a reliable mechanism for

detecting of the network traffic YouTube (720p), as a number of inversions u for the corresponding service is, as expected, close to the theoretical value $M_u = 5000$, the null hypothesis is rejected.

Table 6 – Results of research of belonging of network traffic samples to one and the same general totality (network traffic YouTube (720p))

Traffic type (service)	Representation of traffic as a packet/s		Representation of traffic as a bit/s	
	Inversions' number u	The decision on testing the hypothesis	Inversions' number u	The decision on testing the hypothesis
YouTube (720p)	5005	Accepted	5006	Accepted
YouTube (360p)	542	Rejected	572	Rejected
Skype (voice)	302	Rejected	300	Rejected
Skype (video)	2140	Rejected	364	Rejected
E-mail	54	Rejected	47	Rejected
HTTP	1732	Rejected	1011	Rejected
FTP	9539	Rejected	9960	Rejected

Let's consider the second case when the observed data of network traffic YouTube (360p) act as the sample x_1, x_2, \dots, x_{100} , and the data of other network traffic alternatively act as the sample y_1, y_2, \dots, y_{100} . The obtained results are shown in Table 8.

The data shown in Table 7 confirm the correctness of detection of network traffic YouTube (360p), as the results of studies of the belonging of samples to one and the same general totality in different presentation forms the number of the observed inversions u is close to the theoretical value $M_u = 5000$ ($u = 5006$ and $u = 5008$, respectively), the null hypothesis is not rejected. It should be also noted that by the Wilcoxon criterion, one should statistically differentiate the network traffic YouTube (360p) from the traffic services of most other services. HTTP traffic is the exception, which in each of the studied methods of presentation (packet/s and bits/s) is statistically indistinguishable from the traffic YouTube (360p), by Wilcoxon criterion belonging of these network traffic samples to the same general totality is not rejected.

Table 7 – Results of research of belonging of network traffic samples to one and the same general totality (network traffic YouTube (360p))

Traffic type (service)	Representation of traffic as a packet/s		Representation of traffic as a bit/s	
	Inversions' number u	The decision on testing the hypothesis	Inversions' number u	The decision on testing the hypothesis
YouTube (720p)	9555	Rejected	9525	Rejected
YouTube (360p)	5006	Accepted	5008	Accepted
Skype (voice)	7364	Rejected	2900	Rejected
Skype (video)	9502	Rejected	7542	Rejected
E-mail	1066	Rejected	590	Rejected
HTTP	5333	Accepted	4766	Accepted
FTP	989	Rejected	998	Rejected

The results of the study of the statistical properties of network traffic Skype (voice) and testing of the hypothesis that supplies statistical data to the same general totality are shown in Table 8.

Table 8 – Results of research of belonging of network traffic samples to one and the same general totality (network traffic Skype (voice))

Traffic type (service)	Representation of traffic as a packet/s		Representation of traffic as a bit/s	
	Inversions' number u	The decision on testing the hypothesis	Inversions' number u	The decision on testing the hypothesis
YouTube (720p)	9795	Rejected	9797	Rejected
YouTube (360p)	2764	Rejected	7171	Rejected
Skype (voice)	5003	Accepted	5008	Accepted
Skype (video)	10000	Rejected	10000	Rejected
E-mail	333	Rejected	212	Rejected
HTTP	3742	Rejected	5684	Rejected
FTP	10000	Rejected	10000	Rejected

The data presented in Table 9 show the difference in the average sense of the properties of the network traffic Skype (voice) and the properties of other services' traffic of a telecommunication system. The observed number of inversions lies in the critical area, indicating that the test samples belong to different general totalities. In other words, using the Wilcoxon criterion allows detecting Skype (voice) traffic with high reliability and distinguishing it from other network traffics.

The results of studies of the network traffic Skype (video) properties are shown in Table 10. The analysis of the obtained results shows that the traffic Skype (video) is statistically distinguishable from other traffic services, and using of the Wilcoxon criterion allows the detection of the corresponding service of a telecommunication system.

Table 10 shows the results of studies of network traffic samples belonging to one and the same general totality, obtained by analyzing statistical properties of the E-mail traffic network. Tables 11 and 12 show the results of similar studies of HTTP and FTP network traffic, respectively. The analysis shows that the network traffic of E-mail, and FTP services are statistically different by the Wilcoxon criterion from other traffic services, and for them there is no similarity observed in any of the investigated samples. At the same time, the statistical properties of the HTTP traffic are similar to the traffic observed in the operation of the service YouTube (360p). This is also confirmed by the data of Table 7.

Table 9 – Results of research of belonging of network traffic samples to one and the same general totality (network traffic Skype (video))

Traffic type (service)	Representation of traffic as a packet/s		Representation of traffic as a bit/s	
	Inversions' number u	The decision on testing the hypothesis	Inversions' number u	The decision on testing the hypothesis
YouTube (720p)	7932	Rejected	9733	Rejected
YouTube (360p)	604	Rejected	2586	Rejected
Skype (voice)	0	Rejected	0	Rejected
Skype (video)	5009	Accepted	5009	Accepted
E-mail	3	Rejected	0	Rejected
HTTP	2699	Rejected	3108	Rejected
FTP	9901	Rejected	10000	Rejected

Table 10 – Results of research of belonging of network traffic samples to one and the same general totality (network traffic E-mail)

Traffic type (service)	Representation of traffic as a packet/s		Representation of traffic as a bit/s	
	Inversions' number u	The decision on testing the hypothesis	Inversions' number u	The decision on testing the hypothesis
YouTube (720p)	947	Rejected	961	Rejected
YouTube (360p)	9016	Rejected	9483	Rejected
Skype (voice)	9774	Rejected	9890	Rejected
Skype (video)	999	Rejected	10000	Rejected
E-mail	5001	Accepted	5001	Accepted
HTTP	8095	Rejected	8320	Rejected
FTP	10000	Rejected	10000	Rejected

Table 11 – Results of research of belonging of network traffic samples to one and the same general totality (network traffic HTTP)

Traffic type (service)	Representation of traffic as a packet/s		Representation of traffic as a bit/s	
	Inversions' number u	The decision on testing the hypothesis	Inversions' number u	The decision on testing the hypothesis
YouTube (720p)	8314	Rejected	9056	Rejected
YouTube (360p)	4734	Accepted	5288	Rejected
Skype (voice)	6297	Rejected	4323	Rejected
Skype (video)	7327	Rejected	6923	Rejected
E-mail	1990	Rejected	1770	Rejected
HTTP	5003	Accepted	5009	Accepted
FTP	9893	Rejected	998	Rejected

Table 12 – Results of research of belonging of network traffic samples to one and the same general totality (network traffic FTP)

Traffic type (service)	Representation of traffic as a packet/s		Representation of traffic as a bit/s	
	Inversions' number u	The decision on testing the hypothesis	Inversions' number u	The decision on testing the hypothesis
YouTube (720p)	559	Rejected	137	Rejected
YouTube (360p)	29	Rejected	7	Rejected
Skype (voice)	0	Rejected	0	Rejected
Skype (video)	195	Rejected	0	Rejected
E-mail	2	Rejected	0	Rejected
HTTP	204	Rejected	4	Rejected
FTP	5007	Accepted	5007	Accepted

The final results of the conducted experimental studies are summarized in Tables 13, 14, which list the number of inversions and the results of testing the hypothesis of homogeneity of network traffic for different forms of representation (packet/s and bits/s, respectively).

Table 13 – The number of inversions and the results of testing the hypothesis of homogeneity of network traffic (packet/s)

	YouTube (720p)	YouTube (360p)	Skype (voice)	Skype (video)	E-mail	HTTP	FTP
YouTube (720p)	5005 «+»	9555 «-»	9795 «-»	7932 «-»	947 «-»	8314 «-»	559 «-»
YouTube (360p)	542 «-»	5006 «+»	2764 «-»	604 «-»	9016 «-»	4734 «+»	29 «-»
Skype (voice)	302 «-»	7364 «-»	5003 «+»	0 «-»	9774 «-»	6297 «-»	0 «-»
Skype (video)	2140 «-»	9502 «-»	10000 «-»	5009 «+»	999 «-»	7327 «-»	195 «-»
E-mail	54 «-»	1066 «-»	333 «-»	3 «-»	5001 «+»	1990 «-»	2 «-»
HTTP	1732 «-»	5333 «+»	3742 «-»	2699 «-»	8095 «-»	5003 «+»	204 «-»
FTP	9539 «-»	989 «-»	10000 «-»	9901 «-»	10000 «-»	9893 «-»	5007 «+»

Table 14 – The number of inversions and the results of testing the hypothesis of homogeneity of network traffic (bits/s)

	YouTube (720p)	YouTube (360p)	Skype (voice)	Skype (video)	E-mail	HTTP	FTP
YouTube (720p)	5006 «+»	9525 «-»	9797 «-»	9733 «-»	961 «-»	9056 «-»	137 «-»
YouTube (360p)	572 «-»	5008 «+»	7171 «-»	2586 «-»	9483 «-»	5288 «+»	7 «-»
Skype (voice)	300 «-»	2900 «-»	5008 «+»	0 «-»	9890 «-»	4323 «-»	0 «-»
Skype (video)	364 «-»	7542 «-»	10000 «-»	5009 «+»	10000 «-»	6923 «-»	0 «-»
E-mail	47 «-»	590 «-»	212 «-»	0 «-»	5001 «+»	1770 «-»	0 «-»
HTTP	1011 «-»	4766 «+»	5684 «-»	3108 «-»	8320 «-»	5009 «+»	4 «-»
FTP	9960 «-»	991 «-»	10000 «-»	10000 «-»	10000 «-»	998 «-»	5007 «+»

The following designations are applied in tables 13, 14:

«+» – the hypothesis of network traffic homogeneity is not rejected,

«-» – the hypothesis of network traffic homogeneity is rejected,

The results of the hypothesis testing shown in Tables 13 and 14 are symmetrical relatively to the main diagonal, which confirms the reliability of the obtained results in each specific experiment.

The analysis of the data provided in Tables 13 and 14 shows that in the process of the study of various telecommunication services network traffic samples in the majority of cases, the hypothesis of homogeneity is rejected, i.e., there is a correct decision on the belonging of the samples to various processes. This provision

may be made the basis of one of the elements of the system for network activity monitoring, i.e. by using the Wilcoxon criterion an initial detection of telecommunications service can be carried out.

One of the most important characteristics of a random variable is the index of dispersion, which allows comparison of the random parameters of the studied process to determine the significance of differences or matching their characteristics. The following section provides a variance analysis of individual services network traffic and TCS services based on an assessment of relations the variances sample, the statistical hypotheses about the homogeneity of the simulation results on this main index are checked.

CONCLUSIONS

1. The results of experimental studies of the statistical properties of network traffic using the correlation analysis of time series confirm the theoretical assumptions that for different types of traffic the result of the BDS-test gives different values that can be taken as a reference, i.e. and on this basis a network activity detection process of a separate service of a telecommunications network can be organized. Thus, the experimental data confirm the theoretical assumption about the possibility of using the values of the BDS-test to detect traces of malicious software in the network traffic.

2. The obtained results of the correlation analysis of the network traffic based on the BDS-test is recommended to be used, first, as part of the analytical component of modern anti-virus systems. Second, the correlation analysis of the network traffic may be used for the organization of one of the main elements of the system for monitoring network activity as a touch subsystem (sensors to collect traffic information) and as the analytical part (decision module component).

3. To solve the problem of individual telecommunications system's services detection in the observed network traffic, an evaluation unit of the significance differences of two or more samples (series) of independent observations in the network traffic (Wilcoxon criterion) is used. It allows to set different data streams belonging to the same general totality with a given accuracy and reliability.

4. Analysis of the obtained experimental research data shows that during the study of samples of network traffic of various telecommunication services in the majority of cases, the hypothesis of homogeneity is rejected, i.e., there is a correct decision on the belonging the samples to different processes. This position is recommended to be used as one of the elements of a system for monitoring network activity, i.e. through the use of the Wilcoxon criterion is offered to produce a primary detection of a telecommunication service.

5. A promising direction for further research is the assess of the relationship of the sample variances, statistical hypothesis testing in the uniformity of simulation results in terms of dispersion. The results of these studies are designed to perform a comparison of the random parameters of the tested process to determine the significance of differences or matching in their characteristics.

REFERENCES

- [1] Kharpuk N. M. The Statistic Analysis of the Network Traffic. Electronic Library of the Belarusian State University – 2008. – P. 116-119. [Electronic Resource]. Access regime: <http://elib.bsu.by/bitstream/123456789/7401/1/6.pdf>
- [2] NIST Special Publication 800-94. Guide to Intrusion Detection and Prevention Systems (IDPS). – Computer Security Division Information Technology Laboratory National Institute of Standards and Technology, Gaithersburg. – 127 pages (February 2007)
- [3] Brian Caswell, Jay Beale, Andrew Baker. Snort Intrusion Detection and Prevention Toolkit. – Syngress Media, U.S. 2006. <http://www.lehmanns.de/shop/sachbuch-ratgeber/21797174-9780080549279- snort-intrusion-detection-and-prevention-toolkit#drm1>
- [4] Ushakov D. V. Development of the Principles of Functioning of Network Intrusion Detection Systems Based on the Model of a Protected Distributed System: Ph. D Dis.: 05.13.19 Moscow, 2005 175 p.
- [5] Zapechnikov S. V., Miloslavskaya N. G., Tolstoy A. I., Ushakov D. V. Information Security in Open Systems. Textbook for high schools. In 2 volumes. – M., 2008. – V. II: Network Protection Tools. – 558 p.
- [6] Comparison of Firewall, Intrusion Prevention and Antivirus Technologies. http://www.juniper.net/solutions/literature/white_papers/200063.pdf
- [7] Intrusion Prevention Systems (IPS). <http://www.securecomputing.com/pdf/Intru-Preven-WP1-Aug03-vF.pdf>
- [8] Intrusion Prevention Systems (IPS). <http://hosteddocs.ittoolbox.com/BW013004.pdf>
- [9] State of the Practice of Intrusion Detection Technologies. <http://www.sei.cmu.edu/pub/documents/99.reports/pdf/99tr028.pdf>
- [10] Wireless Intrusion Detection and Response. http://users.ece.gatech.edu/~owen/Research/Conference%20Publications/wireless_IAW2003.pdf
- [11] Anomaly Detection in IP Networks. <http://users.ece.gatech.edu/~jic/ sig03.pdf>
- [12] Design and Implementation of an Anomaly Detection System: an Empirical Approach. <http://luca.ntop.org/ADS.pdf>
- [13] Host-Based Intrusion Detection Systems. <http://staff.science.uva.nl/~delaat/snb-2004-2005/p19/report.pdf>
- [14] Olifer V. G., Olifer N. A. computer Networks. Principles, Technologies, Protocols. Spb.: Piter, 2010. – 944 p.
- [15] Smirnov N. V., Dunin-Barkovski I. V., Course on Probability Theory and Mathematical Statistics for Technical Applications. Ed. 2. – M.: Nauka, 1969.-512 p.
- [16] Sheffe G., Variance Analysis: Trans. From Eng. Ed. 2. M.: Nauka, 1980. – 512 p.
- [17] Kuznetsov A. A. Method of Structural Identification of Information Flows in Telecommunication Networks Based on BDS-test / A. A. Kuznetsov, S. G. Semenov, S. N. Simonenko, E. V. Masleshko// Scientific and technical journal "Science and Technology of the Air Force of Ukraine". Publication 2 (4) – Kharkiv: KhAFU. – 2010. – P. 131 - 137.
- [18] Semenov S. The method of processing and identification of telecommunication traffic based on BDS-tests / S. Semenov, A. Smirnov., E. Meleshko // The book of materials International Conference «Statistical Methods of Signal and Data Processing (SMSDP-2010)» – Kiev, Ukraine, National Aviation University “NAU-Druk” Publishing House, October 13-14, 2010. – C.166-168. – engl.
- [19] B. LeBaron "A Fast Algorithm for the BDS Statistic", Studies in Nonlinear Dynamics and Econometrics. 1997. Vol. 2. No. 2. P. 53-59.
- [20] D. Chappell J. Padmore and C. Ellis. "A note on the distribution of BDS statistics for a real exchange rate series", Oxford Bulletin of Economics and Statistics, 58, 3, 561- 566, 1996.

Area-Delay Efficient Binary Adders in QCA

¹, D.Thirupathi Reddy M.Tech, ², Soma Prneeth Reddy ,
³, Katasani Sandeep Kumar Reddy, ⁴, Suddamalla Nagadastagiri Reddy,
⁵, S.K. khasid UG Students[B.Tech],

Dept of ECE Mekapati RajaMohan Reddy Institute of Technology and Science . Nellore,
India,

ABSTRACT:

As transistors decrease in size more and more of them can be accommodated in a single die, thus increasing chip computational capabilities. However, transistors cannot get much smaller than their current size. The quantum-dot cellular automata (QCA) approach represents one of the possible solutions in overcoming this physical limit, even though the design of logic modules in QCA is not always straightforward. In this brief, we propose a new adder that outperforms all state-of-the art competitors and achieves the best area-delay tradeoff.

The above advantages are obtained by using an overall area similar to the cheaper designs known in literature. The 64-bit version of the novel adder spans over 18.72 μm^2 of active area and shows a delay of only nine clock cycles, that is just 36 clock phases.

KEYWORDS -Verilog HDL, Xilinx 14.3.

I. INTRODUCTION

Quantum-dot cellular automata (QCA) are an attractive emerging technology suitable for the development of ultra dense low-power high-performance digital circuits. Quantum-dot cellular automata (QCA) which employs array of coupled quantum dots to implement Boolean logic function. The advantage of QCA lies in the extremely high packing densities possible due to the small size of the dots, the simplified interconnection, and the extremely low power delay product. A basic QCA cell consists of four quantum dots in a square array coupled by tunnel barriers. Electrons are able to tunnel between the dots, but cannot leave the cell. If two excess electrons are placed in the cell, Coulomb repulsion will force the electrons to dots on opposite corners. There are thus two energetically equivalent ground state polarizations can be labeled logic “0” and “1”. The basic building blocks of the QCA architecture are AND, OR and NOT. By using the Majority gate we can reduce the amount of delay. i.e by calculating the propagation and generational carries.

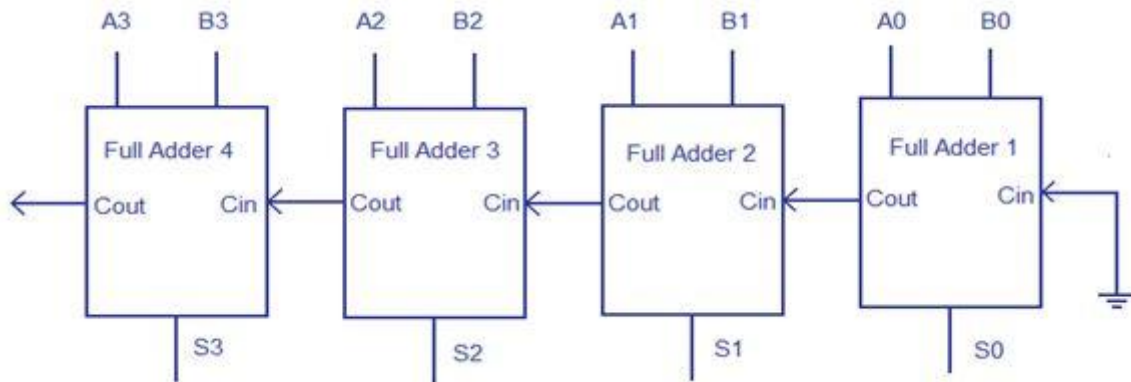
II. REGULAR METHOD

A. Description

Multiple full adder circuits can be cascaded in parallel to add an N-bit number. For an N-bit parallel adder, there must be N number of full adder circuits. A ripple carry adder is a logic circuit in which the carry-out of each full adder is the carry in of the succeeding next most significant full adder. It is called a ripple carry adder because each carry bit gets rippled into the next stage. In a ripple carry adder the sum and carry out bits of any half adder stage is not valid until the carry in of that stage occurs. Propagation delays inside the logic circuitry is the reason behind this. Propagation delay is time elapsed between the application of an input and occurrence of the corresponding output.

Consider a NOT gate, When the input is “0” the output will be “1” and vice versa. The time taken for the NOT gate’s output to become “0” after the application of logic “1” to the NOT gate’s input is the propagation delay here. Similarly the carry propagation delay is the time elapsed between the application of the carry in signal and the occurrence of the carry out (Cout) signal.

B. RCA architecture



C. Basic Full adder block

To understand the working of a ripple carry adder completely, you need to have a look at the full adder too. Full adder is a logic circuit that adds two input operand bits plus a Carry in bit and outputs a Carry out bit and a sum bit.. The Sum out (Sout) of a full adder is the XOR of input operand bits A, B and the Carry in (Cin)bit. Truth table and schematic of a 1 bit Full adder is shown below

There is a simple trick to find results of a full adder. Consider the second last row of the truth table, here the operands are 1, 1, 0 ie (A, B, Cin). Add them together ie $1+1+0 = 10$. In binary system, the number order is 0, 1, 10, 11..... and so the result of $1+1+0$ is 10 just like we get $1+1+0 = 2$ in decimal system. 2 in the decimal system correspond to 10 in the binary system. Swapping the result “10” will give $S=0$ and $Cout = 1$ and the second last row is justified.

Inputs			Outputs	
A	B	Cin	Cout	S
0	0	0	0	0
1	0	0	0	1
0	1	0	0	1
1	1	0	1	0
0	0	1	0	1
1	0	1	1	0
0	1	1	1	0
1	1	1	1	1

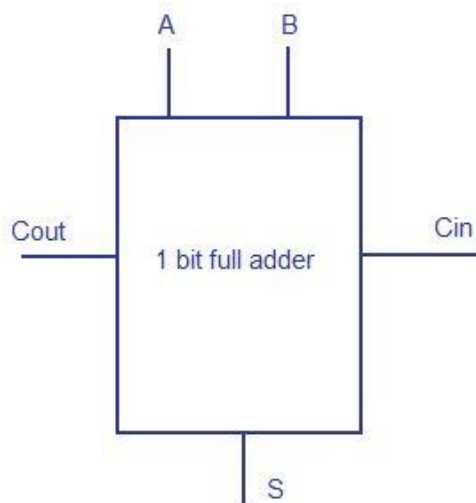


Fig ; 1 bit full adder schematic and truth table

III. PROPOSED METHOD

A.Description

Quantum Dot Cellular Automata (sometimes referred to simply as quantum cellular automata, or QCA) are proposed models of quantum computation, which have been devised in analogy to conventional models of cellular automata introduced by von Neumann. Standard solid state QCA cell design considers the distance between quantum dots to be about 20 nm, and a distance between cells of about 60 nm. Just like any CA, Quantum (-dot) Cellular Automata are based on the simple interaction rules between cells placed on a grid. A QCA cell is constructed from four quantum dots arranged in a square pattern. These quantum dots are sites electrons can occupy by tunneling to them.

B. Cell Design

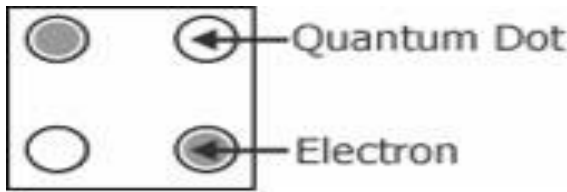


Fig: Simplified Diagram of QCA Cell

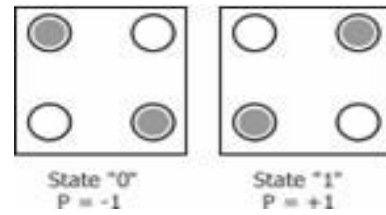


Fig :Four Dot Quantum Cell

C. Structure of Majority gate

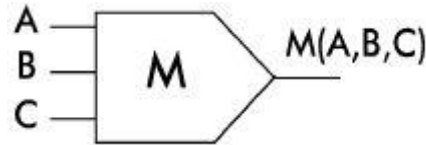


Fig: Structure of Majority gate

D. QCA Majority Gate:

The QCA majority gate performs a three-input logic function. Assuming the inputs are A ,B and C, the logic function of the majority gate is

$$M = AB + BC + CA$$

E. Architecture of Basic Novel 2-bit adder

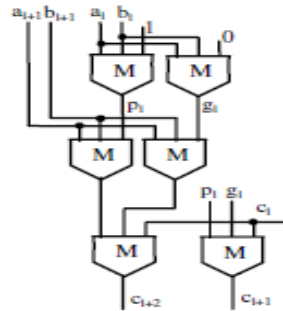
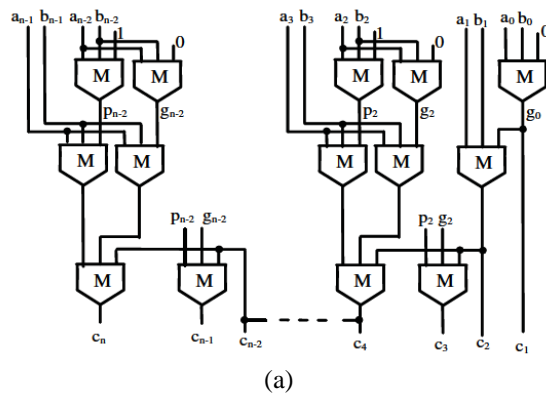
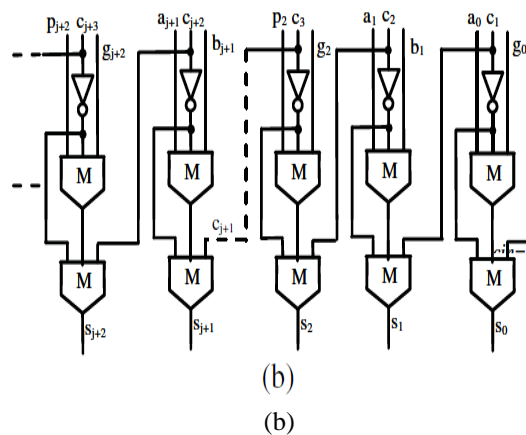


Fig: ARCHITECTURE OF BASIC NOVEL 2-BIT ADDER

To introduce the novel architecture proposed for implementing ripple adders in QCA, let consider two n -bit addends $A = a_{n-1}, \dots, a_0$ and $B = b_{n-1}, \dots, b_0$ and suppose that for the i th bit position (with $i = n - 1, \dots, 0$) the auxiliary propagate and generate signals, namely $p_i = a_i + b_i$ and $g_i = a_i \cdot b_i$, are computed. c_i being the carry produced at the generic $(i-1)$ th bit position, the carry signal c_{i+2} , furnished at the $(i+1)$ th bit position.



Fig Novel n -bit adder (a) carry chain and (b) sum block.

IV. CONCLUSION

The reduced number of gates of this work offers the great advantage in the reduction of area and also the total delay. The QCA architecture is therefore, low area, low delay, simple and efficient for VLSI hardware implementation. It would be interesting to test the design of the modified 128-bit Novel adders.

V. ACKNOWLEDGMENT

The authors would like to thank D.Thirupathi Reddy, the VLSI Division, MRRITS, Udayagiri, India, for their contributions to this work.

REFERENCES

- [1] C. S. Lent, P. D. Tougaw, W. Porod, and G. H. Bernstein, "Quantum cellular automata," *Nanotechnology*, vol. 4, no. 1, pp. 49–57, 1993.
- [2] M. T. Niemer and P. M. Kogge, "Problems in designing with QCAs Layout = Timing," *Int. J. Circuit Theory Appl.*, vol. 29, no. 1, pp. 49–62, 2001.
- [3] J. Huang and F. Lombardi, *Design and Test of Digital Circuits by Quantum-Dot Cellular Automata*. Norwood, MA, USA: Artech House, 2007.
- [4] W. Liu, L. Lu, M. O'Neill, and E. E. Swartzlander, Jr., "Design rules for quantum-dot cellular automata," in *Proc. IEEE Int. Symp. Circuits Syst.*, May 2011, pp. 2361–2364.
- [5] K. Kim, K. Wu, and R. Karri, "Toward designing robust QCA architectures in the presence of sneak noise paths," in *Proc. IEEE Design, Autom. Test Eur. Conf. Exhibit.*, Mar. 2005, pp. 1214–1219.
- [6] K. Kong, Y. Shang, and R. Lu, "An optimized majority logic synthesis methodology for quantum-dot cellular automata," *IEEE Trans. Nanotechnology*, vol. 9, no. 2, pp. 170–183, Mar. 2010.
- [7] K. Walus, G. A. Jullien, and V. S. Dimitrov, "Computer arithmetic structures for quantum cellular automata," in *Proc. Asilomar Conf. Signals, Syst. Comput.*, Nov. 2003, pp. 1435–1439.



D.Thirupathi Reddy B.Tech from JNTU Anantapur University, M.Tech from JNTU Anantapur University. He is working as Assistant Professor ECE Department of Mekapati Rajamohan Reddy Institute of Technology and Science, Udayagiri, SPSRNellore, Dt, A.P, INDIA-524226. He was the member for Techno vision-2K5, Techno vision-2K6, and Techno vision-2K13 held in the Rajamohan Reddy Institute of Technology and Science, Udayagiri, SPSRNellore, Dt, A.P. He published one International journal. He attended work shop on "cadence tool", Faculty Development programs and technical symposiums.



Soma Praneeth Reddy, Studying B.Tech(ECE) at Mekapati RajaMohanReddy Institute of Technology and Science(MRRITS), SPSR Nellore,AP,and doing projectwork on Area-Delay Efficient Binary Adders In QCA with Reduced Area&Delay Application , Attended one national level technical seminars, one national level workshop.



Katasani Sandeep kumar reddy ,Studying B.Tech(ECE) at Mekapati RajaMohanReddy Institute of Technology and Science(MRRITS), SPSR Nellore,AP,and doing projectwork on Area-Delay Efficient Binary Adders In QCA with Reduced Area&Delay Application.



Suddamalla Nagadastagiri Reddy, Studying B.Tech(ECE) at Mekapati RajaMohanReddy Institute of Technology and Science(MRRITS), SPSR Nellore,AP,and doing projectwork on Area-Delay Efficient Binary Adders In QCA with Reduced Area&Delay Application.Attended More than three national level technical seminars,two national level workshops.



S.k.Khasid, Studying B.Tech(ECE) at Mekapati RajaMohanReddy Institute of Technology and Science(MRRITS), SPSR Nellore,AP,and doing projectwork on Area-Delay Efficient Binary Adders In QCA with Reduced Area&Delay Application.

Efficient Multicast Algorithms for Wireless Mesh Networks

Dr.Sivaagorasakthivelmurugan¹, P.Ravi Shankar²

Associate Professor¹, Assistant Professor²

Department of EEE¹, Department of EEE²,

SreeSakthi Engineering College, Nehru Institute of Engineering and Technology,
Coimbatore

ABSTRACT

Wireless Mesh Networks (WMN) are promising and emerging technology for providing low cost and high quality internet service to the end user. The Lookup algorithm (LU) in wireless infrastructure enables the possibility of ID assignment of peers and 1-hop broadcast between peers through cross-layering technique. Thus message overhead reduces and increase information retrieval performance. Channel assignment (CA) algorithm builds efficient multilevel trees and reduces the number of relay nodes and hop distances of the trees. The algorithms use dedicated channel assignment strategies to reduce the interference to improve the network capacity. The result of our study enables efficient resource sharing and best throughput is performed in wireless mesh network.

Keywords – Wireless Mesh Network, Cross-layering technique, Channel Assignment.

I. INTRODUCTION

Wireless mesh network is the next generation technology for providing low cost and efficient internet access to the end users. Mesh networks are classified by the use of multiple channels and multiple interfaces. Wireless mesh networks come in a range of architectures and functional components. The wireless mesh networks are comprised into, classification of mesh networks, communication technologies for mesh networks and the key differences between mesh networks and traditional wireless multi-hop networks. Mesh networks comprise of three types of nodes: Mesh Routers (or Access Points - APs), Mesh Clients and Gateway Routers. Gateway routers at the top border provide wired connectivity to the Internet. The mesh routers at the other border act as access points for mesh clients and user networks. Peer-to-peer systems and applications are distributed systems without any centralized control or hierarchical organization, where the software running at each node is equivalent in functionality. A review of the features of recent peer-to-peer applications yields a long list: redundant storage, permanence, selection of nearby servers, anonymity, search, authentication, and hierarchical naming. Despite this rich set of features, the core operation in most peer-to-peer systems is efficient location of data items. The contribution of this paper is a scalable protocol for lookup in a dynamic peer-to-peer system with frequent node arrivals and departures.

Three features that distinguish Lookup algorithm from many other lookup protocols are its simplicity, provable correctness, and provable performance. Chord is simple, routing a key through a sequence of other nodes toward the destination. A node requires information about other nodes for efficient routing, but performance degrades gracefully when that information is out of date. This is important in practice because nodes will join and leave arbitrarily, and consistency of even state may be hard to maintain. Only one piece of information per node needs to be correct in order for Chord to guarantee correct routing of queries; lookup program has a simple algorithm for maintaining this information in a dynamic environment. Traditional casting protocols for wireless networks assume that each node is equipped with one interface. A mesh network provides the nodes with multiple interfaces that can be used to improve the throughput substantially. However, channel assignment is subject to the number of available channels and interfaces, the network topology, the communication requests, and other factors. Interference cannot be completely eliminated due to the limited number of available channels. An inappropriate channel assignment strategy will result in throughput reduction due to the multichannel hidden terminal problem [3], disconnection of the topology [4], or unfair bandwidth allocation to various users [5].

The rest of this paper is structured as follows. Section 2 describes the design model and its function. Section 3 consists of distributed lookup protocol. Section 4 presents the functions of channel assignment protocol. Section 5 demonstrates about algorithms performance through simulation and experiments on a deployed prototype. Finally, we describe outline for future work in Section 6 and summarize our contributions in Section 7.

II. SYSTEM MODEL

A. Introduction

THE design simplifies the systems based on by addressing many problems and by introducing basic techniques for channel assignment algorithms followed by design considerations for CA algorithms in WMNs.

B. Design Consideration

The design simplifies the design of mesh systems and applications based on it by addressing these difficult problems:

Load balance: Chord acts as a distributed hash function, spreading keys evenly over the nodes; this provides a degree of natural load balance.

Decentralization: Chord is fully distributed: no node is more important than any other. This improves robustness and makes Chord appropriate for loosely-organized peer-to-peer applications.

Scalability: The cost of a Chord lookup grows as the log of the number of nodes, so even very large systems are feasible. No parameter tuning is required to achieve this scaling.

The following are examples of applications for lookup provide a good foundation.

Cooperative Mirroring, as outlined in a recent proposal [6]. Imagine a set of software developers, each of whom wishes to publish a distribution. Demand for each distribution might vary dramatically, from very popular just after a new release to relatively unpopular between releases. An efficient approach for this would be for the developers to cooperatively mirror each others' distributions. Ideally, the mirroring system would balance the load across all servers, replicate and cache the data, and ensure authenticity. Such a system should be fully decentralized in the interests of reliability, and because there is no natural central administration.

Time-Shared Storage for nodes with intermittent connectivity. If a person wishes some data to be always available, but is only occasionally available, they can offer to store others' data while they are up, in return for having their data stored elsewhere when they are down. The data's name can serve as a key to identify the (live) Chord node responsible for storing the data item at any given time. Many of the same issues arise as in the Cooperative Mirroring application, though the focus here is on availability rather than load balance. To improve the throughput of WMNs, many studies have been conducted on how to assign orthogonal channels to adjacent wireless links to minimize interference. It is known that 802.11b/g and 802.11a provide 3 and 12 nonoverlapping channels, respectively. Although 802.11a provides more nonoverlapping channels than 802.11b/g, it has several drawbacks. Because 802.11a works on a higher frequency spectrum (5 GHz) than 802.11b/g (2 GHz), it is more difficult to penetrate walls and other obstructions, and thus 802.11a has a shorter range. Through experiments, we observe that the interference between two links depends on both their physical distance and channel separation [6]. Unlike the traditional interference model, the interference range is no longer a constant. Instead, it varies with the channel separation. Let I_c be the interference range of two links with channel separation c . That means, when the channel separation of two links is c , they will interfere with each other if their distance is less than I_c , and otherwise not. For example, $I_0 \approx \frac{1}{4} 2R$, which means the same channel can be used on two links without any interference only when they are over twice the transmission range away.

III. LOOKUP ALGORITHM

The Lookup protocol specifies how to find the locations of keys, new nodes join the system, and how to recover from the failure (or planned departure) of existing nodes. This section describes a simplified version of the protocol that does not handle concurrent joins or failures. Section 5 describes enhancements to the base protocol to handle concurrent joins and failures.

A. Hashing Function

Consistent hashing assigns keys to nodes as follows. Identifiers are ordered in an *identifier circle with m* modulo K is assigned to the first node whose identifier is equal to or follows in the identifier space. This node is called the *successor node* of key denoted by *successor*. If identifiers are represented as a circle of number is the first node clockwise from Figure 2 shows an identifier circle with the circle has three nodes: 0, 1, and 3. The successor of identifier 1 is node 1, so key 1 would be located at node 1. Similarly, key 2 would be located at node 3, and key 6 at node 0. Consistent hashing is designed to let nodes enter and leave the network with minimal disruption. To maintain the consistent hashing mapping when a node joins the network, certain keys previously assigned to successor now become assigned to leaves the network, all of its assigned keys are reassigned to successor. No other changes in assignment of keys to nodes need occur. In the example above, if a node were to join with identifier 7, it would capture the key with identifier 6 from the node with identifier 0. The following results are proven in the papers that introduced consistent hashing [11, 13].

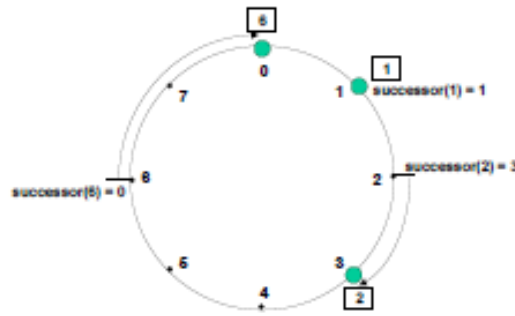


Figure 1: an identifier circle consisting of the three nodes 0, 1, and 3

A very small amount of routing information suffices to implement consistent hashing in a distributed environment. Each node need only be aware of its successor node on the circle. Queries for a given identifier can be passed around the circle via these successor pointers until they first encounter a node that succeeds the identifier; this is the node the query maps to. A portion of the Chord protocol maintains these successor pointers, thus ensuring that all lookups are resolved correctly. However, this resolution scheme is inefficient: it may require traversing all N nodes to find the appropriate mapping. To accelerate this process, Chord maintains additional routing information. This additional information is not essential for correctness, which is achieved as long as the successor information is maintained correctly. As before, let m be the number of bits in the key/node identifiers. Each node, maintains a routing table with m entries, called the *finger table*.

The pseudo code that implements the search process is shown in Figure 2. The notation $n.foo()$ stands for the function $foo()$ being invoked at and executed on node n . Remote calls and variable references are preceded by the remote node identifier, while local variable references and procedure calls omit the local node. Thus $n.foo()$ denotes a remote procedure call on node n , while $n.bar$, without parentheses, is an RPC to lookup a variable bar on node n . $find_successor$ works by finding the immediate predecessor node of the desired identifier; the successor of that node must be the successor of the identifier. We implement $find_predecessor$ explicitly, because it is used later to implement the joint operation. In a dynamic network, nodes can join (and leave) at any time. The main challenge in implementing these operations is preserving the ability to locate every key in the network. To achieve this goal, Chord needs to preserve two invariants:

1. Each node's successor is correctly maintained. For every key K , node $successor(k)$ is responsible for k . In order for lookups to be fast, it is also desirable for the finger tables to be correct. To preserve the invariants stated above, Chord must perform three tasks when a node joins the network:

1. Initialize the predecessor and fingers of node n .
2. Update the fingers and predecessors of existing nodes to reflect the addition of n .
3. Notify the higher layer software so that it can transfer state associated with keys that node is now responsible.

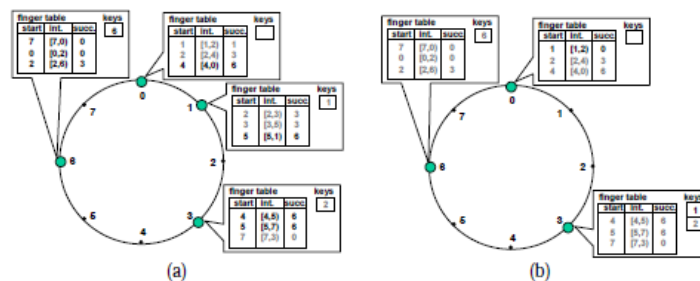


Figure 2: (a) Finger tables and key locations after node 6 joins. (b) Finger tables and key locations after node 3 leaves.

IV. CHANNEL ASSIGNMENT ALGORITHM

Routing protocols do exist to offer efficient multicasting service for conventional multihop wireless networks, such as MANETs and wireless sensor networks. Since the nodes become increasingly mobile or the networks only have scarce resources such as power constraints and limited computing ability, most previous work pays much attention to energy efficiency and how to build the multicast structure without knowing the global topology. As a result, the multicast structure should be distributably constructed, energy efficient, and should take care of the topology change as well as group member management, which may conflict with maximizing the throughput of the network to some extent. However, since mesh networks are deployed to provide last-mile Internet access for enterprises or communities, the throughput and the network capacity are the

major concerns. Deployed at fixed locations, mesh routers have limited mobility. Furthermore, they are computationally powerful and do not rely on battery power compared with their counterparts in MANETs or sensor networks, which help to achieve sufficient network capacity to meet the requirement of applications such as audio or video sharing among end users. Thus, we need to create a multicast structure that aims to deliver the packets rapidly to the multireceivers(multireceivers are defined as the multicast group members except for the source node) without worrying about the energy consumption and topology changes.

A common method for multicast is to build a multicast tree,where the source node is usually the gateway. In this paper, we first propose the LCA algorithm, which can be achieved by the following steps. First, the nodes obtain their level information. The BFS is used to traverse the whole network. All the nodes are partitioned into different levels according to the hop count distances between the source and the nodes.

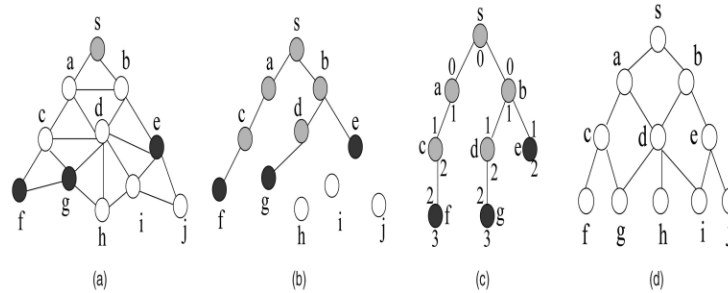


Figure 3: An example for CA and tree mesh. (a) Network topology, (b) multicast tree, (c) channel assignment, and (d) tree mesh. Figs. 3a and 3d give an example of the original network channel at the same level. For example, in Fig. 3c, since g is in the transmission range of both c and d, there will be interference when c and d use the same channel. Second, when the number of available channels is more than that of the levels, some channels will not be utilized, which is a waste of channel diversity. Third, the channel assignment does not take the overlap property of the two adjacent channels into account. As we know channel i and channel i+1 are adjacent in frequency, so they partially interfere with each other. Thus, the channel i for level i still has some interference effect with the channel i+1 for level i+1.

V. SIMULATION RESULTS

A. Delay Comparison

Total number of network-level packets exchange by no. of nodes to maintain the overlay, and to resolve the queries. the delay is the average time it takes for a packet to reach the destination after it leaves the source.

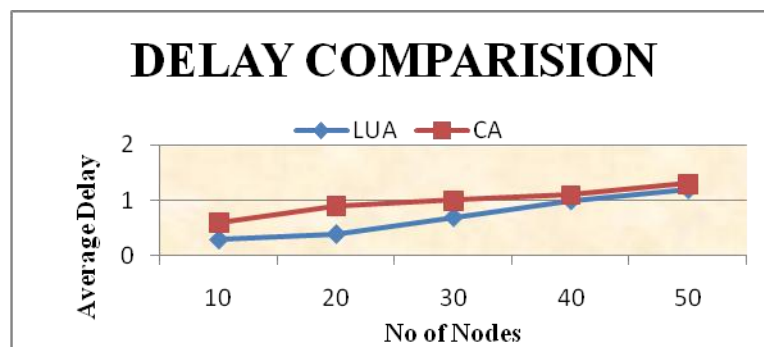


Figure 4: Delay Comparison

From figure 4 shows the comparison of average delay between the number of nodes and the performance of lookup algorithm and channel assignment algorithm where the delay in channel assignment is large compared to the lookup algorithm is less.

B. Average Response Time

Percentage of queries which are successfully resolved; a query on key k is successfully resolved if the ip address of the peer responsible for key k is returned to the peer which issued the query.

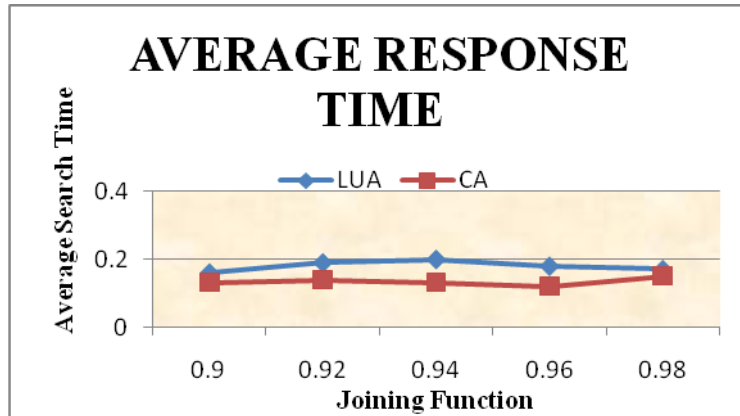


Figure 5: Average Response Time

The above Figure 5 shows the comparison between average search time and joining function of the nodes. It compares the successful queries of the nodes between the LUA algorithm and CA algorithm lookup algorithm will outperform more loss when compare to the channel assignment algorithm.

C. Throughput Comparison

The throughput is the average number of packets each multireceiver receives during a time unit.

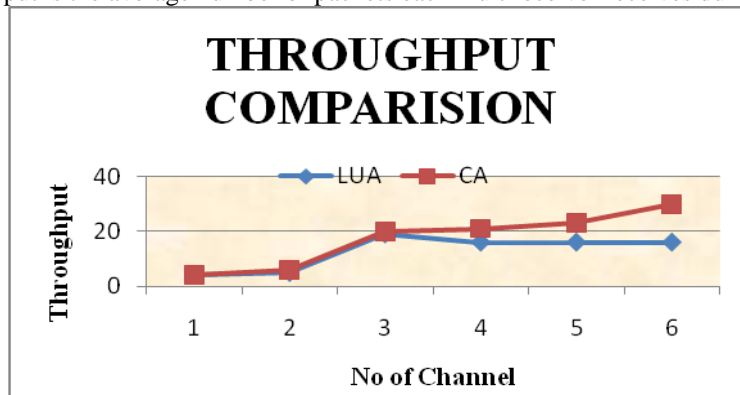


Figure 6: Throughput Comparison

The above figure6 shows the comparison of throughput between the number of channels from the comparison it is clearly knows that the channel increases from the number of nodes channel assignment algorithm performs high throughput when compare to lookup algorithm.

D. Average Query Response Time

For successful queries, the time elapsed between the instant the query is issued by node n and the instant answer is received at the node n.

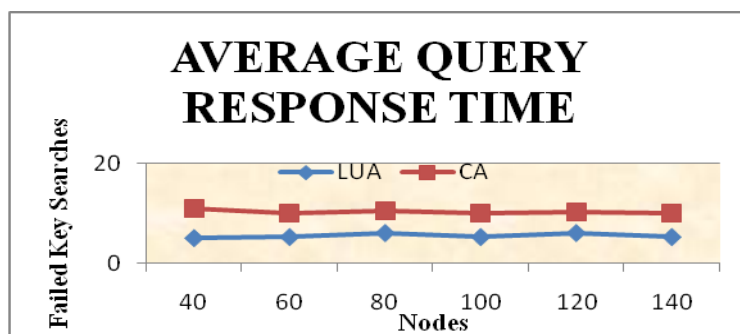


Figure 7: Average Query Response Time

Figure 7 we consider number of nodes and its successful query rates of the nodes during the joining functions in the channel assignment between more number of nodes.

VI. CONCLUSION

In this paper, we carefully evaluated the performance of lookup algorithm and channel assignment algorithm through NS2 (network simulator-2). The proposed algorithm utilized for implementing file/resource sharing application and the dedicated channel assignment helps to further reduce the interference in wireless mesh networks. Although our performance evaluation shows the outperform of overlay maintenance and single channel assignment in terms of throughput delay.

In future further improve the message overhead and to improve throughput and reduce delay in the multi channel multi interfaces.

REFERENCES

- [1] Al Hamra, C. Barakat, and T. Turletti, "Network Coding for Wireless Mesh Networks: A Case Study," Proc. IEEE Int'l Symp. World of Wireless, Mobile and Multimedia (WoWMoM), 2006.346 IEEE TRANSACTIONS ON MOBILE COMPUTING, VOL. 9, NO. 3, MARCH 2010
- [2] M. Caesar, M. Castro, E.B. Nightingale, G. O'Shea, and A. Rowstron, "Virtual Ring Routing: Network Routing Inspired by DHTs," Proc. ACM SIGCOMM, pp. 351-362, 2006.
- [3] Canali, M.E. Renda, and P. Santi, "Evaluating Load Balancing in Peer-to-Peer Resource Sharing Algorithms for Wireless Mesh Networks," Proc. IEEE Workshop Enabling Technologies and Standards for Wireless Mesh Networking (MeshTech), pp. 603-609, 2008.
- [4] M. Conti, E. Gregori, and G. Turi, "A Cross-Layer Optimization of Gnutella for Mobile Ad Hoc Networks," Proc. ACM MobiHoc, May 2005.
- [5] Cramer and T. Fuhrmann, "Performance Evaluation of Chord in Mobile Ad Hoc Networks," Proc. ACM Int'l Workshop Decentralized Resource Sharing in Mobile Computing and Networking (MobiShare), pp. 48-53, 2006.
- [6] M. Denny, M. Franklin, P. Castro, and A. Purakayastha, "Mobiscope: A Scalable Spatial Discovery Service for Mobile Network Resources," Proc. Int'l Conf. Mobile Data Management (MDM), 2003.
- [7] P. Desnoyers, D. Ganesan, and P. Shenoy, "TSAR: A Two Tier Sensor Storage Architecture Using Interval Skip Graphs," Proc. ACM Conf. Embedded Networked Sensor Systems (SenSys), Nov. 2005.
- [8] T. Fuhrmann, "Scalable Routing for Networked Sensors and Actuators," Proc. IEEE Comm. Soc. Conf. Sensor and Ad Hoc Comm. Networks (SECON), pp. 240-251, 2005.
- [9] K. Ramachandran, E.M. Belding, K. Almeroth, and M. Buddhiko, "Interference-Aware Channel Assignment in Multi-Radio Wireless Mesh Networks," Proc. IEEE INFOCOM, 2006.
- [10] J. Tang, G. Xue, and W. Zhang, "Maximum Throughput and Fair Bandwidth Allocation in Multi-Channel Wireless Mesh Networks," Proc. IEEE INFOCOM, 2006.
- [11] Mishra, V. Shrivastava, and S. Banerjee, "Partially Overlapped Channels Not Considered Harmful," Proc. ACM SIGMETRICS/Performance, 2006.
- [12] P. Li, N. Scalabrino, Y. Fang, E. Gregori, and I. Chlamtac, "Channel Interference in IEEE 802.11b Systems," Proc. IEEE Global Telecomm. Conf. (GLOBECOM), 2007.
- [13] T.H. Cormen, C.E. Leiserson, R.L. Rivest, and C. Stein, Introduction to Algorithms. The MIT Press, 2001.
- [14] <http://www.isi.edu/nsnam/ns/index.html>, 2009.
- [15] Royer and C. Perkins, "Multicast Operation of the Ad-Hoc on Demand Distance Vector Routing Protocol," Proc. ACM MobiCom, 1999.

Subaltern Voice in Shakespeare: A Study in The Tempest

Tribeni Mandal,

Asst.Prof., Science College, Kokrajhar, Affiliated to Gauhati University

ABSTRACT:

The term “subaltern” is an allusion to the work of Antonio Gramsci (1891-1973), an Italian Marxist. It means a person or group of persons belonging to an inferior rank and station, may be for race, class, gender, sexual orientation, ethnicity or religion. In 1980s, there arose a group named Subaltern Studies Group (SSG). It was influenced by the scholarship of Eric Stokes and Ranajit Guha. They tried to formulate a new narrative of the history of India and South Asia. They focused on the subalterns or the non-elites as agents of social and political change. This paper in its present form is the result of a study on Shakespeare and the subaltern where an analysis will be made on some of the works of Shakespeare and his treatment of the marginalized section of the society in them with a special reference to the subaltern characters in *The Tempest*. This paper uses Gramsci’s conception of hegemony where it is “a condition in which the supremacy of a social group is achieved not only by physical force” but also through consensual submission of the very people who were dominated (Litowitz 2000,p.518). According to Gramsci there are two levels of hegemony. “These two levels correspond on one hand to the function of ‘hegemony’ which the dominant group exercises throughout society and on the other hand to that of ‘direct domination’ or command exercised through the state and the ‘juridical’ government” (Gramsci 1971,p.12). In *The Tempest* one can find a reflection of England’s colonial expansion. The play has been undoubtedly interpreted as a play about colonialism. It is simply for Prospero’s coming to Sycorax’s island, subduing her, ruling and imposing his own culture on the natives. Prospero tries to civilize and educate Caliban but with the accompaniment of politics of dominization over the colonized.

KEY WORDS : Subaltern, Antonio Gramsci, Italian Marxist, Subaltern Studies Group (SSG), Eric Stokes, Ranajit Guha, Shakespeare, Marginalised.

I. INTRODUCTION

The term subaltern refers to any person or group of inferior rank and station, may be for race, class, gender, sexual orientation, ethnicity or religion. It is the social group who is socially, politically and geographically outside of the hegemonic power structure of the colony and of the colonial homeland. It is derived from the cultural hegemony work of Antonio Gramsci, which identified the social groups who are excluded from a society’s established structures for political representation, the means by which people have a voice in their society. In Post-colonial theory, the term Subaltern describes the lower classes and the social groups who are at the margins of a society. But Gayatri Spivak advised against a too broad application of the term. The subalterns are peoples who have been silenced in the administration of the colonial states they constitute. Gayatri Spivak in an essay titled, “Can the subaltern Speak?” wrote: The Subaltern cannot speak. There is no virtue in global laundry lists with woman as a pious. Representation has not withered away. The female intellectual has a circumscribe task which she must not disown with a flourish. (p.308) She put emphasis on the pitiable condition of women who are not only oppressed by patriarchy but also by colonialism. The most famous name among all Subaltern Historians is unquestionably Ranajit Guha. The most powerful example of subaltern historical scholarship is his *Elementary Aspects of Peasants Insurgency in Colonial India* where he offers a fascinating account of the peasants’ insurgent consciousness, rumours, mystic visions, religiosity and bonds of community.

Shakespeare’s plays often resurface with female characters which tell us not only his view of women but also their status in Shakespeare’s time. These characters are of a bawdy woman like the Nurse in *Romeo and Juliet*, Margaret in *Much Ado About Nothing* or Audrey in *As You Like It*; the tragic innocent woman like Juliet in *Romeo and Juliet*, Lavinia in *Titus Andronicus*, or Ophelia in *Hamlet*; the scheming *Femme Fatal* like

lady Macbeth in *Macbeth* or King Lear's daughters, Goneril and Regan in *King Lear*; the witty woman like Katherine in *The Taming of The Shrew*; the married woman who dresses as men like Rosalind in *As You Like It* and Viola in *Twelfth Night*; women falsely accused of Adultery like Desdemona in *Othello* and Hero in *Much Ado About Nothing*. The construction of female characters in Shakespeare's plays reflects the Elizabethan image of woman in general. They have been bound to rules and conventions of the Patriarchal Elizabethan era. In his comedies the world of women is safe where she is happy and comes to full flowering. Shakespeare has created every shade of womanhood, from Miranda's simplicity and innocence to Cleopatra's eternal courtesan. His women are extremely individualized even when they resemble the particular one. Coming to the tragic heroines, they are pathetic, helpless and are always eclipsed by the towering personality of the hero. Except Cleopatra, everyone from Ophelia to Desdemona and Cordelia are all helpless and pathetic. Shakespeare's women are very practical, lively and resourceful. They take the stage in the grip of their hand. One can find the simplicity in thought, frankness and eloquency in discourse in the characters of Rosalind, Portia and Viola. Shakespeare's heroines are uplifted by love and they are self-sacrificing, passionate, virtuous and chaste.

II. Objectives And Methodology

The objective of the paper is to make an analysis of the subaltern characters in Shakespeare with a special emphasis on the characters in *The Tempest*. The methodology used here is analytical and help of secondary sources of information has been taken like journals, articles, books etc.

III. DISCUSSION

Helen Zimmern, in the preface to the English translation of Louis Lewe's Study *The Women of Shakespeare*, argued in 1895 that "of Shakespeare's dramatis personae, his women are perhaps the most attractive, and also, in a sense, his most original creations, so different are they, as a whole, from the ideals of the feminine type prevalent in the literature of his day." In Shakespeare's plays female characters play an important role for the dramatic run of events. Women in Elizabethan period were considered as the weaker sex and they represented virtues like obedience, silence, sexual chastity, piety, humility, constancy and patience. Women in that period were the housewives and mothers. But within this deprived, tight and organized schedule, they have been represented in their most diverse ways by the Bard. In Shakespeare's time women had less freedom than their male counterparts. Women who were born high are presented in his plays as mere possessions only who would have been passed from father to the husbands. They are socially bound and restricted within a framework in such a way that they are unable to move or see the world around them without servants or maids. They are always under the strict guidance of their men.

Women in Shakespeare's plays who are socially low are shown as sexually aware. Women are never totally free in the plays of Shakespeare for they are always in the possession of either the husbands or the fathers. Some are even owned by their employers. Shakespeare suspected women in power and are thus portrayed having a questionable moral. Here one can take the case of Gertrude and Lady Macbeth where the former is shown marrying her husband and the latter is shown as a lady who compels her husband into murder and both of them meet their fate as a penalty for their own act. No doubt, Shakespeare gave enough space to his female protagonists still his plays do not address the role of women royalty. In both *Hamlet* and *Macbeth*, Shakespeare implicitly states the danger of women being in power. The real political issues of the Elizabethan era were dramatized through the portrayal of the character of Hamlet's mother, Gertrude and also through Lady Macbeth's passionate and uncontrolled ambition for power. Gender anxieties are reflected and the chaos created as such from this kind of anxiety is revealed. Female leadership is thus questioned by Shakespeare. Desire for stability clearly demonstrates itself in both *Macbeth* and *Hamlet*. In *Macbeth*, a suggestion of Kingship and power leads Lady Macbeth to convince and instigate her husband to commit a crime by murdering the King and crowning himself. In *Hamlet*, Gertrude the mother of Hamlet marries Claudius, the uncle and the murderer of his father. Their union throws the power of the crown in dispute between Hamlet, the King's son and Claudius, now husband of the Queen. In both these plays, women and their actions lead to instability in the state and a break of peace occurs as a result. Each drama reflects social anxieties from female rule. Lady Macbeth's disruption emerges from her ambition and this ambition is made high by her gender. After reading *Macbeth*'s revelation of the witches' predictions, she thinks that only her insistence will lead Macbeth to acquire the position of a King. Lady Macbeth is exemplified as a negative anode of female ambition and power. In Lady

Macbeth the feminine desires for power were seen unnatural:

Come you spirits

That tend on mortal thoughts, unsex me here

And fill me, from the crown to the toe, top-full

of direst cruelty!

Here one can find the tension, the political gender tensions already existent in the Elizabethan world. Shakespeare defeminizes Lady Macbeth to give her ambitions credibility. He takes Lady Macbeth and her oddity so far as to reverse the gender roles of Macbeth. Weakness, as always is associated with the female but here, Lady Macbeth assumes Macbeth's bloody obligation and vice-versa. The female cannot, although, survive in a world of men and thus Lady Macbeth's strength deteriorates and she falls into periods of lunacy and sleepwalking. She puts forward that none can call their power to account but she is mistaken by the power of her own conscience. Her act of suicide indicates a personal trial and conviction. The irony underlies in the death of Lady Macbeth where the political structure is normalized with a return of male rule. Shakespeare reflects the culture of Elizabethan era through lady Macbeth's tragic fall from her ambition leading to power. On the one hand, Lady Macbeth is portraiture of the unnatural and ambiguous aspects of female political power and gender; hamlet, on the other hand, brings forward the issues of sovereignty and sexuality which again was very much prominent within the Elizabethan world. Unlike Elizabeth, Hamlet's Gertrude, chose a new King for Denmark. By marrying Claudius the absolute power was also shifted to him by the Queen. The fate of the state and particularly of Gertrude depended upon her new husband. Claudius murdered his own brother and so he can never be the right heir to the throne. He married Gertrude not for the reason that he loved her but for the selfish motive of acquiring the throne. The woman was only a source and not the means. She was used as a tool and thus a distrust of males is shown who achieve power through marriage to the female monarch. Thus Hamlet pronounces his uncle as a person who intends to harm others through sexual manipulations:

A murderer and a villain;
A slave that is not the twentieth part the tithe
of your precedent lord; a vice of Kings;
A cutpurse of the empire and the rule,
That from a shelf the precious diadem stole,
And put it in his pocket.

Hamlet condemns his mother and declares her characterless. For she married his uncle within less than a month of his father's demise. Hamlet accused his mother and generalized: "Frailty, thy name is woman." In both Hamlet and Macbeth, some points reflect the Elizabethan desire for a stable male monarch. A society full of disorderliness is presented before the readers where the cause of this disorderliness is nothing but female ambition or exploitation. In both the plays the female power exists and they suffer a lot too which again tries to show that women, however, cannot overcome the patriarchal system. Within these two plays one can view the potential conflicts arising from female power. But both the plays end with the diminution of female sovereign authority and Shakespeare's political resolution is represented by the females' destruction and the state's return to normalcy and patriarchal framework. If we take into account Shakespeare's comedies we can find that the female characters are undoubtedly strong and intelligent. They are sometimes shown as superior to men who are just to the contrary of his tragic heroines and in contrary to that of the Elizabethan society women. May be this is why he uses disguises through which his female characters speak freely and discards the force imposed upon them by their men. Character traits like adaptability, intelligence, strong will-power, self-awareness can be found in Rosalind of *As You Like It*, Viola of *Twelfth Night*, Beatrice of *Much Ado About Nothing* and Katherine of *The Taming of The Shrew*. In Elizabethan society women were compelled to do whatever best suited men and were never allowed control of their own consequences.

They were overall adaptable to their situation. Here one can take the examples of Rosalind and Viola who changed their identities to become men in order to get protection. Beatrice and Katherine were not confident enough for they were more direct and witty in their discourse. These women showed their intelligence through their discourse. Rosalind trains Orlando to be a better husband while she is disguised as a man in the forest and Orlando believes him. Viola parallels Rosalind and expresses her ideas of love to Orsino who likes him. Beatrice and Katherine on the other hand argue with men, attack them, and use their wit in order to equal their intelligence and self-respect. These women are aware of the society's expectations and also are aware of their self-awareness. Elizabethan audience would uproar with such ideas of gender equality if only Shakespeare would not have shown it as a fiction. Fiction is revealed by the mystical connotation of the forest scene and the presence of Hymen, the God of marriage. Viola was left alone but she acquired the right to marry Orsino only when her brother was there to give her away to Orsino. It shows that without a man to give her away the marriage would not have been possible. Beatrice and Katherine were witty enough using their sharp tongues. They were not willing to accept everything that was thrust upon them. But everything ends up happily for they tie the knots in a mutual understanding. Shakespeare, in no way had to remain attached to the expectations of Elizabethan society and he made this true by ending up all his comedy heroines becoming wives. Marriage was unavoidable for the

Elizabethan heroines and all the four female heroine's problems were resolved by the acceptance and protection of men. In *The Tempest* Shakespeare has used the fairy machinery with magic spells and enchantments. In his early plays the fairies were used for merry making and to create fun but in *The Tempest* one can see that these fairies are totally under the control of a male named Prospero. It is this man without whose permission and direction the fairies cannot act. The spirits do not possess any kind of independence and opportunity of action but it is only Prospero the wizard like man by whose orders they do act. One can see Ariel too who instead of possessing so much of powers cannot act on his own for he is bound to perform anything and everything only by his master's command. It is clearly revealed that he and all his fairylanders can only act by the command of a mortal lord. That Ariel is a diminutive being is found in these lines:

Where the bee sucks there suck I
In a cowslip's bell I lie:
There I couch when owls do cry,
On the bat's back do I fly
After summer merrily.

In *The Tempest* Shakespeare introduced the fairies as the means of redressing the wrong done to one mortal by another. The fairies and their powers are exploited by Prospero in such a way that they are compelled to fall on their knees and make amends. The title "*The Tempest*" itself tells the reader or shows the viewer that it is about a storm----- a violent storm in the sea as well as in the mind of the major character in the play that is Prospero. Prospero is the Duke of Milan but he is wronged by his own brother Antonio. He was also accompanied by Alonso in this deed. They have been stranded on an island for twelve years. Miranda, Prospero's three years old daughter was also with him. They were provided with enough food, clothes, water and good books of Prospero's by the counselor Gonzalo. Here, Prospero the possessor of great magical spell is served by spirits and specially Ariel. Although Ariel is portrayed as a very mischievous spirit still one cannot deny the fact that he is a sincere and obedient one for he does act with the command of only Prospero who he thinks is his master. This is perhaps because he was saved by Prospero from Sycorax who was supposed to trap him in a tree. Ariel is overall a loyal. In this play Prospero is portrayed as a character who always goes on performing his magical spells with the help of his slave and spirit Ariel. But whatever he did was only to show all the wrong doers the right way and to reveal the truth before the audience. He did not do anything for mere fun. He also performed his magic to bring Miranda, his only daughter closer to Ferdinand so that they fall in extreme love and become one. Prospero cannot be an evil soul and so also the case with Ariel. Both performed magical spells to do the right things and to show others the right way. This is proved at the end of the play when one finds that Prospero being wronged by so many other than his brother Antonio forgives them. No doubt he warns them not to repeat the same further. And when everything is alright he buries his magic properties and throws his book of magic in the waters.

A colonist can love the place where he builds a colony like his own country. But he only explores and exploits it for mere selfish ends and then leaves it like anything -----And this is very true of Prospero. This shows his colonial mentality. Caliban is a reflection of the native and Prospero a colonist. Prospero's treatment of Caliban is clear from Caliban's speech where he speaks thus-----

I must eat my dinner
This island is mine, by Sycorax my mother
Which thou tak'st from me.

Prospero rules with a hegemonic attitude of a colonizer in the island. He is portrayed as a dictatorial colonial ruler who treats the native (Caliban) like a slave and abandons the colony as soon as his job is completed.

IV. CONCLUSION

In *The Tempest*, one can find a male character that seems to be doing magic with the help of a spirit where the spirit was treated as a slave by the protagonist of the play. But the spirit, Ariel's loyalty is not sublimed. Here Shakespeare did not try to bring Ariel's loyalty, obedience and sincerity to the forefront. He was a subaltern character for he was not of this world but of the other. Without the presence of Ariel in *The Tempest* there would not have been the tempest and the play as a result would have been paralyzed from being developed. Undoubtedly, Shakespeare's plays reflect the Elizabethan image of women in general where women were bound to rules and conventions of the Patriarchal Elizabethan era. Shakespeare wanted to portray women as witty and strong but this was only for his great admiration to Queen Elizabeth. He, at last, could not but take the help of male characters thus weakening the wit and strength of their female counterparts only because he was aware of the society where he existed and was also conscious of the uproar and chaos that might be the outcome of such a play where women would be shown as a powerful one, equal to men in all respects. For Elizabethan audience was not at all happy by the rule of a queen, they wanted a patriarchal system.

In Hamlet and Macbeth one can find characters like Gertrude and Lady Macbeth on the one hand and on the other in The Tempest one can find the character of Ariel-----all them being the subalterns in their own way. Gertrude and Lady Macbeth were given importance as far as their male counterparts were helped, exalted or supported by them. As soon as the male counterparts did fall their importance in the plays were lost and they fell down from the top position to somewhere where they were lost at once. Likewise in The Tempest the spirit Ariel was the most important character without whose contribution there would not have been any development in the play and where Prospero's actions totally depended upon Ariel. But to our surprise Ariel was only in the play acting as a mere slave to Prospero and individually his character does not find any such ground on which he can stand firm. It seems as if without Prospero there would not have been Ariel but would there have been Prospero and his resourceful magical spells without Ariel, is a thing to be considered. However, Caliban is not only a deformed slave but a native of the island over whom Prosper rules. Prospero thinks Caliban is genetically inferior-----

A devil, a born devil, on whose nature

Nurture can never stick;

Caliban is a symbol of colonial injustice. He is a symbol of European imperialism and colonization. He was disinherited, exploited and subjugated. He was torn between his own culture and a culture that was imposed on him by Prospero. Caliban finally repents for his rebelliousness and promises to remain obedient and sincere to Prospero ever after.

V. ACKNOWLEDGEMENT

The author is thankful to the Head, Department of English, Diphu University Campus, Karbi Anglong , Dr. Bishnu Charan Dash for being the torch bearer and also a guide throughout the preparation of this piece of writing. The author declares this paper to be her original work and that; this paper has not previously formed the basis for publication in any other journal.

REFERENCES

- [1] Guha, Ranajit, 1982.(Ed.) Subaltern Studies, Writings on South Asian History and Society (7 volumes). Delhi: OUP.
- [2] Sarkar, Sumit. 1997. "The Decline of the Subaltern" in Writing Social History, Delhi: OUP.
- [3] Das, B.K. 2005. Twentieth Century Literary Criticisms. Delhi: Atlantic.
- [4] Gandhi Leela. 199. Post Colonial Theory: A Critical Introduction, Delhi: OUP.
- [5] Shakespeare, William, Macbeth, in The Complete Works of William Shakespeare (Ware, Hertfordshire, England: Wordsworth Editions, Ltd., 1996), I.v.25-28.
- [6] Macbeth,I.v.40-43.
- [7] Ibid,II.ii.63-64.
- [8] Ibid, v.i.37.
- [9] Shakespeare, William, Hamlet, in The Complete Works of William Shakespeare (Ware, Hertfordshire, England: Wordsworth Editions, Ltd., 1996), I.ii.8-10,14.
- [10] Ibid, I.ii.152-53.
- [11] Ibid, III.iv.97-102.
- [12] Ibid, I.ii.8-9.
- [13] Ibid, III.iv.139-40.
- [14] Shakespeare, William, The Oxford Shakespeare. New York: Oxford University Press, 2002.
- [15] Shakespeare, William, The Tempest, in The Complete Works of William Shakespeare (Ware, Hertfordshire, England: Wordsworth Editions, Ltd., 1996).

Modeling of Sokoto Cement Production Process Using A Finite Automata Scheme: An Analysis Of The Detailed Model

¹Z. Ibrahim, ²A.A. Ibrahim and ³I. A. Garba
^{1,2}Department of Mathematics, Sokoto State University, Sokoto
³Department of Mathematics, UsmanuDanfodiyo University, Sokoto

ABSTRACT

This research intends to establish the detailed model and study the models as established in the compact scheme earlier on presented. In this case, the research focuses on the study of the algebraic theoretic properties and relationship between the processes of production viewed as sub-states of a designed automata scheme. The transitions were then linked up in an algorithm that also specifies the movement from one state to another. A transition matrix was then generated from the resulting transition table leading up to a construction of an optimal production model for the Sokoto Cement production system.

KEY WORDS: Limestone, Cement, States, Finite Automata Scheme and Transitions matrix

I. INTRODUCTION

Cement is a fine powder which sets after a few hours when mixed with water, and then hardens in a few days into a solid strong material, therefore, Cement is a hydraulic binder, which hardens when water is added to it [5]. There are 27 types of common cement which can be grouped into 5 general categories and 3 strength classes: ordinary, high and very high. In addition, some special cements exist like sulphate resisting cement, low heat cement and calcium aluminat cement. Cement plants are usually located closely either to hot spots in the market or to areas with sufficient quantities of raw materials. The aim is to keep transportation costs low in taking the basic constituents for cement (limestone and clay) from quarries to these areas. Basically, cement is produced in two steps: first, clinker is produced from raw materials and in the second step cement is produced from cement clinker. The first step can be a dry, wet, semi-dry or semi-wet process according to the state of the raw material. According to [2], the raw materials are delivered in bulk, crushed and homogenised into a mixture, which is fed into a rotary kiln, which is an enormous rotating pipe of 60 to 90 m long and up to 6 m in diameter. The kiln is heated by a 2000°C flame inside of it and is slightly inclined to allow for the materials to slowly reach the other end, where it is quickly cooled to 100-200°C for clinker formation. There are four basic oxides in the correct proportions that make cement clinker: calcium oxide (65%), silicon oxide (20%), alumina oxide (10%) and iron oxide (5%).

These elements mixed homogeneously (called "raw meal" or slurry) when heated by the flame at a temperature of approximately 1450°C to form the new compounds: silicates, aluminates and ferrites of calcium responsible for the hydraulic hardening of cement through hydration of these compounds. These solid grains obtained as the final product of this phase is called "clinker" and are stored in huge silos for the next process. The second phase is handled in a cement grinding mill, which may be located in a different place to the clinker plant. Gypsum (calcium sulphates) and possibly additional cementitious (such as blastfurnace slag, coal fly ash, natural pozzolanas, etc.) or inert materials (limestone) are added to the clinker and grounded to produce a fine and homogenous powder called cement. The cement is then stored in silos before being dispatched either in bulk or bagged.

Portland cement

The American Society for Testing and Materials (ASTM) in [7], defines Portland cement as "hydraulic cement which not only hardens by reacting with water but also forms a water-resistant product, produced by pulverizing clinkers consisting essentially of hydraulic calcium silicates, usually containing one or more of the forms of calcium sulfate as an inter-ground addition." The low cost and widespread availability of the limestone, shale, and other naturally occurring materials make Portland cement one of the lowest-cost materials widely used over the last century throughout the world.

Description of the Study Area

According to [1], the Iullemeden Basin of West Africa covering an estimated area of 700,000km² extends into northwestern Nigeria where it is referred to as the "Sokoto Basin". The Sokoto Basin lies in the sub-Saharan Sudan belt of West Africa in zone of Savanna-type vegetation generally classified as semi-arid. It lies between latitudes 10° and 14° N and longitudes 3° and 7° E and covering an area of about 65,000 square kilometres. The area is bounded on the north and west by Niger Republic and on the southwest by Benin Republic. Although the Sokoto Basin of Nigeria appears extensive in area extent, it only represents about one-tenth of the entire Iullemeden Basin of West Africa [1]. The basin broadly covers an area underlain predominantly by crystalline rocks to the east and sedimentary terrain to the northwestern half. The cement plant (the Cement Company of Northern Nigeria) is located in Kalambaina, which is about 6 km from the capital – Sokoto and is (13° 21' 16" N and 5° 5' 37" E) in Wamakko local government area of Sokoto State, one of the notable areas of the Sokoto Basin with the large deposits of limestone and other minerals. The sedimentary rock in this study area is classified as Sokoto group, which included the Kalambaina formation made up of limestone (Adelana, Olasehinde and Vrbka, 2003).

1.3 Sokoto Cement

The Sokoto cement, produced by the Cement Company of Northern Nigeria, is a Portland cement and its production started from 1966. The Company is situated in Kalambaina area of Wamakko Local Government Area of Sokoto State where there is abundance of Limestone which constitutes the major raw materials. The first phase of its production is: Quarrying, Raw material preparation and Clinkering while the second phase which is the Cement milling consists of: Grinding and packaging.

II. APPLICATION OF FINITE AUTOMATA SCHEMES IN CEMENT PRODUCTION PROCESS

According to [4], the use of the word 'automata' harks back to the early days of the subject in the 1950's when they were viewed as abstract models of real circuits. The term 'finite automata' describes a class of models of computation that are characterized by having finite states. A Finite State Machine (FSM) or Finite-State Automaton (plural: automata), or simply a State Machine, is a mathematical model computation used to design both computer programs and sequential logic circuits. It is conceived as an abstract machine that can be in one of a finite number of states, the machine is in only one state at a time; the state it is in at any given time is called the current state. An automaton can change from one state to another when initiated by a triggering event or condition, this is called a transition. A particular finite state machine is defined by a list of its states, and the triggering condition for each transition. The fact that, automata models are abstract models of real circuits motivates me to use the model in design and analysis of the production system of Sokoto cement on the ground that the system has finite states of production process with a finite link from one state to the other expressed in terms of machine sequence. A detailed approach to modeling a cement production process should include all stages of production and transitions from the raw material to the finished cement. In particular, finite automata models have been used to model and develop a control for manufacturing systems [8]. In cement production process, the state of machine changes after each instruction is executed, and each state is completely determined by the prior state and the input. The machine simply starts at an initial state, changes from state to state until it reaches the final state [6].

A typical production system is composed of multiple machines and workstations that perform various operations on a part of production, and a material handling system that interconnect these machines and workstations. Parts are processed to completion by transiting them through various machines and workstations according to their individual process plan. After processing is complete these parts leave the system and proceed to the next state until the final state of production is reached [9]. For most manufacturing systems however, operation runs sequentially reaching desirable or pre-specified states. Each product goes through its own part of states until it reaches completion, i.e., the final state [3].

2.1 Notations

According to [4], a deterministic finite automaton (DFA) consists of;

- [1] a finite set of states (often denoted Q)
- [2] a finite set Σ of symbols (alphabet)
- [3] a transition function that takes as argument a state and a symbol and returns a state (often denoted δ)
- [4] a start state often denoted q_0
- [5] a set of final or accepting states (often denoted F)

[6] We have $q_0 \in Q$ and $F \subseteq Q$

So a DFA is mathematically represented as a 5-tuple $(Q, \Sigma, \delta, q_0, F)$

The transition function δ is a function in

$$Q \times \Sigma \rightarrow Q$$

$Q \times \Sigma$ is the set of 2-tuples (q, a) with $q \in Q$ and $a \in \Sigma$

Without loss of generality, we shall represent the detailed model of the cement production process using a finite automata scheme. This is to provide for an algebraic theoretic treatment and analysis of the model with a view to developing functional and ordered relations among the different components and subcomponents of the production systems as well as to undertake an optimization of the process. The model will therefore, be based on pre-defined assumptions of the deterministic automata having the following notational symbols:

q^0_1 = at the quarry level

q^0_2 = crushing of the lime stone

q^0_3 = stock piling

q^0_4 = raw mill

q^0_5 = silo

q^1_1 = preheating

q^1_2 = rotary kiln

q^1_3 = cooler

q^2_1 = mixing with gypsum

q^2_2 = grinding the mixture

q^2_3 = the cement

q^3_1 = packaging

q^3_2 = store

$t1_1$ = Process to second state of production from quarry to crushing

$t1_2$ = Process to second state of production from crushing to stockpile

$t1_3$ = Process to second state of production from stockpile to raw mill

$t1_4$ = Process to second state of production from raw mill to the silo

$t1_5$ = Completely processing to second state of production

$t2_1$ = Process to third state of production from preheating to the rotary kiln

$t2_2$ = Process to third state of production from rotary kiln to cooler

$t2_3$ = Completely processing to the third state of production

$t3_1$ = Process to the final state of production from mixing with gypsum to grinding

$t3_2$ = Process to the final state of production from grinding to having the finished cement

$t3_3$ = Completely processing to the final state of production; cement being stored

$t3_4$ = Cement packaging

t_* = Impossible process

So that, $Q = (q^0_1, q^0_2, q^0_3, q^0_4, q^0_5, q^1_1, q^1_2, q^1_3, q^2_1, q^2_2, q^2_3, q^3_1, q^3_2)$

$$\Sigma = (t1_1, t1_2, t1_3, t1_4, t1_5, t2_1, t2_2, t2_3, t3_1, t3_2, t3_3, t3_4)$$

The transition function of this scheme is denoted as:

$\delta: Q \times \Sigma \rightarrow Q$, where δ, Q, Σ are as defined above.

It therefore, follows that the underlined model has the state parameters thus:

- $\delta(q0_1, t1_1) = q0_2$
- $\delta(q0_2, t1_2) = q0_3$
- $\delta(q0_3, t1_3) = q0_4$
- $\delta(q0_4, t1_4) = q0_5$
- $\delta(q1_1, t2_1) = q1_2$
- $\delta(q1_2, t2_2) = q1_3$
- $\delta(q1_3, t2_3) = q2_1$
- $\delta(q2_1, t3_1) = q2_2$
- $\delta(q2_2, t3_2) = q2_3$
- $\delta(q2_3, t3_3) = q3_1$
- $\delta(q3_1, t3_4) = q3_2$

Construction of the Detailed Model of the Finite Automata for the Cement Production Process

The detailed model of the cement production process is obtained from compact model of the production system by taking into consideration additional processes and activities in line with the different components and subcomponents of the production system. As mentioned earlier, a state in the compact model has several sub states in the production system. Therefore, the detailed model identifies these sub-states and incorporates them in the production complex.

The detailed model of the complete cement production process has thirteen (13) sub-states made up of the following:

- [1] the raw material state
- [2] clinker process state
- [3] cement milling state
- [4] finished cement state

The raw material state which is the initial stage of production has 5 sub-states comprising of quarry, crushing, stockpiling, raw milling and silo. The clinker state is the second stage and it has 3 sub-states of preheating, rotary kiln and cooling leading up to the third stage of production which is called the cement milling state. The milling state has 3 sub-states: mixing with additives, grinding and powdering. The finished cement state which is the final stage also has 2 sub-states that is packaging and storing.

Based on these defined parameters the detailed model of the Sokoto Cement production process can be designed using a finite automata scheme as in the fig. 1.

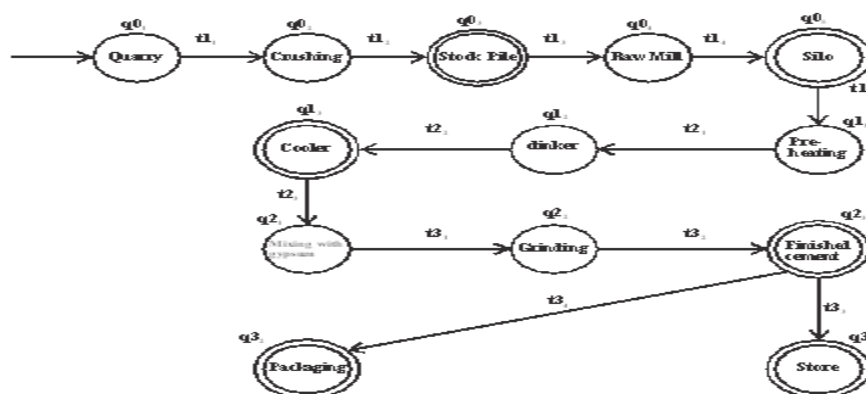


Fig 1. Detailed model of the SokotoCement production as a finite automata scheme

Figure 1, depicts the deterministic finite automata (DFA) model with a fixed number of states and we can only be in one state at a time and the transition table of the model is constructed using adjacency scheme as shown in table 1.

Table 1: the Transition Table of the detailed model of the Sokoto Cement production process

	$q0_1$	$q0_2$	$q0_3$	$q0_4$	$q0_5$	$q1_1$	$q1_2$	$q1_3$	$q2_1$	$q2_2$	$q2_3$	$q3_1$	$q3_2$
$q0_1$	1	$t1_1$	t_*										
$q0_2$	0	1	$t1_2$	t_*									
$q0_3$	0	0	1	$t1_3$	t_*								
$q0_4$	0	0	0	1	$t1_4$	t_*							
$q0_5$	0	0	0	0	1	$t1_5$	t_*						
$q1_1$	0	0	0	0	0	1	$t2_1$	t_*	t_*	t_*	t_*	t_*	t_*
$q1_2$	0	0	0	0	0	0	1	$t2_2$	t_*	t_*	t_*	t_*	t_*
$q1_3$	0	0	0	0	0	0	0	1	$t2_3$	t_*	t_*	t_*	t_*
$q2_1$	0	0	0	0	0	0	0	0	1	$t3_1$	t_*	t_*	t_*
$q2_2$	0	0	0	0	0	0	0	0	0	1	$t3_2$	t_*	t_*
$q2_3$	0	0	0	0	0	0	0	0	0	0	1	$t3_3$	t_*
$q3_1$	0	0	0	0	0	0	0	0	0	0	0	1	$t3_4$
$q3_2$	0	0	0	0	0	0	0	0	0	0	0	0	1

From the automata model of fig. 1 one can observe in the adjacency matrix of table 1, as follows:

- [1] That the upper diagonal elements are non-zero, indicating a one way directional connectivity of the respective process in the different stages of production.
- [2] That the diagonal elements are 1s indicating there is a delay (time lag) in between processes.
- [3] The lower diagonal elements are 0s indicating the non-reversibility of processes at this level of production.

2.3 The Transition Matrix of the Finite Automata Scheme of Sokoto Cement Production Process

Among the targets of this research work is to develop an optimal production model for Sokoto Cement. In view of this, a transition matrix is hereby generated from the transition table as in Table 1. This is done, first by developing an algorithm to generate elements of the transition matrix using the parameters of the automata model of fig. 1 and denoting all backward (reversed) operations act as ($t0_0$). The non-zero elements are those computed using the algorithm 2.4 which is used to construct the transition matrix in Table 2:

2.4 Algorithm

Assign: t_{ij} a transition from major production state to a sub-state, where i = major state of production and j = sub state of production.

Assign: t_{rc} is an element of the matrix where r = row number and c = column number

Then $t_{rc} = (i + j)r$ (1)

At $i = 1$, compute $t_{rc} = (i + j)r$ for $j \leq 5$

At $i = 2$, compute $t_{rc} = (i + j)r$ for $j \leq 3$

At $i = 3$, compute $t_{rc} = (i + j)r$ for $j \leq 4$

end if $i > 3$
end.

Accordingly the following matrix is obtained.

Table 2: Transition Matrix of the Sokoto Cement Production Process

$$\begin{bmatrix} 1 & 2 & 0 & 0 & 0 & 0 & 0 & 0 & 0 & 0 & 0 & 0 & 0 \\ 0 & 1 & 6 & 0 & 0 & 0 & 0 & 0 & 0 & 0 & 0 & 0 & 0 \\ 0 & 0 & 1 & 12 & 0 & 0 & 0 & 0 & 0 & 0 & 0 & 0 & 0 \\ 0 & 0 & 0 & 1 & 20 & 0 & 0 & 0 & 0 & 0 & 0 & 0 & 0 \\ 0 & 0 & 0 & 0 & 1 & 30 & 0 & 0 & 0 & 0 & 0 & 0 & 0 \\ 0 & 0 & 0 & 0 & 0 & 1 & 18 & 0 & 0 & 0 & 0 & 0 & 0 \\ 0 & 0 & 0 & 0 & 0 & 0 & 1 & 28 & 0 & 0 & 0 & 0 & 0 \\ 0 & 0 & 0 & 0 & 0 & 0 & 0 & 1 & 40 & 0 & 0 & 0 & 0 \\ 0 & 0 & 0 & 0 & 0 & 0 & 0 & 0 & 1 & 36 & 0 & 0 & 0 \\ 0 & 0 & 0 & 0 & 0 & 0 & 0 & 0 & 0 & 1 & 50 & 0 & 0 \\ 0 & 0 & 0 & 0 & 0 & 0 & 0 & 0 & 0 & 0 & 1 & 66 & 0 \\ 0 & 0 & 0 & 0 & 0 & 0 & 0 & 0 & 0 & 0 & 0 & 1 & 84 \\ 0 & 0 & 0 & 0 & 0 & 0 & 0 & 0 & 0 & 0 & 0 & 0 & 1 \end{bmatrix}$$

III. DISCUSSION OF RESULT

From Table 2, taking the difference of the t_{rc} (ie, $t_{rn} - t_{rn-1}$) and summing up these differences we have.

$$\left. \begin{aligned} \sum_{r=1}^5 (t_m - t_{m-1}) &= 30, & i=1 \\ \sum_{r=6}^8 (t_m - t_{m-1}) &= 22, & i=2 \\ \sum_{r=9}^{12} (t_m - t_{m-1}) &= 48, & i=3 \end{aligned} \right\} \quad (2)$$

The summation of the three processes of production is 100 which indicate the attainment of complete production process.

$$\text{ie } \sum_{r=1}^{12} (t_m - t_{m-1}) = 100 \quad (3)$$

Now using equation (2), at $i=1$ yields 30% of production while putting $i=2,3$ yields 22% and 48% of production respectively. This signifies that any problem that causes a break in the chain of production will be measured with respect to the total production process. According to [9], in manufacturing process break in production process cannot be ruled out. In most cases the effect of this abnormality cannot be immediately ascertained by the manufacturers. This research will immediately show the extent of the break on the production process which analytically shows the manufacturer areas of concentration to optimize the process. The larger the percentage summation of a level of major state of production, the critical that level of production is. From this, the manufacturer knows exactly what is at stake at every level of production.

IV. CONCLUSION

The transition matrix generated from the resulting transition table lead to the construction of an optimal production model for the Sokoto Cement Production Process. However, for both the diagnosis and remedies to be more effective and timely, there is the need to consider further the detailed analysis of the sub-stages of the major sub-states of the cement production process or even look more critically into the languages of the individual state's automaton in future research.

REFERENCES

- [1] Adelana S. M. A., Olasehinde P. I. and Vrbka P. (2003), Isotope and Geochemical Characterization of Surface and Subsurface Waters in the Semi-Arid Sokoto Basin, Nigeria: *African Journal of Science and Technology (AJST)*, Science and Engineering Series Vol. 4 No. 2 pp. 80-89.
- [2] Jacob J. P. (2009). Sustainable Benefits of Concrete Structures, European Concrete Platform ASBL, 1050 Brussels, Belgium.
- [3] Kim N., Shin D, Wusk R. A. and Rothrock L. (2010). Using Finite State Automata for Formal Modeling of affordances in Human-Machine Cooperative Manufacturing System: *International Journal of Production Research*, vol. 48, No. 5 Pg. 1303 – 1320.
- [4] Lawson M. V. (2005). Lecture Note, Department of Mathematics, School of Mathematic and Computer Science Hderiott Watt University.
- [5] Lea F.M. (1970). *The Chemistry of Cement and Concrete* (3rd edition); Edward Arnold Publishers Ltd.
- [6] O'Castillo O. L. and Tapia C. G. (2009). An Environmental and Production Policy Application of Multi-objective Mathematical Programming for Cement Manufacturing in the Philippines. www.math.upd.edu.ph.
- [7] Sarier N. (2013), *Nanotechnology Applications in Civil Engineering*, ce.iku.edu.tr/lcourses/CE08085.
- [8] Smith P., Esta C., Jha S. and Kong S. (2008). *Deflating the Big Bang: Fast and Scalable Deep Packet Inspection with Extended Finite Automata*, Seattle, Washington, USA.
- [9] Yalcin A., Tai T. and Boucher T. O. (2004). Deadlock Avoidance in Automated Manufacturing Systems Using Finite Automata and State Space Search. www.researchgate.net

Clustering Techniques to Analyze Communication Overhead in Wireless Sensor Network

Prof. Arivanantham Thangavelu¹, Prof. Abha Pathak²

¹(Department of Information Technology, Pad.Dr.DYPIET, Pune-18,

²(Department of Information Technology, Pad.Dr.DYPIET, Pune-18,

ABSTRACT:

Wireless Sensor network is a tiny sensor device about a cubic size having sensors and small battery, which enables applications that connect the physical world with pervasive networks. These sensor devices do not only have the ability to communicate information across the sensor network, but also to cooperate in performing more complex tasks, like signal processing, data aggregation and compression in the network rather than out of the network. The major problem with wireless sensor network is their limited source of energy, the coverage constraint and high traffic load. In this paper we introduce various clustering techniques which are to be used to reduce communication overhead and increase network's lifetime. In the present work, the comparative evaluation of communication overhead for the wireless sensor network based on clustering technique is carried out.

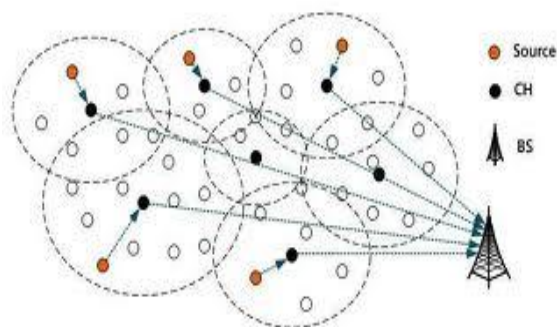
Keywords– Wireless sensor network (WSN), Clustering, K-means algorithm, Fuzzy clustering algorithm.

I. INTRODUCTION

Wireless Sensor Networking is a network of wireless sensor nodes deployed in an area. The wireless sensor network consists of the sensor nodes. The components of wireless sensor networks are sensing unit, processing unit and communication unit. The sensing unit senses the surroundings and acquires the data. The processing unit processes the acquired data and removes the redundancy. The communication unit acts as a transceiver, i.e. it receives the data and also transmits it. Wireless Sensor Networks (WSN) now-a-days is very popular for its specialty. WSN applications are having wide variety of domain. It include right from military application to farming application. The surveillance system for enemy or threat, the precision agriculture where farmer can control the temperature, humidity, etc. are the few examples of WSN applications. Health domain is having full of challenges with which the WSN can play important role in monitoring and disseminating the data to base station. Every application of WSN comprises of a set of sensor nodes and the base station called as sink. It is a sort of distributed system where all the nodes can work together to convey the data up to the sink. The entire node senses the data, depending on the application and sends it to the sink. The data may be reaching up to the destination in a single hop or through multi hop. In single hop, the data acquired by each node is transmitted to the base station directly. In multi hop, the data to be transmitted to the base station is through a number of nodes, i.e. the nodes transmit their data to the next node which is then transmitted to the next node, and finally to the base station.

II. CLUSTERING

In order to reduce the energy consumption a clustering and node redundancy approach has been extensively studied. In Clustering approach, sensor nodes are divided into clusters. Each cluster has a leader which is called cluster head (CH) aggregate all the data received by members of cluster and sends aggregated data to Base Station (BS). Clustering allows aggregation of data. It helps in removing the redundant data and combining the useful data. It limits the data transmission. The cluster system gives an impression of a small and very stable network. It also improves the network lifetime by reducing the network traffic.



III. CLUSTERING ALGORITHM

Clustering algorithms are designed to reach goals like a specific cluster structure and cluster-head distribution respectively. Also load-distribution among CHs, energy saving, high connectivity, and fault tolerance are often emphasized goals. Clustering provides re-source utilization and minimizes energy consumption in WSNs by reducing the number of sensor nodes that take part in long distance transmission. Cluster based operation consists of rounds. These involve cluster heads selection, cluster formation, and transmission of data to the base station. The operations are explained below.

1) Cluster Head Selection

In order for a node to become cluster head in a cluster the following assumptions were made.

- All the nodes have the same initial energy.
- There are S nodes in the sensor field.
- The number of clusters is K .

Based on the above assumptions, the average number of sensor nodes in each cluster is M where

$$M = S/K$$

After M rounds, each of the nodes must have been a cluster head (CH) once.

2) Cluster Formation

The next step in the clustering phase is cluster formation after CHs have been elected. Below gives the description of new cluster formation.

Step 1: The new cluster heads elected above broadcast advertisements (ADV) message to all non-cluster nodes in the network using Carrier Sense Multiple Access (CSMA) MAC Protocol.

Step 2: Each sensor node determines which clusters it will join, by choosing CH that requires minimum communication energy.

Step 3: Each non-cluster node uses CSMA to send message back to the CHs informing them about the cluster it wants to belong.

Step 4: After CHs have received messages from all nodes, Time Division Multiple Access (TDMA) scheduling table will be created and send it to all nodes. This message contains time allocated to each node to transmit to the CH within each cluster.

Step 5: Each sensor node uses TDMA allocated to it to transmit data to the CH with a single-hop transmission and switch off its transceiver whenever the distance between the node and CH is more than one hop to conserve energy. To avoid a single node transmitting data multiple times in one round, we set a threshold value G . G is the total time of all nodes in the cluster forwarding their data to the CH in one round.

Step 6: CHs will issue new TDMA slots to all nodes in their clusters when allocated time for G has elapsed, for each node to know exact time it will transmit data to avoid data collision during transmission that can increase energy consumption.

Step 7: CH transceiver is always turn-on to receive data from each node in its cluster and prepare them for inter-clusters transmission. Inter-cluster transmission is of two types: single hop and multi-hop [23,24]. We adopted multi-hop transmission in order to save more energy during inter-cluster transmission.

3) Transmission of Data

After all data has been received, the CH performs data fusion function by removing redundant data and compresses the data into a single packet. This packet is transmitted to the base station via multi hops transmission. After a certain period which is calculated in advance, the next round starts with the election of new CHs using our initial algorithm as described in 1 above and formation of new clusters as explained in 2.

3.1 K-means Clustering

K-means is one of the simplest algorithms that solve the well known clustering problem. The efficient cluster head selection method using K-means algorithm to maximize the energy efficiency of wireless sensor network. It is based on the concept of finding the cluster head minimizing the sum of Euclidean distances between the head and member nodes. The K-Means method is numerical, unsupervised, non-deterministic and iterative technique. It is used to partition an image into K clusters. The procedure follows a simple and easy way to classify a given data set through a certain number of clusters (assume k clusters) fixed a priori. The main idea is to define k centroids, [5] one for each cluster. These centroids should be placed in a cunning way because of different location causes different result. So, the better choice is to place them as much as possible far away from each other. The next step is to take each point belonging to a given data set and associate it to the nearest centroid. When no point is pending, the first step is completed and an early group age is done. At this point we need to re-calculate k new centroids as barycenters of the clusters resulting from the previous step. After we have these k new centroids, a new binding has to be done between the same data set points and the nearest new centroid. A loop has been generated. As a result of this loop we may notice that the k centroids change their location step by step until no more changes are done. In other words centroids do not move anymore. K-Means clustering generates a specific number of disjoint, flat (non-hierarchical) clusters. It is well suited to generating global clusters. K-means clustering is responsible for reducing communication overhead, energy consumption in wireless sensor network and increases network's lifetime The basic K-mean algorithm describes following:

Step1. Choose the number K of clusters either manually, randomly or based on some heuristic.

Step2. Generate K clusters and determines the cluster's center.

Step3. Assign each pixel in the image to the cluster that minimizes the variance between the pixel and the cluster center

Step4. Re-compute cluster centers by averaging all of the pixels in the cluster.

Step5. Repeat steps 3 and 4 until some convergence criterion is met.

3.2 Fuzzy Clustering

In hard clustering, data is divided into distinct clusters, where each data element belongs to exactly one cluster. Fuzzy clustering methods, however, allow the objects to belong to several clusters simultaneously, with different degrees of membership. In many situations, fuzzy clustering is more natural than hard clustering. Objects on the boundaries between several classes are not forced to fully belong to one of the classes, but rather are assigned membership degrees between 0 and 1 indicating their partial membership. Fuzzy clustering is a process of assigning these membership levels, and then using them to assign data elements to one or more clusters. One of the most widely used fuzzy clustering algorithms is the Fuzzy C-Means (FCM) Algorithm. The algorithm of fuzzy c-means clustering is as follows:

Step1. Choose a number of clusters in a given image.

Step2. Assign randomly to each point coefficients for being in a cluster.

Step3. Repeat until convergence criterion is met.

Step4. Compute the center of each cluster.

Step5. For each point, compute its coefficients of being in the cluster [4-5].

IV. SIMULATION RESULT

Simulation was carried out in Matlab. As seen from Figure (1) communication overheads increases significantly when velocity of sinks nodes increases using K-means clustering algorithm.

Figure (2) shows using Fuzzy clustering algorithm communication overhead increases with velocity on sink node and drops at the end.

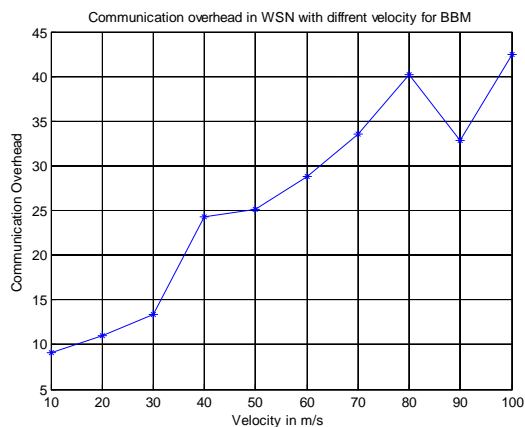


Figure (1)

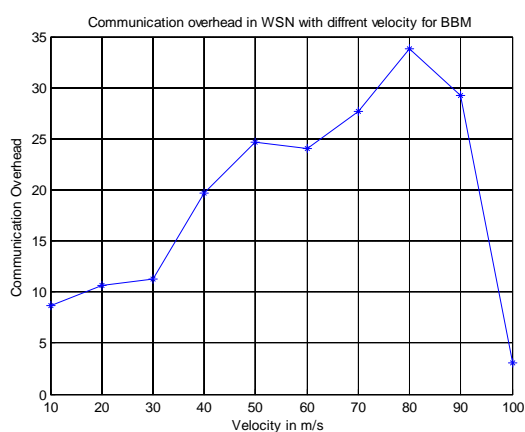


Figure (2)

V. CONCLUSION

As a result of these experiments, we evaluated the communication overhead in WSN using K-means clustering algorithm and Fuzzy clustering algorithm. We find that FCA is stable and energy efficient algorithm because it gives the low communication overhead as compare to K-means algorithm.

REFERENCES

- [1] Shiv Prasad Kori and Dr R K baghel "Evaluation of Communication Overheads in Wireless Sensor Networks" *International Journal of Engineering Research (ISSN: 2319- 6890) Volume No.2, Issue No.2, pp: 167-171 01 April 2013.*
- [2] Zhang/RFID and Sensor Networks AU7777_C012 Page Proof Page 323 2009-6-24 "Clustering in Wireless Sensor Networks".
- [3] Kavita Musale and Sheetal Borde "Analysis of Cluster Based Routing Protocol for Mobile Wireless Sensor Network" *International Journal of Advanced Trends in Computer Science And Engineering, Vol.2, No.1, Pages: 124-129 (2013)*
- [4] Pallavi Mathur , Soumya Saxena and Meghna Bhardwaj "Node clustering using K Means Clustering in Wireless Sensor Networking "National Conference in Intelligent Computing & Communication.
- [5] A Tutorial on Clustering Algorithms.
- [6] S. Adaekalavan and C. Chandrashekar "A Comparative Analysis of Fuzzy C- Means Clustering and Harmonic K Means Clustering Algorithms" *European Journal of Scientific Research ISSN 1450-216X Vol.65 No.1 (2011)*
- [7] Mrs. Bharati R.Jipkate and Dr. Mrs. V.Gohokar "A Comparative Analysis Of Fuzzy C-Means Clustering and K-Means Clustering Algorithm" *International Journal of Computational Engineering Research / ISSN: 2250- 3005 IJCER | May-June 2012*
- [8] Mathworks (<http://www.mathworks.com>)